Automated Modelling and Simulation of Automated Vehicles

Hong Chen

A Thesis

in the

Department of Mechanical Engineering

Presented in Partial Fulfilment of the Requirements

for the Degree of Master of Applied Science

at

Concordia University

Montréal, Québec, Canada

June 1996

© Hong Chen

ISBN   0-612-18379-3

Canada

Abstract

Automated Modelling and Simulation of Automated Vehicles

Hong Chen

A systematic methodology is presented for modelling and simulation of the dynamics of a class of automated vehicles, sometimes known as wheeled mobile robots (WMRs) or automated guided vehicles (AGVs). In this research, vehicles which operate essentially with four degrees of freedom (forward, lateral, roll and yaw) are studied, although the methodology can be extended to cover bounce and pitch modes.

Automated vehicles are widely used in many manufacturing industries. Examples include materials handling for payloads ranging from lightweight office supplies to heavy automotive engine blocks or newsprint rolls. The number of wheels and their configurations vary from one application to another, which may also require a corresponding mix of driving wheel units, steering wheel units and driving-steering wheel units, or simply casters to provide adequate loading support. Driving and steering are usually carried out with DC motors employing control loops of varying degrees of sophistication.

Thus, the methodology is designed to cater for arbitrary wheel configurations, a combination of sprung and unsprung masses, generation of tractive forces, rolling friction and lateral forces (side friction) at wheel-ground contact points, nonholonomic constraints of the automated vehicle system, etc. The model is built systematically by considering the vehicle main body and each wheel unit as separate rigid bodies, going through the necessary force balances and the characteristics of the salient components (such as vehicle main body and

each wheel unit), and assembling the dynamic model for the vehicle as an entire system. In this modelling process, the user keeps tab of all variables and equations being generated, so that (s)he can keep track of the number of redundancies in the resulting model. Formal structure of the model also leads to a corresponding structure for simulation on digital computer.

As illustrations, four automated vehicles are examined to show how the methodology may be put to use. These case studies demonstrate that this methodology produces results very easy, providing the much needed help for investigating performance of different designs of automated vehicles.

To my Parents,

ZONG SHUN CHEN and ZHI HUA DOU

and my Son,

FAN MARK LI

Without your love and support this would not have been possible

Acknowledgements

The author wishes to extend her sincerest gratitude and appreciation to Dr. R. M. H. Cheng for having rendered supervision, constructive criticism, moral and financial support during the course of this thesis work. Special thanks are due to Dr. M. G. Mehrabi and Dr. R. Rajagopalan for their helpful suggestions and moral support. Thanks are also due to the resourceful Mr. G. Huard for his technical support. Many thanks are due to the faculty, staff and students of the Centre for Industrial Control who over the years have provided a rich shared resource of ideas and information. The author wishes to thank her sisters Jie and Tao, who have been so supportive during this research, as always. Finally, the author would like to thank Bruce Roussel for proofreading the English of this thesis, and for his continual faith and encouragement.

Table of Contents

List of Figures

List of Tables

Nomenclature

α_i	Slip angle of wheel unit i (rad); the angle between the wheel plane and velocity vector $\mathbf{V}_{B_i}$ (direction of wheel travel)
β_{A_i}	Direction angle (rad); the angle between the x-axis of frame $\{Q\}$ and velocity vector $\mathbf{V}_{A_i}$ (only for casters)
β_{B_i}	Direction angle (rad); the angle between the x-axis of frame $\{Q\}$ and velocity vector $\mathbf{V}_{B_i}$
γ	Angular velocity of the vehicle about the yaw (z) axis of frame $\{Q\}$ (rad/s)
δ_i	Steering angle of a steering or driving-steering wheel unit i (rad); the angle between the wheel plane and the x-axis of frame $\{Q\}$
$\dot{\delta}_i$	Steering rate of the steering or driving-steering wheel unit (rad/s)
ζ_i	Caster free rotating angle (rad); the angle between the wheel plane and the x-axis of frame $\{Q\}$
$\ddot{\zeta}_i$	Caster angular acceleration (rad/s^2)
θ	Heading angle of the vehicle (rad); the angle between the X-axis of inertial frame $\{I\}$ and the x-axis of reference frame $\{Q\}$ (rad)
ξ_i	Angle between the steering column and the x_{B_i}-axis for Type A steerable wheel unit (where $\xi_i = \text{sign}(y_{a_i}) \dfrac{\pi}{2} + \delta_i$, and $\dot{\xi}_i = \dot{\delta}_i$)
ρ	Angular velocity of the vehicle about the roll (x) axis of frame $\{Q\}$ (rad/s)
$\sum X$	Total external forces acting on the vehicle along the x-axis (N)
$\sum Y$	Total external forces acting on the vehicle along the y-axis (N)
$\sum L$	Total external moments acting on the vehicle about the x-axis (N.m)
$\sum N$	Total external moments acting on the vehicle about the z-axis (N.m)
φ	Rolling angle of the vehicle (rad)

ω_i	Angular velocity of the driving or driving-steering wheel unit i (rad/s)
$\dot{\omega}_i$	Angular acceleration of the driving or driving-steering wheel unit i (rad/s^2)
$\mathbf{a}$	Acceleration vector of the vehicle with respect to inertial frame $\{I\}$
$\mathbf{a}_{A_i}$	Linear acceleration vector of joint A_i with respect to frame $\{Q\}$
$\mathbf{a}_Q$	Acceleration vector of the vehicle with respect to reference frame $\{Q\}$ (m/s^2)
A_i	Joint used to represent the connection between the vehicle main body and a wheel unit
$\{A_i\}$	Wheel reference frame located at joint A_i. The x_{A_i}, y_{A_i} and z_{A_i} axes of this frame are parallel to the x, y and z axes of the frame $\{Q\}$
$\mathbf{A}_{A_i}$	Linear acceleration vector of joint A_i with respect to frame $\{I\}$
$\mathbf{A}_{B_i}$	Linear acceleration vector of joint B_i with respect to frame $\{I\}$
b_i	Steering column length (m)
B_i	Joint used to represent the connection between the steering column and a wheel
$\{B_i\}$	Steering coordinate frame located at joint B_i. The x_{B_i}, y_{B_i} and z_{B_i} axes of this frame are parallel to the x, y and z axes of the frame $\{Q\}$
C_{α_i}	Cornering stiffness of the wheel (N.rad^{-1})
C_φ	Rolling stiffness of the system (N.m.rad^{-1})
C_i	Wheel-ground contact point used to represent the location of the wheel unit on the ground
$\{C_i\}$	Wheel-ground contact point frame located at wheel-ground contact point C_i. The x_{C_i}, y_{C_i} and z_{C_i} axes of this frame are parallel to the x, y and z axes of the frame $\{Q\}$
d_i	Offset of the steering column of steerable wheel units or casters (m)
D_i	Viscous damping factor of the drive motor (N.m.s.rad^{-1})

$\{D_i\}$	An imaginary frame, attached to the centre of mass for each wheel unit. The x_{D_i}, y_{D_i} and z_{D_i} axes of this frame are parallel to the x, y and z axes of frame $\{Q\}$
f_{r_i}	Rolling resistance factor of each wheel unit
F_{c_i}	Side resistance force of caster i, which is the force acting at wheel-ground contact point C_i by the ground (N)
F_{f_i}	Frictional force acting on each wheel unit at wheel-ground contact point C_i by the ground (N)
F_{l_i}	Lateral force acting on each wheel unit at wheel-ground contact point C_i by the ground (N)
F_{t_i}	Tractive force applied on the driving or driving-steering wheel i (N)
F_{x_i}	Reaction force which is the x-component of the resultant force acting on each wheel unit by the vehicle main body at joint A_i (or B_i) (N)
F_{x_i}'	Reaction force which is the x-component of the resultant force acting on the vehicle main body by each wheel unit at joint A_i (or B_i) (N)
F_{y_i}	Reaction force which is the y-component of the resultant force acting on the wheel unit by the vehicle main body at joint A_i (or B_i) (N)
F_{y_i}'	Reaction force which is the y-component of the resultant force acting on the vehicle main body by each wheel unit at joint A_i (or B_i) (N)
$F_{z_{C_i}}$	Vertical force acting on the wheel-ground contact point C_i by the ground (N)
F_{z_i}	Reaction force which is the z-component of the resultant force acting on the wheel unit by the vehicle main body at joint A_i (or B_i) (N)
F_{z_i}'	Normal force which is the z-component of the resultant force acting on the vehicle main body by each wheel unit at joint A_i (or B_i) (N)
g	Constant of gravity (m s^{-2})
h	Distance between the x-axis and the total mass centre m (m)
h_s	Distance between the rolling (x)-axis and the sprung mass centre (m)

i	Subscript index utilized to identify association with distinct wheel units
$\{I\}$	Inertial frame fixed on the ground
$I_{A_{s_i}}$	Moment of inertia of a steering wheel about the z_{A_i} axis (kg.m^2)
I_{B_i}	Moment of inertia of a driving wheel about its rotation axis (kg.m^2)
I_{S_x}	Moment of inertia of the vehicle about the x-(roll) axis (kg.m^2)
I_{xz}	Moment of inertia of the vehicle about the xz-plane (kg.m^2)
I_z	Moment of inertia of the vehicle about the z-axis (kg.m^2)
I_{s_i}	Polar moment of inertia of the caster (kg.m^2)
J_i	Moment of inertia referred to motor shaft (kg.m^2)
k_1	Coefficient of rolling friction
k_2	Coefficient of rolling friction (s.m^{-1})
k_{cnI}	Coefficient of side friction
k_e	Voltage constant of the motor (Volt.s.m^{-1})
k_t	Torque constant of drive motor (N.m.A^{-1})
L_ρ	Damping coefficient of suspension system (N.m.s.rad^{-1})
L	Inductance of the motor (H)
m	Total mass of the vehicle: summation of the sprung mass m_s and unsprung mass m_u (kg)
m_i	Mass of the each wheel unit (kg)
m_s	Sprung mass of the vehicle (kg)
m_u	Unsprung mass of the vehicle (kg)
n_c	Total number of casters employed on the automated vehicle system
n_d	Total number of driving wheel units employed on the automated vehicle

n_{ds}	Total number of driving-steering wheel units employed on the automated vehicle system
n_s	Total number of steering wheel units employed on the automated vehicle
N_i	Motor shaft-wheel axle gear ratio
$\mathbf{P}$	Position vector of the vehicle with respect to inertial frame $\{I\}$ (m)
$\mathbf{P}_{b_i}$	Position vector of joint B_i with respect to frame $\{Q\}$ (m)
$\mathbf{P}_{A_i}$	Position vector of joint A_i with respect to inertial frame $\{I\}$ (m)
$\mathbf{P}_{B_i}$	Position vector of joint B_i with respect to inertial frame $\{I\}$ (m)
$\{Q\}$	Reference frame attached to the vehicle main body
R_i	Radius of each wheel unit i (m)
R	Resistance of the motor (Ω)
T_D	Moment produced by spring damping of the suspension system
T_{f_i}	Static friction of drive motor (N.m)
T_{ω_i}	Tractive torque applied on driving or driving-steering wheel i (N.m)
T_G	Moment is due to the weight of the sprung mass
T_S	Moment produced by the spring forces of the suspension system
u	Longitudinal instantaneous linear velocity of the vehicle along the x-axis of frame $\{Q\}$ (m/s)
v	Lateral instantaneous linear velocity of the vehicle along the y-axis of frame $\{Q\}$ (m/s)
$\mathbf{v}_{A_i}$	Linear velocity vector of joint A_i with respect to frame $\{Q\}$
v_{xyA_i}	Magnitude of the velocity vector $\mathbf{v}_{A_i}$ in the xy-plane at joint A_i
$\mathbf{v}_{B_i}$	Linear velocity vector of joint B_i with respect to frame $\{Q\}$

$v_{xy_{B_i}}$ Magnitude of the velocity vector v_{B_i} in the xy-plane at joint B_i

$v_{j_{x_i}}$ Linear velocity of j_i along the x_{j_i}-axis with respect to frame $\{j_i\}$ (m/s) (where j represents joints A and B, wheel-ground contact point C, or the centre of mass D)

$v_{j_{y_i}}$ Linear velocity of j_i along the y_{j_i}-axis with respect to frame $\{j_i\}$ (m/s) (where j represents joints A and B, wheel-ground contact point C, or the centre of mass D)

V_X Instantaneous linear velocity of the vehicle along the X-axis of frame $\{I\}$ (m/s)

V_Y Instantaneous linear velocity of the vehicle along the Y-axis of frame $\{I\}$ (m/s)

V Velocity vector of the vehicle with respect to inertial frame $\{I\}$ (m s^{-1})

V_{A_i} Linear velocity vector of joint A_i with respect to frame $\{I\}$ (m s^{-1})

V_{B_i} Linear velocity vector of joint B_i with respect to frame $\{I\}$ (m s^{-1})

V_Q Velocity vector of the vehicle with respect to reference frame $\{Q\}$ (m/s)

W Total weight of the vehicle (kg)

$(x_{j_i}, y_{j_i}, z_{j_i})$ Locations of joints A_i and B_i, and the wheel-ground contact point C_i or the centre of mass of wheel unit i with respect to frame $\{Q\}$ (where $j = A, B, C, D$)

X_i, Y_i Total external forces acting on each wheel unit at wheel-ground contact point C_i along the x-and y-axes of the frame $\{Q\}$ (N)

Chapter 1

INTRODUCTION

1.1 Introduction to Automated Vehicles and their Applications

Automated Vehicles, also known as Wheeled Mobile Robots (WMRs) or Automated Guided Vehicles (AGVs), are driverless vehicles which usually move along a path on the floor defined by a buried guide wire or a painted line. Imai, Fujiwara and Kawashima [1] characterize automated vehicles as having five major properties: *navigating function*, *travelling route*, *position accuracy*, *energy savings* and *communication function*. Automated vehicles are highly sophisticated and increasingly popular as material handling and transportation devices in flexible manufacturing systems, airports, nuclear stations and military installations. They are also widely being used in offices and a variety of other applications.

Compared with other materials handling equipment alternatives such as pushcarts, forklifts or fixed automation (conveyors and the like), there are many benefits provided by using automated vehicle systems. Lane [2] cites the primary benefit of an automated vehicle system as its flexibility enabling 'smart' assembly, as well as efficient space utilization, safety and low overall operating cost. For example, system installation, phase-in and startup times are faster than other handling systems. Relocating an automated vehicle system is less costly and faster when assembly lines are to expected to be altered in the future, or should new assembly lines be added. With many wireless systems the guide path can be modified in a matter of minutes and even wire-guided vehicles can be dynamically rerouted to respond to changing priorities within an existing system. Automated vehicles are nearly as flexible as a

1

forklift or pushcart, travelling virtually anywhere within a facility to pick up or deliver a load. But unlike conveyors, they are not permanent: they are only present when working in a given area. Since they can park in an out of the way location, they do not create physical restrictions within the factory to nearly the extent that conveyors do. Automated vehicle systems can share their space with other equipment such as forklifts, allowing for clear aisles and improved overall space utilization within the factory. In addition, they are safer than competitive technologies, since most vehicles are equipped with obstacle-detection sensors and will avoid obstacles in their path or stop before hitting them. Unlike forklifts, there is no operator error.

Automated vehicle-based assembly systems are replacing conveyorized assembly lines, offering more flexibility, productivity and better quality control. Large or small p Jucts may be assembled directly on automated vehicles. Castleberry [3] describes how automated vehicles constitute ideal material handling systems because they handle a variety of parts in random order, can be reprogrammed to handle new parts and new routes, and can handle a well-defined family of parts in a predetermined sequence. Moreover, although automated vehicle systems are significantly more expensive than forklifts or other manual equipment, they can pay for themselves rapidly by reducing operating costs, especially in multi-shift operations. Nelms [4] and Delta Air Lines Inc. [5] report the acquisition cost of automated vehicle systems as often comparable to that of conveyors for the same application, but overall operating costs - particularly in the area of maintenance - are usually significantly lower. Dunkin [6] cites the Japanese as leading the way in use of mechanized and automated materials handling systems as a means to free workers for more creative tasks.

Automated vehicle systems are increasingly a key factor for staying competitive in world markets. They use advanced guidance and control systems that provide both flexibility and accuracy. They also have free-ranging ability [7]. Lai and Hsieh [8] and Tanya and Sanljiv [9] report that with the increasing interest in automating factories, automated vehicle systems (which include all flexible and driverless material handling methods) have gained importance not only in warehousing but also for carrying work in process in manufacturing facilities. Automated vehicles have become an integral part of today's manufacturing and warehousing environments. In addition, automated vehicle systems provide the efficiency of automation at a cost that is comparable to conventional equipment.

Applications of automated vehicle systems traditionally have involved moving large, heavy and pallet loads throughout distribution warehouses and highly automated manufacturing facilities, especially in the automotive industry. In the high production processes workpiece flow tends to be complicated, it is difficult to lay out loading and unloading positions regularly. It is therefore necessary to use the automated vehicles which have the ability to move quickly along often intricate routes. Automated vehicle systems have been widely used for non-condition flow applications in many manufacturing processes. Smaller automated vehicle systems are also being used for delivering raw materials, totes in light manufacturing and assembly facilities, as well as in office and other applications. Smith and Sarin [9] report that in more than a dozen US hospitals, automated vehicles already carry food trays down halls, through doors and onto elevators. A miniature mobile robot equipped with video cameras is used for inspecting otherwise inaccessible locations [10].

Furthermore, in recent years novel technologies are delivered to market more rapidly

3

because of the many advanced guidance and control capabilities available in automated vehicles With control systems becoming more intelligent, applications of automated vehicle systems are becoming larger and more complex. In addition, new guidance technologies allow vehicles to be used in areas where buried wire would have been impractical or impossible. In other words, automated vehicles can be applied in industry by following the desired paths other than those marked by reflective tape, paint or buried wire. For example, Saha and Angeles [11] report dead-reckoning techniques which allow applications without physical guidepaths. Other examples include undersea exploration [12], nuclear and explosive handling [13], security [14], military [15], as well as hospital, clearing, assembling, printing and airlines [16]. Automated vehicle system applications have thus been extraordinarily extended from their earliest and most conventional roles.

1.2 Historical Background of Automated Vehicles

1.2.1 Development of Automated Vehicles in Industry

Probably the first automated vehicle was introduced in 1953 by Barret Electric [2][6], which was a towing tractor modified to follow a guide wire. Throughout the 1960s and early 1970s, automated vehicle designs did not vary much from the towing-tractor type that were used primarily in warehouses. In the mid 1970s, unit load automated vehicles, which had been developed in Europe, were introduced into the U.S. These vehicles were used almost exclusively to connect with automated storage and retrieval systems. Over the last 10 to 15 years, a variety of new vehicle types have appeared including forklift vehicles that move loads vertically as well as horizontally. They can be used to store loads in pallet racks, and smaller

4

vehicles are used for office and light industrial applications. Some automated vehicles are designed to be used as assembly platforms for manufacturing operations.

Early automated vehicles were guided by a wire embedded in the floor and were able to make only the simplest routing decisions. Rapid development in electronics technology during the 1960s and 1970s also allowed automated vehicle capabilities to increase rapidly. Control systems became "smarter," allowing applications to become larger and more complex. However, until the early 1980s wire guidance remained the only viable guide path option. Since then there has been an explosion of new technologies for automated vehicle guidance. Two principal categories of guidance systems have evolved. The first type are guide paths, such as reflective tape [17], reference markers, or magnets embedded in the floor [18]. The second group of technologies use dead-reckoning [11][19]. All of these technologies permit automated vehicles to be used in areas where buried wire would have been impractical or impossible. This contributed to a significant growth in automated vehicle installations.

During the 1970s and early 1980s automated vehicle applications continued to become larger and more complex, using new guidance and control capabilities. Recently, applications have also been made to smaller plants, with fewer vehicles covering less distance with less complex routing and control schemes. During this time, automated vehicles have moved from being a tool used by only the largest companies to one used by smaller companies in simple but effective applications.

1.2.2 Development of Automated Vehicles at Concordia University

During past decade, there have been a number of experimental automated vehicles

successfully developed in the Centre for Industrial Control (CIC) of the Department of

Mechanical Engineering at Concordia University. The earliest one, named CONCIC-1, was

built in 1985. Cheng, Coubert, Surpaceanu, Favreau, and Fahim [20] describe this vehicle as

a light-duty, high-speed automated vehicle guided by camera vision and capable of following

a floor guide path. It can be used as an automated tractor or a unit load transporter. A

photograph of the CONCIC-1 automated vehicle is shown in Fig.1.1. It has a triangular

wheel-base configuration with one driving-steering wheel at the front, and two caster wheels
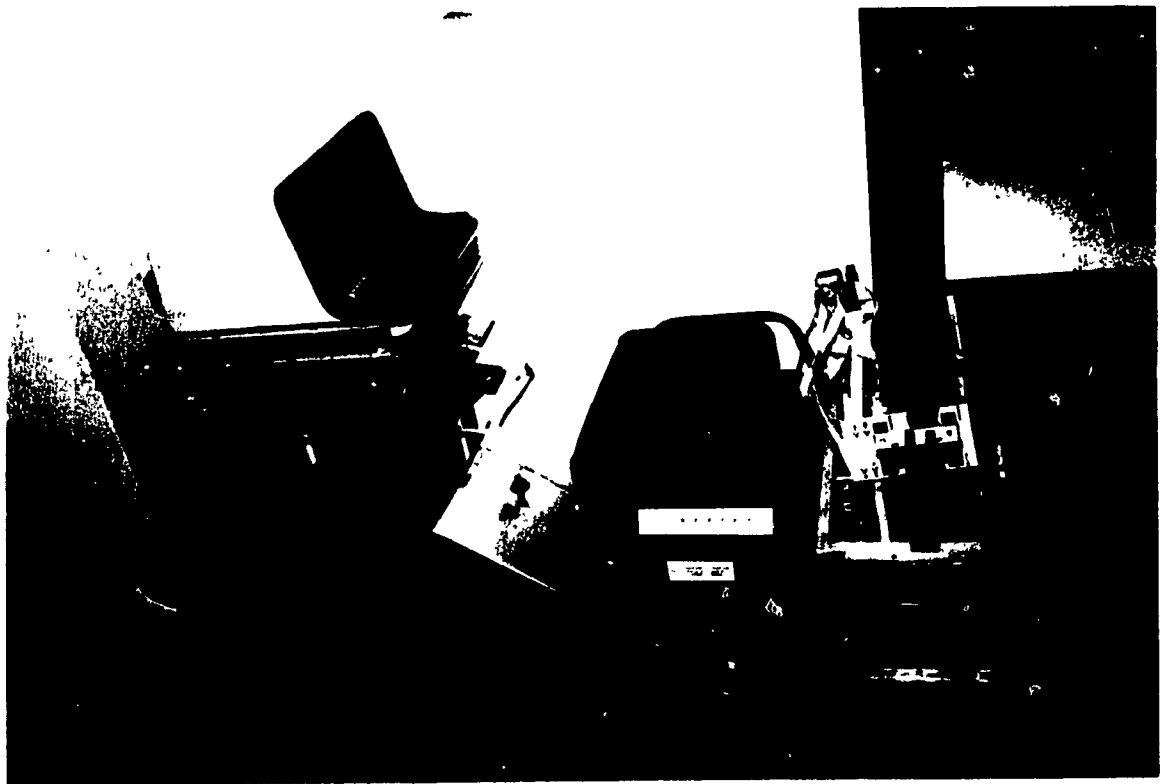
Figure 1.1: Photograph of CONCIC-1 [20].

at the rear. The driving mechanism consists of a DC motor which is engaged to the driving

wheel via a belt and chain transmission. The steering mechanism is made up of a DC motor

which drives the steering axis via a chain drive. CONCIC-1 has four major functions which

include *System Management*, *Sensing Function*, *Motion Control* and *Data Acquisition*. The controller of CONCIC-1 has been designed and built as a modular structure comprising three microprocessors which execute specific operations such as motion control or analysis of the guide path image with the necessary hardware to communicate with the central computer. Although CONCIC -1 worked well with various types of paths, the tricycle mechanical configuration limits the turning radius, and therefore tracking at intersections becomes more difficult. More details about the CONCIC-1 design can be found in [20].

The second prototype automated vehicle, named CONCIC-2 [17][21] was built in 1988. Compared with CONCIC-1, it has a very flexible mechanical design meeting various industrial needs. It can offer different wheelbase configurations by relocating the wheels. This flexible mechanical structure is also very useful for intensive investigation of the dynamic performance of automated vehicles with different wheel configurations. Fig.1.2 shows a photograph of the CONCIC-2. This vehicle, built by Rajagopalan [17], consists of two motorized driving wheel units at the mid-length of the vehicle, and two casters, one located in fron. and one at the rear. Each motorized wheel is controlled by a velocity servo loop that is built by using an LM628 servo controller, a digital-to-analog converter, and an amplifier, as well as an on-board microcomputer unit serving as a main controller. An optical camera is mounted in the front or the back of the vehicle to recognize the location of the vehicle relative to the tape on the floor and junctions. Ultrasonic sensors and wireless devices are employed on the vehicle to detect obstacles and communicate with the control station [17][22]. A two degrees-of-freedom dynamic model of CONCIC-2 has been developed by Cheng and Huang [21][23]. This dynamic model has been verified with experimental results.

7

Furthermore, a method to develop the equations of motion for an AGV with different wheel configurations is suggested by Huang in Appendix A of [21].
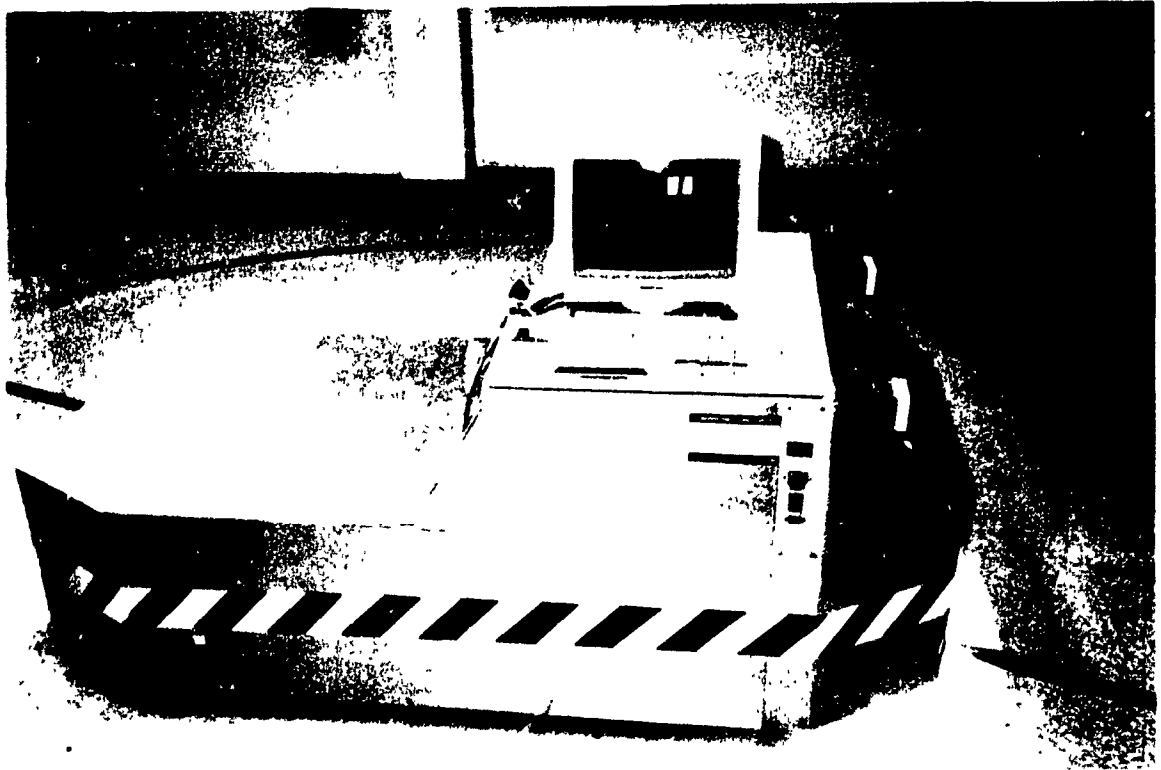
1. Prototype AGV   3. Ultrasonic Sensors

2. Terminal   4. Track with road signs

5. Keyboard

Figure 1.2: Photograph of the CONCIC-2 [17].

The third experimental vehicle is named CONCIC-3, and was built in 1993. It was conceived by Cheng and Mehrabi [19][24] as a test bed for dynamic modelling and control experimentation of automated transit vehicles (ATV). CONCIC-3 is equipped with two integral driving-steering wheel units located in the front and rear of the vehicle, as well as two

casters located one on each side of the automated vehicle for load support and stability. Each driving-steering unit has a driving motor geared to a solid rubber wheel and a steering motor with a ring type reduction gear.

Mehrabi [19] suggested two dynamic models, a complex nonlinear model and a simplified linear model. The nonlinear dynamic model operates with three degrees of freedom (yaw, lateral and roll). The simplified model was obtained by linearizing the nonlinear model. Lateral and yaw motions are the only two motions retained in the linear model. The effect of changes in total mass, sprung mass, inertia parameters, stiffness, damping, geometric and kinematic parameters of the vehicle system on the responses of the lateral, roll and yaw motions of the system have been studied using sensitivity theory. Results show how variations in these parameters influence the motion of the vehicle. In particular, the sprung mass, roll moments of inertia and roll damping directly affect the roll motion, but they do not have an important effect on yaw and lateral motion. Geometric kinematic parameters are most influential on both roll, yaw and lateral motion of the vehicle. These factors should therefore be considered most carefully during the design stage.

The linear model was used to simulate vehicle responses as well as to provide a linear plant to design control laws based on linear control theory. It was confirmed in [19] that simulations of the open loop responses of the detailed nonlinear model and the simplified linear model remain close to each other under typical operating conditions. In order to obtain satisfactory performance of an automated vehicle, a number of motion control strategies have been developed based on a differential drive model and a tricycle model. For the class of differential drive vehicles which has two independent side driving wheels, a control structure

has been proposed by using the kinematic relations of the system. Performance of the controlled system is also investigated in these simulations.

For the tricycle model which has a steering wheel at front end of the vehicle, two control schemes have been proposed. One is a nonlinear control scheme which was developed based on the dynamic equations for the system. Simulations demonstrate an improvement in path tracking of the vehicle (approximately 25 percent less overshoot). Another strategy is a controller which was designed using optimal control theory and the linearized dynamic model of the vehicle. This controller is unable to compensate for errors produced due to path curvature. An integral action is incorporated in the controller to enhance vehicle performance in curve tracking. Although the performance of both controllers appears satisfactory in the simulation results, the nonlinear controller shows superior performance for the system in path following. Other experimental AGVs have also been built at CIC.

1.3 Literature Review

1.3.1 Introduction

Imai, Fujiwara, and Kawashima [1], Jarvis [25], and Lai and Hsieh [8] describe automated vehicle systems as performing the following four basic functions:

(i) **Navigating function.** In high production processes, workpiece flow tends to be complex, making it difficult to lay out loading and unloading positions regularly. It is therefore necessary that automated vehicles have the ability to move quickly along often intricate routes.

(ii) **Travelling route.** With conventional types of automated vehicles, setting or

changing the travelling route is a major task. The capability of more advanced systems to making easy alteration of the travelling route is therefore an important issue.

(iii) **Positioning accuracy.** Workpieces must continually be transferred between automated vehicle systems and manufacturing equipment. If positioning accuracy is poor, it may be costly to adapt the loading mechanism or to correct vehicle positioning. To reduce this labour and cost, automated vehicles should be capable of accurate positioning.

(iv) **Communication function.** In an advanced job-shop-type production, production information should be matched with the flow of the workpieces. Thus the automated vehicles should be provided with an advanced communication function.

In order to give proper consideration to all the above functions, research in the area of automated vehicles involves multidisciplinary knowledge. The main areas can be generally classified as: guidance (including sensing and navigation), kinematic and dynamic modelling, motion control and planning, and design and manufacture. Each of these plays an important role for the entire automated vehicle system.

1.3.2 Guidance (Sensing and Navigation) Techniques

There are two general categories of automated vehicle guidance systems. Each type has particular applications for which it is best suited. One type uses guide path systems external to the vehicle, whereas the other uses dead reckoning as a means of navigation. Possible ways in which external guide path systems may be implemented include the following.

(i) an energized wire loop as discussed by Boegli [26], in which the path is not easily

modified, since installation of the wire is expensive.

(ii) optical sensors or beacons coupled with on board triangulation to compute the instantaneous vehicle position and orientation as reported by Rajagopalan and Cheng [17][27].

(iii) discrete magnetic marker reference/sensing systems as reported by Matsumoto and Tomizuka [19], and Hessburg and Peng [28] that are based on a series of magnetic markers placed in the centre of a predetermined vehicle path. Corridor effect magnetometers, mounted on front centre of the vehicle, acquire the field from the markers.

Another technique to guide the vehicle is called "*dead-reckoning*" guidance, as reported by Mehrabi [18], and Cheng and Rajagopalan [29]. This method does not rely on use of any physical guide paths. To move the vehicle along a prescribed path, the wheel motion parameters are plotted from a mathematical description of this path. The path of the automated vehicle can be easily modified by simply redefining the path in the computer memory.

1.3.3 Kinematic and Dynamic Modelling

It is well known that kinematics and dynamics of a manipulator form the basis of its control, trajectory planning and path planning. Similarly, kinematics and dynamics for an automated vehicle are also very important for analysis of its motion feasibility, control, trajectory planning and other more complicated problems. Kinematics and dynamics of various automated vehicles have been investigated extensively over the past the two decades.

12

Muri and Neuman [30][31][32], Wang [33], d'Andrea-Novel [34], Cyril, Cheng and Sankar [35], Lilly [36] and Craig [37] treat automated vehicles as examples of mechanical systems with nonholonomic constraints because they require rolling contact between two or more rigid bodies. Automated vehicle systems are also distinct from stationary robots in other ways. For example, in contrast to robotic manipulators, which are holonomic systems, rolling robots are non-holonomic systems Rolling constraints in the wheels make kinematic and dynamic analyses more complicated than those of holonomic systems. Consequently, the following important characteristics of automated vehicle systems require special consideration in the kinematic and dynamic modelling process: (1) closed-chain mechanisms, (2) friction, (3) higher-pair joints, (4) unactuated joints, (5) unsensed joints.

Muir and Neuman [30][31] also give important guidance for kinematic and dynamic modelling of automated guided vehicles. They have listed the important differences between conventional stationary manipulators and automated vehicles. For the sake of completeness these are presented below. Firstly, stationary manipulators are open-chain mechanisms, whereas the wheels of an automated vehicle form a closed-chain when in contact with the surface-of-travel. Secondly, automated vehicle mobility comes from the translational friction between wheel-ground contact points (or patches), whereas friction between joints is usually neglected for stationary manipulators. Lack of sufficient friction at wheel-ground contact points (or patches) will lead to wheel slippage, a problem not encountered in stationary manipulator operation. Thirdly, all prismatic or revolute stationary manipulator joints are *lower-pairs*. A lower pair allows common surface contact between adjacent links providing holonomic constraint. The "joints" and wheel-ground contact points of automated vehicles

13

are higher-pairs, and higher-pairs allow point or line contact providing nonholonomic (velocity) constraints. Next, to control the motion of an open chain, all joints must be actuated and all of the joint positions (or angles) and velocities must be sensed. In contrast, a closed-chain mechanism may be adequately controlled with some joints unactuated, and its motions may be adequately comprehended with some joints unsensed. Finally, higher-pair wheel "joints" of automated vehicles do not allow actuation and sensing of the rotational degree of freedom of each wheel about the wheel-ground contact point.

Furthermore, as pointed out by Muir and Neuman [30], the Lagrange and Newton-Euler formulations are most widely applied to the dynamic modelling of stationary manipulators. However, since the dry or viscous friction at joints is not accounted for in these two methodologies, and automated vehicles are closed-chains for which the kinematic and dynamic equations of motion must be computed in parallel and sufficient friction must be encountered, neither Lagrange nor Newton-Euler formulations may therefore be applied for wheeled mobile robot dynamic modelling.

There are many studies on the topic of kinematic modelling [11][22][29][31][32][33]. One interesting investigation is a unified approach to both direct and inverse kinematic analysis for four kinds of wheeled robots developed by Wang, Linnett and Roberts [33]. In this approach, a general mathematical model for automated vehicles without kinematic constraints is given. The general constraint equations are based on the indefinite requirement for any types of automated vehicles consisting of wheels connected to the rigid body. Specifically, these systems roll without any side-slip. Finally, the kinematics of four types of vehicles are developed by considering the general mathematical model, constraint equations,

as well as specified vehicle path, such as a straight line, circular path, or more general curve of the form y = f(x). These four types of vehicles are specified as: *ordinary car-like robots* (such as passenger cars, single unit trucks, single unit buses and articulated trucks), *dual drive robots* (dual drive motors with various casters), *synchro drive and steering robots*, and *omnidirectional robots*. All above examples illustrate the general procedure of deriving direct and inverse kinematics of an automated vehicle.

Another example is the kinematic model of an automated vehicle with an inclined steering column and offset distance as reported by Cheng and Rajagopalan [29]. This vehicle is considered to have two degrees of freedom, forward linear velocity and angular velocity. It consists of a three-wheeled configuration and a driving-steering wheel with an inclined steering column and offset distance, and two driving wheels employed at front and rear of the vehicle respectively. From the kinematic model, a criterion is derived to test the existence of the inverse kinematic solution. This criterion is a function of the geometric parameters of the automated vehicle and the steering angle of the front wheel. It represents the range of steering angle for which the inverse kinematic solution exists. In addition, this criterion also indicates the proximity of a unique solution for the motion parameters of the wheels, i.e., the wheel angular velocity, steering angle, and steering rate for desired values of the motion parameters of the automated vehicle.

Simularly, there are many studies on the topic of dynamic modelling [11][18][19][21][23][24][30][34][35][37][38][39][40][41][42][43]. A dynamic model (as well as the guidance system) of a three-wheel electric wheelchair (two driving wheels and a caster) have been developed by Johnson in 1983 [39]. In this model, the electric wheelchair

15

is considered to consist of three rigid bodies and D'Alembert's Principle is applied. Other studies concerning vehicle handling and stability have been made by Verma and Gillespie [40], Tousi and Bajaj [41], and Mehrabi [19]. Three-DOF nonlinear and linear dynamic models which incorporate lateral, yaw and roll motion as well as wheel-surface interaction forces, and 2-DOF linearized models that eliminate the roll motion have been investigated by Cyril, Cheng and Sankar [35], and Huang [21].

A nonlinear eight DOF handling model, in which the modes are defined as: 1. lateral velocity, 2. longitudinal velocity, 3. vehicle yaw rate, 4. vehicle roll, 5 -8. angular velocity of each of the four wheels, has been used to examine the effects of roll stiffness on handling and performance by Constantine, Bowman and Law [44]. This model was originally developed by Xia [43] [44] based on a 1984 Honda Accord (a 4-door sedan with front wheel drive). It represents a four wheeled automobile consisting of a sprung mass and front and rear unsprung masses. Based on this dynamic model, various control strategies have been devised and investigated which vary the total roll stiffness and / or the roll couple distribution in order to improve cornering ability and stopping distance. The results demonstrate that through active roll control, several benefits may be achieved, such as improved vehicle trajectory, better control ability and stability, and more predictability from the driver's viewpoint.

1.3.4 Control Strategies

Matsumoto and Tomizuka [18] and Hessburg, Peng, and Tomizuka [28] report research activity in automated vehicle control in three main areas. These are (1) longitudinal control which controls the vehicle forward speed, (2) lateral control which controls the vehicle

16

following a given path, and (3) yaw motion control which controls the desired direction of the vehicle. These three areas are of primary importance in automated vehicle control research.

The conventional approaches for control of automated vehicle systems are based on the information concerning position, velocity or both. Such simple position / velocity control schemes are often applied in situations where the system dynamics and the load disturbances are not significant. Many examples of control schemes based on vehicle kinematics are documented by Muir and Neuman [33], Rajagopalan [17][27], Cyril, Cheng, and Sankar [35], and Cheng and Rajagopalan [29].

However, when an automated vehicle is travelling in a straight line at high speed or entering a curved section of roadway, centripetal forces and side forces acting on the vehicle will become significant. In conventional servo control, which is based on velocity control, the required current is provided by amplifiers as demanded by the motors. Actual speed of wheels may therefore be reduced due to the existence of significant dynamic forces. Thus, sophisticated control schemes should be developed to handle the effects of the speed and path of the vehicle travelling, as well as the forces acting on the vehicle. In other words, advanced control schemes must take into account the influence of vehicle dynamics and provide adaptive cruise and steering control to meet varying needs in the operating environment.

Fortunately, modern parallel processing technology makes dynamic control possible. Model-based control is ideally suited to a powerful computational environment centred at the coordination stage. Lee and Chang [45] have pioneered research into the development of environments which support techniques for reducing dynamic calculation time by parsing

17

finite-difference equations into a format suitable for parallel processing. In this way, feedback and dynamic calculations are performed on separate processors.

The feasibility of implementing model-based control techniques on existing hierarchical control architectures for industrial manipulators has been experimentally evaluated by Leahy [46], Craig, Hsu, and Sastry [47], and Khosal and Kanada [48]. A major class of existing manipulators have been retrofitted to receive the benefits of dynamic-based control without any hardware modifications. In addition, An and Hollerbach [49] and Leahy [50] report experimental evaluation of model-based techniques demonstrating the potential for improving tracking accuracy with higher-speed trajectories.

Parallel processors make dynamic model-based control feasible, however there have been far fewer reported applications to automated vehicles than for stationary robotic manipulators. Nevertheless, recently model-based control techniques have been applied to automated vehicle systems by Hessburg and Peng [28], Matsumoto and Tomizuka [18], Canudas and Roskam [51], Rajagopalan and Cheng [52], Feng, Koren and Borenstein [53], and Koshiyama and Yamafuji [54].

Hessburg and Peng [28] and Matsumoto and Tomizuka [18] have implemented two control strategies based on the dynamics of four wheel steering vehicles. These two strategies provide lateral control, vehicle lateral velocity and yaw rate control using any two of three possible independent control inputs. The three possible inputs are: a differential driving torque between the two front wheels, a differential driving torque between the two rear wheels, and front and rear wheel steering angles. The analysis shows that considering the front and rear wheels independently allows a wider variation of lateral velocity and yaw rate in the steady

state.

The problem of controlling a two DOF automated vehicle under path and input torque constraints is considered by Canudas and Roskam [51], and a dynamics-based control scheme is proposed. In [52][53][54], computed torque control is introduced based on the dynamics of 2-DOF vehicles. The advantage of the model-based approach is in that sensor information on the actual vehicle dynamics are used. Required current is provided by the amplifiers only after the actuators experience the effect of the centripetal forces and side forces acting on the wheels. The speed of the vehicle can thus be kept constant for a variety of desired paths, since the compute torque control scheme pre-computes the current required to smoothly negotiate trajectory curvature ahead of the vehicle, without having to reduce forward speed. Each of aforementioned studies thus reveals the superiority of dynamic model-based control.

1.3.5 Tracking Control and Motion Planning

Tracking control and motion planning with nonholonomic constraints are fundamentally different from tracking control and motion planning with holonomic constraints. Li [55], Toumassoud and Jehl [56], and Sarkar, Yun and Kumar [57] point out that rolling engenders nonholonomic constraints in an otherwise holonomic system. Li [55] studied the motion of two rigid bodies rolling relative to one another. One example considers a vehicle wheel and the curved surface on which it travels. Li addressed this problem by specifying rolling without slipping (nonholonomic) motion instead of sliding (holonomic) motion. Advantages of this approach are as follows: (1) problems of wear associated with the contacting bodies is eliminated, and (2) associated control problems become much simpler. This is because in

19

order to control sliding motion, the coefficient of friction has to be known exactly, which is generally difficult.

Tracking control and motion planning of automated vehicle systems is always based on the assumption that the vehicle has pure rolling without slip motion. Many studies have been carried out on this subject, such as a stable tracking control method for a nonholonomic vehicle proposed by Kanayama [54]. Kanayama proved the stability of the control rule by using a Liapunov function.

Over the past decade, tracking control and motion planning for automated vehicles has been investigated extensively based on kinematic modelling. However, work based on dynamic modelling automated vehicles with nonholonomic constraints is much more recent (d'Andréa-Novel, 1991[34], Canudas de wit 1991 [51], Sarkar, Yun, Kumar 1994 [57]). For example, Sarkar, Yun, Kumar [57] developed a unified approach to control of automated vehicle systems subject to both holonomic and nonholonomic constraints.

1.4 Scope of the Thesis

1.4.1 Objectives of this Research

There is some information in the technical literature on the subject of dynamic modelling of automated vehicles. No attention has been paid to development of systematic methodologies for dynamic modelling of automated vehicles. However, more sophisticated control laws typically require a dynamic model, since behaviour of a vehicle may thus be predicted from dynamic parameters. Dynamic models are also useful for preliminary evaluation of performance characteristics of new automated vehicle designs.

20

The objective of this thesis is to present a systematic methodology for modelling and simulation of the dynamics of a class of automated vehicles. This type of vehicle may have any combination of four types of arbitrarily-located wheel units. These units are (1) motorized driving wheels, (2) motorized steering wheels, (3) motorized driving-steering wheels, and (4) free-rotating casters. Vehicles which have four degrees of the freedom (forward, lateral, roll and yaw) are examined, although the methodology is extendable to include bounce and pitch modes if the dynamics warrant their inclusion. Furthermore, based on the assumption that the wheel-ground contact region satisfies conditions of point contact, pure rolling and non-slipping, nonholonomic constraints of the automated vehicle system are explored. This model does not consider the dynamics of each wheel suspension independently, but rather as a single parameter for the entire vehicle which affects rolling.

The methodology is designed to cater to n arbitrary wheel configurations, a combination of sprung and unsprung masses, generation of tractive forces, rolling friction and lateral forces (side friction) at wheel-ground contact points. It builds up the model systematically by considering the vehicle main body and each wheel unit as separate rigid bodies, going through the necessary force balances and characteristics of the salient components, as well as assembling the dynamic model for the vehicle as an entire system. In this modelling process, a table is created to track all variables used and equations being generated which are finally assembled into a model of the entire system.

Formal structure of the model also leads to parallel structure for simulating the model digitally on the computer. Application of the present methodology generates a set of nonlinear ordinary differential equations which, depending on configuration, may be as high as eighth

21

order. Nonlinearities arise from terms involving steering angle, which is dependent on desired paths and vehicle forward, lateral and yaw velocities.

Four automated vehicle systems are examined to show how the methodology may be put to use. This methodology is seen to produce results in a very short time, providing the much needed help for investigating the performance of different designs of automated vehicles. In addition, this methodology can be used provide a check on the results obtained by more conventional approaches to dynamic modelling.

1.4.2 Layout of the Thesis

Chapter 2 deals with notational conventions for coordinate systems for representation of position, velocity and acceleration of the vehicle. Chapter 2 also deals with characterization of different wheel types and nonholonomic constraints of the wheel-ground contact points. In Chapter 3, equations of motion are derived for each component of the vehicle system, and the entire vehicle system. Chapter 4 presents the procedure for automated dynamic modelling and simulation in a step-by-step format. Chapter 5 discusses four examples to illustrate the methodology for dynamic modelling and simulation. Chapter 6 presents conclusions and future work. Appendix A reviews the fundamentals of rigid body dynamics. Appendix B derives each of the four types of wheel models considered by the present methodology. Appendix C discusses the analysis of vertical forces and loads acting on each wheel. Appendix D gives the system parameters of two examples.

Chapter 2

REPRESENTATION OF AUTOMATED VEHICLE SYSTEMS

2.1 Introduction

Automated vehicles generally consist of a rigid vehicle main body equipped with n arbitrarily located non-deformable wheels, as shown in Fig 2.1. Typically, the number of wheels employed on automated vehicles, and their wheel configurations vary from one to another depending on the application. The four most common types of wheel units generally utilized on automated vehicles are: motorized driving wheel units, motorized steering wheel units, motorized driving-steering wheel units and free rotating casters. In this research, an automated vehicle is constrained to move on a smooth horizontal plane, hence only some of the possible degrees of freedom (DOFs) are actuated. These DOFs are defined as follows: longitudinal velocity u along the x axis, lateral velocity v along the y axis, roll rate p about the x axis, yaw rate γ about the z axis. Linear translation along the z-axis (bounce) and rotation about the y-axis (pitch) are taken as negligible. In addition, a combination of sprung mass m_s, unsprung masses m_u and total mass of the vehicle system are also considered explicitly. In order to systematically analyze automated vehicle systems, some general assumptions, joint definitions and generalized coordinates will be given in this chapter. The position and velocity of an automated vehicle, and characterization of wheel units will be also discussed in detail. In addition, based on the assumption that the wheel-ground contact region satisfies conditions of point contact, pure rolling and non-slipping, nonholonomic constraints of the automated vehicle system will be explored.

23
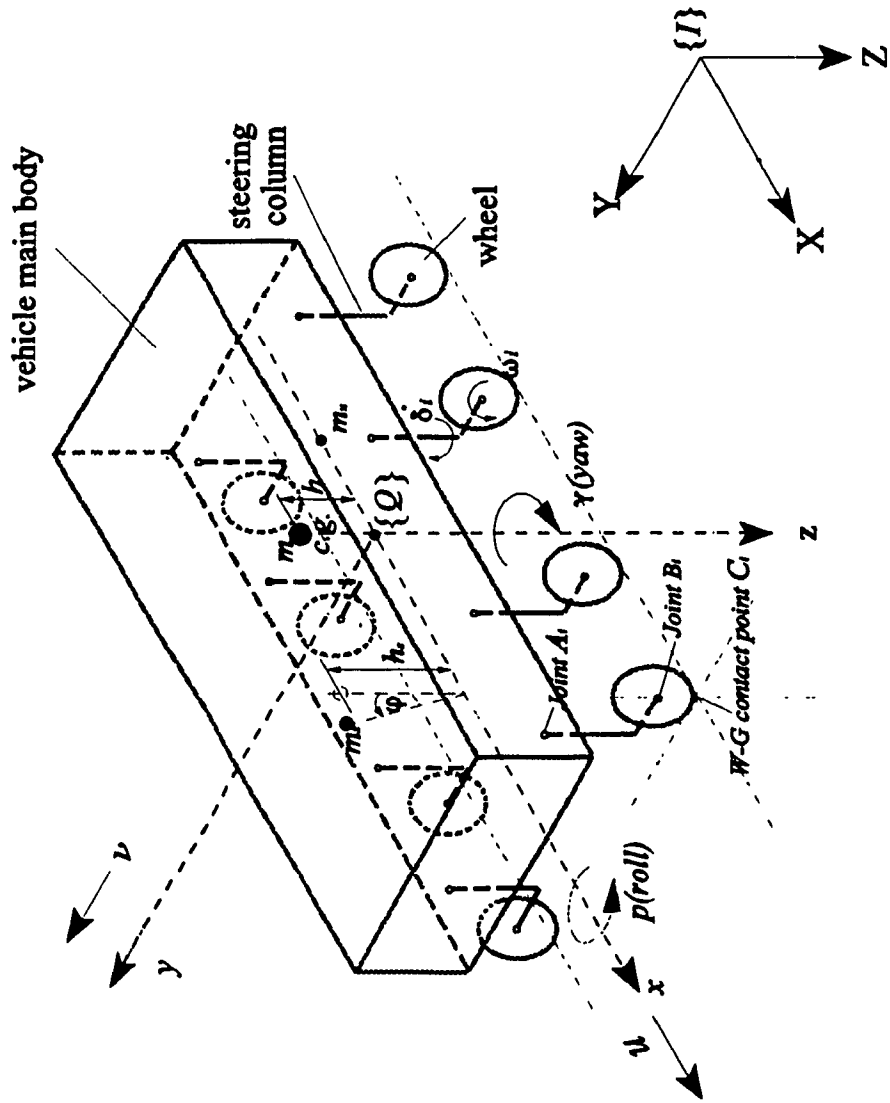
Figure 2.1: Schematic of an Automated Vehicle.

2.2 Definitions, Assumptions and Notational Conventions

2.2.1 Assumptions and Notational Conventions

The mechanics of wheels are discussed in general in Appendix B. The present work considers a simplified wheel model, i.e., a wheel assumed to be non-deformable, with wheel-ground contact region assumed to be a point contact. Employing wheels of this type, the automated vehicles considered in this work are further assumed to consist of a rigid main body [39] supported by n arbitrarily-located non-deformable wheel units (as shown in Fig. 2.1). These wheel units may each be of one of the following four types (as shown in Fig.2.2):

      (i) Motorized driving wheel units (or driven wheel units),

      (ii) Two types of motorized steering wheel units (Type A & B),

      (iii) Two types of motorized driving-steering wheel units (Type A & B),

      (iv) Free rotating casters,

and all types of wheel units can be classified into two categories: rotatable wheel units and fixed wheel units based on the assumption that wheel planes remain vertical. If a wheel can rotate about a vertical axis, it is defined as a rotatable wheel unit such as a steering wheel unit, driving-steering wheel unit or caster, otherwise it is defined as a fixed wheel unit (driving or driven wheel unit).

The four degrees of freedom considered as actuated in an automated vehicle constrained to move on a smooth horizontal plane are defined as follows [44]:

      (i) longitudinal velocity u along the x axis,

      (ii) lateral velocity v along the y axis,

      (iii) roll rate p about the x axis,

(v) yaw rate γ about the z axis.

Linear translation along the z-axis (bounce) and rotation about the y-axis (pitch) are taken as negligible. In addition, the sprung mass m_s, unsprung masses m_u and total mass m are considered explicitly.

For added convenience in the subsequent analysis of automated vehicle systems with arbitrarily wheel configurations, some generalized joints, and specific notational conventions are introduced. These conventions are as follows: (1) the vehicle main body and individual wheel units are taken as independent rigid bodies. (2) the physical interaction or connection between the vehicle main body and each wheel unit is represented by each individual joint. For example, Fig.2.3 shows a exploded view of an automated vehicle with three wheels configuration. A driving-steering wheel unit (wheel unit 1) and two driving wheel units (wheel unit 2 and wheel unit 3), are located at the front and rear of the vehicle respectively. The joint A_1 represents the connection between the vehicle main body and the steering column of wheel unit 1. The joint B_1 is used to represent the connection between the steering column and driving wheel of wheel unit 1. The joints B_2 and B_3 are used to represent the connection between the vehicle main body and driving wheels of wheel unit 2 and wheel unit 3. The lower-case indicia notation i ($i = 1, 2, 3$) is used to identify association with distinct wheel units.

One general requirement of the mechanical design for an automated vehicle system is that all wheel units connected to the rigid body should roll without any side-slip [32][33]. Consequently, the assumptions are made that there is no longitudinal slip and no side slip at the wheel-ground contact points. In addition, the load acting on each wheel can be

precalculated by following the instructions indicated in Appendix C, or simply assuming that each wheel supports an equal load. Details of the load redistribution are discussed in Appendix C.

a) driving wheel   b) steering wheel   c) driving-steering wheel   d) caster
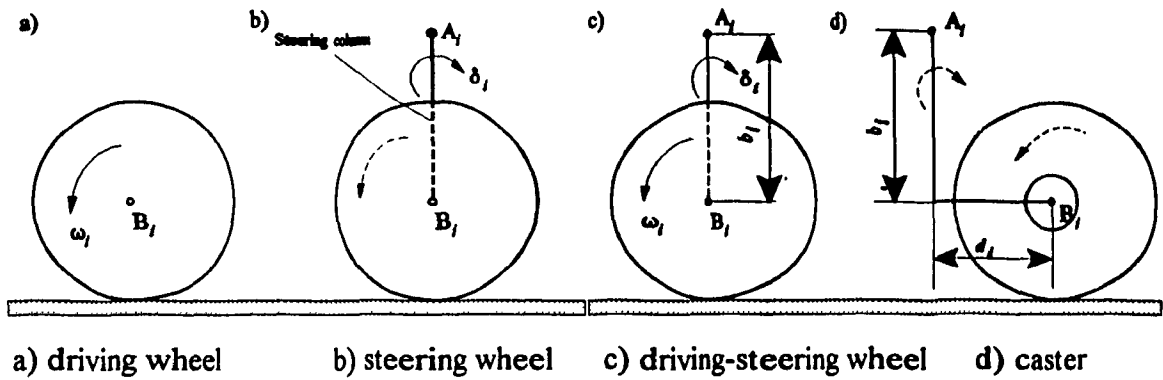
Figure 2.2: Profile Views of the Four Types of Wheel Units.
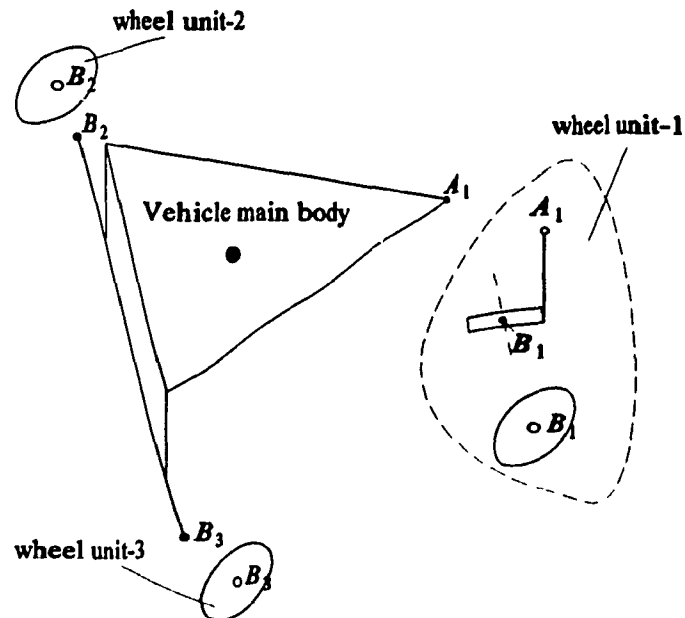
Figure 2.3: Exploded View of an Automated Vehicle with Three Wheels Configuration.

2.2.2 Defining General Joints and Wheel-Ground Point

In this research, the vehicle main body and each wheel unit attached to the vehicle main body are considered independently. However, the dynamic or kinematic relationship between vehicle main body and each wheel unit must be provided. In addition, the position and orientation of a wheel relative to an appropriately-defined reference point must be specified. Accordingly, for convenience in analysis of these relationships, some generalized joints are suggested, such as the joints A_i, B_i and the wheel-ground contact point C_i shown in Figs. 2.1, 2.4 and 2.5. Joints A_i, B_i are used to represent the physical interaction between two rigid bodies in an entire vehicle system. Furthermore, some joints introduce steering variables (δ_i) or powering variables (ω_i) to the vehicle system. A wheel-ground contact point C_i is used to represent the location of the wheel on the ground. A lower-case indicia notation i ($i = 1$, $2, ..., n$) is used to identify distinct wheel units.

Generally, two types of rotatable wheel units (here only indicate the steerable wheel units) are employed on automated vehicle systems. The most common type, henceforth referred to in this thesis as Type A, is shown in Fig.2.4, and consists of a vertical steering column whose offset is perpendicular to the wheel plane. Another type is shown in Fig.2.5, henceforth referred to in this thesis as Type B, and consists of an inclined steering column with offset parallel to the wheel plane. Type B wheel units are often located on the front of three-wheeled vehicle [17]. Both types of rotatable wheel units are located on the vehicle main body through joint A_i, and the steering column and wheel plane are connected by the joint B_i, as shown in Figs. 2.4 and 2.5. Consequently, in order to consider a rotatable wheel unit as a driving-steering wheel unit, it is required to rotate the wheel either about a fixed

28
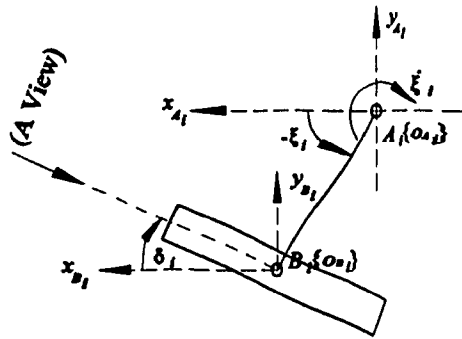
(Plane View)
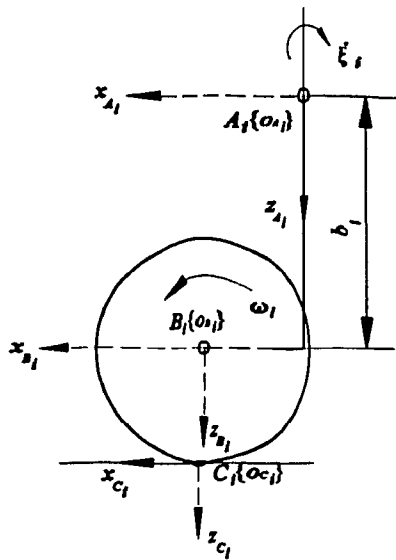
(Profile View)
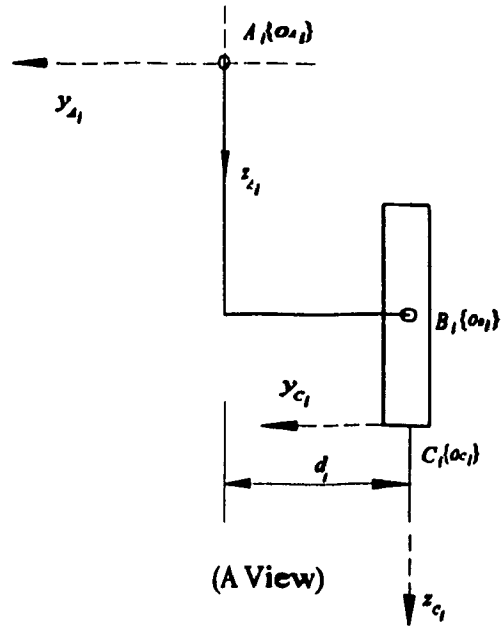
(A View)

Figure 2.4: Subcoordinates Assignment and Wheel Parameter Definition
for Type A wheel unit.

29

a) Profile View   **b) Plan View**
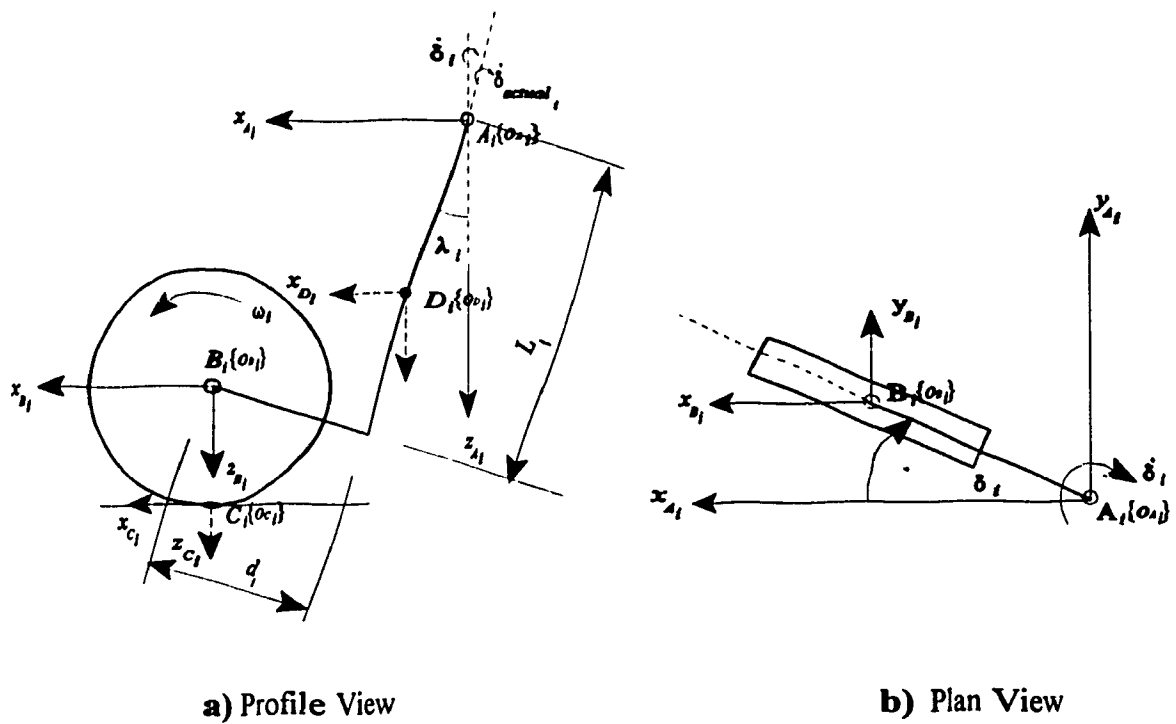
Figure 2.5: Subcoordinates Assignment and Wheel Parameter Definitions
for Type B wheel unit.

vertical axis at the joint A_i, or a horizontal axis at the joint B_i by the powered DC motors.

Thus, joint A_i will introduce a steering variable (δ_i), and joint B_i will introduce a powering

variable (ω_i) into the entire vehicle system.

For a driving wheel unit, the wheel plane is fixed relative to the vehicle main body,

that is, no steering column is involved, hence the joint A_i does not exist. Each driving wheel

unit is connected directly to the vehicle main body by joint B_i, and introduces one powering

variable (ω_i) into the vehicle system. Steering wheel units resemble driving-steering wheel

units in that they rotate about both vertical and horizontal axes through joints A_i and B_i.

Consequently, there are also two joints A_i and B_i involved in this type of wheel unit. However,

30

it is unlike the driving-steering wheel unit in that the powered variable (ω_i) is dependent on other motion parameters of the vehicle system, and the joint B_i thus does not introduce any variables to the vehicle system. Only joint A_i introduces a steering variable (δ_i) into the vehicle system. Casters rotate about a vertical axis at joint A_i and a horizontal axis at joint B_i as shown in Fig. 2.2, but introduce no joint variables into the vehicle system. This is because casters can freely rotate about their vertical and horizontal axes. Caster motion thus completely depends on other motion parameters in the system.

The total number of joints, steering and power variables introduced into the automated vehicle system can therefore be determined from the number and types of wheel units employed. This may be summarized as follows:

(i) driving wheel units each introduce one joint (B_i) and one powering variable (ω_i) into the automated vehicle system,

(ii) steering wheel units each introduce two joints (A_i and B_i) and one steering variable (δ_i) into the automated vehicle system,

(iii) driving-steering wheel units each introduce two joints (A_i and B_i), one steering variable (δ_i) and one powering variable (ω_i) into the automated vehicle system,

(iv) caster units each introduce two joints (A_i and B_i), but neither steering variable (δ_i) nor powering variable (ω_i) into the automated vehicle system.

Consequently, if the total numbers of driving wheel units, steering wheel units, driving-steering wheel units and casters employed by an automated vehicle system are n_d, n_s, n_{ds} and n_c respectively, then the total number of variables introduced to the system can be determined by the following equation:

$$N_{var} = n_d + n_s + 2n_{ds} . \tag{2.1}$$

31

2.2.3 Defining Coordinate Frames

Fig.2.6 shows plan and profile views of the general model for an automated vehicle considered by this thesis. In order to describe the position, orientation and motion of the vehicle, two primary coordinates are used: an inertial frame $I\{O,X,Y,Z\}$, and a reference frame $Q\{o, x, y, z\}$. The inertial reference frame $I\{O, X, Y, Z\}$ is fixed to the ground and used to describe motion parameters of the vehicle in terms of the position of reference point $Q(o, x, y, z)$ and orientation angle θ of the vehicle. The XY-plane of this frame is chosen to be parallel to the ground, with the Z-axis perpendicular to the ground and positive downwards. The X-axis and Y-axis directions are determined by the right hand rule. Reference frame $Q\{o, x, y, z\}$, defined as attached to the vehicle main body, is used as a reference frame for describing the location or motion of any joint (point) connected to the vehicle main body. The x-axis of this frame is defined as coincident with the vehicle rolling axis, and passes through the centre of the unsprung mass. In addition, the x-axis is also parallel to the longitudinal axis of the vehicle [60] (refer to Figs.2.1 and 2.6). The forward direction is defined as positive. The z-axis is defined to pass through the mass centroid of the vehicle parallel to the Z-axis of frame $\{I\}$ with downward positive. The intersection of the z-axis and rolling (x) axis of frame $\{Q\}$ is taken as the origin (o, x, y, z) of frame $\{Q\}$, and the y-axis direction is determined by the right hand rule.

In order to analyse the dynamic or kinematic relationships between the vehicle main body and each wheel unit, as well as the position and orientation of a wheel relative to the reference frame $Q\{o, x, y, z\}$ and inertial frame $I\{O, X, Y, Z\}$, a set of convenient generalized sub-coordinate systems are introduced. These sub-coordinate systems are denoted by

32

$A_i\{o_{A_i}, x_{A_i}, y_{A_i}, z_{A_i}\}, B_i\{o_{B_i}, x_{B_i}, y_{B_i}, z_{B_i}\}, C_i\{o_{C_i}, x_{C_i}, y_{C_i}, z_{C_i}\}$, and $D_i\{o_{D_i}, x_{D_i}, y_{D_i}, z_{D_i}\}$

as shown in Figs. 2.4 and 2.5. They are located at joints A_i, B_i, the wheel-ground contact point C_i, or the centre of mass of the wheel unit D_i respectively. The x_{j_i}, y_{j_i}, z_{j_i} $(j = A, B, C$ and $D)$ axes of all sub-coordinate systems are chosen parallel to the x, y, z axes of the reference frame $Q(o, x, y, z)$.

2.3 Position and Velocity of an Automated Vehicle

For an automated vehicle system, knowledge of the position and velocity of the vehicle are essential to any subsequent dynamic analysis. As shown in Figs. 2.1 and 2.6, the vehicle position with respect to the inertial frame $\{I\}$ in the plane can be completely specified by the following five variables:

- X_Q, Y_Q, Z_Q: coordinates of the reference point Q in the inertial frame $\{I\}$,

- φ: rotation angle of the reference point Q with respect to the inertial frame $\{I\}$,

- θ: orientation of the vehicle with respect to the inertial frame $\{I\}$.

A vector $\mathbf{P}$ is defined to represent these variables as follows:

$$\mathbf{P} = (\ X_Q\ Y_Q\ Z_Q\ \varphi\ \theta\ )^T.\tag{2.2}$$

Recall that the vehicle is assumed to have four DOFs: longitudinal velocity u along the x axis, lateral velocity v along the y axis, roll rate p about the x axis and yaw rate γ about the z axis. Consequently, linear translational velocities of the automated vehicle with respect to frame $\{I\}$ can be represented as:

$$V = \begin{pmatrix} \dot{X}_Q \\ \dot{Y}_Q \\ \dot{Z}_Q \end{pmatrix} = Rotate \ (Z, \ \theta) \ Rotate \ (X, \ \varphi) V_Q$$

$$= \begin{bmatrix} \cos(\theta) & -\sin(\theta) & 0 \\ \sin(\theta) & \cos(\theta) & 0 \\ 0 & 0 & 1 \end{bmatrix} \begin{bmatrix} 1 & 0 & 0 \\ 0 & \cos(\varphi) & -\sin(\varphi) \\ 0 & \sin(\varphi) & \cos(\varphi) \end{bmatrix} \begin{pmatrix} u \\ v \\ w \end{pmatrix}$$

$$= \begin{bmatrix} \cos(\theta) & -\sin(\theta)\cos(\varphi) & \sin(\theta)\sin(\varphi) \\ \sin(\theta) & \cos(\theta)\cos(\varphi) & -\cos(\theta)\sin(\varphi) \\ 0 & \sin(\varphi) & \cos(\varphi) \end{bmatrix} \begin{pmatrix} u \\ v \\ w \end{pmatrix} \qquad (2.3)$$

Linear accelerations of the vehicle with respect to inertial frame $\{I\}$ can be represented as:

$$a = \begin{pmatrix} \ddot{X}_Q \\ \ddot{Y}_Q \\ \ddot{Z}_Q \end{pmatrix} = \begin{bmatrix} -\sin(\theta) & -\cos(\theta)\cos(\varphi) & \cos(\theta)\sin(\varphi) \\ \cos(\theta) & -\sin(\theta)\cos(\varphi) & \sin(\theta)\sin(\varphi) \\ 0 & 0 & 0 \end{bmatrix} \begin{pmatrix} u \\ v \\ w \end{pmatrix} \dot{\theta}$$

$$+ \begin{bmatrix} 0 & \sin(\theta)\sin(\varphi) & \sin(\theta)\cos(\varphi) \\ 0 & -\cos(\theta)\sin(\varphi) & -\cos(\theta)\cos(\varphi) \\ 0 & \cos(\varphi) & -\sin(\varphi) \end{bmatrix} \begin{pmatrix} u \\ v \\ w \end{pmatrix} \dot{\varphi} \qquad (2.4)$$

$$+ \begin{bmatrix} \cos(\theta) & -\sin(\theta)\cos(\varphi) & \sin(\theta)\sin(\varphi) \\ \sin(\theta) & \cos(\theta)\cos(\varphi) & -\cos(\theta)\sin(\varphi) \\ 0 & \sin(\varphi) & \cos(\varphi) \end{bmatrix} \begin{pmatrix} a_x \\ a_y \\ a_z \end{pmatrix}$$

where the bounce mode of the system is considered negligible, and the distance from the ground to the origin of the reference frame $\{Q\}$ is constant. Thus, there is no linear translation along the z axis, i.e., Z_Q = constant, $w = 0$ and $a_z = 0$. In other words, for a four

DOFs vehicle system, the variables involved in the Z direction, such as Z_Q, w and a_r, or z_{a_i}, z_{b_i} and z_{c_i}, do not need to be considered in Eqns. (2.2), (2.3), (2.4) or later equations. The purpose of retaining Z direction variables is to provide a structure of system equations which is easily extended from four DOFs to a six DOFs.
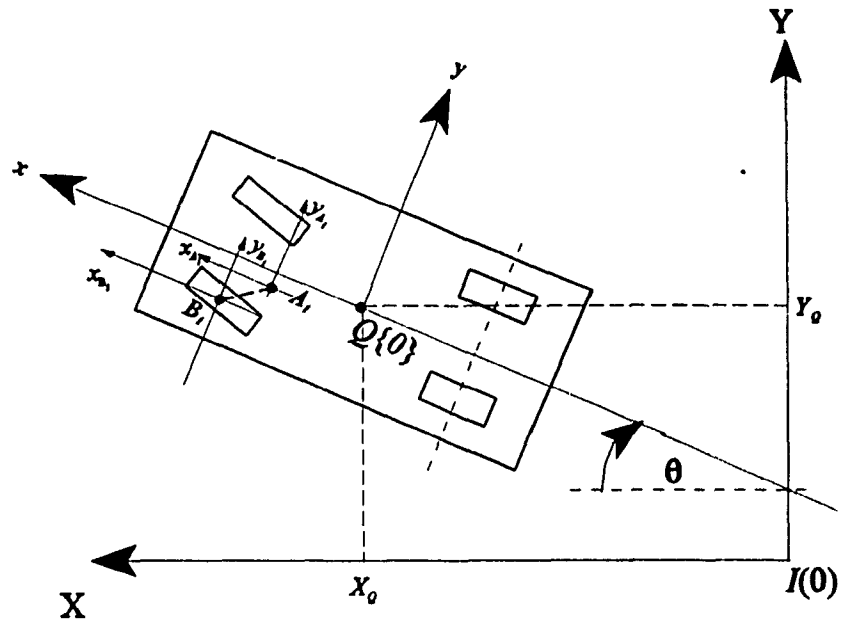
a) Plan View
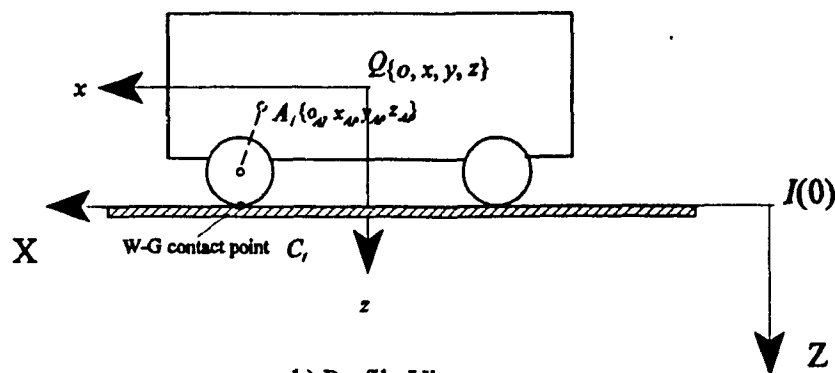
b) Profile View

Figure 2.6: Coordin..tes Assignment and Position of a Vehicle in the Plane Motion.

Furthermore, if roll motion is not involved, the vehicle only contains three DOFs. In this case, the reference frame $\{Q\}$ can be simply located on the mass centre, and positions and velocities can be determined from Eqns. (2.2), (2.3), (2.4) by taking roll angle φ and rolling rate $\dot{\varphi}$ as zero.

2.4 Characterization of a Wheel

Definitions for generalized joints, coordinate systems and notional conventions have been discussed in detail in Section 2.2. In this section, the characterization of a wheel will be detailed which makes use of these conventions (see Figs. 2.7 and 2.8).
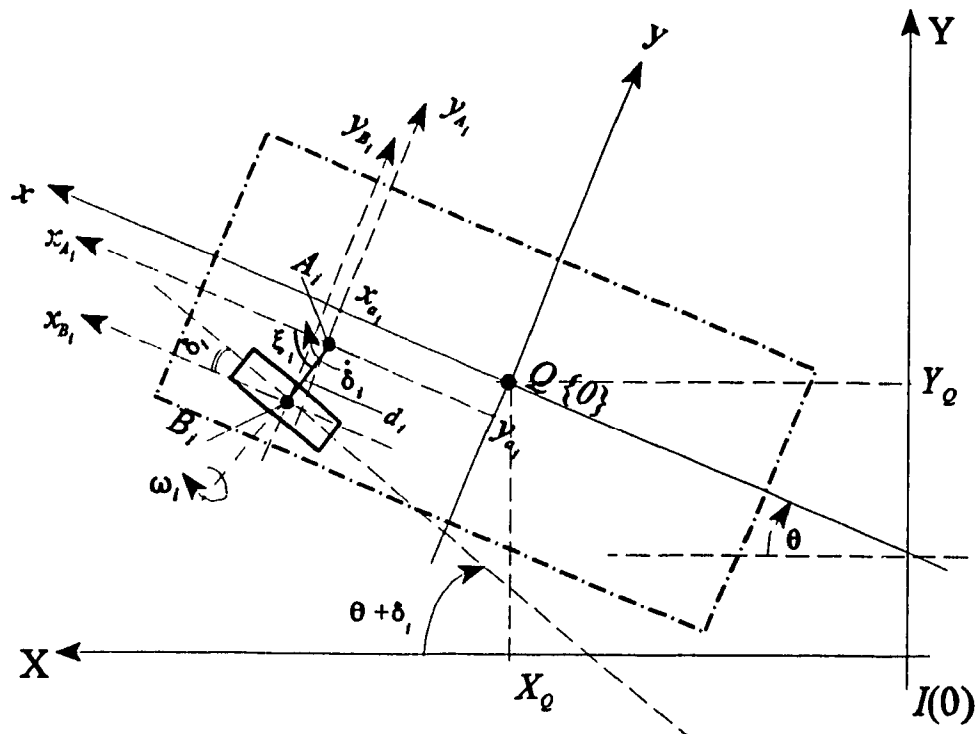
Figure 2.7: Characterization of a Type A Wheel in an Automated Vehicle System.
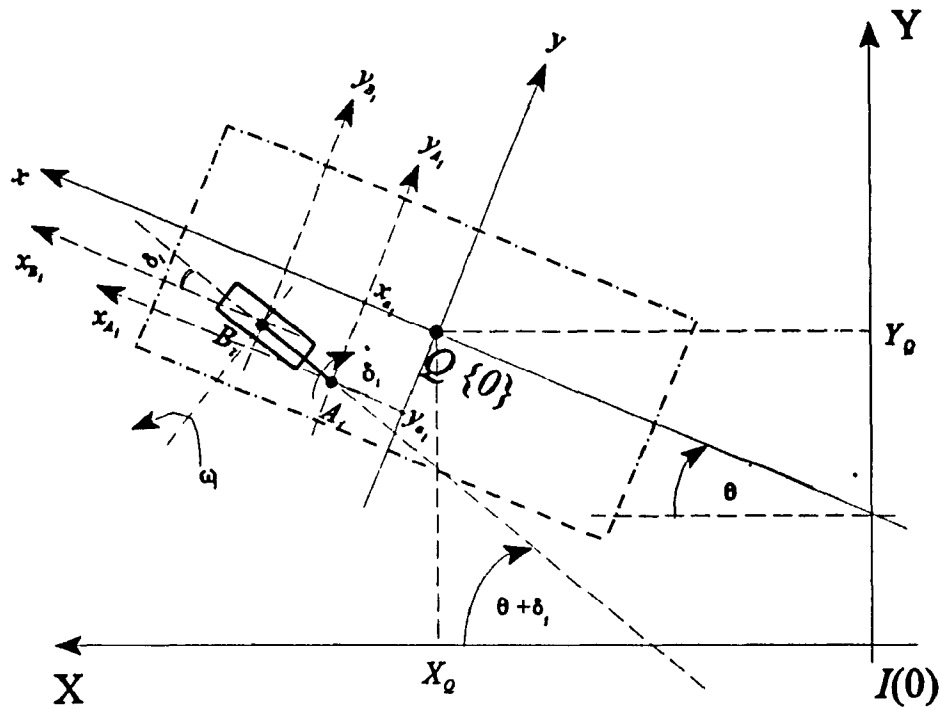
Figure 2.8: Characterization of a Type B Wheel in an Automated Vehicle System.

2.4.1 Description of Joint A_i and Direction Angle β_{A_i}

As discussed previously, a joint A_i is generally used to represent the physical interaction or connection between the vehicle main body and a wheel unit which may be a steering wheel unit, driving-steering wheel unit, or caster. The motion of point A_i on the vehicle main body is identical to the motion of joint A_i on the wheel unit. Therefore, we use A_i to represent any point in the rigid body when discussing the motion of the rigid body and also use it to represent a wheel unit connected to the corresponding point when discussing steering angle. As shown in Fig.2.7, the position of the joint A_i with respect to frame $\{Q\}$ is specified by three constants x_{a_i}, y_{a_i} and z_{a_i} (whose signs depend on the location of joint A_i). Thus, referring to

37

Appendix A, Eqns. (A.1), (A.2), (A.3), (A.4), the linear velocities of the joint A_i with respect to the reference frame $\{Q\}$ can be represented as follows:

$$
\mathbf{v}_{A_i} = \begin{pmatrix} v_{x_{A_i}} \\ v_{y_{A_i}} \\ v_{z_{A_i}} \end{pmatrix} = \begin{pmatrix} u \\ v \\ 0 \end{pmatrix} + \begin{bmatrix} 0 & -\gamma & 0 \\ \gamma & 0 & -p \\ 0 & p & 0 \end{bmatrix} \begin{pmatrix} x_{e_i} \\ y_{e_i} \\ z_{e_i} \end{pmatrix} ,
\tag{2.5}
$$

and the linear accelerations of joint A_i with respect to frame $\{Q\}$ can be represented as:

$$
\mathbf{a}_{A_i} = \begin{pmatrix} \dot{d}_{x_{A_i}} \\ \dot{d}_{y_{A_i}} \\ \dot{v}_{z_{A_i}} \end{pmatrix} = \begin{pmatrix} a_x \\ a_y \\ a_z \end{pmatrix} + \begin{bmatrix} 0 & -\dot{\gamma} & 0 \\ \dot{\gamma} & 0 & -\dot{p} \\ 0 & \dot{p} & 0 \end{bmatrix} \begin{pmatrix} x_{e_i} \\ y_{e_i} \\ z_{e_i} \end{pmatrix}
$$
$$
+ \begin{bmatrix} 0 & -\gamma & 0 \\ \gamma & 0 & -p \\ 0 & p & 0 \end{bmatrix} \left(\begin{pmatrix} u \\ v \\ w \end{pmatrix} + \begin{bmatrix} 0 & -\gamma & 0 \\ \gamma & 0 & -p \\ 0 & p & 0 \end{bmatrix} \begin{pmatrix} x_{e_i} \\ y_{e_i} \\ z_{e_i} \end{pmatrix} \right) .
\tag{2.6}
$$

In addition, the x-axis of the frame as defined in Section 2.2.3 is coincident with the vehicle rolling axis, and roll motion of the vehicle is exclusively caused by the suspension system [60]. Vehicle rolling motion therefore cannot be transmitted to the wheel unit through the vehicle main body connection joint. In Eqns. (2.5) and (2.6), the roll rate p and rolling acceleration $\dot{p}$ are assumed negligible. The magnitude of the projection of the velocity vector $\mathbf{v}_{A_i}$ in the $x_{A_i} y_{A_i}$ plane with respect to frame $\{Q\}$ is:

$$
v_{(xy)_{A_i}} = \sqrt{v_{x_{A_i}}{}^2 + v_{y_{A_i}}{}^2} = \sqrt{(u - \gamma y_{e_i})^2 + (v + \gamma x_{e_i})^2} ,
\tag{2.7}
$$

and the direction of $\mathbf{v}_{A_i}$ in the $x_{A_i}y_{A_i}$ plane of frame $\{Q\}$ can be represented by the angle β_{A_i}:

$$\beta_{A_i} = \tan^{-1}\frac{v_{y_{A_i}}}{v_{x_{A_i}}} = \tan^{-1}\frac{v + \gamma x_{a_i}}{u - \gamma y_{a_i}} .$$

(2.8)

Eqn. 2.8 defines the direction angle of joint A_i, which is the angle between velocity vector $\mathbf{v}_{(xy)A_i}$ and the x_{A_i}-axis. The sign of direction angle β_{A_i} depends on the sign of the ratio $(v_{y_{A_i}}/v_{x_{A_i}})$. If $(v_{y_{A_i}}/v_{x_{A_i}}) > 0$, then β_{A_i} is a positive (clockwise) angle (see Fig. B.12 in Appendix B), otherwise it is negative.

Eqns. (2.5) and (2.6) give the mathematical description of any joint $A_i(x_{a_i}, y_{a_i}, z_{a_i})$ on the vehicle main body in terms of the velocities and accelerations of the reference frame $Q\{o, x, y, z\}$. The position of joint A_i with respect to the reference frame $\{Q\}$ can be expressed in the inertial frame $\{I\}$ by the following transformation:

$$\mathbf{P}_{A_i} = \begin{bmatrix} X_{A_i} \\ Y_{A_i} \\ Z_{A_i} \end{bmatrix} = \begin{bmatrix} x_{a_i}\cos(\theta) - y_{a_i}\sin(\theta) + X_Q \\ x_{a_i}\sin(\theta) + y_{a_i}\cos(\theta) + Y_Q \\ Z_Q - z_{a_i} \end{bmatrix},$$

(2.9)

and the linear velocities of joint A_i with respect to the inertial frame $\{I\}$ can be obtained by differentiating Eqn. (2.9) with respect to time as follows:

$$\mathbf{V}_{A_i} = \begin{bmatrix} \dot{X}_{A_i} \\ \dot{Y}_{A_i} \\ \dot{Z}_{A_i} \end{bmatrix} = \begin{bmatrix} (-x_{a_i}\sin(\theta) - y_{a_i}\cos(\theta))\dot{\theta} + \dot{X}_Q \\ (x_{a_i}\cos(\theta) - y_{a_i}\sin(\theta))\dot{\theta} + \dot{Y}_Q \\ 0 \end{bmatrix}.$$

(2.10)

Differentiating Eqn. (2.10) with respect to time yields:

$$
\mathbf{A}_{A_I} = \begin{bmatrix} \ddot{X}_{A_I} \\ \ddot{Y}_{A_I} \\ \ddot{Z}_{A_I} \end{bmatrix} = \begin{bmatrix} (-x_c \cos(\theta) + y_{a_I} \sin(\theta))\dot{\theta}^2 + (-x_{a_I}\sin(\theta) - y_{a_I}\cos(\theta))\ddot{\theta} + \ddot{X}_Q \\ (-x_{a_I}\sin(\theta) - y_{a_I}\cos(\theta))\dot{\theta}^2 + (x_{a_I}\cos(\theta) - y_{a_I}\sin(\theta))\ddot{\theta} + \ddot{Y}_Q \\ \ddot{Z}_Q \end{bmatrix} \quad (2.11)
$$

Eqn. (2.11) represents the accelerations of joint A_I with respect to the inertial frame $\{I\}$. Eqns. (2.9), (2.10), (2.11) demonstrate that the complete mathematical description of any point (joint) A_I $(x_{a_I}, y_{a_I}, z_{a_I})$ on the vehicle main body can be obtained from the position, orientation, and their derivatives of the reference point (or frame) $\{Q\}$ with respect to the inertial frame $\{I\}$ (where Z_Q = constant, so that $\dot{Z}_{A_I} = 0$, $\ddot{Z}_{A_I} = 0$).

2.4.2 Description of Joint B_I and Direction Angle β_{B_I}

Figs. (2.4) and (2.5) illustrate the configuration of Types A and B rotatable wheel units. In both cases, the centre of the wheel is connected to the vehicle main body by a steering column $A_I B_I$, which can rotate about a fixed vertical axis (z_{A_I}) at joint A_I. The centre of each wheel is indicated as joint B_I, which represents the physical interaction or connection between a wheel plane and a steering column. In this section, these two types of rebatable wheel units are studied in detail.

2.4.2.1 Type A Rotatable Wheel Unit

Figs. 2.4 and 2.7 illustrate a Type A rotatable wheel unit and the relationship between a Type

40

A wheel unit and the vehicle main body, respectively. The position of joint B, with respect to

joint A, can be specified by one constant and one variable: an offset d_i and an angle $\xi_i(t)$. The

offset d_i is the horizontal distance between joints A_i and B_i as shown in Fig. 2.4. The angle

$\xi_i(t)$ is the angle between the x_{A_i} axis and the steering column A_iB_i, with positive clockwise

as shown in Fig. 2.7. The orientation of the wheel plane with respect to the x_{B_i} axis of the sub-

coordinate frame $B_i\{ o_{B_i}, x_{B_i}, y_{B_i}, z_{B_i} \}$ is defined as the steering angle $\delta_i(t)$, with positive

clockwise as shown in Fig.2.7. Assuming the steering column A_iB_i is perpendicular to the

wheel plane, the angle $\xi_i(t)$ is equal to sign $(y_{a_i}) \dfrac{\pi}{2} + \delta_i(t)$ and sign $(y_{a_i}) = \dfrac{y_{a_i}}{|y_{a_i}|}$.

Based on the above descriptions, and the discussions in Appendix A and Section

2.4.1, it is apparent that when the geometric relationship between any point and a reference

point on the rigid body is known, the mathematical description of this point can be completely

characterized in terms of the reference point. Thus, the instantaneous position of joint B_i with

respect to the frame $\{Q\}$ can be written as:

$$
\mathbf{P}_{b_i} = \begin{bmatrix} x_{b_i} \\ y_{b_i} \\ z_{b_i} \end{bmatrix} = \begin{bmatrix} d_i \cos(\xi_i) + x_{a_i} \\ d_i \sin(\xi_i) + y_{a_i} \\ z_{a_i} + b_i \end{bmatrix} ,
\tag{2.12}
$$

with $\xi_i = \text{sign}(y_{a_i})\dfrac{\pi}{2} + \delta_i(t)$, and the instantaneous position of joint B_i with respect to frame

$\{I\}$ can be determined by using $\{ x_{b_i}, y_{b_i}, z_{b_i} \}$ to replace $\{ x_{a_i}, y_{a_i}, z_{a_i} \}$ in Eqn. (2.9), which

then becomes:

$$
\mathbf{P}_{B_i} = \begin{bmatrix} X_{B_i} \\ Y_{B_i} \\ Z_{B_i} \end{bmatrix} = \begin{bmatrix} (d_i \cos(\xi_i) + x_{a_i})\cos(\theta) - (d_i \sin(\xi_i) + y_{a_i})\sin(\theta) + X_Q \\ (d_i \cos(\xi_i) + x_{a_i})\sin(\theta) + (d_i \sin(\xi_i) - y_{a_i})\cos(\theta) + Y_Q \\ Z_Q - (z_{a_i} + b_i) \end{bmatrix} .
\tag{2.13}
$$

The linear velocities and accelerations of joint B_i with respect to frame $\{Q\}$ can be calculated by replacing $(x_{b_i}, y_{b_i}, z_{b_i})$ with $(x_{a_i}, y_{a_i}, z_{a_i})$ in Eqns. (2.5) and (2.6). In addition, the velocity magnitude $(v_{(xy)_{B_i}})$ of joint B_i in the $x_{B_i}y_{B_i}$ plane with respect to the frame $\{Q\}$, and the direction angle (β_i) of joint B_i can be determined from Eqns. (2.7) and (2.8) by replacing (x_{b_i}, y_{b_i}) with (x_{a_i}, y_{a_i}). The velocity magnitude $(v_{(xy)_{B_i}})$ is as follows:

$$
\begin{aligned}
v_{(xy)_{B_i}} &= \sqrt{v_{x_{B_i}}^2 + v_{y_{B_i}}^2} \\
&= \sqrt{(u - \gamma(d_i \sin(\xi_i) + y_{a_i}))^2 + (v + \gamma(d_i \cos(\xi_i) + x_{a_i}))^2} \;,
\end{aligned}
\tag{2.14}
$$

and the direction angle of the joint B_i is:

$$
\beta_{B_i} = \tan^{-1} \frac{v_{y_{B_i}}}{v_{x_{B_i}}} = \tan^{-1} \frac{(v + \gamma(d_i \cos(\xi_i) + x_{a_i}))}{(u - \gamma(d_i \sin(\xi_i) + y_{a_i}))} .
\tag{2.15}
$$

Similarly, β_{B_i} is defined as the direction angle of joint B_i, which is the angle between velocity vector $v_{(xy)_{B_i}}$ and the x_{B_i}-axis. The sign of β_{B_i} depends on the sign of the ratio $(v_{y_{B_i}}/v_{x_{B_i}})$. If $(v_{y_{B_i}}/v_{x_{B_i}}) > 0$, β_{B_i} is positive (clockwise - see Fig. B.12, Appendix B), otherwise it is negative.

In the same manner as joint A_i, the instantaneous linear velocities of joint B_i with respect to the inertial frame $\{I\}$ can be obtained by differentiating Eqn. (2.13) with respect to time as follows:

$$
\mathbf{V}_{B_i} = \begin{bmatrix} \dot{X}_{B_i} \\ \dot{Y}_{B_i} \\ \dot{Z}_{B_i} \end{bmatrix} = \begin{bmatrix} -(d_i \cos(\xi_i) + x_{a_i})\sin(\theta) - (d_i \sin(\xi_i) + y_{a_i})\cos(\theta) \\ (d_i \cos(\xi_i) + x_{a_i})\cos(\theta) - (d_i \sin(\xi_i) + y_{a_i})\sin(\theta) \\ 0 \end{bmatrix} \dot{\theta} \qquad (2.16)
$$

$$
+ \begin{bmatrix} -\sin(\xi_i)\cos(\theta) - \cos(\xi_i)\sin(\theta) \\ -\sin(\xi_i)\sin(\theta) + \cos(\xi_i)\cos(\theta) \\ 0 \end{bmatrix} d_i \dot{\xi}_i + \begin{bmatrix} \dot{X}_Q \\ \dot{Y}_Q \\ \dot{Z}_Q \end{bmatrix},
$$

where $\dot{\xi}_i(t) = \dot{\delta}_i(t)$. The linear accelerations of point B_i with respect to inertial frame $\{I\}$ can be obtained by differentiating Eqn. (2.16) with respect to time. From the above discussion, we can conclude that Eqns. (2.13) and (2.16) give the complete mathematical description of positions and velocities of joint B_i for the Type A wheel unit. In addition, Eqns. (2.12) through (2.16) are also suitable for three DOFs vehicle systems, where the suspension is neglected.

Furthermore, if the column A_iB_i is fixed, the angle $\xi_i(t)$ becomes constant ($\xi_i = \text{sign}(y_{a_i}) \dfrac{\pi}{2}$), and the steering angle $\delta_i(t)$ becomes equal to zero. In this case, the wheel unit is regarded as unrotatable, and can be considered a motorized driving wheel unit or driven wheel unit. As a result, we can say that for an unrotatable wheel unit, joint B_i is coincident with joints A_i. Joint B_i is then used to represent the physical interaction or connection between a wheel plane and the vehicle main body. The complete mathematical description of the position, velocity and acceleration of joint B_i with respect to the reference frames $\{Q\}$ and the inertial frame $\{I\}$ can be determined in the same way as for joint A_i, which is described in Section 2.4.1.

43

2.4.2.2 Type B Rotatable Wheel Unit

As shown in Figs. 2.5 and 2.7, the geometric relationship between joints B_i and A_i can be described by three constants (steering column length L_i, offset d_i, and angle λ_i), and a steering variable $\delta_i(t)$. The mathematical description of the joint B_i can be completely characterized by the reference point A_i. Thus, the instantaneous position of joint B_i with respect to frame $\{Q\}$ can be written as:

$$
\mathbf{P}_{b_i} = \begin{bmatrix} x_{b_i} \\ y_{b_i} \\ z_{b_i} \end{bmatrix} = \begin{bmatrix} \Delta_i \cos(\delta_i) + x_{a_i} \\ \Delta_i \sin(\delta_i) + y_{a_i} \\ z_{a_i} + b_i \end{bmatrix}, \tag{2.17}
$$

and the instantaneous position of joint B_i with respect to the reference frame $\{Q\}$ can be transformed to the inertial frame $\{I\}$ as follows:

$$
\mathbf{P}_{B_i} = \begin{bmatrix} X_{B_i} \\ Y_{B_i} \\ Z_{B_i} \end{bmatrix} = \begin{bmatrix} (\Delta_i \cos(\delta_i) + x_{a_i})\cos(\theta) - (\Delta_i \sin(\delta_i) + y_{a_i}))\sin(\theta) + X_Q \\ (\Delta_i \cos(\delta_i) + x_{a_i})\sin(\theta) + (\Delta_i \sin(\delta_i) + y_{a_i})\cos(\theta) + Y_Q \\ Z_Q - (z_{a_i} + b_i) \end{bmatrix}, \tag{2.18}
$$

where $\Delta_i = d_i \cos(\lambda_i) + L_i \sin(\lambda_i) = constant$, $b_i = L_i \cos(\lambda_i) - d_i \sin(\lambda_i) = constant$, and the effective steering angle $\delta_i = \tan^{-1}[\cos(\lambda_i) \tan \delta_{actual_i}]$[22]. The linear velocities and accelerations of joint B_i with respect to frame $\{Q\}$ can be calculated by replacing $(x_{b_i}, y_{b_i}, z_{b_i})$ with $(x_{a_i}, y_{a_i}, z_{a_i})$ in Eqns.(2.5) and (2.6). The velocity magnitude $(v_{(xy)_{B_i}})$ of joint B_i in the $x_{B_i} y_{B_i}$ plane with respect to frame $\{Q\}$, and the direction angle (β_i) of joint B_i can be determined from Eqns. (2.7) and (2.8) by replacing (x_{b_i}, y_{b_i}) with (x_{a_i}, y_{a_i}). The

44

velocity magnitude $(v_{(xy)_{B_i}})$ is as follows:

$$v_{(xy)_{B_i}} = \sqrt{v_{x_{B_i}}{}^2 + v_{y_{B_i}}{}^2}$$

$$= \sqrt{(u - \gamma y_{b_i})^2 + (v + \gamma x_{b_i})^2} \qquad (2.19)$$

$$= \sqrt{(u - \gamma(\Delta_i \sin(\delta_i) + y_{a_i}))^2 + (v + \gamma(\Delta_i \cos(\delta_i) + x_{a_i}))^2} ,$$

and the direction angle of joint B_i is:

$$\beta_{B_i} = \tan^{-1} \frac{v_{y_{B_i}}}{v_{x_{B_i}}} = \tan^{-1} \frac{v + \gamma(\Delta_i \cos(\delta_i) + x_{a_i})}{u - \gamma(\Delta_i \sin(\delta_i) + y_{a_i})} . \qquad (2.20)$$

If required, the instantaneous velocity and acceleration of the mass centre $D_i\{x_{d_i}, y_{d_i}, z_{d_i}\}$ of the wheel unit with respect to frame $\{Q\}$ can be also obtained using $\{x_{d_i}, y_{d_i}, z_{d_i}\}$ to replace $\{x_{a_i}, y_{a_i}, z_{a_i}\}$ in Eqns. (2.5) and (2.6). The instantaneous linear velocity of joint B_i with respect to the inertial frame $\{I\}$ can be obtained by differentiating Eqn. (2.18) with respect to time.

$$\mathbf{V}_{B_i} = \begin{bmatrix} V_{x_{B_i}} \\ V_{y_{B_i}} \\ V_{z_{B_i}} \end{bmatrix} = \begin{bmatrix} -(\Delta_i \cos(\delta_i) + x_{a_i})\sin(\theta) - (\Delta_i \sin(\delta_i) + y_{a_i})\cos(\theta) \\ (\Delta_i \cos(\delta_i) + x_{a_i})\cos(\theta) - (\Delta_i \sin(\delta_i) + y_{a_i})\sin(\theta) \\ 0 \end{bmatrix} \dot{\gamma}$$

$$\qquad (2.21)$$

$$+ \begin{bmatrix} -\sin(\delta_i)\cos(\theta) - \cos(\delta_i)\sin(\theta) \\ -\sin(\delta_i)\sin(\theta) + \cos(\delta_i)\cos(\theta) \\ 0 \end{bmatrix} \Delta_i \dot{\delta}_i + \begin{bmatrix} \dot{X}_Q \\ \dot{Y}_Q \\ \dot{Z}_Q \end{bmatrix} .$$

45

In addition, the linear acceleration of point B_i with respect to inertial frame $\{I\}$ can be obtained by differentiating Eqn. (2.21) with respect to time. To summarize, it may be seen that Eqns. (2.17) through (2.21) give the complete mathematical description of position and velocity for joint B_i of a Type B wheel unit with respect to the inertial frame $\{I\}$.

2.5 Kinematic Nonholonomic Constraints at Wheel-Ground Contact Point C_i

Automated vehicles are examples of multi-input nonholonomic systems [61]. As pointed out in Section 2.2.2, if the system employs n_d driving wheel units, n_s steering wheel units, n_{ds} driving-steering wheel units and n_c casters, then $(n_d + n_s + 2 \times n_{ds})$ input variables will be introduced to the automated vehicle system. However, those variables may be subject to geometric, kinematic or other constraints within the automated vehicle system. The kinematic constraints of each wheel are discussed in this section, based on the mathematical descriptions of wheel units provided in Sections 2.4.1 and 2.4.2. A general requirement in the mechanical design of automated vehicle systems is that all wheels connected to the rigid body should roll without side-slip [30][32][[33][34]. In this research, we assume that all input variables satisfy this condition.

All input variables may thus be determined using the geometric relationship of a wheel unit with respect to the frames $\{Q\}$ and $\{I\}$, and the assumption that all wheels connected to the rigid body roll without side-slip. Stated otherwise, the wheel-ground contact points should satisfy the conditions of pure rolling and non slipping [30][31][32][33][38]. These conditions are henceforth referred to as kinematic constraints 1 and 2, respectively.

Kinematic constraint 1 (pure rolli. g): The component of the velocity at the wheel-

46

ground contact point in the plane of the wheel should be zero, i.e.,

$$v_{c_{i_{plane}}} = v_{B_{i_{plane}}} - R_i \, \omega_i = 0 \tag{2.22}$$

where $v_{B_{i_{plane}}} = V_{X_{B_i}} \cos(\theta + \delta_i) + V_{Y_{B_i}} \sin(\theta + \delta_i)$, which is the velocity of the centre of wheel i in the direction of the wheel plane.

In accordance with the definitions in Sections 2.4.1 and 2.4.2, the method of determination for velocities $V_{X_{B_i}}$, $V_{Y_{B_i}}$ depends on the type of wheel unit employed. For a driving wheel unit, these velocities should be calculated by Eqn. (2.10). For a Type A steering wheel unit, these velocities should be calculated by Eqn. (2.16). For a Type B steering wheel unit, these velocities should be calculated by Eqn. (2.21). Substituting Eqns. (2.10), (2.16) and (2.21) into kinematic constraint 1 yields the angular velocities for each type of motorized wheel unit as follows:

(i) For a driving wheel unit or a Type A steering wheel unit,

$$\omega_i = \frac{\dot{X}_Q \cos(\theta + \delta_i) + \dot{Y}_Q \sin(\theta + \delta_i) + (x_{a_i} \sin(\delta_i) - y_{a_i} \cos(\delta_i))\gamma}{R_i} \tag{2.23 (a)}$$

(ii) For a Type B steering wheel unit,

$$\omega_i = \frac{\dot{X}_Q \cos(\theta + \delta_i) + \dot{Y}_Q \sin(\theta + \delta_i) + (x_{a_i} \sin(\delta_i) - y_{a_i} \cos(\delta_i) - \text{sign}(y_a)d_i)\gamma}{R_i} \tag{2.23(b)}$$

where R_i = the radius of wheel i, and the angular acceleration of a motorized wheel unit (for both cases listed above) can be determined by differentiating Eqns. (2.23 (a)) and (2.23 (b)) with respect to time as follows:

47

$$\dot{\omega}_i = \frac{Num1 + Num2 + Num3}{R_i},\qquad\qquad (2.24)$$

where

$$Num1 = \ddot{X}_Q \cos(\theta + \delta_i) - \dot{X}_Q \sin(\theta + \delta_i)(\dot{\gamma} + \dot{\delta}_i),$$

$$Num2 = \ddot{Y}_Q \sin(\theta + \delta_i) + \dot{Y}_Q \cos(\theta + \delta_i)(\dot{\gamma} + \dot{\delta}_i),$$

and

$$Num3 = \begin{cases} (x_{a_i}\cos(\delta_i)+y_{a_i}\sin(\delta_i))\dot{\delta}_i\dot{\gamma} +(x_{a_i}\sin(\delta_i)-y_{a_i}\cos(\delta_i))\ddot{\gamma} & \text{for 2.23 (a),} \\[2ex] (x_{a_i}\cos(\delta_i)+y_{a_i}\sin(\delta_i))\dot{\delta}_i\dot{\gamma} +(x_{a_i}\sin(\delta_i)-y_{a_i}\cos(\delta_i)-\text{sign}\,(y_{a_i})d_i)\ddot{\gamma} & \text{for 2.23 (b).} \end{cases}$$

Kinematic constraint 2 (non-slipping): The velocity component of the wheel-ground contact point C_i orthogonal to the wheel plane is zero, i.e.,

$$v_{C_{i\,vertical}} = -V_{X_{B_i}} \sin(\theta + \delta_i) + V_{Y_{B_i}} \cos(\theta + \delta_i) = 0,\qquad\qquad (2.25)$$

Rearranging Eqn. (2.25) yields the steering angle of driving-steering wheel units and steering wheel units as follows:

$$\delta_i = \tan^{-1}\left(\frac{V_{Y_{B_i}}}{V_{X_{B_i}}}\right) - \theta,\qquad\qquad (2.26)$$

Substituting $V_{X_{B_i}}$, $V_{Y_{B_i}}$ from Eqns. (2.10), (2.16) and (2.21) into Eqn. (2.25) and rearranging gives the following results:

48

(i) For a steering wheel unit with no offset, or a Type A steering wheel unit, the steering angle can be determined by:

$$\delta_i = \tan^{-1}\frac{-\dot{X}_Q \sin(\theta) + \dot{Y}_Q \cos(\theta) + x_{a_i}\gamma}{\dot{X}_Q \cos(\theta) + \dot{Y}_Q \sin(\theta) - y_{a_i}\gamma}, \qquad (2.27(a))$$

and the steering rate of above steering wheel unit can be obtained by differentiating Eqn.(2.27(a)) with respect to the time.

(ii) For a Type B steering wheel unit, the steering rate can be determined by following equation:

$$\dot{\delta}_i = \frac{-\dot{X}_Q \sin(\theta+\delta_i) + \dot{Y}_Q \cos(\theta+\delta_i) + (x_{a_i}\cos(\delta_i) + y_{a_i}\sin(\delta_i))\gamma}{\Delta_i} + \gamma, \quad (2.27(b))$$

In the above equation, the steering angle as a function of time can be calculated by applying the initial conditions $\delta(0)_i$, $\dot{X}_Q(0)$, $\dot{Y}_Q(0)$ and $\gamma(0)$, with $\Delta_i = d_i\cos(\lambda_i) + L_i\sin(\lambda_i)$. From the above equations, it is evident that if desired linear and angular velocities, as well as the trajectory of the vehicle with respect to the inertial frame { I } are given, then angular velocity ω_i and angular acceleration $\dot{\omega}_i$, as well as the steering angles δ_i or steering rate $\dot{\delta}_i$ of a motorized driving-steering wheel can be determined by the kinematic constraints 1 and 2.

2.6 Summary

In this chapter, general assumptions, definitions and conventional notations are introduced and discussed in detail. Expressions for the positions and velocities of three and four DOFs

49

automated vehicles have been derived based on these usages. Two kinematic (Nonholonomic) constraints are detailed, both of which must be satisfied by all wheel units utilized on the types of vehicles considered in this thesis. These constraints are the pure rolling and non-slipping conditions at wheel-ground contact points.

In addition, the vehicle main body and each wheel unit are considered as individual rigid bodies [38][39]. Joints A_i and B_i are introduced for assembly of these components. The lower-case i $\{i = 1, 2, 3, ... , n\}$ is utilized to indicate different wheel units and their parameters. There are five coordinate frames defined to describe the position and velocity of an automated vehicle system. Detailed derivations are given for velocity magnitudes of joints A_i and B_i with respect to the reference frame $\{Q\}$. The direction angles β_{A_i} and β_{B_i} are also defined in order to describe the velocity vectors at joints A_i and B_i.

Moreover, based on the derivations in Sections 2.4.1 and 2.4.2, we can conclude that if the geometric relationship of joint A_i with respect to the reference point (frame) $\{Q\}$ is known, then the characteristics of joint A_i can be completely described. These characteristics are described by a set of equations written in terms of the position, velocity, orientation, and their time derivatives for reference point (frame) $\{Q\}$ with respect to the inertial frame $\{I\}$. Similarly, if the geometric relationship of joint B_i with respect to joint A_i is known, then the characteristics of joint B_i are also completely described by a set of equations in terms of the position, velocity, orientation, and their derivatives for the reference frame $\{Q\}$ with respect to the inertial frame $\{I\}$.

In summary, we can say that the complete mathematical description of joints A_i and B_i of a wheel unit with respect to the reference frame $\{Q\}$ and the inertial frame $\{I\}$ can be

50

combined with the kinematic constraints to either design the control law or compute the simulation input motion parameters $\{\omega_p, \delta_i\}$ and $\{\omega_p, \dot{\delta}_i\}$ of all kinematical constraints wheel units. The theory of combining the mathematical description and of joints for a wheel unit together may also used to develop the general kinematic model for arbitrary wheel configurations, but this is beyond the scope of the present thesis.

Chapter 3

EQUATIONS OF MOTION FOR AUTOMATED VEHICLE SYSTEMS

3.1 Introduction

The dynamics of automated vehicle systems, considered as multi-closed-chain mechanisms, are significantly more complex than single-closed-chain mechanisms (such as the slider crank mechanism, for example). The Lagrangian approach and D'Alembert's principle (the reader is referred to Appendix A) are often applied to problems in automated vehicle dynamics. D'Alembert's principle is used for the present work, in which the approach is as follows. Firstly, inertia forces and moments of the entire vehicle system are examined. Secondly, the automated vehicle system is broken down into individual components at each joint (as defined in Chapter 2), and the dynamical equations for each of these components is derived separately. A distinct set of dynamical equations which can be used to govern each wheel unit and the vehicle main body are thus obtained. Thirdly, based on an understanding of the reaction forces between each component taken as rigid bodies as well as the external forces acting on each rigid body, an appropriate system of dynamical equations is formulated for a complete automated vehicle by reassembling the components. Finally, a set of second-order nonlinear ordinary differential equations are obtained which govern the entire vehicle system. The dynamical model of the automated vehicle are obtained from these equations.

3.2 Derivation of Equations of Motion for Automated Vehicles

A schematic of a four DOF automated vehicle model is shown in Fig. 3.1. The vehicle has longitudinal velocity u, lateral velocity v, yaw rate γ and roll rate p. Sprung mass m_s and unsprung mass m_u are also shown. In addition, the vehicle is assumed symmetric with respect to the xoz plane. Thus, locations of sprung mass m_s, unsprung mass m_u, and total mass m of the vehicle are assumed to be located in the xoz plane of frame $\{Q\}$. Furthermore, as discussed in Chapter 2, the x and z axes of reference frame $\{Q\}$ are chosen to pass through the centres of the unsprung mass m_u and total mass m of the vehicle, respectively. Locations of the sprung mass m_s, unsprung mass m_u, and total mass m of the vehicle with respect to the reference frame $\{Q\}$ are specified by the following constants:

h = distance between the centre of the total mass (c.g) and the x-axis,

c = distance between the centre of the sprung mass (s) and the z-axis,

h_s = distance between the centre of the sprung mass (s) and the x-axis,

e = distance between the centre of the total unsprung mass (u) and the z-axis.

Mass centres of the total mass m, the sprung mass m_s and unsprung mass m_u are denoted as c.g., s and u respectively. Total mass m is equal to the sprung mass m_s plus the total unsprung mass m_u, i.e.:

$$m = m_s + m_u \, ,$$

$$m_u = \sum_{i=1}^{n} m_{u_i} \, . \tag{3.1}$$

When the vehicle is in static equilibrium, moments produced by the sprung mass and unsprung

53

mass should be balanced. Consequently, moments about the x and y axes must be zero, which are:

$$m_s \, g \, c = m_u \, g \, e \, ,$$

$$\sum_{i=1}^{n} m_{u_i} \, y_i = 0 \, .$$

(3.2)

where $m_u \, e = \sum_{i=1}^{n} m_{u_i} \, x_i$, and

m_{u_i} = each individual unsprung mass unit (i.e., each wheel unit),

x_i = distance between the centre of each individual unsprung mass unit and the z-axis.

Figure 3.1: Schematic of the Four Degrees of Freedom (DOF) Vehicle Model.

54

3.2.1 Inertial Forces of the Vehicle Along the x and y Axes

According to the description in Appendix A, accelerations of any point located on the vehicle main body can be determined by Eqn. (A.2.2). Thus, replacing point $P_i(x, y, z)$ by the location of the sprung mass centre s $(c, o, -h_s)$ with respect to the reference frame $\{Q\}$ into Eqn.(A.2.2), acceleration of the centre of the sprung mass m_s along the x-axis can be obtained as:

$$a_{s_x} = \dot{u} - \gamma v - \gamma^2 c - \gamma \rho h_s .\qquad\qquad (3.3)$$

Similarly, based on the location of the unsprung mass u given by: $x_u = -e$, $y_u = 0$, $z_u = 0$, the acceleration of the unsprung mass m_u along x axis can be determined by:

$$a_{u_x} = \dot{u} - \gamma v + \gamma^2 e ,\qquad\qquad (3.4)$$

The equation of motion of the vehicle along the x axis will therefore be given by:

$$\sum X = m_s \, a_{s_x} + m_u \, a_{u_x} .\qquad\qquad (3.5\ a)$$

Substituting Eqns. (3.1) through (3.4) into Eqn. (3.5a) yields the equation of the motion of the vehicle along the x axis:

$$\sum X = m \ (\dot{u} - \gamma v) - \gamma \rho h \, m_s ,\qquad\qquad (3.5\ b)$$

where the total external forces acting on the vehicle are $\sum X$. In addition, acceleration of the centre of the sprung mass s along the y axis, also obtained from Eqn. (A.2.2), is as follows:

$$a_{s_y} = \dot{v} + \gamma u + \dot{\gamma} c + \rho h_s ,\qquad\qquad (3.6)$$

55

and the acceleration of the centre of the unsprung mass u along the y axis can be determined by:

$$a_{u_y} = \dot{v} + \gamma u - \dot{\gamma} e .$$

(3.7)

Therefore the equation of motion of the vehicle along the y axis will be:

$$\sum Y = m_s \, a_{s\,y} + m_u \, a_{u\,y} .$$

(3.8 a)

Substituting Eqns. (3.1) and (3.2), and expressions for a_{s_y} and a_{u_y} into Eqn. (3.8 a) yields the equation of the motion of the vehicle along the y axis, which can be expressed as follows:

$$\sum Y = m \ (\dot{v} + \gamma u) + m_s \, \dot{p} h_s .$$

(3.8 b)

3.2.2 Moment of Inertia of the Vehicle With Respect to the x and z Axes

Since the x (rolling) axis passes through the unsprung mass centre, the unsprung mass m_u cannot produce any rolling motion about it. Consequently, the only contribution to moments about the x axis is due to the sprung mass m_s. Referring to Appendix A, Eqns. (A.5) and (A.2.2), the total moment of inertia of each elemental mass δm with respect to the x axis is:

$$\begin{aligned}
\sum L &= \sum \delta m \ (y \, a_z - z \, a_y) \\
&= \sum \delta m \ [y \ (p \, \dot{v}) - y \, z \ (p^2) + x \, y \ (p \, \gamma) + y^2 \ (\dot{p}) \\
&\quad - z \ (\dot{v} + \gamma \, u) + y \, z \ (\gamma^2 + p^2) - x \, z \ (\dot{\gamma}) + z^2 \ (\dot{p})] .
\end{aligned}$$

(3.9)

The following results are therefore obtained due to the fact that both sides of the vehicle are

symmetric with respect to the xoz plane:

$$\sum \delta m \; y = 0 \;,$$

$$\sum \delta m \; y \; z = I_{s_y z} = 0 \;,$$

$$\sum \delta m \; z = - m_s \, h_s \;,$$

$$\sum \delta m \; x \; y = I_{s_x y} = 0 \;,$$

$$\sum \delta m \; (y^2 + z^2) = I_{s_x} \;,$$

$$\sum \delta m \; x \; z = I_{s_x z} \;.$$

(3.10)

Substituting the above equations into Eqn. (3.9), the moment of inertia of the vehicle may be rewritten in the following form:

$$\sum L = \sum \delta m \; (y^2 + z^2) \, \dot{p} - \sum \delta m \; (xz\dot{\gamma}) - \sum \delta m \; z(\dot{v} + \gamma u)$$
$$= I_{s_x} \, \dot{p} + m_s h_s \; (\dot{v} + \gamma u) - I_{xz} \dot{\gamma} \;.$$

(3.11)

In the above equation, $\sum L$ is the external moment acting on the vehicle about x axis. I_{s_x} is the moment of inertia of the sprung mass m_s with respect to the x axis. The moment of inertia of the sprung mass with respect to the x'- axis is $I_{s_x'}$ which passes through the centre of the sprung mass s and is parallel to the x-axis (see Fig.3.1). According to the parallel-axis theorem [63], $I_{s_x} = I_{s_x'} + m_s h_s$, and the product of inertia ($I_{s_{xz}}$) of the sprung mass with respect to the x- and z-axes also have to satisfy the expression $I_{xz} = I_{s_{xz}} + I_{u_{xz}}$. In addition, since the centre of the unsprung mass is located on the x-axis and is symmetric to the xoz-plane, we have $I_{u_{xz}} = 0$ and $I_{xz} = I_{s_{xz}}$.

Similarly, according to Appendix A, Eqns. (A.5) and (A.2.2), the total moment of

inertia of each δm with respect to the z-axis can be expressed as:

$$\sum N = \sum \delta m \ (x \ a_y - y \ a_x)$$

$$= \sum \delta m \ (\ x[(\dot{v} + \gamma u) - (\gamma^2 + p^2)x + (\dot{\gamma})x + (\dot{p})z \ ] \qquad (3.12)$$

$$- y \ [(\dot{u} - \gamma v) - (\gamma^2)x + (\dot{\gamma})y + (\gamma p)z \ ]) \ .$$

Substituting Eqn. (3.10) into the above equation, the moment of inertia of the vehicle can be rewritten as follows:

$$\sum N = I_z \dot{\gamma} - I_{xz} \dot{p} \ , \qquad (3.13)$$

where the external moment acting on the vehicle about the z-axis is $\sum N$. Rolling and yaw accelerations of reference frame $\{Q\}$ of the vehicle are $\dot{p}$ and $\dot{\gamma}$, respectively.

3.2.3 Outline of Results in Sections 3.2.1 and 3.2.2

Expressions involving longitudinal velocity, lateral velocity, yaw and roll of the vehicle have been completely described. A set of second-order nonlinear ordinary differential equations, which incorporate sprung and unsprung masses, have also been derived to govern the motions of the vehicle. These equations are summarized as follows:

$$\sum X = m \ (\dot{u} - \gamma v) - \gamma p \ h_s \ m_s \ ,$$

$$\sum Y = m \ (\dot{v} + \gamma u) + m_s \dot{p} \ h_s \ ,$$

$$\sum L = I_{x_s} \dot{p} + m_s h_s \ (\dot{v} + \gamma u) - I_{xz} \dot{\gamma} \ , \qquad (3.14)$$

$$\sum N = I_z \dot{\gamma} - I_{xz} \dot{p} \ .$$

If a vehicle is modelled by the above equations, but has no roll motion (i.e., only three DOFs), the centre of total mass of the vehicle becomes the origin of the reference frame $\{Q\}$, and Eqns. (3.14) simplify to:

$$\sum X = m\ (\dot{u} - \gamma v)\ ,$$

$$\sum Y = m\ (\dot{v} + \gamma u)\ ,$$

$$\sum N = I_z \dot{\gamma}\ . \tag{3.15}$$

In the equations ((3.14) and (3.15)) of motion for three and four DOFs vehicles, the external forces and moments acting on the vehicle are yet to be determined. The following two sections examine each individual rigid body component of the vehicle system for the purpose of obtaining these forces and moments. These components include the vehicle main body and individual wheel units.

3.3 Equations of Motion for the Components of a Vehicle System

As discussed in Chapter 1, automated vehicle configurations vary significantly from one application to the next. The consequent objective of this research is to provide a methodology for formulation of dynamical equations for a class of automated vehicles which contain arbitrary wheel configurations. In order to achieve this target, this section examines the vehicle main body, and driving, steering and driving-steering wheel units, as well as casters as individual rigid bodies. The method of the body-centred system (refer to Appendix A) is utilized, and equations of motion for each rigid body will be derived in this section. In addition, the joint notation A_i (or B_i) described in detail in Chapter 2 is used to represent connections between the vehicle main body and each wheel as shown in Figs.3.2 through 3.6.

59
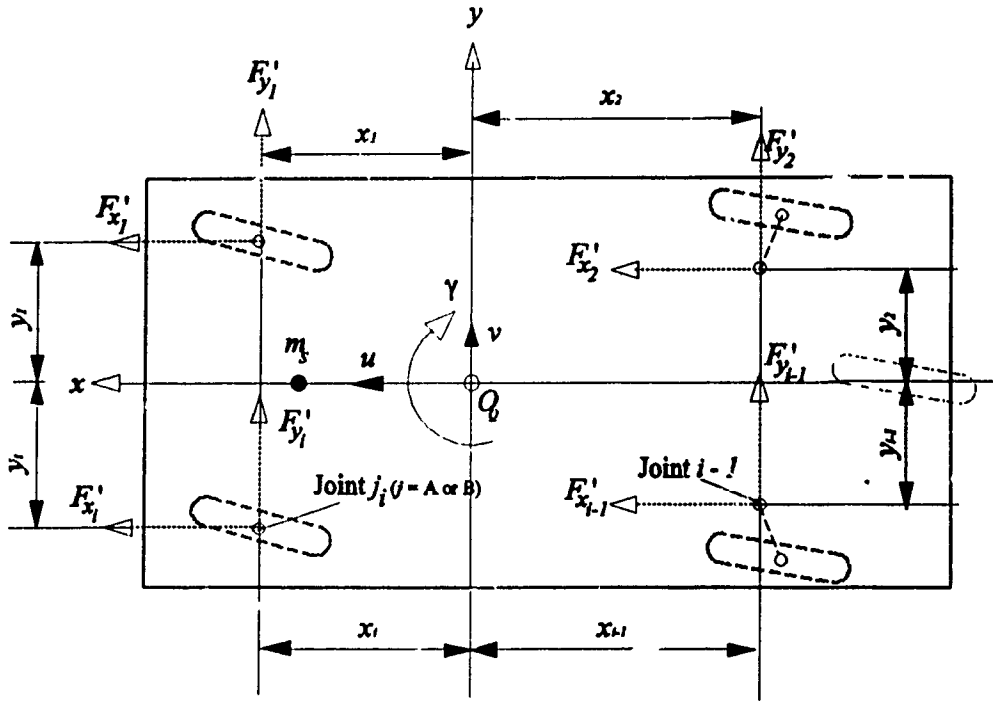
a) Plan View
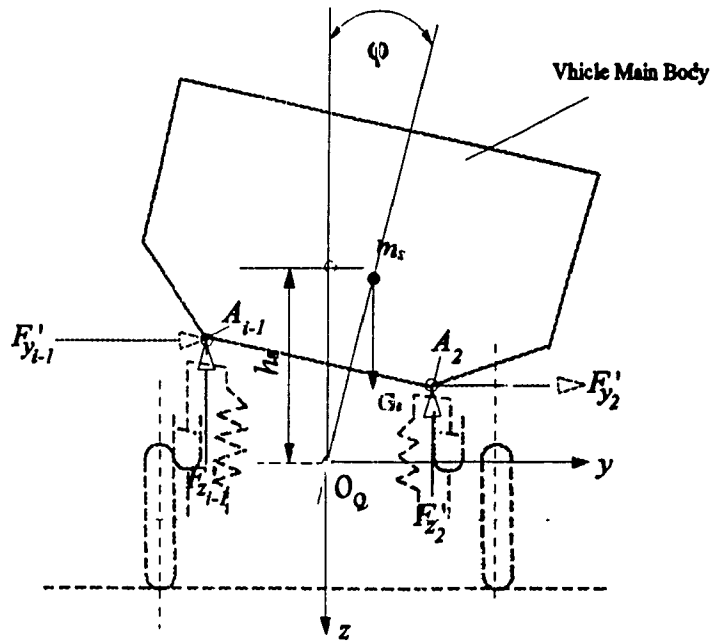
b) Back View

Figure 3.2: A Free Body Diagram of Vehicle Main Body.

60

3.3.1 Equations of Motion for the Vehicle Main Body

Fig.3.2 shows a free body diagram of a vehicle main body, supported by n wheel units which may include n_d driving wheel units, n_s steering wheel units, n_{ds} driving-steering wheel units and n_c casters ($n = n_d + n_s + n_{ds} + n_c$). Each wheel-main body joint is denoted as either A_i or B_i ($i = 1, 2, ..., n$) (notation defined in Chapter 2, Sections 2.4.1 and 2.4.2). There are three reaction forces acting on each joint. These three reaction forces can be indicated with their components along the x, y, z axes as F'_{r_i}, F'_{y_i}, F'_{s_i}. Directions of these three forces (F'_{x_i}, F'_{y_i}, F'_{s_i}) are defined as parallel to the x, y, z axes, respectively, of reference frame $\{Q\}$.

3.3.1.1 Inertia Forces of the Vehicle Main Body Along the x and y Axes

According to D'Alembert's principle, inertia forces of the vehicle main body along x and y axes can be obtained from Eqns. (3.5 b) and (3.8 b) as follows (refer to Section 3.2):

$$\Sigma X' - m_s \, a_{s_x} = m_s(\dot{u} - \gamma v - \gamma^2 c - \gamma p h_s) \, ,$$

$$\Sigma Y' = m_s \, a_{s_y} = m_s(\dot{v} + \gamma u + \dot{\gamma} c + p h_s) \, , \tag{3.16}$$

where total external forces acting on the vehicle main body by each wheel unit along the x and y axes are represented by $\Sigma X'$ and $\Sigma Y'$, respectively.

3.3.1.2 External Forces of the Vehicle Main Body Along the x and y Axes

As shown in Fig.3.2, the total external forces $\Sigma X'$ and $\Sigma Y'$ are the summation of total forces acting through each joint B_i ($i = 1, 2, ..., n_d$), and the total forces acting through each joint

61

A_i ($i = n_d + 1$, $n_d + 2$, ..., $n_d + n_s + n_{ds} + n_c$) along the x and y axes. The total external forces acting on the vehicle main body along the x and y axes can therefore be expressed by the following equations:

$$\Sigma X' = \sum_{i=1}^{n_d} F'_{x_i} + \sum_{i=n_d+1}^{n_d+n_s} F'_{x_i} + \sum_{i=n_d+n_s+1}^{n_d+n_s+n_{ds}} F'_{x_i} + \sum_{i=n_d+n_s+n_{ds}+1}^{n} F'_{x_i} ,$$

$$\Sigma Y' = \sum_{i=1}^{n_d} F'_{y_i} + \sum_{i=n_d+1}^{n_d+n_s} F'_{y_i} + \sum_{i=n_d+n_s+1}^{n_d+n_s+n_{ds}} F'_{y_i} + \sum_{i=n_d+n_s+n_{ds}+1}^{n} F'_{y_i} ,$$

(3.17)

where the total number of driving wheels, steering wheels, driving-steering wheels and casters are denoted as n_s, n_s, n_{ds} and n_c respectively, and the total number of wheels is n ($= n_s + n_s + n_{ds} + n_c$).

3.3.1.3 Moments of Inertia of the Vehicle Main Body About the x and z Axes

As pointed out in Section 3.2.2, vehicle rolling motion is caused by the sprung mass, thus the total moment of inertia of the vehicle about the x-axis equals the moment of inertia of the vehicle main body about the x-axis. The moment of inertia of the vehicle main body about the x-axis can be determined by Eqn. (3.11), rewritten as:

$$\Sigma L' = I_{s_x} \dot{p} + m_s h_s (\dot{v} + \gamma u) - I_{s_x} \dot{\gamma} ,$$

(3.18)

where the external moment acting on the vehicle main body about the x-axis is $\Sigma L'$, the moment of inertia of the sprung mass m_s with respect to the x-axis is I_{s_x}, and the product of inertia of the sprung mass with respect to the x and z axes is I_{s_x}.

62

The total moment of inertia of each δm_s with respect to the z-axis can be determined by the following equation (refer to Eqns. (3.10) and (3.12), and Appendix A Eqns. (A.5) and (A.2.2)):

$$\Sigma N' = \sum \delta m_s (x \, a_y - y \, a_x)$$

$$= \sum \delta m_s (\, x[(\dot{v} + \gamma u) - (\gamma^2 + p^2)x + (\dot{\gamma})x + (\dot{p})z \,] \qquad (3.19)$$

$$- y \,[(\dot{u} - \gamma v) - (\gamma^2)x + (\dot{\gamma})y + (\gamma p)z \,]) \,,$$

where since both sides of the vehicle main body are symmetric with respect to the xoz plane,

$$\sum \delta m_s \, y = 0 \,,$$

$$\sum \delta m_s \, y \, z = 0 \,,$$

$$\sum \delta m_s \, z = -m_s h_s \,,$$

$$\sum \delta m_s \, xy = 0 \,, \qquad\qquad\qquad (3.20)$$

$$\sum \delta m_s \, (y^2 + z^2) = I_{s_z} \,,$$

$$\sum \delta m_s \, xz = I_{s_{zx}} \,.$$

Then, the moment of inertia of the vehicle main body can be simplified as follows:

$$\Sigma N' = I_{s_z} \dot{\gamma} - I_{s_{zx}} \dot{p} \,. \qquad\qquad\qquad (3.21)$$

The total external moment acting on the vehicle main body about the z-axis is $\sum N'$

3.3.1.4 External Moment of the Vehicle Main Body About the x and z Axes

Fig.3.3 shows schematically the external moments acting on the unsprung mass. There are

63

three external moments acting on the vehicle main body about the x-axis [60]. Firstly, the moment T_S is produced by the spring forces of the suspension system. It is defined as:

$$T_S = (C_{\varphi_1} + C_{\varphi_2} + \ldots\ldots + C_{\varphi_n}) \; \varphi \; = \sum_{i=1}^{n} C_{\varphi_i} \varphi \; = C_{\varphi} \varphi \; . \tag{3.22 a}$$

Secondly, the moment T_D is produced by spring damping in the suspension system. It is defined as:

$$T_D = (\frac{\partial L_1}{\partial p_1} + \frac{\partial L_2}{\partial p_2} + \ldots\ldots + \frac{\partial L_n}{\partial p_n}) \; \dot{\varphi} \; = \sum_{i=1}^{n} \frac{\partial L_i}{\partial p_i} \dot{\varphi} \; = L_p \, p \; . \tag{3.22 b}$$

The total number of wheel units employed on the vehicle is n. Thirdly, the moment T_G is due to the weight of the sprung mass, and is:

$$T_G = G_s h_s \sin(\varphi) \approx m_s g h_s \varphi \; , \tag{3.22 c}$$

Hence, the summation of moments about the x (rolling) axis is as follows:

$$\Sigma L' = T_G - T_S - T_D \; . \tag{3.23}$$

Here, the sprung mass is m_s, and the equivalent rolling stiffness is C_{φ}, for which $[C_{\varphi}] =$ [N·m·rad^{-1}], and L_p is the damping coefficient of the entire suspension system, for which $[L_p]$ = [N·m·s·rad^{-1}] and g is the acceleration of gravity. The distance from the origin O_Q to the centre of sprung mass is h_s .
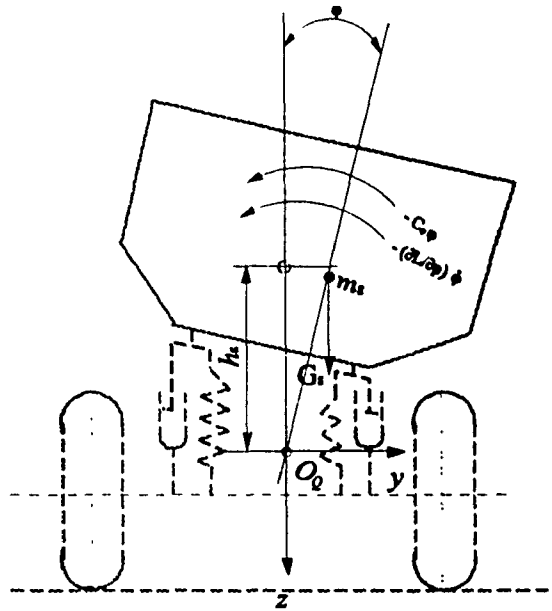
Figure 3.3: Schematic of External Moments Acting on the Sprung Mass.
(Vehicle Main Body)

Furthermore, as described in Appendix C for a four DOFs vehicle system, the load

acting on each wheel is redistributed during rolling motion. Friction in the left and right

wheels may not be equal, and the lateral forces of each wheel also may not be equal. As a

result, the forces $(F'_{x_i}, i = 1, 2, ..., n)$ acting on each joint by each wheel unit are not

necessarily equal to one another. In addition, the forces $(F'_{y_i}, i = 1, 2, ..., n)$ are also not

necessarily equal to one another. These differences give rise to moments of the vehicle main

body about the z-axis, and the summation of moments about the z-axis can be represented as

follows (see Fig. 3.2 a)):

$$\Sigma N' = -\sum_{i=1}^{n} (F'_{x_i} y_i) + \sum_{i=1}^{n} (F'_{y_i} x_i) . \tag{3.24}$$

65

3.3.1.5 Equations of Motion

The total external forces $\Sigma X'$ and $\Sigma Y'$ of the vehicle main body along the x and y axes have been represented in Eqn. (3.17). In addition, the external moments $\Sigma L'$ and $\Sigma N'$ of the vehicle main body about the y and z axes have been represented by Eqns. (3.23) and (3.24). Substituting these external forces and moments into Eqns. (3.16), (3.18) and (3.21) results in four second-order nonlinear ordinary differential equations representing a four DOFs vehicle main body motion:

$$m_s(\dot{u} - \gamma v - \gamma^2 c - \gamma p h_s) = \sum_{i=1}^{n_d} F_{x_i} + \sum_{i=n_d+1}^{n_d+n_s} F_{x_i} + \sum_{i=n_d+n_s+1}^{n_d+n_s+n_{ls}} F_{x_i} + \sum_{i=n_d+n_s+n_{ls}+1}^{n} F_{x_i} \, ,$$

$$m_s(\dot{v} + \gamma u + \dot{\gamma} c + p h_s) = \sum_{i=1}^{n_d} F_{y_i} + \sum_{i=n_d+1}^{n_d+n_s} F_{y_i} + \sum_{i=n_d+n_s+1}^{n_d+n_s+n_{ls}} F_{y_i} + \sum_{i=n_d+n_s+n_{ls}+1}^{n} F_{y_i} \, ,$$

$$I_{s_x} \dot{p} + m_s h_s (\dot{v} + \gamma u) - I_{s_{xz}} \dot{\gamma} = T_G - T_S - T_D \, ,$$

$$I_{s_z} \dot{\gamma} - I_{s_{xz}} \dot{p} = -\sum_{i=1}^{n} (F'_{x_i} y_{a_i}) + \sum_{i=1}^{n} (F'_{y_i} x_{a_i}) \, . \qquad (3.25)$$

3.3.2 Equations of Motion for Driving Wheel Units

A driving wheel unit is regarded as a rigid body as shown in Fig.3.4. The wheel can only rotate about its own horizontal axis, therefore there is only a single degree of freedom introduced in the vehicle system. In this case, the driving wheel unit will be adjoined on the vehicle main body through the joint B_i (the wheel rotation axis) directly. The driving wheel unit exerts a tractive force on the vehicle main body through the joint B_i. Generally, two sub-coordinates systems, $B_i\{x_{B_i}, y_{B_i}, z_{B_i}\}$ and $C_i\{x_{C_i}, y_{C_i}, z_{C_i}\}$ are used to describe this wheel

unit. System B_i is attached at the intersection of the wheel plane and its rotation axis which

is fixed on the vehicle main body. System C_i is fixed at the wheel-ground contact point. The

x_{j_i}, y_{j_i}, z_{j_i} ($j = B$ or C) axes of these two coordinate systems are parallel to the x, y, z axes

of reference frame $\{Q\}$.
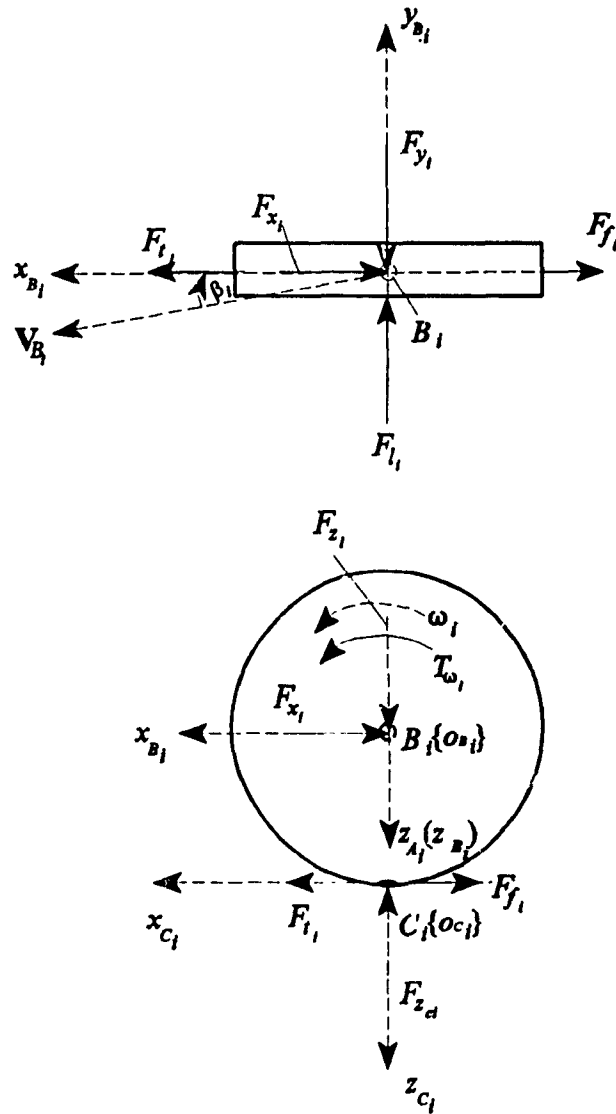
Figure 3.4: Free Body Diagram of Driving Wheel Unit.

67

In addition, as discussed in Appendix B, there are four external forces: tractive force F_{t_i}, friction force F_{f_i}, lateral force F_{l_i} and normal force F_{zc_i}, acting on the wheel-ground contact through the ground. The three reaction forces F_{x_i}, F_{y_i}, F_{z_i} act on joint B_i through the vehicle main body. Directions of these forces are indicated in Fig. 3.4. Assume the centre of the wheel (B_i) is the centre of mass of the driving wheel unit, and linear velocities along the x_{B_i} and y_{B_i} axes are $v_{x_{B_i}}$ and $v_{y_{B_i}}$, and the angular acceleration of the driving wheel about the y_{B_i} axis is $\dot{\omega}_i$. Then, applying Eqn. (A.5), the equations of motion for a driving wheel can be represented as follows:

$$\sum X_{B_i} = m_i \, \dot{v}_{B_{x_i}} = (F_{t_i} - F_{f_i}) - F_{x_i} \, ,$$

$$\sum Y_{Bi} = m_i \, \dot{v}_{B_{y_i}} = F_{l_i} - F_{y_i} \, ,$$

$$\sum Z_{Bi} = F_{z_i} + m_i g - F_{zc_i} = 0 \, ,$$

$$\sum M_{B_i} = I_{B_i} \, \dot{\omega}_i = (F_{t_i} - F_{f_i}) R_i \, ,$$

(3.26)

where the total external force acting on the unit in the x-direction (which is also the direction of the wheel heading) is $\sum X_{B_i}$. The total external force acting on the unit in the y-direction which is also the direction perpendicular to the wheel plane is $\sum Y_{B_i}$. The total external force acting on the unit in the z-direction is $\sum Z_{B_i}$. The total moment of the driving wheel about its horizonal axis is $\sum M_{B_i}$. The moment of inertia of a driving wheel about its rotation axis (y_{B_i}) is I_{B_i}. The radius of a driving wheel is R_i, and the tractive force of a driving wheel is $F_{t_i} = T_{\omega_i}/R_i$. The torque applied on the driving wheel is T_{ω_i} [N.m].

According to Appendix B, frictional and lateral forces of the wheel may be determined

68

from Eqns. (B.1) and (B.3) as:

$$F_{f_i} = f_r F_{zc_i} \, ,$$

$$F_{l_i} = C_{s_i} \alpha_i \, ,$$
(3.27)

with $f_r = k_1 (1 + k_2 v_{B_i})$ and $k_1 = 0.007, k_2 = 0.01$ [s/m], and the cornering stiffness of the wheel i is C_{s_i} [N/deg]. The magnitude of velocity for the centre of the wheel is v_{B_i}, which can be determined from Eqn.(2.7) in Section 2.4.1 as:

$$v_{B_i} = \sqrt{(u - \gamma y_{b_i})^2 + (v + \gamma x_{b_i})^2} \, ,$$
(3.28)

and the slip angle can be determined from Eqns. (2.8) and it's definition (refer to Appendix B, Fig. B.1) as:

$$\alpha_i = \beta_i - \delta_i = \tan^{-1} \frac{v + \gamma x_{b_i}}{u - \gamma y_{b_i}} \, ,$$
(3.29)

where the steering angle is equal to zero, and the linear velocities of the vehicle with respect to the frame $\{Q\}$ are u and v, and yaw rate of the vehicle is γ. The location of the joint B_i with respect to the reference frame $\{Q\}$ in the xy plane is (x_{b_i}, y_{b_i}).

Rearranging Eqn.(3.26), the reaction forces $(F_{x_i}, F_{y_i}, F_{z_i})$ can be obtained as follows:

$$F_{x_i} = (F_{t_i} - F_{f_i}) - m_i v_{B_{x_i}} \, ,$$

$$F_{y_i} = F_{l_i} - m_i v_{B_{y_i}} \, ,$$
(3.30)

$$F_{z_i} = F_{zc_i} - m_i g \, ,$$

with a tractive force $F_{t_i} = T_{c_i} / R_i$, and the normal force F_{zc_i} has been determined in Appendix C.

In addition, the wheel angular velocity ω_i and acceleration $\dot{\omega}_i$ may be determined from kinematic constraint 1 discussed in Section 2.5, which can be rewritten as follows:

$$\omega_i = \frac{\dot{X}_Q \cos(\theta) + \dot{Y}_Q \sin(\theta) - y_{b_i} \dot{\gamma}}{R_i},$$

$$\dot{\omega}_i = \frac{\ddot{X}_Q \cos(\theta) - \dot{X}_Q \sin(\theta)\gamma + \ddot{Y}_Q \sin(\theta) + \dot{Y}_Q \cos(\theta)\gamma - y_{b_i}\ddot{\gamma}}{R_i}.$$

(3.31)

where the desired linear velocities and accelerations of the vehicle with respect to the inertial frame $\{I\}$ are defined as $\dot{X}_Q$, $\dot{Y}_Q$ and $\ddot{X}_Q$, $\ddot{Y}_Q$ respectively. The desired angular acceleration of the vehicle and the orientation of the vehicle with respect to the inertial frame $\{I\}$ are defined as $\dot{\gamma}$ and θ respectively. Generally, all of these desired variables must be specified as inputs to the system. Then, based on the desired trajectory (position and velocity) of the vehicle with respect to the inertial frame $\{I\}$, the required angular velocity and acceleration of a motorized driving wheel unit, as well as the tractive force may be determined by applying the appropriate kinematic constraints.

3.3.3 Equations of Motion for Steering Wheel Units

Based on the mechanics of wheels as discussed in Appendix B, a steering wheel is considered as a free body as shown in Figs. 3.5 and 3.6. There are two sub-coordinate systems A_i $\{x_{A_i}, y_{A_i}, z_{A_i}\}$, and $C_i\{x_{C_i}, y_{C_i}, z_{C_i}\}$ employed in steering wheel units. Unlike driving wheel units, steering wheel units cannot introduce tractive forces to the vehicle system, but can transfer torque to the vehicle main body and pilot the direction of motion of the vehicle by

70

rotation of the wheel around a vertical axis (the z_{A_i}-axis). At any instant, there is an equivalent fixed angle between the x_{A_i}-axis (or the x-axis of reference frame $\{Q\}$), and the direction of travel of the steering wheel (the plane of the wheel). This angle is defined as the steering angle δ_i, and the sign of the steering angle is defined as positive when the steering wheel rotates clockwise as seen from above. Types A and B steering wheel units each have distinct equations of motion which will now be considered.

Type A Steering Wheel Units: This type of steering wheel unit is shown in Fig. 3.5. Assume the centre of mass of this unit is located at the centre of the wheel, and a sub-coordinate system $B_i\{x_{B_i}, y_{B_i}, z_{B_i}\}$ is located at the mass centre of the steering wheel unit, which is parallel to the reference frame $Q\{x, y, z\}$. Let the linear velocities along the x_{B_i} and y_{B_i} axes be $v_{x_{B_i}}$ and $v_{y_{B_i}}$, respectively. The angular velocity of the steering unit about the z_{A_i}-axis is defined as $\dot{\xi}_i$ (where $\xi_i = \text{sign}(y_{a_i})\dfrac{\pi}{2} + \delta_i$ and $\dot{\xi}_i = \dot{\delta}_i$). Then, using D'Alembert's principle applied to the "body-centred system" (refer to Appendix A, Section A.2), the equations of motion of a Type A steering wheel unit may be derived from Eqn. (A.5) and expressed as follows:

$$\sum X_{B_{x_i}} = m_i \, (\dot{v}_{B_{x_i}} - \dot{\delta}_i v_{B_{y_i}}) \ ,$$

$$\sum Y_{B_{y_i}} = m_i \, (\dot{v}_{B_{y_i}} + \dot{\delta}_i v_{B_{x_i}}) \ ,$$

$$\sum Z_{B_{z_i}} = F_{z_i} + m_i g - F_{z_{C_i}} = 0 \ ,$$

$$\sum N_{A_{z_i}} = I_{z_{A_i}} \ddot{\xi}_i = I_{z_{A_i}} \ddot{\delta}_i \ .$$

$$(3.32)$$

where $\sum X_{B_i}$ is the total external force of the steering wheel along the x_{B_i}-axis, $\sum Y_{B_i}$ is the

71

total external force of the steering wheel along the along the y_{B_i}-axis, and $\sum Z_{B_i}$ is the total

external force of the steering wheel along the z_{B_i}-axis. The total moment of the steering wheel

about the z_{A_i}-axis is $\sum N_{A_i}$. The linear accelerations along the x_{B_i} and y_{B_i} axes are $v_{x_{B_i}}$ and

$v_{y_{B_i}}$, respectively. The angular acceleration of the steering wheel about the z_{B_i} axis is $\ddot{\delta}_i$.

Figure 3.5: Free Body Diagram of Type A Steering Wheel Unit.

As shown in Fig. 3.5, there are three external forces which are friction force F_{f_i}, lateral force F_{l_i} and the normal force $F_{z_{C_i}}$ acting on the wheel-ground contact point C_i by the ground. The direction of the lateral force F_{l_i} is always against the slip direction. In addition, three reaction forces F_{x_i}, F_{y_i}, F_{z_i} act on joint A_i by the vehicle main body. Directions of these forces are indicated in Fig. 3.5. The total external forces acting on the steering wheel along the x_{B_i} and y_{B_i} axes, and the total moment of the steering wheel about the z_{A_i}-axis can be represented by the following equations:

$$\sum X_{B_i} = -F_{f_i} \cos \delta_i + |F_{l_i}| \cos \left(\delta_i - \text{sign}\,(\alpha_i)\frac{\pi}{2}\right) - F_{x_i} \,,$$

$$\sum Y_{B_i} = -F_{f_i} \sin \delta_i + |F_{l_i}| \sin \left(\delta_i - \text{sign}\,(\alpha_i)\frac{\pi}{2}\right) - F_{y_i} \,, \qquad (3.33)$$

$$\sum Z_{B_i} = F_{z_i} + m_i\, g - F_{z_{C_i}} \,,$$

with the steering torque $T_{s_i} = I_{z_{A_i}} \ddot{\delta}_i$, and the moment of inertia of the steering wheel about the z_{A_i}-axis is $I_{z_{A_i}}$. Substituting Eqn. (3.32) into Eqn. (3.33) yields the equations of motion for Type A steering wheel units, which are as follows:

$$m_i\, (\dot{v}_{B_{x_i}} - \dot{\delta}_i v_{B_{y_i}}) = -F_{f_i} \cos \delta_i + |F_{l_i}| \cos \left(\delta_i - \text{sign}\,(\alpha_i)\frac{\pi}{2}\right) - F_{x_i} \,,$$

$$m_i\, (\dot{v}_{B_{y_i}} + \dot{\delta}_i v_{B_{x_i}}) = -F_{f_i} \sin \delta_i + |F_{l_i}| \sin \left(\delta_i - \text{sign}\,(\alpha_i)\frac{\pi}{2}\right) - F_{y_i} \,,$$

$$0 = F_{z_i} + m_i\, g - F_{z_{C_i}} \,, \qquad (3.34)$$

Rearranging Eqn. (3.34), the reaction forces acting on the steering wheel by the vehicle main body along the x, y and z axes can be obtained by the following equations:

$$F_{x_i} = -F_{f_i} \cos \delta_i + |F_{l_i}| \cos (\delta_i - \text{sign}(\alpha_i)\frac{\pi}{2}) - m_i (\dot{v}_{B_{x_i}} - \dot{\delta}_i v_{B_{y_i}}),$$

$$F_{y_i} = -F_{f_i} \sin \delta_i + |F_{l_i}| \sin (\delta_i - \text{sign}(\alpha_i)\frac{\pi}{2}) - m_i (\dot{v}_{B_{y_i}} + \dot{\delta}_i v_{B_{x_i}}),$$

$$F_{z_i} = F_{z_{C_i}} - m_i g, \tag{3.35}$$

In the above equations, the friction force F_{f_i} and lateral force F_{l_i} can be obtained from Appendix B, Eqns. (B.1), and (B.3). In addition, assuming the normal force $F_{z_{C_i}}$ has been calculated (for further details, refer to Appendix C). The velocity magnitude $(v_{(xy)_{B_i}})$ of joint B_i in the $x_{B_i} y_{B_i}$ plane with respect to frame $\{Q\}$ can be obtained from Eqn. (2.14) in Section 2.4.2.1 as follows:

$$v_{(xy)_{B_i}} = \sqrt{v_{x_{B_i}}^2 + v_{y_{B_i}}^2} \tag{3.36 a}$$

$$= \sqrt{(u - \gamma(d_i \sin(\xi_i) + y_{a_i}))^2 + (v + \gamma(d_i \cos(\xi_i) + x_{a_i}))^2},$$

and the direction angle (β_i) of joint B_i can be determined from Eqns.(2.15) as:

$$\beta_{B_i} = \tan^{-1} \frac{v_{y_{B_i}}}{v_{x_{B_i}}} = \tan^{-1} \frac{v + \gamma((d_i \cos(\xi_i) + x_{a_i})}{u - \gamma(d_i \sin(\xi_i) + y_{a_i})}, \tag{3.36 b}$$

Thus, the slip angle α_i is:

$$\alpha_i = \beta_i - \delta_i = \tan^{-1} \frac{v + \gamma(d_i \cos(\xi_i) + x_{a_i})}{u - \gamma(d_i \sin(\xi_i) + y_{a_i})} - \delta_i, \tag{3.36 c}$$

where the locations of joints A_i with respect to reference frame $\{Q\}$ are x_{a_i} and y_{a_i}. The

steering column rotation angle is $\xi_i = \text{sign}(y_{a_i})\dfrac{\pi}{2} + \delta_i$. In addition, referring to Section 2.5,

the steering angle may decided by applying kinematic constraint 2 for Type A steering wheel

units. Thus, the steering angle can be determined from Eqn.(2.27a) as:

$$\delta_i = \frac{-\dot{X}_Q \sin(\theta) + \dot{Y}_Q \cos(\theta) + x_{a_i}\gamma}{\dot{X}_Q \cos(\theta) + \dot{Y}_Q \sin(\theta) - y_{a_i}\gamma} . \qquad (3.37)$$

In the above equation, linear velocities of the vehicle with respect to the inertial frame $\{I\}$ are

represented as $\dot{X}_Q$ and $\dot{Y}_Q$, respectively. The angular velocity of the vehicle is γ. The

orientation of the vehicle with respect to the inertial frame $\{I\}$ is θ.

Type B Steering Wheel Units: Define another sub-coordinate system $D_i\{x_{D_i}, y_{D_i}, z_{D_i}\}$ as

located at the mass centre of the steering wheel unit, parallel to reference frame $Q\{x, y, z\}$,

as shown in Fig. 3.6. Let the linear velocities along the x_{D_i} and y_{D_i} axes be $v_{x_{D_i}}$ and $v_{y_{D_i}}$,

respectively. The angular velocity of the steering wheel about the z_{D_i}-axis is $\dot{\delta}_{D_i}$ (where

$\dot{\delta}_{D_i} = \dot{\delta}_{A_i} = \dot{\delta}_i$). Similarly, based on D'Alembert's principle applied to "body-centred

system" [21][39][60](refer to Appendix A, Section A.2), the equations of motion of the

steering wheel unit can be derived from Eqn. (A.5), and expressed as follows:

$$\sum X_{D_{x_i}} = m_i (\dot{v}_{D_{x_i}} - \dot{\delta}_i v_{D_{y_i}}) ,$$

$$\sum Y_{D_{y_i}} = m_i (\dot{v}_{D_{y_i}} + \dot{\delta}_i v_{D_{x_i}}) , \qquad (3.38)$$

$$\sum N_{D_{z_i}} = I_{z_{D_i}} \ddot{\delta}_i .$$

where $\sum X_{D_i}$ is the total external force of the steering wheel along the x_{D_i}-axis, and $\sum Y_{D_i}$ is the total external force of the steering wheel along the y_{D_i} axis. The total moment of the steering wheel about the z_{D_i}-axis is $\sum N_{D_i}$. The linear accelerations along the x_{D_i} and y_{D_i} axes are $v_{x_{D_i}}$ and $v_{y_{D_i}}$, respectively. The angular acceleration of the steering wheel about the z_{D_i} axis is $\dot{\delta}_i$.
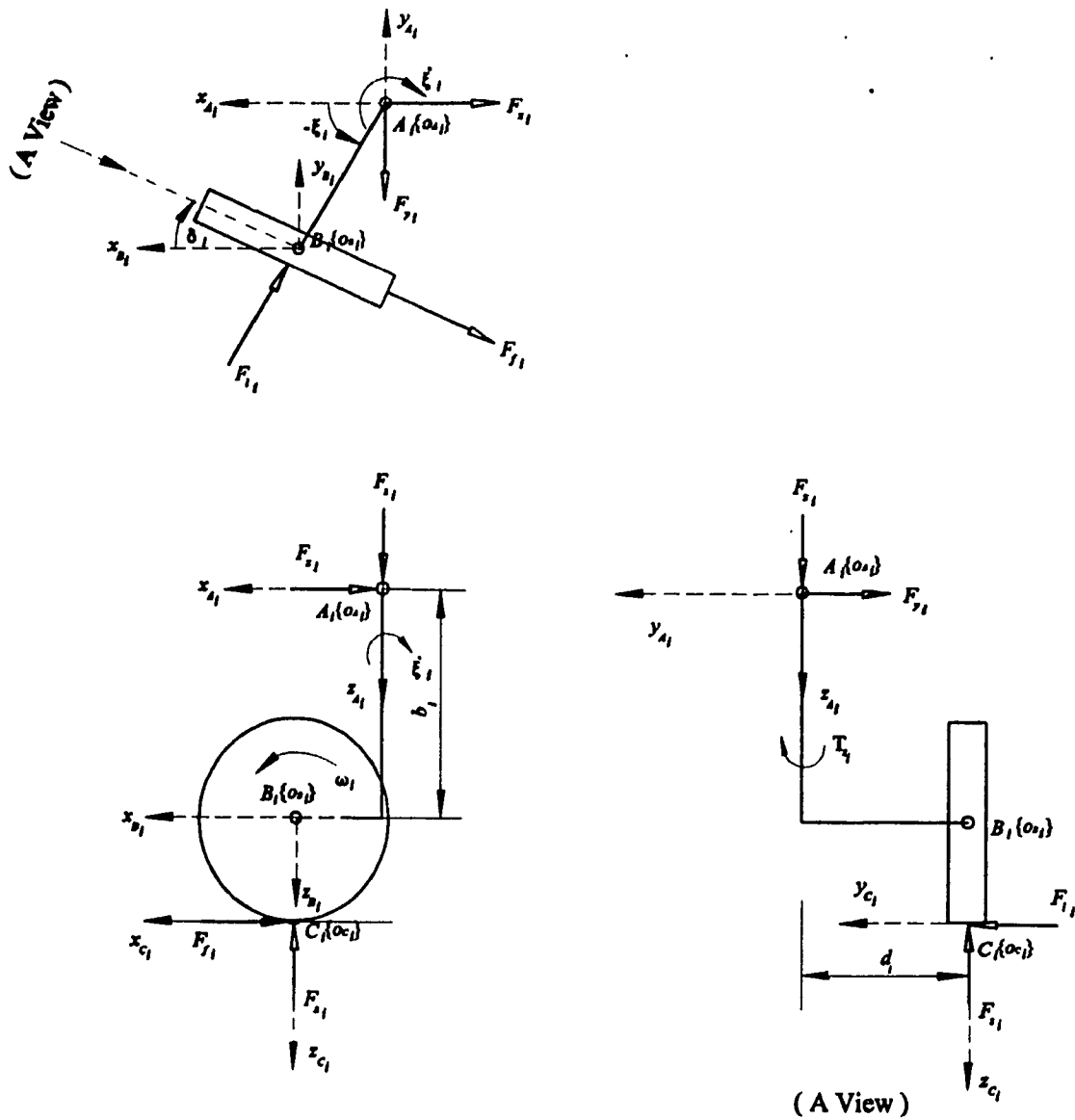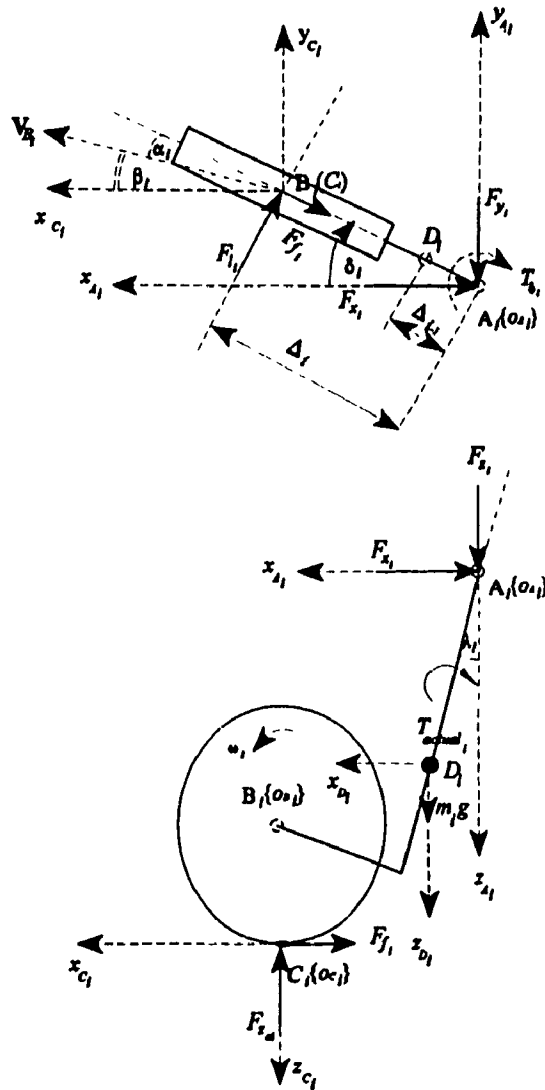

Figure 3.6: Free Body Diagram of Type B Steering Wheel Units.

76

There are three external forces which are friction force F_{f_i}, lateral force F_{l_i} and the normal force F_{zc_i} acting on the wheel-ground contact point C_i through the ground. In addition, three reacting forces F_{x_i}, F_{y_i}, F_{z_i} are acting on joint A_i by the vehicle main body. Directions of these forces are illustrated in Fig. 3.6. The total external forces acting on the steering wheel along the x_{D_i} and y_{D_i} axes, and the total moment of the steering wheel about the z_{D_i}-axis can be represented by the following equations:

$$\sum X_{D_i} = -F_{f_i} \cos \delta_i + |F_{l_i}| \cos (\delta_i - \text{sign}(\alpha_i)\frac{\pi}{2}) - F_{x_i},$$

$$\sum Y_{D_i} = -F_{f_i} \sin \delta_i + |F_{l_i}| \sin (\delta_i - \text{sign}(\alpha_i)\frac{\pi}{2}) - F_{y_i},$$

$$\sum Z_{D_i} = F_{z_i} + m_i g - F_{zc_i},$$

$$\sum N_{D_i} = (-F_{x_i} \sin \delta_i + F_{y_i} \cos \delta_i) \Delta_{l_i} + F_{l_i}(\Delta_i - \Delta_{l_i}),$$

(3.39)

where the direction of the lateral force F_{l_i} is always opposite to the direction of the slip angle α_i. Substituting Eqn. (3.38) into Eqn. (3.39), the equations of motion for the Type B steering wheel unit can be represented as follows:

$$m_i (\dot{v}_{D_{x_i}} - \dot{\delta}_i v_{D_{y_i}}) = -F_{f_i} \cos \delta_i + |F_{l_i}| \cos (\delta_i - \text{sign}(\alpha_i)\frac{\pi}{2}) - F_{x_i},$$

$$m_i (\dot{v}_{D_{y_i}} + \dot{\delta}_i v_{D_{x_i}}) = -F_{f_i} \sin \delta_i + |F_{l_i}| \sin (\delta_i - \text{sign}(\alpha_i)\frac{\pi}{2}) - F_{y_i},$$

$$0 = F_{z_i} + m_i g - F_{zc_i},$$

$$I_{z_{D_i}} \ddot{\delta}_i = (-F_{x_i} \sin \delta_i + F_{y_i} \cos \delta_i) \Delta_{l_i} + F_{l_i}(\Delta_i - \Delta_{l_i}).$$

Rearranging above equation, the reaction forces acting on the steering wheel by the vehicle

77

main body along the x, y and z axes can be obtained as the following equations:

$$F_{x_i} = -F_{f_i} \cos \delta_i - F_{l_i} \cos (\frac{\pi}{2} - \delta_i) - m_i (\dot{v}_{D_{x_i}} - \dot{\delta}_i v_{D_{y_i}}) \ ,$$

$$F_{y_i} = -F_{f_i} \sin \delta_i + F_{l_i} \sin (\frac{\pi}{2} - \delta_i) - m_i (\dot{v}_{D_{y_i}} + \dot{\delta}_i v_{D_{x_i}}) \ ,$$

$$F_{z_i} = F_{z_{C_i}} - m_i g \ , \tag{3.40}$$

and the moment acting on the mass centre of the steering wheel will be obtained by the following equation:

$$I_{z_{D_i}} \ddot{\delta}_i = m_i ((\dot{v}_{D_{x_i}} - \dot{\delta}_i v_{D_{y_i}}) \sin \delta_i - (\dot{v}_{D_{y_i}} + \dot{\delta}_i v_{D_{x_i}}) \cos \delta_i) \Delta_{l_i} + F_{l_i} \Delta_i \ , \tag{3.41}$$

where the horizontal distance between the centre of the mass of the steering wheel and joint A_i is Δ_{l_i}. The moment of inertia of the steering wheel about the z_{D_i}-axis is $I_{z_{D_i}}$. Similarly, in the above equations, the friction force F_{f_i} and lateral force F_{l_i} can be obtained from Appendix B, Eqns. (B.1), and (B.3). In addition, assuming the normal force $F_{z_{C_i}}$ has been determined (for further details refer to Appendix C). The velocity magnitude $(v_{(xy)_{B_i}})$ of joint B_i in the $x_{B_i} y_{B_i}$ plane with respect to frame $\{Q\}$ can be obtained from Eqn. (2.19) in Section 2.4.2.2 as:

$$v_{(xy)_{B_i}} = \sqrt{v_{x_{B_i}}^2 + v_{y_{B_i}}^2} \tag{3.42 a}$$

$$= \sqrt{(u - \gamma(\Delta_f \sin (\delta_i) + y_{a_i}))^2 + (v + \gamma(\Delta_f \cos (\delta_i) + x_{a_i}))^2} \ ,$$

and the direction angle (β_i) of joint B_i can be determined from Eqn. (2.20) as:

78

$$\beta_{B_i} = \tan^{-1} \frac{v_{y_{B_i}}}{v_{x_{B_i}}} = \tan^{-1} \frac{v + \gamma(\Delta_i \cos(\delta_i) + x_{a_i})}{u - \gamma(\Delta_i \sin(\delta_i) + y_{a_i})} . \tag{3.42 b}$$

Thus, the slip angle α_i is:

$$\alpha_i = \beta_i - \delta_i = \tan^{-1} \frac{v + \gamma(\Delta_i \cos(\delta_i) + x_{a_i})}{u - \gamma(\Delta_i \sin(\delta_i) + y_{a_i})} - \delta_i , \tag{3.43 c}$$

where the locations of joints A_i with respect to the reference frame $\{Q\}$ are x_{a_i} and y_{a_i}.

Eqn. (3.41) describes the mathematical constraint of the Type B steering wheel unit, which requires that angular acceleration and steering rate of the steering wheel depend on the accelerations and velocities of the mass centre of the steering wheel unit, which in turn depends on the vehicle motion. In this case, the steering angle may be decided by applying the kinematic constraint discussed in Section 2.5. Thus, the rate of change of steering angle of the Type B steering wheel unit can be determined from Eqn.(2.27b), and is:

$$\dot{\delta}_i = \frac{-\dot{X}_Q \sin(\theta + \delta_i) + \dot{Y}_Q \cos(\theta + \delta_i) + (x_{a_i} \cos(\delta_i) + y_{a_i} \sin(\delta_i))\gamma}{\Delta_i} + \gamma . \tag{3.44}$$

The steering rate and steering angle of the steering wheel with respect to time can be determined by applying the initial conditions of the vehicle system, namely $\delta_i(0) = 0$, and $\dot{X}(0)_P$, $\dot{Y}(0)_i$ and $\theta(0)$ into Eqn. (3.39). These are:

$$\dot{\delta}_i(0) = \frac{-\dot{X}(0)_Q \sin\theta_0 + \dot{Y}(0)_Q \cos\theta_0 + (x_{a_i})\gamma(0)}{\Delta_i} + \gamma(0) , \tag{3.45}$$

79

and

$$\delta_i(t) = \int_0^t \left(\frac{-\dot{X}_Q \sin(\theta+\delta_i) + \dot{Y}_Q \cos(\theta+\delta_i) + (x_{a_i}\cos(\delta_i) + y_{a_i}\sin(\delta_i))\gamma}{\Delta_i} + \gamma \right) dt, \tag{3.46}$$

In the above equations, $\Delta_i = d_i\cos(\lambda_i) + L_i\sin(\lambda_i)$, and the linear velocities of the vehicle with respect to inertial frame I are represented as $\dot{X}_Q$ and $\dot{Y}_Q$, respectively. Yaw and roll modes of angular acceleration of the vehicle are represented as $\dot{\gamma}$, $\dot{\rho}$, respectively. The orientation of the vehicle with respect to inertial frame $\{I\}$ is θ.

In the special where the offset $\Delta_i = 0$ or $d_i = 0$, the steering angle of the steering wheel unit can be determined by the following equation:

$$\delta_i = \frac{-\dot{X}_Q \sin(\theta) + \dot{Y}_Q \cos(\theta) + x_{a_i}\gamma}{\dot{X}_Q \cos(\theta) + \dot{Y}_Q \sin(\theta) - y_{a_i}\gamma}. \tag{3.47}$$

3.3.4 Equations of Motion for Driving-Steering Wheel Units

A driving-steering wheel unit is a wheel unit capable of simultaneously performing driving and steering functions. Driving-steering wheel units generally introduce a tractive force to the vehicle main body through joint B_i. They also introduce a torque to the vehicle main body through joint A_i, and lead the direction of the vehicle by rotating about the vertical axis (z_{A_i}). Considering a driving-steering wheel as a rigid body, three sub-coordinate systems, $A_i\{x_{A_i}, y_{A_i}, z_{A_i}\}$, $B_i\{x_{B_i}, y_{B_i}, z_{B_i}\}$, $C_i\{x_{C_i}, y_{C_i}, z_{C_i}\}$ are employed on joints A_i and B_i, and the wheel-ground contact point C_i. However, if the wheel unit centre of mass is not coincident

with the centre of the wheel, there is an additional sub-coordinate system $D_i\{x_{D_i}, y_{D_i}, z_{D_i}\}$ located on the centre of mass of the driving-steering wheel unit.

Referring to Sections 3.3.2 and 3.3.3, we can conclude that for a driving-steering wheel unit, there are four external forces, namely, tractive force F_{t_i}, friction force F_{f_i}, lateral force F_{l_i} and normal force $F_{z_{C_i}}$ acting on the wheel-ground contact point through the ground. Three reactive forces F_{x_i}, F_{y_i}, F_{z_i} act on joint A_i through the vehicle main body. The equations of motion of this system can be determined by combining the equations of motion for driving wheel units and steering wheel units. Two types of driving-steering wheel units are discussed in this section, similar to those mentioned in Section 3.3.3.

Type A Driving-Steering Wheel Units: As shown in Fig. 3.7, three sub-coordinate systems $A_i\{x_{A_i}, y_{A_i}, z_{A_i}\}$, $B_i\{x_{B_i}, y_{B_i}, z_{B_i}\}$, $C_i\{x_{C_i}, y_{C_i}, z_{C_i}\}$ are used. Assuming the wheel unit centre of mass is coincident with the centre of the wheel plane, the equations of motion of this type of wheel unit become:

$$\sum X_{B_{x_i}} = m_i \left(\dot{v}_{B_{x_i}} - \dot{\delta}_i v_{B_{y_i}} \right) ,$$

$$\sum Y_{B_{y_i}} = m_i \left(\dot{v}_{B_{y_i}} + \dot{\delta}_i v_{B_{x_i}} \right) ,$$

$$\sum Z_{B_{z_i}} = F_{z_i} + m_i g - F_{z_{C_i}} = 0 , \qquad\qquad (3.48)$$

$$\sum M_{B_i} = I_{B_i} \dot{\omega}_i ,$$

$$\sum N_{A_{z_i}} = I_{z_{A_i}} \ddot{\xi}_i = I_{z_{A_i}} \ddot{\delta}_i ,$$

where the linear accelerations of driving-steering wheel units along the x_{B_i} and y_{B_i} axes are $v_{x_{B_i}}$ and $v_{y_{B_i}}$ respectively. The angular acceleration of the driving disk about its horizontal axis

81

is $\dot{\omega}_i$, and steering rate about the fixed vertical axis z_{B_i} is $\dot{\delta}_i$. The total external force of this

unit along the x_{B_i}-axis is $\sum X_{B_i}$, the total external force of this unit along the along the y_{B_i}-

axis is $\sum Y_{B_i}$, and the total external force of this unit along the z_{B_i}-axis is $\sum Z_{B_i}$. The total

moment of the driving wheel about its horizontal axis is $\sum M_{B_i}$. The total moment of the

steering wheel about the z_{A_i}-axis is $\sum N_{A_i}$. The moment of inertia of a wheel plane about its

rotation axis is I_{B_i}, and the moment of the inertia of a wheel unit about a fixed vertical axis

at joint A_i is $I_{s_{A_i}}$.

Figure 3.7: A Free Body Diagram of Type A Driving-Steering Wheel Units.

Referring to Fig.3.7, the total external forces acting on the driving-steering wheel along the x_{B_i}, y_{B_i} and z_{A_i} axes can be represented by the following equations:

$$\sum X_{B_i} = (F_{t_i} - F_{f_i}) \cos \delta_i + |F_{l_i}| \cos (\delta_i - \text{sign}(\alpha_i)\frac{\pi}{2}) - F_{x_i} \ ,$$

$$\sum Y_{B_i} = (F_{t_i} - F_{f_i}) \sin \delta_i + |F_{l_i}| \sin (\delta_i - \text{sign}(\alpha_i)\frac{\pi}{2}) - F_{y_i} \ , \qquad (3.49)$$

$$\sum Z_{B_i} = F_{z_i} + m_i g - F_{zc_i} \ ,$$

with the applied tractive torque $T_{\omega_i} = I_{B_i} \dot{\omega}_i$ and the steering torque $T_{s_i} = I_{s_{A_i}} \ddot{\delta}_i$. Substituting Eqn. (3.48) into Eqn. (3. 49), the equations of motion for the driving-steering wheel unit can be represented as follows:

$$m_i (\dot{v}_{B_{x_i}} - \dot{\delta}_i v_{B_{y_i}}) = (F_{t_i} - F_{f_i}) \cos \delta_i + |F_{l_i}| \cos (\delta_i - \text{sign}(\alpha_i)\frac{\pi}{2}) - F_{x_i} \ ,$$

$$m_i (\dot{v}_{B_{y_i}} + \dot{\delta}_i v_{B_{x_i}}) = (F_{t_i} - F_{f_i}) \sin \delta_i + |F_{l_i}| \sin (\delta_i - \text{sign}(\alpha_i)\frac{\pi}{2}) - F_{y_i} \ ,$$

$$\qquad (3.50)$$

$$0 = F_{z_i} + m_i g - F_{zc_i} \ .$$

Rearranging above equation, the reaction forces acting on joint A_i of the driving-steering wheel unit by the vehicle main body along the x, y and z axes can be determined by the follows:

$$F_{x_i} = (F_{t_i} - F_{f_i}) \cos \delta_i - F_{l_i} \cos (\frac{\pi}{2} - \delta_i) - m_i (\dot{v}_{B_{x_i}} - \dot{\delta}_i v_{B_{y_i}}) \ ,$$

$$F_{y_i} = (F_{t_i} - F_{f_i}) \sin \delta_i + F_{l_i} \sin (\frac{\pi}{2} - \delta_i) - m_i (\dot{v}_{B_{y_i}} + \dot{\delta}_i v_{B_{x_i}}) \ ,$$

$$\qquad (3.51)$$

$$F_{z_i} = F_{zc_i} - m_i g \ .$$

In Eqn. (3.51), the friction force F_{f_t} and lateral force F_{l_t} can be obtained from Appendix B,

Eqns. (B.1), and (B.3). The normal force F_{zc_t} has been precalculated in Appendix C. In

addition, the velocity magnitude $v_{(xy)_{B_t}}$, the direction angle of the joint B_t, and the slip angle

α_t can be determined by Eqns. (2.14), (2.15) and (3.29) respectively. Applying kinematic

constraints 1 and 2 discussed in Section 2.5, the angular velocity and acceleration of the

driving wheel can be determined by Eqns. (2.23 a) and (2.24 a), and the steering angle can

be determined by Eqn.(2.27a).

Type B Driving-Steering Wheel Units: Fig.3.8 shows a free body diagram of a Type B

driving-steering wheel unit. Assuming the centre of mass of the driving-steering wheel unit

is D_t, an additional sub-coordinate system $D_t\{x_{D_t}, y_{D_t}, z_{D_t}\}$ is employed. Linear velocities

along the x_{D_t} and y_{D_t} axes are $v_{x_{D_t}}$ and $v_{y_{D_t}}$, and the angular velocity of the driving-steering

wheel unit about the z_{D_t}-axis is $\dot{\delta}_{D_t}$ (where $\dot{\delta}_{D_t} = \dot{\delta}_{A_t} = \dot{\delta}_t$). Angular acceleration of the

driving disk about its horizontal axis is $\dot{\omega}_t$. Based on D'Alembert's principle applied to the

"body-centred system" [39][60](refer to Appendix A, Section A.2), the equations of motion

of the Type B driving-steering wheel unit can be derived from Eqn. (A.5), and are as follows:

$$\sum X_{D_{x_t}} = m_t \ (v_{D_{x_t}} - \dot{\delta}_t v_{D_{y_t}}) \ , $$

$$\sum Y_{D_{y_t}} = m_t \ (v_{D_{y_t}} + \dot{\delta}_t v_{D_{x_t}}) \ , $$

$$\sum Z_{D_{z_t}} = F_{z_t} + m_t \ g - F_{zc_t} = 0 \ , \qquad\qquad (3.52)$$

$$\sum M_{B_t} = I_{B_t} \ \dot{\omega}_t \ , $$

$$\sum N_{D_{z_t}} = I_{z_{D_t}} \ddot{\delta}_t \ . $$

where $\sum X_{D_t}$ is the total external force acting on this unit along the x_{D_t} direction, which is also

84

the forward direction of vehicle motion. The total external force acting on this wheel unit along the y_{D_i} direction is ΣY_{D_i}. The total external force acting on this wheel unit along the z_{D_i} direction is ΣZ_{D_i}, which is identically zero. The total moment of the driving disk of the wheel unit about its horizontal axis is ΣM_{B_i}. The total moment of the driving-steering wheel unit about the z_{D_i}-axis is ΣN_{D_i}. The moment of inertia of a driving-steering wheel unit about its vertical axis (z_{D_i}) is $I_{s_{D_i}}$, and the moment of inertia of a driving disk about its rotation axis is I_{B_i}.

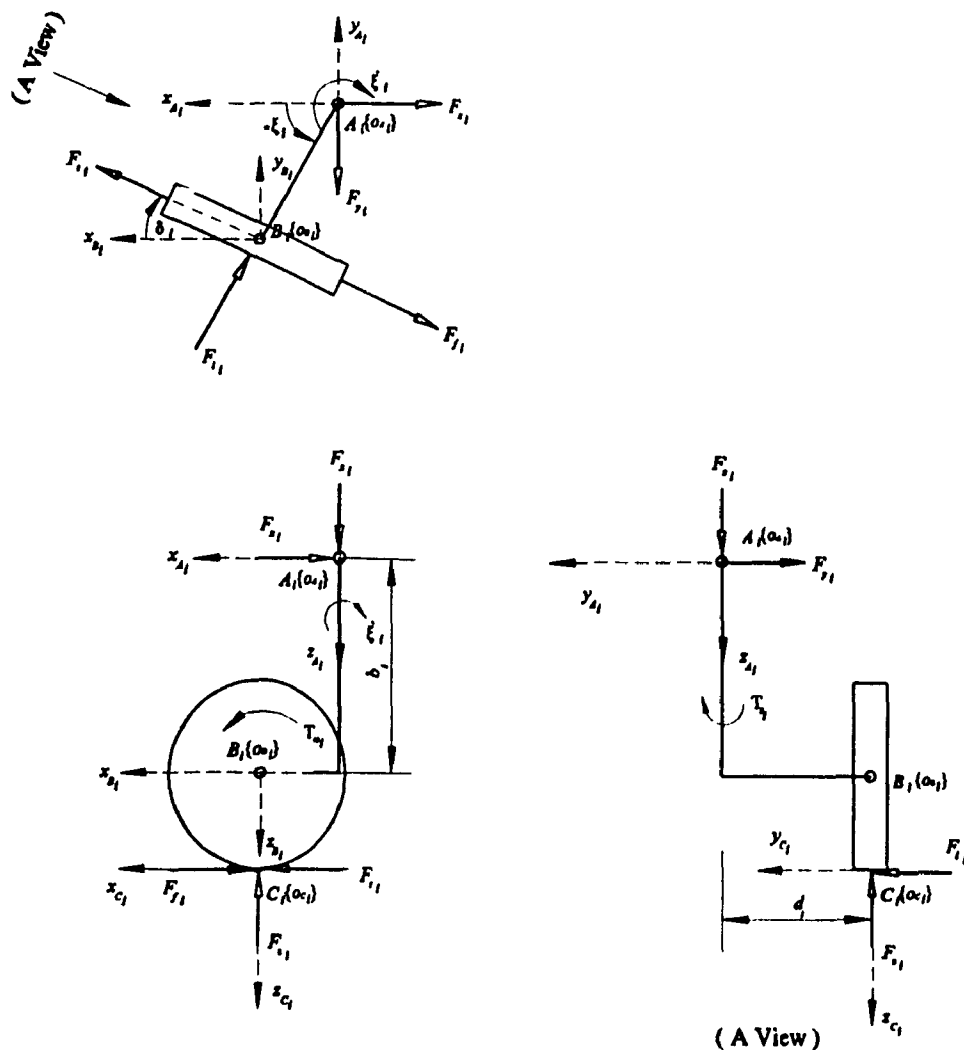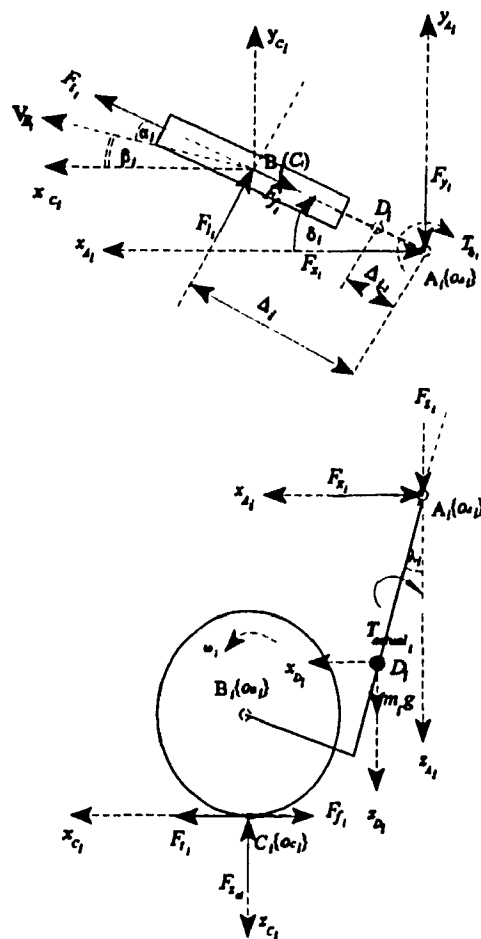**Figure 3.8:** A Free Body Diagram of Type B Driving-Steering Wheel Units.

Referring to Fig.3.8, the total external forces acting on the Type B driving-steering wheel unit along the x_{D_i}, y_{D_i} and z_{D_i} axes can be represented by the following equations:

$$\sum X_{D_i} = (F_{t_i} - F_{f_i})\cos\delta_i + |F_{l_i}|\cos(\delta_i - \text{sign}(\alpha_i)\frac{\pi}{2}) - F_{x_i},$$

$$\sum Y_{D_i} = (F_{t_i} - F_{f_i})\sin\delta_i + |F_{l_i}|\sin(\delta_i - \text{sign}(\alpha_i)\frac{\pi}{2}) - F_{y_i},$$

$$\sum Z_{D_i} = F_{z_i} + m_i g - F_{z_{C_i}},$$

$$\sum N_{D_i} = (-F_{x_i}\sin\delta_i + F_{y_i}\cos\delta_i)\Delta_{i_1} + F_{l_i}(\Delta_i - \Delta_{i_1}),$$

(3.53)

and the torque applied on the drive disk is T_{ω_i}, so that the tractive force is $F_{t_i} = T_{\omega_i}/R_i$. The horizontal distance between wheel-ground contact point and the z_{A_i}-axis is Δ_i, and the horizontal distance between the mass centre and the z_{A_i}-axis is Δ_{i_1}, and the radius of the driving disk is R_i. Substituting Eqn. (3. 52) into Eqn. (3.53), the equations of motion for the Type B driving-steering wheel unit can be represented as follows:

$$m_i(\dot{v}_{D_{x_i}} - \dot{\delta}_i v_{D_{y_i}}) = (F_{t_i} - F_{f_i})\cos\delta_i + |F_{l_i}|\cos(\delta_i - \text{sign}(\alpha_i)\frac{\pi}{2}) - F_{x_i},$$

$$m_i(\dot{v}_{D_{y_i}} + \dot{\delta}_i v_{D_{x_i}}) = (F_{t_i} - F_{f_i})\sin\delta_i + |F_{l_i}|\sin(\delta_i - \text{sign}(\alpha_i)\frac{\pi}{2}) - F_{y_i},$$

$$0 = F_{z_i} + m_i g - F_{z_{C_i}},$$

(3.54)

$$I_{z_{D_i}}\ddot{\delta}_i = (-F_{x_i}\sin\delta_i + F_{y_i}\cos\delta_i)\Delta_{i_1} + F_{l_i}(\Delta_i - \Delta_{i_1}).$$

Rearranging Eqn. (3.54), the reaction forces (F_{x_i}, F_{y_i}, F_{z_i}) acting by the vehicle main body can be expressed as follows:

86

$$F_{x_i} = (F_{t_i} - F_{f_i}) \cos \delta_i + |F_{l_i}| \cos (\delta_i - \text{sign}(\alpha_i)\frac{\pi}{2}) - m_i (\dot{v}_{D_{x_i}} - \dot{\delta}_i v_{D_{y_i}}) \, ,$$

$$F_{y_i} = (F_{t_i} - F_{f_i}) \sin \delta_i + |F_{l_i}| \sin (\delta_i - \text{sign}(\alpha_i)\frac{\pi}{2}) - m_i (\dot{v}_{D_{y_i}} + \dot{\delta}_i v_{D_{x_i}}) \, , \qquad (3.55)$$

$$F_{z_i} = F_{z_{C_i}} - m_i g \, ,$$

and the moment acting on the centre of mass of the driving-steering unit can be expressed using the following equation:

$$I_{z_{D_i}} \ddot{\delta}_i = m_i ((\dot{v}_{D_{x_i}} - \dot{\delta}_i v_{D_{y_i}}) \sin \delta_i - (\dot{v}_{D_{y_i}} + \dot{\delta}_i v_{D_{x_i}}) \cos \delta_i) + F_{l_i} \Delta_i \, . \qquad (3.56)$$

Eqn. (3.56) represents the mathematical constraint of the Type B driving-steering wheel unit. Similarly, in the above equations, the friction force F_{f_i} and lateral force F_{l_i} can be obtained from Appendix B, Eqns. (B.1), and (B.3). The normal force $F_{z_{C_i}}$ has been precalculated in Appendix C. The velocity magnitude $v_{(xy)_{B_i}}$, the direction angle of joint B_i, and the slip angle α_i can be determined by Eqns. (2.19), (2.20) and (3.43 c), respectively. Applying kinematic constraints 1 and 2, which are discussed in Section 2.5, the angular velocity and acceleration of the driving wheel can be determined by Eqn. (2.23 b) and (2.24 b), and the steering angle can be determined by Eqn. (2.27b).

3.3.5 Equations of Motion for Casters

A caster, considered as a rigid body [21][39], is shown schematically in Fig.3.9. The function of a caster is similar to that of a steering wheel unit, in that it can lead the direction of the vehicle by freely rotating about its pivot point A_i (i.e., the vertical axis z_{A_i}). However, no torque can be transferred to the vehicle main body through the pivot point A_i. Define the velocity along the direction of the caster heading as V_{h_i}, and the velocity perpendicular to the caster plane as V_{p_i}. Referring to Fig. 3.9, we can see that when the direction of the caster heading is not parallel to the velocity of the pivot point A_i, i.e., the velocity vector V_{A_i} at the pivot point is not aligned with the wheel plane of the caster, the pivot point leads the caster sideways as well as forward. Consequently, a side-friction force F_{C_i} acts at the contact point C_i in the direction opposite to the perpendicular velocity V_{v_i} to prevent side-slip. A torque due to the offset Δ_i and the side-friction force F_{C_i} causes the caster to rotate about the pivot point until the plane of the caster is in line with the velocity vector V_{A_i}.

Referring to Fig.3.9, there are two sub-coordinate systems $A_i\{ x_{A_i}, y_{A_i}, z_{A_i} \}$ and $C_i\{ x_{C_i}, y_{C_i}, z_{C_i} \}$ attached to the caster. The sub-coordinate system $D_i\{ x_{D_i}, y_{D_i}, z_{D_i} \}$ is located at the mass centre of the caster. Denote the linear velocity along the axes x_{D_i} and y_{D_i} as $v_{x_{D_i}}$ and $v_{y_{D_i}}$ respectively, and the angular velocity of the caster about the z_{D_i}-axis as ζ_{D_i} (where $\zeta_{D_i} = \zeta_{A_i}$). The equations of motion of the caster can be derived from Appendix A, Eqn. (A.3), and expressed as:

$$\sum X_{D_{x_i}} = m_i (\dot{v}_{D_{x_i}} - \zeta_i v_{D_{y_i}}) \,,$$

$$\sum Y_{D_{y_i}} = m_i (\dot{v}_{D_{y_i}} + \zeta_i v_{D_{x_i}}) \,, \tag{3.57}$$

$$\sum N_{D_{z_i}} = I_{z_{D_i}} \dot{\zeta}_i \,,$$

where m_i is the mass of the caster and the total external forces acting on the caster along the x_{D_i} and y_{D_i} axes are $\sum X_{D_i}$ and $\sum Y_{D_i}$. The total moment acting on the caster about the z_{D_i} -axis is $\sum Z_{D_i}$.
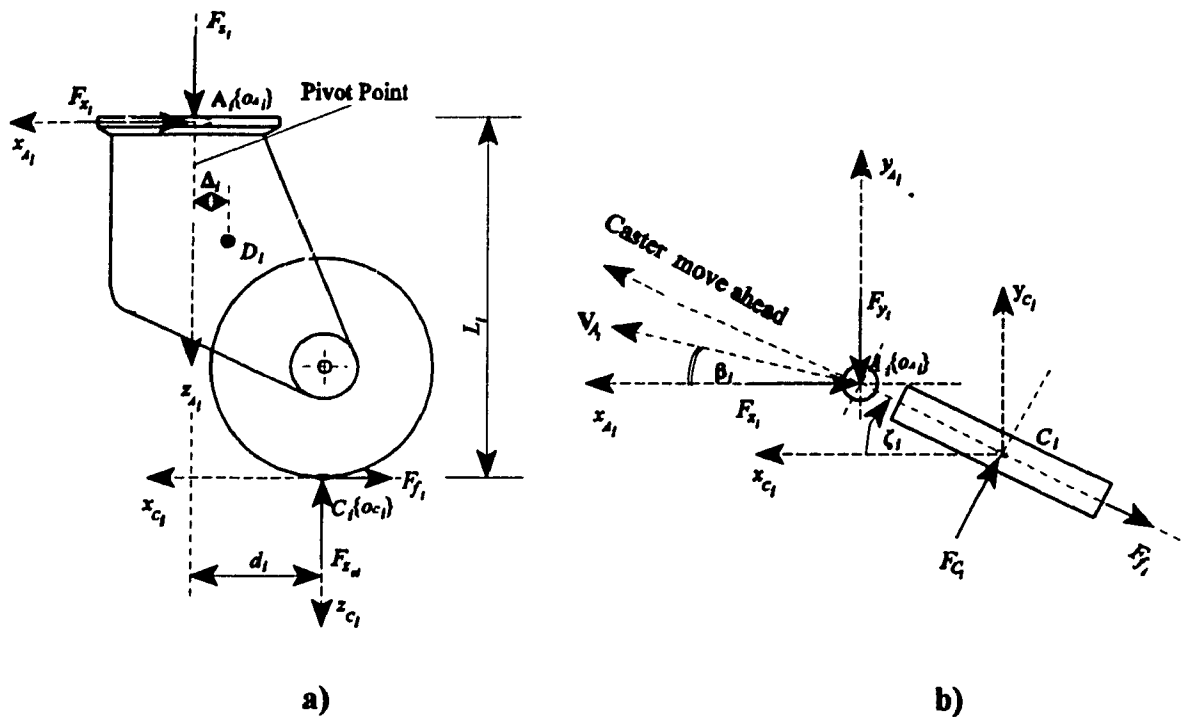
Figure 3.9: A Free Body Diagram of a Caster.

As shown in Fig. 3.9 b), the angle between the x_{C_i} -axis and the caster heading is defined as ζ_i, with positive clockwise as seen from above. The direction of the side-friction force F_{C_i} is always opposite to the trend of the side-slip. It depends on the direction of the pivot point velocity V_{A_i} (i.e., the direction angle β_i) and the direction of the caster heading (i.e., the angle ζ_i). If $[\beta_i - \zeta_i]$ is positive, the side-friction force F_{C_i} is negative; otherwise the side-friction force F_{C_i} is positive. If $[\beta_i - \zeta_i]$ is zero, the perpendicular velocity v_{v_i} is equal to zero and the side-friction force F_{C_i} is identically zero. According to Huang [21], the side-

friction force F_{C_i} can derived by following equation:

$$F_{C_i} = -k_{ai} \, F_{s_i} \, \text{sign} \, (\beta_i - \zeta_i) \, . \tag{3.58}$$

Thus, the total external forces $\sum X_{D_i}$ and $\sum Y_{D_i}$ and moments $\sum N_{D_i}$ of the caster can be represented by the following equations:

$$\sum X_{D_i} = -F_{f_i} \cos \zeta_i + F_{C_i} \cos \left(\zeta_i + \text{sign} \, (\zeta_i) \frac{\pi}{2} \right) - F_{x_i} \, ,$$

$$\sum Y_{D_i} = -F_{f_i} \sin \zeta_i + F_{C_i} \sin \left(\zeta_i + \text{sign} \, (\zeta_i) \frac{\pi}{2} \right) - F_{y_i} \, ; \tag{3.59}$$

$$\sum N_{D_i} = (F_{x_i} \sin \zeta_i - F_{y_i} \cos \zeta_i) \Delta_{l_i} + F_{C_i} (\Delta_i - \Delta_{l_i}) \, .$$

Substituting Eqn. (3.59) into Eqn. (3.57), the equations of motion of the caster can be rewritten as:

$$m_i \, (\dot{v}_{D_{x_i}} - \dot{\zeta}_i v_{D_{y_i}}) = -F_{f_i} \cos \zeta_i + F_{C_i} \cos \left(\zeta_i + \text{sign} \, (\zeta_i) \frac{\pi}{2} \right) - F_{x_i} \, ,$$

$$m_i \, (\dot{v}_{D_{y_i}} + \dot{\zeta}_i v_{D_{x_i}}) = -F_{f_i} \sin \zeta_i + F_{C_i} \sin \left(\zeta_i + \text{sign} \, (\zeta_i) \frac{\pi}{2} \right) - F_{y_i} \, , \tag{3.60}$$

$$I_{s_{D_i}} \, \ddot{\zeta}_i = (F_{x_i} \sin \zeta_i - F_{y_i} \cos \zeta_i) \Delta_i + F_{C_i} (\Delta_i - \Delta_{l_i}) \, .$$

Rearranging Eqn. (3.60), the reaction forces acting on the caster through the vehicle main body can be obtained as:

$$F_{x_i} = -F_{f_i} \cos \zeta_i + F_{C_i} \cos \left(\zeta_i + \text{sign} \, (\zeta_i) \frac{\pi}{2} \right) - m_i \, (\dot{v}_{D_{x_i}} - \dot{\zeta}_i v_{D_{y_i}}) \, ,$$

$$F_{y_i} = -F_{f_i} \sin \zeta_i + F_{C_i} \sin \left(\zeta_i + \text{sign} \, (\zeta_i) \frac{\pi}{2} \right) - m_i \, (\dot{v}_{D_{y_i}} + \dot{\zeta}_i v_{D_{x_i}}) \, ,$$

$$F_{z_i} = F_{z_{C_i}} - m_i \, g \, , \tag{3.61}$$

90

where the horizontal distance between the centre of the mass of this unit and the pivot axis

(z_{A_i}) is Δ_{t_1}, and the polar moment of the caster about this axis can be represented as:

$$I_{z_{D_i}} \check{\zeta}_i = F_{c_i} \Delta_i .$$

(3.62)

3.3.6 Section Summary

In this section, the D'Alembert method is used to derive the equations of motion of each component of the vehicle system. These components are the vehicle main body, driving wheel units, Type A and B steering wheel units, Type A and B driving-steering units, and casters. Expressions are found for the tractive forces, torques and / or steering angles of each wheel unit, subject to kinematic constraints. These constraints are (i) pure rolling, and (ii) non-slipping at the wheel-ground contact point. For each wheel unit, expressions for reaction forces acting by the vehicle main body are established.

3.4 Dynamic Equations of the Automated Vehicle

In the previous sections, characteristics of the vehicle main body and wheel units have been discussed in detail by considering them as separate rigid bodies. Equations of motion have been derived for each of these components. The forces acting on each wheel unit by the vehicle main body also have been determined. The objective of this section is to derive a dynamical formulation for the vehicle system by examining interconnection forces between the vehicle main body and each wheel through joints A_i and B_i. The external forces and moments acting on the vehicle system by the ground are formulated by integrating wheel unit with the vehicle main body.

91

3.4.1 Equation of Motion of the Vehicle Along the x-Axis

Since the forces acting on each joint A_i (or B_i) of the vehicle main body by each wheel unit are equal and opposite to the forces acting on each wheel unit by the vehicle main body at joints A_i (or B_i), we may formulate expressions for the external forces acting on the vehicle main body in the normalized forms F_{x_i}', F_{y_i}' and F_{z_i}' with respect to the x, y and z axes of frame $\{Q\}$ (see Fig.3.2). From Section 3.3, the total external fores acting on the vehicle main body along the x-axis can be derived by substituting F_{x_i}' ($= -F_{x_i}$ and $i = 1, 2, ..., n$) from Eqns. (3.30), (3.35 or 3.40), (3.51 or 3.55), and (3.61) into (3.17), resulting in the following equation:

$$
\sum X' = \sum_{i=1}^{n_d} F_{x_i}' + \sum_{i=n_d+1}^{n_d+n_s} F_{x_i}' + \sum_{i=n_d+n_s+1}^{n_d+n_s+n_{ds}} F_{x_i}' + \sum_{i=n_d+n_s+n_{ds}+1}^{n} F_{x_i}'
$$

$$
= \sum_{i=1}^{n_d} ((F_{t_i} - F_{f_i}) - m_i \, v_{B_{x_i}})
$$

$$
+ \sum_{i=n_d+1}^{n_d+n_s} (-F_{f_i} \cos \delta_i + |F_{l_i}| \cos (\delta_i - \text{sign}(\alpha_i)\frac{\pi}{2}) - m_i (v_{B_{x_i}} - \dot{\delta}_i v_{B_{y_i}}))
$$

$$
+ \sum_{i=n_d+n_s+1}^{n_d+n_s+n_{ds}} ((F_{t_i} - F_{f_i}) \cos \delta_i + |F_{l_i}| \cos (\delta_i - \text{sign}(\alpha_i)) - m_i (v_{B_{x_i}} - \dot{\delta}_i v_{B_{y_i}}))
$$

$$
+ \sum_{i=n_d+n_s+n_{ds}+1}^{n} (-F_{f_i} \cos \zeta_i + F_{c_i} \cos (\zeta_i + \text{sign}(\zeta_i)\frac{\pi}{2}) - m_i (v_{D_{x_i}} - \dot{\zeta}_i v_{D_{y_i}})) ,
$$

where, n_s, n_s n_{ds} and n_c are the number of driving wheel units, steering wheel units, driving-steering wheel units and casters, respectively, and the total number of wheel units is n. Rearranging the above equation, and letting:

$$\sum_{i=1}^{n} m_i \, a_{x_i} = \sum_{i=1}^{n_d} m_i \, \dot{v}_{B_{x_i}} + \sum_{i=n_d+1}^{n_d+n_s} m_i \, (\dot{v}_{B_{x_i}} - \delta_i \dot{v}_{B_{y_i}})$$

$$(3.63)$$

$$+ \sum_{i=n_d+n_s+1}^{n_d+n_s+n_{ds}} m_i \, (\dot{v}_{B_{x_i}} - \delta_i \dot{v}_{B_{y_i}}) + \sum_{i=n_d+n_s+n_{ds}+1}^{n} m_i \, (\dot{v}_{D_{x_i}} - \zeta_i \dot{v}_{D_{y_i}}) \, ,$$

gives the total external fores acting on the vehicle main body along the x-axis:

$$\sum X' = \sum_{i=1}^{n_d} (F_{t_i} - F_{f_i}) - \sum_{i=n_d+1}^{n_d+n_s} (F_{f_i} \cos \delta_i + |F_{l_i}| \cos (\delta_i - \text{sign} (\alpha_i)\frac{\pi}{2})$$

$$+ \sum_{i=n_d+n_s+1}^{n_d+n_s+n_{ds}} ((F_{t_i} - F_{f_i}) \cos \delta_i + |F_{l_i}| \cos (\delta_i - \text{sign} (\alpha_i)\frac{\pi}{2})) \qquad (3.64)$$

$$+ \sum_{i=n_d+n_s+n_{ds}+1}^{n} (-F_{f_i} \cos \zeta_i + F_{c_i} \cos (\zeta_i + \text{sign} (\zeta_i)\frac{\pi}{2}) - \sum_{i=1}^{n} m_i \rho_{x_i} \, .$$

where the mass of each wheel unit is m_i, which is also defined as the unsprung mass m_{u_i} in Section 3.2. The acceleration of the centre of mass of each wheel unit along the x-axis is a_{x_i}. The inertial force due to the total unsprung mass along the x-axis should be equal to the summation of inertial forces caused by each individual wheel unit along the x-axis, thus we have that:

$$m_u a_{u_x} = \sum_{i=1}^{n} m_i \rho_{x_i} \, . \qquad (3.65)$$

Merging Eqns. (3.64), (3.65) and (3.16) yields the following equation:

$$m_s a_{s_x} + m_u a_{u_x} = \sum_{i=1}^{n_d} (F_{t_i} - F_{f_i}) - \sum_{i=n_d+1}^{n_d+n_s} (F_{f_i} \cos \delta_i + |F_{l_i}| \cos (\delta_i - \text{sign}\,(\alpha_i)\frac{\pi}{2}))$$

$$+ \sum_{i=n_d+n_s+1}^{n_d+n_s+n_{ds}} ((F_{t_i} - F_{f_i}) \cos \delta_i + |F_{l_i}| \cos (\delta_i - \text{sign}\,(\alpha_i)\frac{\pi}{2})) \qquad (3.66)$$

$$+ \sum_{i=n_d+n_s+n_{ds}+1}^{n} (-F_{f_i} \cos \zeta_i + F_{c_i} \cos (\zeta_i + \text{sign}\,(\zeta_i)\frac{\pi}{2})),$$

which illustrates that the summation of inertial forces due to both the sprung mass and

unsprung mass is equal to the total external forces acting on the vehicle by the ground along

the x-axis. Again substituting a_{s_x} and a_{u_x} from Eqns. (3.3) and (3.4) into the above equation,

the equation of motion of the vehicle along the x-axis can be represented as:

$$\sum X = m (\dot{u} - \gamma v) - \gamma p h_s m_s$$

$$= \sum_{i=1}^{n_d} (F_{t_i} - F_{f_i}) - \sum_{i=n_d+1}^{n_d+n_s} (F_{f_i} \cos \delta_i + |F_{l_i}| \cos (\delta_i - \text{sign}\,(\alpha_i)\frac{\pi}{2}))$$

$$+ \sum_{i=n_d+n_s+1}^{n_d+n_s+n_{ds}} ((F_{t_i} - F_{f_i}) \cos \delta_i + |F_{l_i}| \cos (\delta_i - \text{sign}\,(\alpha_i)\frac{\pi}{2})) \qquad (3.67)$$

$$+ \sum_{i=n_d+n_s+n_{ds}+1}^{n} (-F_{f_i} \cos \zeta_i + F_{c_i} \cos (\zeta_i + \text{sign}\,(\zeta_i)\frac{\pi}{2})),$$

In the above equation, the tractive force is F_{t_i} ($= \dfrac{I_{B_i} \dot{\omega}_i}{R_i}$), and $\dot{\omega}_i$ is the angular

acceleration of the driving wheel which may be determined from the kinematical constraints

discussed in the previous section, or by other means. The friction force, lateral force and side

force of the caster are F_{f_i} ($= f_r F_{z_{C_i}}$), F_{l_i} ($= C_{s_i} \alpha_i$) and F_{c_i} respectively. The slip angle,

steering angle and caster rotation angle are α_i, δ_i, ζ_i, respectively. All of these variables

94

have been discussed in previous sections of this Chapter and Appendix B.

3.4.2 Equation of Motion of the Vehicle Along the y-Axis

Similarly, the equation of motion of the vehicle system along the y-axis can determined by integrating each wheel unit with the vehicle main body. Substituting F_{y_i}' ($= -F_{y_i}$ and $i = 1$, 2, ..., n) from Eqns. (3.30), (3.35 or 3.40), (3.51 or 3.55), and (3.61) into (3.17), we have the total external forces acting on the vehicle main body by each wheel unit along the y-axis, which can be expressed as the following equation:

$$\sum Y' = \sum_{i=1}^{n_d} F_{y_i}' + \sum_{i=n_d+1}^{n_d+n_s} F_{y_i}' + \sum_{i=n_d+n_s+1}^{n_d+n_s+n_{dr}} F_{y_i}' + \sum_{i=n_d+n_s+n_{dr}+1}^{n} F_{y_i}'$$

$$= \sum_{i=1}^{n_d} (F_{l_i} - m_i\, v_{B_{y_i}}) + \sum_{i=n_d+1}^{n_d+n_s} (\, -F_{f_i} \sin\delta_i + |F_{l_i}| \sin(\delta_i - \text{sign}\,(\alpha_i)\frac{\pi}{2}) - m_i\,(v_{B_{y_i}} + \delta_i v_{B_{x_i}})\,)$$

$$+ \sum_{i=n_d+n_s+1}^{n_d+n_s+n_{dr}} (\, (F_{t_i} - F_{f_i}) \sin\delta_i + |F_{l_i}| \sin(\delta_i - \text{sign}\,(\alpha_i)\frac{\pi}{2}) - m_i\,(v_{B_{y_i}} + \delta_i v_{B_{x_i}})\,)$$

$$+ \sum_{i=n_d+n_s+n_{dr}+1}^{n} (\, -F_{f_i} \sin\zeta_i + F_{C_i} \sin(\zeta_i + \text{sign}\,(\zeta_i)\frac{\pi}{2}) - m_i\,(v_{D_{y_i}} + \zeta_i v_{D_{x_i}})\,) \,,$$

Let:

$$\sum m_i\, a_{y_i} = \sum_{i=1}^{n_d} (\, m_i\, v_{B_{y_i}}) + \sum_{i=n_d+1}^{n_d+n_s} m_i\,(v_{B_{y_i}} + \delta_i v_{B_{x_i}})$$

$$+ \sum_{i=n_d+n_s+1}^{n_d+n_s+n_{dr}} m_i\,(v_{B_{y_i}} + \delta_i v_{B_{x_i}}) + \sum_{i=n_d+n_s+n_{dr}+1}^{n} m_i\,(v_{D_{y_i}} + \zeta_i v_{D_{x_i}}) \,, \tag{3.68}$$

then,

95

$$\sum Y' = \sum_{i=1}^{n_d} F_{l_i} + \sum_{i=n_d+1}^{n_d+n_s} (-F_{f_i} \sin \delta_i + |F_{l_i}| \sin(\delta_i - \text{sign}\,(\alpha_i)\frac{\pi}{2})$$

$$+ \sum_{i=n_d+n_s+1}^{n_d+n_s+n_{lr}} (\,(F_{l_i} - F_{f_i}) \sin \delta_i + |F_{l_i}| \sin(\delta_i - \text{sign}\,(\alpha_i)\frac{\pi}{2})\,) \tag{3.69}$$

$$+ \sum_{i=n_d+n_s+n_{lr}+1}^{n} (\,-F_{f_i} \sin \zeta_i + F_{c_i} \sin(\zeta_i + \text{sign}\,(\zeta_i)\frac{\pi}{2})) - \sum_{i=1}^{n} m_i\, a_{y_i}\;,$$

As with Section 3.2, the mass of each wheel unit is m_i, which is the same as the unsprung mass m_{u_i}. The acceleration of the centre of mass of each wheel unit along the y-axis is a_{y_i}. The inertial force due to the total unsprung mass along the y-axis is equal to the summation of inertial forces from each individual wheel unit along the y-axis, thus:

$$m_u a_{u_y} = \sum_{i=1}^{n} m_i \rho_{y_i}\;. \tag{3.70}$$

Merging Eqns. (3.69), (3.70) and (3.16), yields the following equation:

$$m_s a_{s_y} + m_u a_{u_y} = \sum_{i=1}^{n_d} F_{l_i} + \sum_{i=n_d+1}^{n_d+n_s} (-F_{f_i} \sin \delta_i + |F_{l_i}| \sin(\delta_i - \text{sign}\,(\alpha_i)\frac{\pi}{2})$$

$$+ \sum_{i=n_d+n_s+1}^{n_d+n_s+n_{lr}} (\,(F_{l_i} - F_{f_i}) \sin \delta_i + |F_{l_i}| \sin(\delta_i - \text{sign}\,(\alpha_i)\frac{\pi}{2})\,) \tag{3.71}$$

$$+ \sum_{i=n_d+n_s+n_{lr}+1}^{n} (\,-F_{f_i} \sin \zeta_i + F_{c_i} \sin(\zeta_i + \text{sign}\,(\zeta_i)\frac{\pi}{2}))\;,$$

which illustrates that the summation of inertial forces caused by both the sprung mass and unsprung mass is equal to the total external forces acting on the vehicle by the ground along

the y-axis. Substituting a_{t_y} and a_{u_y} from Eqns. (3.6) and (3.7) into the above equation, the

equation of motion of the vehicle along the y-axis can be represented as follows:

$$\sum Y = m \ (\dot{v} + \gamma u) + m_s \ \dot{p} h_s$$

$$= \sum_{i=1}^{n_d} F_{t_i} + \sum_{i=n_d+1}^{n_d+n_s} (-F_{f_i} \sin \delta_i + |F_{t_i}| \sin (\delta_i - \text{sign}(\alpha_i)\frac{\pi}{2})$$

$$+ \sum_{i=n_d+n_s+1}^{n_d+n_s+n_{dr}} (\ (F_{t_i} - F_{f_i}) \sin \delta_i + |F_{t_i}| \sin (\delta_i - \text{sign}(\alpha_i)\frac{\pi}{2}) \ ) \qquad \text{(3.72)}$$

$$+ \sum_{i=n_d+n_s+n_{dr}+1}^{n} (\ -F_{f_i} \sin \zeta_i + F_{c_i} \sin (\zeta_i + \text{sign}(\zeta_i)\frac{\pi}{2})) \ .$$

3.4.3 Equation of Rolling Motion of the Vehicle Above the x-Axis

Since the vehicle rolling motion is caused only by the sprung mass, the rolling motion of the

vehicle system is equal to the rolling motion of the vehicle main body. Therefore the equation

of motion of the vehicle system can be obtained from Eqn. (3.25), and is as follows:

$$I_{t_x} \dot{p} + m_s h_s \ (\dot{v} + \gamma u) - I_{t_{xz}} \dot{\gamma} = T_G - T_S - T_D , \qquad \text{(3.73)}$$

where the moment T_S, produced by the spring forces of the suspension system, is defined as:

$$T_S = (C_{\varphi_1} + C_{\varphi_2} + \ldots\ldots + C_{\varphi_n}) \ \varphi = \sum_{i=1}^{n} C_{\varphi_i} \ \varphi = C_\varphi \ \varphi ,$$

and the moment T_D, produced by the spring damping forces of the suspension system, is

defined as:

97

$$T_D = (\frac{\partial L_1}{\partial p_1} + \frac{\partial L_2}{\partial p_2} + \dots\dots + \frac{\partial L_n}{\partial p_n}) \dot\varphi = \sum_{i=1}^{n} \frac{\partial L_i}{\partial p_i} \dot\varphi = L_p \, p \, ,$$

where the total number of employed wheels is n. The moment T_G is due to the weight of the sprung mass, and is:

$$T_G = G_S \, h_t \, \sin(\varphi) \approx m_s \, g \, h_t \, \varphi \, ,$$

Here, the equivalent rolling stiffness is C_θ, for which $[C_\theta] = [\text{N·m·rad}^{-1}]$, and L_p is the damping coefficient of the entire suspension system, for which $[L_p] = [\text{N·m·s·rad}^{-1}]$ and g is the acceleration of gravity.

3.4.4 Equation of Yaw Motion of the Vehicle About the z-Axis

In the four degree of freedom vehicle system, the load on each wheel is redistributed during rolling motion. Friction in the left and right wheels is not equal, and the lateral forces of front and rear wheels are also not equal. These differences give rise to moments about the z-axis, i.e., these differences will cause the yaw motion of the vehicle. Furthermore, for certain types of desired vehicle paths, yaw motion is necessary. In such cases, unequal tractive forces or steering angles may occur on each wheel unit. Using the same approach as for deriving the equations of motion of the vehicle along the x and y axes, the equation of yaw motion of the vehicle system about the z-axis can be determined by integrating each wheel unit with the vehicle main body.

Substituting F_{x_i}' and F_{y_i}' ($i = 1, 2, \dots, n$) from Eqns.. (3.30), (3.35 or 3.40), (3.51 or 3.55), and (3.61) into (3.17), the summation of moments about the z-axis of the vehicle system can be represented as follows:

98

$$\sum N' = -\sum_{i=1}^{n} (F'_{x_i} y_{e_i}) + \sum_{i=1}^{n} (F'_{y_i} x_{e_i})$$

$$= -\sum_{i=1}^{n_d} (F_{t_i} - F_{f_i}) y_{e_i} + \sum_{i=n_d+1}^{n_d+n_s} (F_{f_i} \cos \delta_i + |F_{l_i}| \cos(\delta_i - \text{sign}(\alpha_i)\frac{\pi}{2})y_{e_i}$$

$$- \sum_{i=n_d+n_s+1}^{n_d+n_s+n_{ds}} ((F_{t_i} - F_{f_i}) \cos \delta_i + |F_{l_i}| \cos(\delta_i - \text{sign}(\alpha_i)\frac{\pi}{2})) y_{e_i}$$

$$+ \sum_{i=n_d+n_s+n_{ds}+1}^{n} (F_{f_i} \cos \zeta_i - F_{C_i} \cos(\zeta_i + \text{sign}(\zeta_i)\frac{\pi}{2})) y_{e_i} + \sum_{i=1}^{n} m_i a_{x_i} y_{e_i}$$

$$+ \sum_{i=1}^{n_d} F_{l_i} x_{e_i} + \sum_{i=n_d+1}^{n_d+n_s} (-F_{f_i} \sin \delta_i + |F_{l_i}| \sin(\delta_i - \text{sign}(\alpha_i)\frac{\pi}{2})) x_{e_i}$$

$$+ \sum_{i=n_d+n_s+1}^{n_d+n_s+n_{ds}} ((F_{t_i} - F_{f_i}) \sin \delta_i + |F_{l_i}| \sin(\delta_i - \text{sign}(\alpha_i)\frac{\pi}{2}) x_{e_i}$$

$$+ \sum_{i=n_d+n_s+n_{ds}+1}^{n} (-F_{f_i} \sin \zeta_i + F_{C_i} \sin(\zeta_i + \text{sign}(\zeta_i)\frac{\pi}{2}) x_{e_i} - \sum_{i=1}^{n} m_i a_{y_i} y_{e_i},$$

Substituting $\sum N'$ from Eqn. (3.19) into the above equation and rearranging it, yields the following:

$$\sum \delta m_i (x a_y - y a_x) + \sum_{i=1}^{n} m_i (a_{y_i} x_{e_i} - a_{x_i} y_{e_i}) = -\sum_{i=1}^{n} (F'_{x_i} y_{e_i}) + \sum_{i=1}^{n} (F'_{y_i} x_{e_i})$$

$$= -\sum_{i=1}^{n_d} (F_{t_i} - F_{f_i}) y_{e_i} + \sum_{i=n_d+1}^{n_d+n_s} (F_{f_i} \cos \delta_i + |F_{l_i}| \cos(\delta_i - \text{sign}(\alpha_i)\frac{\pi}{2})y_{e_i}$$

$$- \sum_{i=n_d+n_s+1}^{n_d+n_s+n_{ds}} ((F_{t_i} - F_{f_i}) \cos \delta_i + |F_{l_i}| \cos(\delta_i - \text{sign}(\alpha_i)\frac{\pi}{2})) y_{e_i}$$

$$+ \sum_{i=n_d+n_s+n_{ds}+1}^{n} (F_{f_i} \cos \zeta_i + F_{C_i} \cos(\zeta_i + \text{sign}(\zeta_i)\frac{\pi}{2})) y_{e_i} \qquad (3.74)$$

$$+ \sum_{i=1}^{n_d} F_{l_i} x_{e_i} + \sum_{i=n_d+1}^{n_d+n_s} (-F_{f_i} \sin \delta_i + |F_{l_i}| \sin(\delta_i - \text{sign}(\alpha_i)\frac{\pi}{2})) x_{e_i}$$

$$+ \sum_{i=n_d+n_s+1}^{n_d+n_s+n_{ds}} ((F_{t_i} - F_{f_i}) \sin \delta_i + |F_{l_i}| \sin(\delta_i - \text{sign}(\alpha_i)\frac{\pi}{2}) x_{e_i}$$

$$+ \sum_{i=n_d+n_s+n_{ds}+1}^{n} (-F_{f_i} \sin \zeta_i + F_{C_i} \sin(\zeta_i + \text{sign}(\zeta_i)\frac{\pi}{2}) x_{e_i},$$

where the term $\sum \delta m_s(xa_y - ya_x)$ represents the inertial moment about the yaw (z) axis caused by the total sprung mass, and the term $\sum_{i=1}^{n} m_i(a_{y_i}x_{e_i} - a_{x_i}y_{e_i})$ represents the summation of inertial moments about the yaw axis caused by each wheel unit (i.e., the unsprung mass). Therefore, the summation of these two terms should be equal to the total inertial moment acting on the entire vehicle system about the yaw axis, which is:

$$\sum N = \sum \delta m_s(xa_y - ya_x) + \sum_{i=1}^{n} m_i(a_{y_i}x_{e_i} - a_{x_i}y_{e_i})$$

$$= I_z\dot{\gamma} - I_{xz}\dot{p}. \qquad (3.75)$$

Substituting Eqn.(3.75) into Eqn. (3.74) yields the equation of motion of the vehicle about the yaw (z) axis:

$$I_z\dot{\gamma} - I_{xz}\dot{p} = -\sum_{i=1}^{n} (F'_{x_i} y_{e_i}) + \sum_{i=1}^{n} (F'_{y_i} x_{e_i})$$

$$= -\sum_{i=1}^{n_d} (F_{t_i} - F_{f_i}) y_{e_i} + \sum_{i=n_d+1}^{n_d+n_s} (F_{f_i} \cos \delta_i + |F_{l_i}| \cos (\delta_i - \text{sign} (\alpha_i)\frac{\pi}{2})y_{e_i}$$

$$- \sum_{i=n_d+n_s+1}^{n_d+n_s+n_{dr}} ((F_{t_i} - F_{f_i}) \cos \delta_i + |F_{l_i}| \cos(\delta_i - \text{sign} (\alpha_i)\frac{\pi}{2})) y_{e_i}$$

$$+ \sum_{i=n_d+n_s+n_{dr}+1}^{n} (F_{f_i} \cos \zeta_i + F_{c_i} \cos (\zeta_i + \text{sign} (\zeta_i)\frac{\pi}{2})) y_{e_i} \qquad (3.76)$$

$$+ \sum_{i=1}^{n_d} F_{t_i}x_{e_i} + \sum_{i=n_d+1}^{n_d+n_s} (-F_{f_i} \sin \delta_i + |F_{l_i}| \sin(\delta_i - \text{sign} (\alpha_i)\frac{\pi}{2}))x_{e_i}$$

$$+ \sum_{i=n_d+n_s+1}^{n_d+n_s+n_{dr}} ((F_{t_i} - F_{f_i}) \sin \delta_i + |F_{l_i}| \sin(\delta_i - \text{sign} (\alpha_i)\frac{\pi}{2})x_{e_i}$$

$$+ \sum_{i=n_d+n_s+n_{dr}+1}^{n} (-F_{f_i} \sin \zeta_i + F_{c_i} \sin (\zeta_i + \text{sign} (\zeta_i)\frac{\pi}{2})x_{e_i} .$$

3.5 Forward Dynamic Model

At this point, the equations of the motion of the vehicle along the x and y axes, as well as the equations of motion of the vehicle about the x and z axes have been completely derived in Eqns. (3.67), (3.72), (3.73) and (3.76). Summarizing these equations, the four DOFs vehicle dynamic model can be represented as follows:

$$\sum X = m \, (\dot{u} - \gamma v) - \gamma p h_i m_s$$

$$= \sum_{i=1}^{n_d} (F_{t_i} - F_{f_i}) - \sum_{i=n_d+1}^{n_d+n_s} (F_{f_i} \cos \delta_i + |F_{l_i}| \cos (\delta_i - \text{sign} (\alpha_i)\frac{\pi}{2}))$$

$$+ \sum_{i=n_d+n_s+1}^{n_d+n_s+n_{ds}} ((F_{t_i} - F_{f_i}) \cos \delta_i + |F_{l_i}| \cos (\delta_i - \text{sign} (\alpha_i)\frac{\pi}{2}))$$

$$+ \sum_{i=n_d+n_s+n_{ds}+1}^{n} (-F_{f_i} \cos \zeta_i + F_{c_i} \cos ((\zeta_i + \text{sign} (\zeta_i)\frac{\pi}{2})) \,,$$

$$\sum Y = m \, (\dot{v} + \gamma u) + m_s \dot{p} h_s$$

$$= \sum_{i=1}^{n_d} F_{l_i} + \sum_{i=n_d+1}^{n_d+n_s} (-F_{f_i} \sin \delta_i + |F_{l_i}| \sin (\delta_i - \text{sign} (\alpha_i)\frac{\pi}{2})$$

$$+ \sum_{i=n_d+n_s+1}^{n_d+n_s+n_{ds}} ((F_{t_i} - F_{f_i}) \sin \delta_i + |F_{l_i}| \sin (\delta_i - \text{sign} (\alpha_i)\frac{\pi}{2}))$$

$$+ \sum_{i=n_d+n_s+n_{ds}+1}^{n} (-F_{f_i} \sin \zeta_i + F_{c_i} \sin ((\zeta_i + \text{sign} (\zeta_i)\frac{\pi}{2})) \,,$$

$$I_{s_x} \dot{p} + m_s h_s (\dot{v} + \gamma u) - I_{s_{xz}} \dot{\gamma} = T_G - T_S - T_D \,, \tag{3.77}$$

101

$$I_z\dot\gamma - I_{xz}\dot{p} = -\sum_{i=1}^{n} (F'_{x_i} y_{e_i}) + \sum_{i=1}^{n} (F'_{y_i} x_{e_i})$$

$$= -\sum_{i=1}^{n_d} (F_{t_i} - F_{f_i}) y_{e_i} + \sum_{i=n_d+1}^{n_d+n_s} (F_{f_i} \cos \delta_i + |F_{t_i}| \cos (\delta_i - \text{sign}(\alpha_i)\frac{\pi}{2}) y_{e_i}$$

$$- \sum_{i=n_d+n_s+1}^{n_d+n_s+n_{dc}} ((F_{t_i} - F_{f_i}) \cos \delta_i + |F_{t_i}| \cos (\delta_i - \text{sign}(\alpha_i)\frac{\pi}{2})) y_{e_i}$$

$$+ \sum_{i=n_d+n_s+n_{dc}+1}^{n} (F_{f_i} \cos \zeta_i + F_{c_i} \cos((\zeta_i + \text{sign}(\zeta_i)\frac{\pi}{2})) y_{e_i}$$

$$+ \sum_{i=1}^{n_d} F_{t_i} x_{e_i} + \sum_{i=n_d+1}^{n_d+n_s} (-F_{f_i} \sin \delta_i + |F_{t_i}| \sin(\delta_i - \text{sign}(\alpha_i)\frac{\pi}{2})) x_{e_i}$$

$$+ \sum_{i=n_d+n_s+1}^{n_d+n_s+n_{dc}} ((F_{t_i} - F_{f_i}) \sin \delta_i + |F_{t_i}| \sin(\delta_i - \text{sign}(\alpha_i)\frac{\pi}{2}) x_{e_i}$$

$$+ \sum_{i=n_d+n_s+n_{dc}+1}^{n} (-F_{f_i} \sin \zeta_i + F_{c_i} \sin((\zeta_i + \text{sign}(\zeta_i)\frac{\pi}{2})) x_{e_i} .$$

This is an eighth-order nonlinear system of ordinary differential equations. In these equations, the tractive force F_{t_i} or the angular acceleration of the driving wheel $\dot\omega_i$, and steering angle δ_i may be determined from kinematic constraints 1 and 2, or by other means. Friction force F_{t_i} and the side force of the caster F_{c_i}, as well as the slip angle α_i and caster rotation angle ζ_i are also detailed in the previous section.

Rewriting Eqn. (3.77) in matrix form, the general forward dynamical model of the vehicle with arbitrary wheel configurations can be expressed as follows:

$$\mathbf{a}_Q = \begin{pmatrix} \dot{u} \\ \dot{v} \\ \dot{p} \\ \dot{\gamma} \end{pmatrix} = A^{-1}(B + D) , \qquad\qquad (3.78)$$

with:

$$A = \begin{bmatrix} m & 0 & 0 & 0 \\ 0 & m & m\,h_s & 0 \\ 0 & m\,h_s & I_{s_x} & -I_{xz} \\ 0 & 0 & -I_{xz} & I_s \end{bmatrix}, \quad B = \left\{ \begin{array}{c} \sum X \\ \sum Y \\ \sum L \\ \sum N \end{array} \right\}, \quad D = \left\{ \begin{array}{c} (vm + h_s m\,p)\gamma \\ -\mu\gamma \\ -m\,h_s\mu\gamma \\ 0 \end{array} \right\}.$$

Eqn. (3.78) represents the acceleration of the automated vehicle with respect to reference frame $\{Q\}$. Then, the acceleration of the vehicle with respect to inertial frame $\{I\}$ can be represented as:

$$\mathbf{a} = T \times \mathbf{a_Q}, \qquad\qquad\qquad (3.79)$$

with the transformation matrix

$$T = \begin{bmatrix} \cos(\theta) & -\sin(\theta)\cos(\varphi) & \sin(\theta)\sin(\varphi) \\ \sin(\theta) & \cos(\theta)\cos(\varphi) & -\cos(\theta)\sin(\varphi) \\ 0 & \sin(\varphi) & \cos(\varphi) \end{bmatrix}.$$

Integrating Eqns. (3.78) and (3.79) with respect to time yields the velocity components of the vehicle with respect to reference frame $\{Q\}$ and inertial frame $\{I\}$, as given by the following equations:

$$V_Q = \left(\begin{array}{c} u \\ v \\ p \\ \gamma \end{array} \right) = \int_0^t A^{-1}(B + D)\, dt, \qquad\qquad (3.80)$$

and

$$V = \int_0^t T \times A^{-1}(B + D)\, dt. \qquad\qquad (3.81)$$

103

Integrating above equation with respect to time yields the positions of the vehicle with respect to the inertial frame $\{I\}$:

$$\begin{pmatrix} X \\ Y \\ \varphi \\ \theta \end{pmatrix} = \int_{0}^{t} T \times \begin{pmatrix} u \\ v \\ p \\ \gamma \end{pmatrix} dt \ . \tag{3.82}$$

3.6 Summary

In this chapter, an automated vehicle is decomposed into distinct individual rigid bodies for the purpose of deriving the equation of the motion. This vehicle consists of the main body, and combination of driving wheel units, steering wheel units, driving-steering units and casters. The vehicle main body and each wheel unit are connected by two possible types of joints represented by the symbols A_i and B_i. The equations of motion of each rigid body have been derived in detail. The dynamical equations of a vehicle with arbitrary wheel configurations has also been developed by integrating the vehicle main body and each wheel unit together. The forward dynamical model has been derived, with position and velocity of the vehicle with respect to the reference frame $\{Q\}$ or inertial frame $\{I\}$ completely specified.

Furthermore, in this model, the sprung mass m_s and unsprung mass m are considered explicitly. Two types of steering wheel or driving-steering wheel units are generally employed on automated vehicle systems. In Sections 3.3.3 and 3.3.4, the characteristics of these two types of wheel units have been studied in detail. The equations of motion of these wheel units have been derived, and kinematic constraints of two types of wheel units also have been detailed.

104

Chapter 4

GENERAL PROCEDURE FOR DERIVATION AND SIMULATION OF AUTOMATED VEHICLE DYNAMICAL MODELS

4.1 Introduction

In Chapter 3, a general procedure is presented for the decomposition of automated vehicle systems into sets of their constituent parts, namely the vehicle main body, driving wheel unit(s), steering wheel unit(s), driving-steering wheel unit(s), and caster(s). General forms for the dynamical equations modelling each of these subsystems are also derived, and the external forces and moments acting on each individual rigid body are studied in detail. Following analysis of the individual vehicle components, Chapter 3 presents the derivation of a dynamical model for an automated vehicle system which incorporates n arbitrarily-configured wheels using D'Alembert's principle. The derivation procedure for this dynamical model is seen to be rather complex, and a more easily followed step-by-step procedure is clearly desirable.

In this chapter, a systematic methodology will be developed for automated dynamic modelling and simulation of automated vehicles. A detailed understanding of automated vehicle dynamics on the part of the user of this method is not required to follow the steps provided in this chapter for derivation of a complete automated vehicle dynamical model. An overview of the general procedure for derivation of vehicle dynamical models incorporating n arbitrarily-configured wheels is presented in the flowchart of Figure 4.1. Required system parameters are summarized in Table 4.1, and assumptions and nomenclature are summarised

in Section 4.2.1.

Table 4.2 serves as a guide allowing the user to keep track of the creation and / or elimination of variables and equations which arise during the dyn\mic model derivation process. This tracking of all variables and equations allows for more rapid assessment of the number of redundancies in the resulting model. Finally, formal structure of the model also leads to a parallel structure for simulation on digital computer. A general simulation flowchart, Fig. 4.5, illustrates the simulation procedure.

| Step 1: Specification of the vehicle system. |
| Types, numbers and locations of the wheels. |

| Step 2: Setting up intermediate variables. |
| β_i, f_{ri} $\{i=1,2,...n\}$, α_i $\{i=1,2,....(n-n_e)\}$, ζ_i $\{i=(n-n_e),(n-n_e-1),....n\}$ |

| Step 3: Calculate external forces (at C_i) |
| F_{ti}, F_{ci}, F_{fi} and F_{ti} . |

| Step 4: Compute external forces contributed |
| by each type of wheel (in x, y directions). |

| Step 5: Compute total forces and moments. |
| $\sum_{i=1}^{n}X_i$, $\sum_{i=1}^{n}Y_i$, $\sum L$, $\sum N$. |

| Step 6: Assemble the motion equation of |
| the vehicle system with external forces & moments. |

| Step 7: Reduction to matrix form; |
| save for acceleration terms. |

| Step 8: Integrating forward dynamical model. |
| Obtain velocities & trajectory of the vehicle. |

Figure 4.1: Flowchart of the Dynamic Modelling Procedure.

4.2 Procedure for Derivation of an Automated Vehicle Dynamical Model

4.2.1 Assumptions and Nomenclature Used in the Model

For convenience, the general assumptions and definitions described in Chapters 2 and 3 are summarized here:

(i) Five generalized coordinate systems are utilized to describe relative motion of each wheel unit with respect to the vehicle main body and the ground. They are fixed to the ground $\{I\}$, the vehicle main body $\{Q\}$, joints A_i $\{A_i\}$, B_i $\{B_i\}$ and the wheel-ground contact point C_i $\{C_i\}$, respectively. The x_{ji}, y_{ji}, z_{ji} (where $j = A, B, C$) axes of frame $\{A_i\}$, $\{B_i\}$ and $\{C_i\}$ are defined to be parallel to the x, y, z axes of frame $\{Q\}$ (Chapter 2, Section 2.2.3).

(ii) For convenience in subsequent analysis, variable and parameter definitions are systematized using the lower-case indicial notation i ($i = 1, 2, \dots \dots, n$), to identify their association with distinct wheel units.

(iii) The term "Joint" is used to represent the physical interaction or connection between any two rigid body components of an automated vehicle system. Joint characteristics are detailed in Sections 2.4.1 and 2.4.2.

(iv) Steering angle δ_i (or caster rotation angle ζ_i) is the angle between the x-axis of the vehicle and the wheel plane . Direction angle β_i is the angle between the x-axis of the vehicle and velocity vector (V_{B_i}) at the centre of the wheel. Slip angle α_i is the angle between the wheel plane and the direction of wheel travel (i.e., the direction of velocity vector (V_{B_i})). This angle is used to compute the lateral force acting on the wheel (All the above-defined angles represent a rotation of the (vertical) wheel disk

plane around the z-axis, and are taken as positive clockwise as viewed from the negative z-direction as shown in Fig. 4.2).

a) Steering angle = δ_i b) Direction angle = β_i c) Slip angle = $\alpha_i = \beta_i - \delta_i$ d) Caster rotation = ζ_i
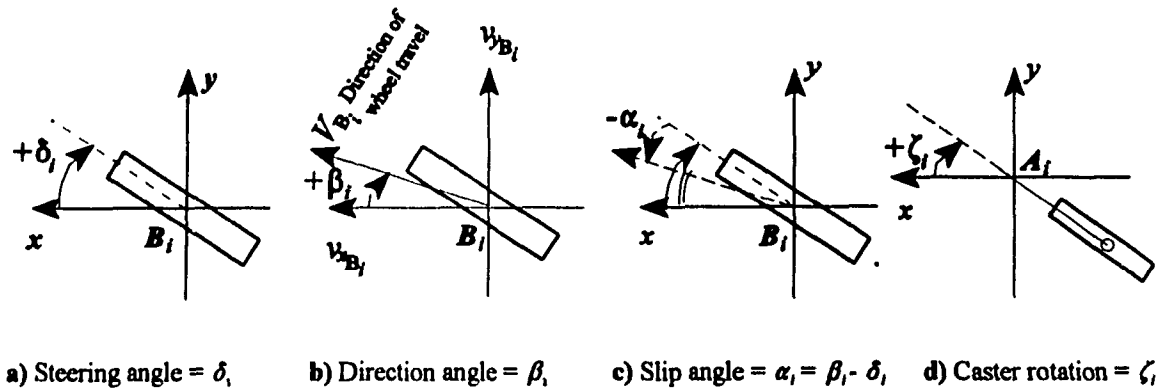
Figure 4.2: Definition of Steering Angle, Direction Angle, Slip angle, and Caster Rotation Angle.

(v) An automated vehicle is assumed to consist of a rigid main body equipped with n independent non-deformable wheel units, which may include:

a) Motorized driving wheel units,

b) Two types of motorized steering wheel units (Chapter 3, Section 3.3.3),

c) Two types of motorized driving-steering wheel units (Section 3.3.4),

d) Free-rotating casters.

(vi) The vehicles have four degrees of freedom (Chapter 2, Section 2.2) :

• Longitudinal velocity u along the x axis,

• Lateral velocity v along the y axis,

109

- Roll rate p about the x axis,

- Yaw rate γ about the z axis.

(vii) The z-direction components (for all coordinate systems) of system variables are not explicitly required by models derived in this thesis, but are retained in order to allow expansion of these models from four to six DOFs if desired.

(viii) The wheel-ground contact region is regarded as point contact (refer to Appendix B). There is no longitudinal slip and no side slip at the wheel-ground contact point.

(ix) The total sprung mass m_s and total unsprung mass m_u are treated explicitly.

(x) Rolling resistance factors for all wheels may be defined as $f_{r_i} = k_1(1 + k_2 v_{xy_i})$, and they can be selected based on other considerations (refer to Appendix B).

(xi) The weight load on each wheel is either assumed uniform, or is precalculated in advance based on the description in Appendix C.

4.2.2 Modelling Procedure

Following the flowchart presented in Fig.4.1, the detailed dynamic modelling procedure can be stated as follows:

Step 1. Specification of the automated vehicle system.

Indicate the types of wheels employed on the vehicle, as well as the number of each of type of wheel and their locations. All wheels should be put in a specific order which as shown by Fig.4.3.

i)
Driving wheel(s)
Number: (n_d)
Location of Joint B_i
$i = 1, 2, ..., n_d$

ii)
Steering wheel(s)
Number: (n_s)
Location of Joints A_i, B_i ,
$i = (n_d+1), (n_d+2), ...(n_d+n_s)$.

iii)
Driving-steering(s)
Number: (n_{ds})
Location of Joints A_i, B_i,
$i = (n_d+n_s+1), ...(n_d+n_s+n_{ds})$.

iv)
Caster(s)
Number: (n_c)
Location of Joint A_i,
$i = (n_d+n_s+n_{ds}+1), ... n$.

Σ

VEHICLE MAIN BODY

Total number of wheels
$n = n_d + n_s + n_{ds} + n_c$
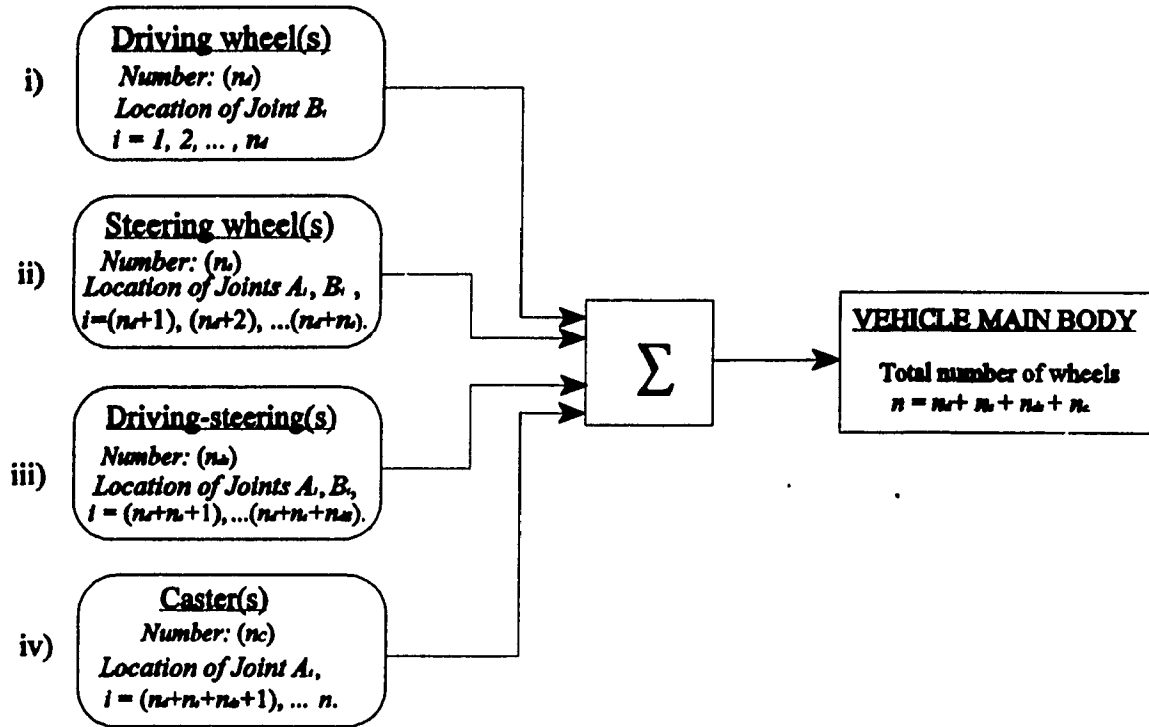
Figure 4.3: Specification of Vehicle Configuration.

i) Driving wheel(s):

Number = n_d,

Location $B_i = (x_{b_i}, y_{b_i}, z_{b_i})$, with $i = 1, 2, ..., n_d$ (in this case joints A_i and B_i can be considered coincident with each other).

ii) Steering wheel(s):

Number = n_s,

Location $A_i = (x_{a_i}, y_{a_i}, z_{a_i})$, with $i = (n_d + 1), (n_d + 2),..., (n_d + n_s)$.

iii) Driving-steering wheel(s):

Number = n_{ds},

Location $A_i = (x_{a_i}, y_{a_i}, z_{a_i})$, with $i = (n_d + n_s + 1), (n_d + n_s + 2),..., (n_d + n_s + n_{ds})$.

111

iv) Caster(s):

Number = n_c,

Location $A_i = (x_{a_i}, y_{a_i}, z_{a_i})$, with ($i = (n_d + n_d + n_s + 1)$, ($n_d + n_d + n_s + 2$), ..., n).

The total number of wheel units n employed on the vehicle and the total number of steering and power variables N_{var} introduced to the system is as follows:

$$n = n_d + n_s + n_{ds} + n_c ,$$

$$N_{var} = n_d + n_s + 2 n_{ds} .$$

(4.1)

The location of joint A_i must be specified by the user, and the location of joint B_i is detailed in Section 2.4.2. For convenience, these locations are summarized here.

(i) For a Type A steering wheel unit or driving-steering wheel unit:

$$\begin{cases} x_{b_i} = x_{a_i} + d_i \cos \xi_i , \\ y_{b_i} = y_{a_i} + d_i \sin \xi_i , \\ z_{b_i} = z_{a_i} + b_i , \end{cases}$$

(4.2 a)

where steering column offset is d_i, the angle between the x_{A_i}-axis and the steering column $A_i B_i$ is ξ_i ($= \text{sign}(y_{a_i})\dfrac{\pi}{2} + \delta_i(t)$), and the length of the steering column is b_i.

(ii) For a Type B steering wheel unit or driving-steering wheel unit:

$$\begin{cases} x_{b_i} = x_{a_i} + \Delta_i \cos \delta_i , \\ y_{b_i} = y_{a_i} + \Delta_i \sin \delta_i , \\ z_{b_i} = z_{a_i} + b_i , \end{cases}$$

(4.2 b)

where the effective offset $\Delta_t = d_f\cos(\lambda_t) + L_f\sin(\lambda_t)$, the effective length of the steering column $b_t = L_f\cos(\lambda_t) - d_f\sin(\lambda_t)$, and the effective steering angle $\delta_t = \tan^{-1}[\cos(\lambda_t)\tan(\delta_{actual_t})]$ (as, for example, in Rajagopalan [17]).

In addition, when the steering column offset is zero, joints A_i and B_i are coincident. The motion of casters completely depends on the motion of the vehicle main body, i.e., joints A_i, thus, the location of joints B_i does not need to be considered. In this step, the number n of joint A_i or B_i locations should be given, and the number $(n_s + n_{ds})$ of joint (B_i) locations should be calculated based on the given location of joint A_i and the type of wheel unit.

Step 2. Setting Up Intermediate Variables (β_i, α_i, ζ_i and f_{r_i}):

Step 2.1. Calculate constrained velocities at joints A_i and B_i, and determine the direction angle (β_i) of each wheel unit as a function of the wheel location and velocity vector. According to the description in Sections 2.4.1 and 2.4.2, the velocity vector at joints A_i and B_i can be expressed as:

$$V_{J_i} = \begin{Bmatrix} v_{x_{J_i}} \\ v_{y_{J_i}} \\ v_{z_{J_i}} \end{Bmatrix} = \begin{Bmatrix} u \\ v \\ 0 \end{Bmatrix} + \begin{bmatrix} 0 & -\gamma & 0 \\ \gamma & 0 & -p \\ -0 & p & 0 \end{bmatrix} \times \begin{Bmatrix} x_{J_i} \\ y_{J_i} \\ z_{J_i} \end{Bmatrix}, \tag{4.3}$$

where j represents joints A_i and B_i, and the rolling velocity p may be neglected because rolling motion does not affect the unsprung mass. The magnitude of each velocity vector in the x, y plane is:

$$v_{xy_{J_i}} = \sqrt{v_{x_{J_i}}^2 + v_{y_{J_i}}^2}. \tag{4.4}$$

113

Thus, constrained velocities and the direction angle of different wheel units can be determined as follows:

i) For driving wheel units ($i = 1, 2, ..., n_d$),

$$\beta_i = \tan^{-1} \frac{v_{y_{B_i}}}{v_{x_{B_i}}} = \tan^{-1} \frac{v + \gamma x_{b_i}}{u - \gamma y_{B_i}} \,.$$

(4.5)

$$v_{(xy)_{B_i}} = \sqrt{v_{x_{B_i}}^2 + v_{y_{B_i}}^2} = \sqrt{(u - \gamma y_{b_i})^2 + (v + \gamma x_{b_i})^2} \,,$$

(4.6)

ii) For steering wheel units ($i = n_d + 1, n_d + 2, ..., n_d + n_s$),

iii) For driving-steering wheel units ($i = n_d + n_s + 1, n_d + n_s + 2, ..., n_d + n_s + n_{ds}$),

$$v_{(xy)_{B_i}} = \begin{cases} \sqrt{(u - \gamma(d_i \sin(\xi_i) + y_{a_i}))^2 + (v + \gamma(d_i \cos(\xi_i) + x_{a_i}))^2} \,, & \text{for case a)}; \\[4mm] \sqrt{(u - \gamma(\Delta_i \sin(\delta_i) + y_{a_i}))^2 + (v + \gamma(\Delta_i \cos(\delta_i) + x_{a_i}))^2} \,, & \text{for case b)}, \end{cases}$$

(4.7)

$$\beta_i = \begin{cases} \tan^{-1} \dfrac{v_{y_{B_i}}}{v_{x_{B_i}}} = \tan^{-1} \dfrac{v + \gamma(d_i \cos(\xi_i) + x_{a_i})}{u - \gamma(d_i \sin(\xi_i) + y_{a_i})} \,, & \text{for case a)} ; \\[5mm] \tan^{-1} \dfrac{V_{y_{B_i}}}{V_{x_{B_i}}} = \tan^{-1} \dfrac{v + \gamma(\Delta_i \cos(\delta_i) + x_{a_i})}{u - \gamma_i(\Delta_i \sin(\delta_i) + y_{a_i})} \,, & \text{for case b)}. \end{cases}$$

(4.8)

where steering angle (δ_i) and steer rate ($\dot{\delta}_i$) of the steering or driving-steering wheel units are determined by applying kinematic constraint 2 at wheel-ground contact

114

points. The steering angle or steering rate can expressed as a function of the desired velocities and trajectory of the vehicle with respect to the inertial frame, and location of the wheel. It can be expressed as follows.

For Type A steering or driving-steering wheel units:

$$\delta_i = \tan^{-1} \frac{-\dot{X}_Q \sin(\theta) + \dot{Y}_Q \cos(\theta) + x_{e_i}\gamma}{\dot{X}_Q \cos(\theta) + \dot{Y}_Q \sin(\theta) - y_{e_i}\gamma} , \qquad (4.8\ a)$$

where the steering rate can be obtained by differentiating the above equation with respect to time. This equation is also applicable when the steering column offset is equal to zero.

For Type B steering or driving-steering wheel units:

$$\dot{\delta}_i = \frac{-\dot{X}_Q \sin(\theta+\delta_i) + \dot{Y}_Q \cos(\theta+\delta_i) + (x_{e_i}\cos(\delta_i) + y_{e_i}\sin(\delta_i))\gamma}{\Delta_i} + \gamma , \qquad (4.8\ b)$$

and the steering angle with respect to time can be calculated by applying the initial conditions $\delta(0)_i$, $\dot{X}_Q(0)$, $\dot{Y}_Q(0)$ and $\gamma(0)$, with $\Delta_i = d_i \cos(\lambda_i) + L_i \sin(\lambda_i)$. Linear velocities of the vehicle with respect to the inertial frame are $\dot{X}_Q(t)$ and $\dot{Y}_Q(t)$, respectively. The yaw rate of the vehicle is $\gamma(t)$ and the orientation of the vehicle is $\theta(t)$.

iv) For casters ($i = n_d + n_s + n_{ds} + 1, n_d + n_s + n_{ds} + 2, \ldots, n_d + n_s + n_{ds} + n_c$),

115

$$v_{(xy)_{A_i}} = \sqrt{v_{x_{A_i}}^2 + v_{y_{A_i}}^2} = \sqrt{(u - \gamma y_{a_i})^2 + (v + \gamma x_{a_i})^2} , \qquad (4.9)$$

$$\beta_i = \tan^{-1} \frac{v_{y_{A_i}}}{v_{x_{A_i}}} = \tan^{-1} \frac{v + \gamma x_{a_i}}{u - \gamma y_{a_i}} . \qquad (4.10)$$

Step 2.2. Calculation of slip angles (α_i), caster rotation angles (ζ_i) and friction factors (f_{r_i}). Based on the analysis wheel models in Appendix B, we can use the following set of equations to determine the slip angles (α_i), caster rotation angles (ζ_i) and friction factors (f_{r_i}) for the entire vehicle system:

$$\begin{cases} \alpha_i = \beta_i - \delta_i , & i = 1, 2, \dots , (n_d + n_s + n_{ds}); \\[2mm] \zeta_i = \dfrac{F_{c_i} \cdot d_i}{I_{s_i}} , & i = (n_d + n_s + n_{ds} + 1) , \dots, (n_d + n_s + n_{ds} + n_c); \\[2mm] f_{r_i} = k_1 (1 + k_2 v_{xy_{j_i}}) , & i = 1, 2, \dots, (n_d + n_s + n_{ds} + n_c). \end{cases} \qquad (4.11)$$

where: $I_{s_i} =$ polar moment of inertia of caster i, $\quad d_i =$ offset of caster i,

k_1 and $k_2 =$ rolling friction coefficients for each wheel (there are alternative models for the friction factors (f_{r_i}) which may also be selected (refer to Appendix B)).

$j = A_i$ and B_i, when wheel unit i is the driving wheel or caster: $j = A_i$, otherwise: $j = B_i$.

In this step, $3n$ intermediate variables must be determined. Furthermore, if the rolling friction factors of wheel units are taken as constants or they are not dependent on the velocity, the magnitudes of velocity vectors V_{A_i} and V_{B_i} do not need to be calculated. The

equations for calculating these velocity magnitudes and friction factors are eliminated in Steps 2.1 and 2.2.

Step 3. Calculation of external forces $(F_{l_i}, F_{f_i}, F_{c_i}$ and $F_{t_i})$ acting on each wheel at the wheel-ground contact point.

Step 3.1. External forces which depends on the slip angle and friction between the wheel and floor.

In Appendix B.2 and B.3, it is shown that the characteristic of the wheel and the floor would influence the forces acting on each wheel unit at the wheel-ground contact point. These external forces are the lateral force F_{l_i}, friction force F_{f_i} and side friction force F_{c_i}, and they are represented as follows:

$$
\begin{cases}
F_{l_i} = -C_{\alpha_i}\alpha_i \,, & i = 1, 2, \ldots, (n_d + n_s + n_{ds}); \\[2mm]
F_{f_i} = f_{r_i}F_{s c_i} \,, & i = 1, 2, \ldots, (n_d + n_s + n_{ds} + n_c); \\[2mm]
F_{c_i} = k_{cn}F_{s c_i}\operatorname{sign}(\beta_i - \zeta_i) \,, & i = (n_d + n_s + n_{ds} + 1) \,, \ldots, (n_d + n_s + n_{ds} + n_c) \,.
\end{cases}
\tag{4.12}
$$

where C_{s_i} = cornering stiffness [N/rad] of the wheel, k_{cn} = coefficient of side friction,

F_{z_i} = load acting on wheel i (this can be precalculated from Appendix C).

Step 3.2. External forces which depends on motor characteristics.

Another external force acting on driving wheel units or driving-steering wheel units is the tractive force F_{t_i} provided by the motor. It is the only force that depends on motor characteristics, but not on the characteristics of the wheel and the floor. A detailed derivation

117

of the tractive force (F_{t_i}) is given in Appendix B.5. The final result for calculating the tractive

force ($i = 1, 2, ..., n_d$ and $i = n_d + n_s + 1, n_d + n_s + 2, ..., n_d + n_s + n_{ds}$) is rewritten here:

$$F_{t_i} = \frac{N_i}{R_i} (K_{T_i} I_i - J_i N_i \dot{\omega}_i - D_i N_i \omega_i - T_{t_i}), \qquad (4.13)$$

In addition, if the apply tractive force F_{t_i} is determined, the required current of each

motorized driving wheel unit can be calculated by following equation:

$$I_i = (\frac{F_{t_i} R_i}{N_i} + J_i N_i \dot{\omega}_i - D_i N_i \omega_i + T_{f_i})/K_{T_i} \qquad (4.14)$$

where N_i = gear ratio,

K_{T_i} = motor torque constant [N.m/A],

I_i = current [A],

J_i = driving wheel moment of inertia [kg.m²],

T_{f_i} = static friction of motor [Nm],

D_i = viscous damping factor [N.m.s/rad],

ω_i and $\dot{\omega}_i$ = angular velocity and acceleration respectively of the driving wheel

unit(s) or driving-steering wheel unit(s), which can be determined by applying kinematic

constraint 1 of the wheel-ground contact points. The angular velocity and acceleration of the

driving wheel(s) can expressed as a function of the desired linear velocities, yaw rate, angular

acceleration and orientation of the vehicle with respect to the inertial frame, and the location

of each wheel and its steering angle. It can be shown that:

i) for a driving wheel unit ($i = 1, 2, ..., n_d$),

$$\omega_i = \frac{\dot{X}_Q \cos(\theta) + \dot{Y}_Q \sin(\theta) - y_{b_i} \gamma}{R_i} , \qquad (4.15)$$

$$\dot{\omega}_i = \frac{\ddot{X}_Q \cos(\theta) + \ddot{Y}_Q \sin(\theta) - (\dot{X}_Q \sin(\theta) - \dot{Y}_Q \cos(\theta))\gamma - y_{b_i} \dot{\gamma}}{R_i} . \qquad (4.16)$$

ii) for Type A driving-steering wheel unit and steering column offset equal to zero

$(i = n_d + n_s + 1, n_d + n_s + 2, ..., n_d + n_s + n_{ds})$,

$$\omega_i = \frac{\dot{X}_Q \cos(\theta + \delta_i) + \dot{Y}_Q \sin(\theta + \delta_i) + (x_{a_i} \sin(\delta_i) - y_{a_i} \cos(\delta_i))\gamma}{R_i} , \qquad (4.17\ a)$$

$$\dot{\omega}_i = \frac{Num1 + Num\,2 + Num3}{R_i} , \qquad (4.18\ a)$$

with : $Num1 = \ddot{X}_Q \cos(\theta + \delta_i) - \dot{X}_Q \sin(\theta + \delta_i)(\gamma + \dot{\delta}_i)$,

$Num2 = \ddot{Y}_Q \sin(\theta + \delta_i) + \dot{Y}_Q \cos(\theta + \delta_i)(\gamma + \dot{\delta}_i)$,

$Num3 = (x_{a_i} \cos(\delta_i) + y_{a_i} \sin(\delta_i))\dot{\delta}_i \gamma + (x_{a_i} \sin(\delta_i) - y_{a_i} \cos(\delta_i))\dot{\gamma}$.

Type B driving steering wheel units:

$$\omega_i = \frac{\dot{X}_Q \cos(\theta + \delta_i) + \dot{Y}_Q \sin(\theta + \delta_i) + (x_{a_i} \sin(\delta_i) - y_{a_i} \cos(\delta_i) - sign(y_e) d_i)\gamma}{R_i} , \qquad (4.17\ b)$$

$$\dot{\omega}_i = \frac{Num1 + Num\,2 + Num3}{R_i} , \qquad (4.18b)$$

119

with: *Num1* $= \ddot{X}_Q \cos(\theta + \delta_i) - \dot{X}_Q \sin(\theta + \delta_i)(\gamma + \dot{\delta}_i)$,

Num2 $= \ddot{Y}_Q \sin(\theta + \delta_i) + \dot{Y}_Q \cos(\theta + \delta_i)(\gamma + \dot{\delta}_i)$,

Num3 $= (x_{a_i} \cos(\delta_i) + y_{a_i} \sin(\delta_i))\dot{\delta}_i \gamma + (x_{a_i} \sin(\delta_i) - y_{a_i} \cos(\delta_i) - \text{sign}(y_{a_i})d_i)\dot{\gamma}$

where R_i = radius of wheel i, δ_i = steer angle [rad], $\dot{\delta}_i$ = steer rate [rad/s].

In this step, one input currents are given, all external forces acting on wheels by the ground have been completely determined. The $2n + n_d + n_{ds}$ external forces must be determined and $2n$ intermediate variables cancel.

Step 4. Calculation of the total external forces acting on each wheel-ground contact point C_i in the x and y directions.

Let the total external force acting at each wheel-ground contact point C_i along the x and y axes be X_i and Y_i respectively. Then, from Eqns. (3.67) and (3.72), it may be shown that the external forces contributed by each type of wheel unit can be expressed as follows:

i) Driving wheel unit ($i = 1, 2, ..., n_d$),

$$\begin{cases} X_i = F_{t_i} - F_{f_i} , \\ \\ Y_i = F_{l_i} . \end{cases}$$ (4.19)

ii) Steering wheel unit ($i = (n_d + 1), (n_d + 2), ..., (n_d + n_s)$),

$$\begin{cases} X_i = (-F_{f_i} \cos \delta_i + |F_{l_i}| \cos(\delta_i - \text{sign}(\alpha_i) \frac{\pi}{2})) , \\ \\ Y_i = (-F_{f_i} \sin \delta_i + |F_{l_i}| \sin(\delta_i - \text{sign}(\alpha_i) \frac{\pi}{2})) . \end{cases}$$ (4.20)

120

iii) Driving-steering wheel unit ($i = (n_d + n_s + 1)$, $(n_d + n_s + 2)$, ..., $(n_d + n_s + n_{ds})$),

$$\begin{cases} X_i = ((F_{t_i} - F_{f_i})\cos\delta_i + |F_{l_i}|\cos(\delta_i - sign(\alpha_i)\frac{\pi}{2})) \, , \\[2em] Y_i = ((F_{t_i} - F_{f_i})\sin\delta_i + |F_{l_i}|\sin(\delta_i - sign(\alpha_i)\frac{\pi}{2})) \, . \end{cases} \qquad (4.21)$$

iv) Caster ($i = (n_d + n_s + n_{ds} + 1)$, $(n_d + n_s + n_{ds} + 2)$, ..., $(n_d + n_s + n_{ds} + n_C)$),

$$\begin{cases} X_i = (-F_{f_i}\cos\zeta_i + F_{C_i}\cos(\zeta_i + sign(\zeta_i)\frac{\pi}{2})). \, , \\[2em] Y_i = (-F_{f_i}\sin\zeta_i + F_{C_i}\sin(\zeta_i + sign(\zeta_i)\frac{\pi}{2})) \, . \end{cases} \qquad (4.22)$$

Step 4, $2n$ algebraic equations are generated.

Step 5. Total forces and moments acting on the vehicle system:

In Step 4, we established the external forces acting on each wheel unit at the wheel-ground contact point. In this step, we summarize the total forces and moments acting on the entire vehicle system throughout the n wheel units.

a) Total external force acting on the vehicle system along the x-direction:

$$\sum_{i=1}^{i=n} X_i = \sum_{i=1}^{n_d} (F_{t_i} - F_{f_i}) + \sum_{i=n_d+1}^{n_d+n_s} (-F_{f_i}\cos\delta_i + |F_{l_i}|\cos(\delta_i - sign(\alpha_i)\frac{\pi}{2}))$$

$$+ \sum_{i=n_d+n_s+1}^{n_d+n_s+n_{ds}} ((F_{t_i} - F_{f_i})\cos\delta_i + |F_{l_i}|\cos(\delta_i - sign(\alpha_i)\frac{\pi}{2})) \qquad (4.23)$$

$$+ \sum_{i=n_d+n_s+n_{ds}+1}^{n} (-F_{f_i}\cos\zeta_i + F_{C_i}\cos(\zeta_i + sign(\zeta_i)\frac{\pi}{2})) \, .$$

121

b) Total external force acting on the vehicle system along the y-direction:

$$\sum_{i=1}^{i=n} Y_i = \sum_{i=1}^{n_d} F_{1_i} + \sum_{i=n_d+1}^{n_d+n_s} (-F_{f_i} \sin\delta_i + |F_{1_i}| \sin(\delta_i - \text{sign}(\alpha_i)\,\frac{\pi}{2}))$$

$$+ \sum_{i=n_d+n_s+1}^{n_d+n_s+n_{dz}} ((F_{t_i} - F_{f_i})\sin\delta_i + |F_{1_i}|\sin(\delta_i - \text{sign}(\alpha_i)\,\frac{\pi}{2})) \qquad (4.24)$$

$$+ \sum_{i=n_d+n_s+n_{dz}+1}^{n} (-F_{f_i} \sin\zeta_i + F_{c_i}\sin(\zeta_i + \text{sign}(\zeta_i)\,\frac{\pi}{2}))\ .$$

c) Total moments acting on the vehicle system about the x (roll) axis:

$$\sum L = m_s\, g\, h_s\, \varphi + C_\varphi\, \varphi + L_p\, p\ . \qquad (4.25)$$

where m_S = sprung mass [kg], $\quad$ g = gravity [m/s²],

φ = rolling angle [rad], $\quad$ p = rolling angular velocity [rad/s],

C_φ = rolling stiffness of the system [N.m.rad⁻¹],

L_p = damping coefficient of suspension system [N.m.s.rad⁻¹],

h_s = distance from the rolling axis to the sprung mass centre [m].

d) Total external moment acting on the vehicle system about the z (yaw) axis:

$$\sum N = -\sum_{i=1}^{n_d} (F_{t_i} - F_{f_i})y_{a_i} + \sum_{i=n_d+1}^{n_d+n_s} (F_{f_i} \cos\delta_i - |F_{1_i}| \cos(\delta_i - \text{sign}(\alpha_i)\,\frac{\pi}{2}))y_{a_i}$$

$$- \sum_{i=n_d+n_s+1}^{n_d+n_s+n_{dz}} ((F_{t_i} - F_{f_i})\cos\delta_i + |F_{1_i}|\cos(\delta_i - \text{sign}(\alpha_i)\,\frac{\pi}{2}))y_{a_i}$$

$$- \sum_{i=n_d+n_s+n_{dz}+1}^{n} (F_{f_i} \cos\zeta_i - F_{c_i} \cos(\zeta_i + \text{sign}(\zeta_i)\,\frac{\pi}{2}))y_{a_i}$$

$$- \sum_{i=1}^{n_d} F_{1_i}x_{a_i} + \sum_{i=n_d+1}^{n_d+n_s} (F_{f_i} \sin\delta_i - |F_{1_i}| \sin(\delta_i - \text{sign}(\alpha_i)\,\frac{\pi}{2}))x_{a_i} \qquad (4.26)$$

$$- \sum_{i=n_d+n_s+1}^{n_d+n_s+n_{dz}} ((F_{t_i} - F_{f_i})\sin\delta_i + |F_{1_i}|\sin(\delta_i - \text{sign}(\alpha_i)\,\frac{\pi}{2}))x_{a_i}$$

$$+ \sum_{i=n_d+n_s+n_{dz}+1}^{n} (F_{f_i} \sin\zeta_i + F_{c_i}\sin(\zeta_i + \text{sign}(\zeta_i)\,\frac{\pi}{2}))x_{a_i}\ .$$

122

Derivations of external moments about the x and z axes are described in detail in Sections 3.4.3 and 3.4.4. In this step, four algebraic equations are generated.

Step 6. Integration of the motion equations of the vehicle system with external forces and moments.

In Section 3.2, the details of an automated vehicle system have been studied. Equations of motion for the vehicle system have been also derived, and are rewritten here:

$$\sum X = m \ (\dot{u} - \gamma v) - \gamma p \ h_s m_s \ ,$$

$$\sum Y = m \ (\dot{v} + \gamma u) + m_s \dot{p} h_s \ ,$$

$$\sum L = I_{x_s} \dot{p} + m_s h_s (\dot{v} + \gamma u) - I_{xz} \dot{\gamma} \ , \tag{4.27}$$

$$\sum N = I_z \dot{\gamma} - I_{xz} \dot{p} \ .$$

Substituting external forces and moments obtained in Step 5 into the above equations, the equations of motion of the vehicle system can expressed as:

$$m(\dot{u} - \gamma v) - \gamma p h_s m_s = \sum_{i=1}^{n_d} (F_{t_i} - F_{f_i}) + \sum_{i=n_d+1}^{n_d+n_s} (-F_{f_i} \cos \delta_i + |F_{t_i}| \cos(\delta_i - \text{sign}(\alpha_i) \frac{\pi}{2}))$$

$$+ \sum_{i=n_d+n_s+1}^{n_d+n_s+n_{dr}} ((F_{t_i} - F_{f_i}) \cos \delta_i + |F_{t_i}| \cos(\delta_i - \text{sign}(\alpha_i) \frac{\pi}{2}))$$

$$+ \sum_{i=n_d+n_s+n_{dr}+1}^{n} (-F_{f_i} \cos \zeta_i + F_{c_i} \cos(\zeta_i + \text{sign}(\zeta_i) \frac{\pi}{2})) \ ,$$

$$m \ (\dot{v} + \gamma u) + m_s \dot{p} h_s = \sum_{i=1}^{n_d} F_{t_i} + \sum_{i=n_d+1}^{n_d+n_s} (-F_{f_i} \sin \delta_i + |F_{t_i}| \sin(\delta_i - \text{sign}(\alpha_i) \frac{\pi}{2}))$$

$$+ \sum_{i=n_d+n_s+1}^{n_d+n_s+n_{dr}} ((F_{t_i} - F_{f_i}) \sin \delta_i + |F_{t_i}| \sin(\delta_i - \text{sign}(\alpha_i) \frac{\pi}{2}))$$

$$+ \sum_{i=n_d+n_s+n_{dr}+1}^{n} (-F_{f_i} \sin \zeta_i + F_{c_i} \sin(\zeta_i + \text{sign}(\zeta_i) \frac{\pi}{2})) \ ,$$

$$I_{s_x} \dot{p} + m_s h_s (\dot{v} + \gamma u) - I_{xz} \dot{\gamma} = m_s g h_s \varphi + C_\varphi \varphi + L_\rho \rho ,$$

$$I_z \dot{\gamma} - I_{xz} \dot{p} = -\sum_{i=1}^{n_d} (F_{t_i} - F_{f_i}) y_{a_i} + \sum_{i=n_d+1}^{n_d+m_s} (F_{f_i} \cos \delta_i - |F_{l_i}| \cos (\delta_i - \text{sign}(\alpha_i)\frac{\pi}{2})) y_{a_i}$$

$$- \sum_{i=n_d+m_s+1}^{n_d+m_s+m_{ds}} ((F_{t_i} - F_{f_i}) \cos \delta_i + |F_{l_i}| \cos (\delta_i - \text{sign}(\alpha_i)\frac{\pi}{2})) y_{a_i}$$

$$- \sum_{i=n_d+m_s+m_{ds}+1}^{n} (F_{f_i} \cos \zeta_i - F_{c_i} \cos ((\zeta_i + \text{sign}(\zeta_i)\frac{\pi}{2})) y_{a_i}$$

$$- \sum_{i=1}^{n_d} F_{l_i} x_{a_i} + \sum_{i=n_d+1}^{n_d+m_s} (F_{f_i} \sin \delta_i - |F_{l_i}| \sin(\delta_i - \text{sign}(\alpha_i)\frac{\pi}{2})) x_{a_i}$$

$$- \sum_{i=n_d+m_s+1}^{n_d+m_s+m_{ds}} ((F_{t_i} - F_{f_i}) \sin \delta_i + |F_{l_i}| \sin(\delta_i - \text{sign}(\alpha_i)\frac{\pi}{2})) x_{a_i}$$

$$+ \sum_{i=n_d+m_s+m_{ds}+1}^{n} (F_{f_i} \sin \zeta_i + F_{c_i} \sin((\zeta_i + \text{sign}(\zeta_i)\frac{\pi}{2})) x_{a_i} .$$

This is an eighth order system of nonlinear ordinary differential equations.

Step 7. Obtainment of the model for vehicle dynamics.

Rearrange the above nonlinear equations in matrix form. The accelerations of the vehicle with respect to frame $\{Q\}$ can be written as:

$$\mathbf{a}_Q = \begin{pmatrix} \dot{u} \\ \dot{v} \\ \dot{p} \\ \dot{\gamma} \end{pmatrix} = A^{-1} (B + D) , \tag{4.29}$$

and the acceleration of the vehicle with respect to inertial frame I can be determined by

$$\mathbf{a} = T \times \mathbf{a}_Q . \tag{4.30}$$

124

where T is the transformation matrix and

$$
A = \begin{bmatrix} m & 0 & 0 & 0 \\ 0 & m & m\,h_s & 0 \\ 0 & m\,h_s & I_{s_x} & -I_{xz} \\ 0 & 0 & -I_{xz} & I_z \end{bmatrix}, \qquad
B = \begin{pmatrix} \sum X \\ \sum Y \\ \sum L \\ \sum N \end{pmatrix}, \qquad
D = \begin{pmatrix} (vm + h_s m_s \rho)\gamma \\ -mu\gamma \\ -m\,h_s\mu\gamma \\ 0 \end{pmatrix}.
$$

Step 8. Integrating the forward dynamical model.

Given the initial position $P_0\{X_Q(0),\ Y_Q(0),\ \varphi(0),\ \theta(0)\}$ and velocities $\{V_x(0),\ V_y(0),\ \rho(0),$

$\gamma(0)\}$ of the vehicle with respect to frame $\{I\}$, the instantaneous velocities and position with

respect to the frame $\{I\}$ can be determined by integrating the above equations, as shown in

Fig. 4.4.
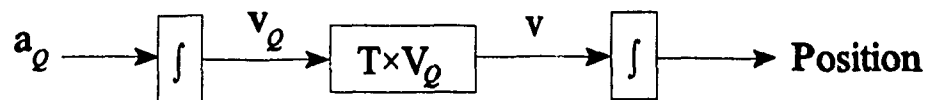
where: T = Transformation matrix

Figure 4.4: Block Diagram for Numerical Integration of Vehicle Dynamical Model.

125

Table 4.1 *Automated Vehicle System Parameters:*

Parameter	Description	Number of occurrences in the model	Value	Units
m	Total mass of the vehicle	1		kg
m_s	Total sprung mass of the vehicle	1		kg
h	Distance between the centre of the total mass and the x (roll) axis	1		m
h_s	Distance between the centre of the sprung mass and the x (roll) axis	.1		m
I_z	Moment of inertia of the vehicle about the z (yaw) axis	1		kg.m^2
I_{xz}	Moment of inertia of the vehicle about the xz plane	1		kg.m^2
I_{s_x}	Moment of the inertia of vehicle about the x (roll) axis	1		kg.m^2
C_φ	Rolling stiffness of the system	1		N.m.rad^{-1}
L_ρ	Damping coefficient of suspension system	1		N.m.s.rad^{-1}
$A_i(x_{a_i}, y_{a_i}, z_{a_i})$	Location of each wheel	$3n$ [3×1]		(m, m, m)
R_i	Radius of the wheel	n		m
m_i	Mass of each wheel unit	n		kg
$I_{A_{x_i}}$	Moment of the inertia of a steering wheel about the z_{A_i} axis	$n_s + n_{ds}$		kg.m^2
J_i	Moment of the inertia refer to motor shaft	$n_d + n_{ds}$		kg.m^2
I_{B_i}	Moment of the inertia of a driving wheel about it's rotation axis	$n_d + n_{ds}$		kg.m^2
I_{s_i}	Polar moment of inertia of the caster	n_c		kg.m^2

C_{a_i}	Cornering stuffiness of the wheel	$n_d + n_s + n_{ds}$		$N.rad^{-1}$
b_i	Length of the steering column	$n_s + n_{ds}*$		m
d_i	Offset of a steer wheel or caster	$n_s + n_{ds} + n_c$		m
k_1	Coefficient of rolling friction	$n*$		
k_2	Coefficient of rolling friction	$n*$		$s.m^{-1}$
k_{cni}	Coefficient of side friction	n_c*		
T_{f_i}	Static friction of the drive motor	$n_d + n_{ds}$		N.m
D_i	Viscous damping factor of the drive motor	$n_d + n_{ds}$		$N.m.s.rad^{-1}$
N_i	Motor shaft-wheel axle gear ratio	$n_d + n_{ds}$		
k_t	Torque constant of drive motor	$n_d + n_{ds}*$		$N.m.A^{-1}$
k_e	Voltage constant of the motor	$n_d + n_s + n_{ds}*$		$Volt.s.m^{-1}$
R	Resistance of the motor	$n_d + n_s + n_{ds}*$		Ω
L	Inductance of the motor	$n_d + n_s + n_{ds}*$		H

n_d = Number of the total driving wheels employed on the automated vehicle system,

n_s = Number of the total steering wheels employed on the automated vehicle system,

n_{ds} = Number of the total driving-steering wheel employed on the automated system,

n_c = Number of the total caster wheel employed on the automated system,

* Those variables may not appear in the model, because there are alternative models for these variables.

Table 4.2 *Vehicle System Variables Calculated During the Modelling Procedure:*

Variable	Description	# of Eqns. involved	Determined by	Eliminated in
$B_i(x_{b_i}, y_{b_i}, z_{b_i})$	Location of joints B_i for the steering & driving-steering wheels	$n_s + n_{ds}$ [3 × 1]	step 1	step 2.1
V_{B_i}	Velocity vector of the vehicle at joints B_i for driving, steering & driving-steering wheel units.	$n_d + n_s + n_{ds}$ [3 × 1]	step 2.1	step 2.1
V_{A_i}	Velocity vector of the vehicle at joints A_i for casters.	n_c [3 × 1]	step 2.1	step 2.1
$v_{xy_i} = v_{xy_{B_i}}$	Magnitude of the V_{B_i} in the xy plane at joints B_i.	$n_d + n_s + n_{ds}$	step 2.1	step 2.2
$v_{xy_i} = v_{xy_{A_i}}$	Magnitude of the V_{A_i} in the xy plane at joints A_i.	n_c	step 2.1	step 2.2
β_i	Direction angle of each wheel	n	step 2.1	step 2.2
δ_i	Steering angle of the steering and driving-steering wheel units	$n_s + n_{ds}$	step 2.1 (Kinematic Constraint II)	*
$\dot{\delta}_i$	Steering rate of steering and driving-steering wheel units	$n_s + n_{ds}$	step 2.1 (Kinematic Constraint II)	step 3.2
α_i	Slip angle of driving, steering & driving-steering wheel units	$n_d + n_s + n_{ds}$	step 2.2	step 3.1
ζ_i	Rotation angle of the caster	n_c	step 2.2	*
f_{r_i}	Rolling friction factor	n	step 2.2	step 3.1
F_{l_i}	Lateral force of each wheel	$n_d + n_s + n_{ds}$	step 3.1	*
F_{c_i}	Side force of the caster	n_c	step 3.1	*
F_{f_i}	Rolling resistance of each wheel	n	step 3.1	*

			Examined in Appendix C	step 3.1
F_{sc_i}	Vertical force acting on wheel-ground contact point by the ground	n	Examined in Appendix C	step 3.1
F_{t_i}	Applied tractive forces of the driving & driving-steering wheel	$n_d + n_{ds}$	step 3.2	*
I_i	Current of the driving motors	$n_d + n_{ds}$	Control Variables	**
ω_i	Angular velocities of the driving wheels	$n_d + n_{ds}$	Kinematic Constraint I	step 3.2
$\dfrac{d\omega_i}{dt}$	Angular accelerations of the driving wheels	$n_d + n_{ds}$	Kinematic Constraint I	step 3.2
X_i, Y_i	Total external forces acting on each wheel-ground contact point along x and y-axis.	n $[\,2 \times 2\,]$	step 4	step 5
$\sum X$	Total external forces acting on the vehicle along the x axis	1	step 5	step 6
$\sum Y$	Total external forces acting on the vehicle along the y axis	1	step 5	step 6
$\sum L$	Total moments acting on the vehicle about the x (roll) axis	1	step 5	step 6
$\sum N$	Total moments acting on the vehicle about the z (yaw) axis	1	step 5	step 6
$\mathbf{a}_Q = (\dot{u} \ \dot{v} \ \dot{p} \ \dot{Y})^T$	Acceleration vector of the vehicle with respect to $\{Q\}$.	1 $[\,4 \times 1\,]$	step 6 & 7	Output variable
$\mathbf{a} = T \times \mathbf{a}_Q$	Acceleration vector of the vehicle with respect to $\{I\}$.	1 $[\,4 \times 1\,]$	step 7	Output variable
$\mathbf{v}_Q = (u \ v \ p \ Y)^T$	Velocity vector of the vehicle system with respect to $\{Q\}$.	1 $[\,4 \times 1\,]$	step 8	Output variable
$\mathbf{v} = T \times \mathbf{v}_Q$	Velocity vector of the vehicle with respect to the frame $\{I\}$.	1 $[\,4 \times 1\,]$	step 8	Output variable
$\mathbf{P} = T \int \mathbf{v}_Q \cdot dt$	Position of the vehicle with respect to the frame $\{I\}$.	1 $[\,4 \times 1\,]$	step 8	Output variable

129

* Those variable will appear in the motion equations (4.28) of the vehicle system.

** Those variables are control variable which may introduce same redundancy to the vehicle system.

Number of the total control variables = $(n_d + n_{d_s})$.

Number of the redundancy of the system = $(n_d + n_{d_s})$ - (DOF of the vehicle on the ground).

4.3 Procedure for Numerical Simulation of Automated Vehicle Dynamics

4.3.1 Description of Dynamical Simulation for an Automated Vehicle

In Section 4.2, the dynamical behaviour of automated vehicle systems is described using a set of spatial force balance equations. The formal structure for derivation of automated vehicle dynamical models has also been developed. This formal structure for the model leads to a parallel structure for simulation of the model on a digital computer. A methodology (based on concepts developed in Section 4.2) is presented for the dynamic simulation of automated vehicle systems.

For this simulation problem, we assume that the following information is given for all wheel units and the vehicle main body:

Given:

$\mathbf{P}_{\bullet} = \{ X(0)_Q, Y(0)_Q, \varphi(0), \theta(0) \}^T$, $\mathbf{V}_{\bullet} = \{ \dot{X}_Q(0), \dot{Y}_Q(0), p(0), \gamma(0) \}^T$ = position and velocity of the automated vehicle with respect to the inertia frame {I} for the current time level.

$\dot{X}_Q(t)$, $\dot{Y}_Q(t)$, $\gamma(t)$ = desired velocities of the vehicle,

130

$m, h, h_s, I_{xx}, I_D, I_{d_z}, k_1, k_2, k_{cn} =$ system parameters,

$n_d, n_p, n_{ds}, n_c =$ number of each type of wheel

$(x_{e_i}, y_{e_i}, z_{e_i}) =$ location of joint $A, \{x_{A_i}, y_{A_i}, z_{A_i}\}$ for the wheel i,

with, $i = 1, 2, ...,(n_d + n_p + n_{ds} + n_c)$,

$R_i, d_i, I_{B_i} =$ the wheel unit i parameters,

$\zeta_i(0) =$ initial angle of the caster,

$\delta_i(0)$ (or $\xi_i(0)$) = initial angle of the steering wheel,

or other system parameters (refer to Table 4.1).

In the solution of the automated vehicle system simulation problem, the following unknown

quantities are desired:

Unknown:

$F_{t_i}, F_{s_i}, F_{c_i} =$ external forces acting on the wheel-ground contact points,

External moments (including the moment at joints B_i and A_i by the actuator i),

F_{t_i} or $I_i =$ required applied tractive force or current for drivable wheel unit i,

$\delta_i =$ required applied steering angle of wheel i

$\zeta_i =$ rotation angle of the caster i,

$a_Q =$ acceleration vector of the vehicle system with respect to the frame $\{Q\}$,

$a =$ acceleration vector of the vehicle system with respect to the frame $\{I\}$,

$P^*, V^* =$ position and velocities for the next time level,

The following intermediate variables are also required to allow determination of unknown

variables from known variables, and their time histories are not usually explicitly required in

the final results. Those variables are:

131

$(x_{B_i}, y_{B_i}, z_{B_i})$ = constrained location of wheel i at joint B_i,

v_{A_i}, v_{B_i} = constrained velocity vector of the vehicle at joints A_i or B_i,

β_i = direction angle of wheel i,

α_i = slip angle of wheel i,

f_{r_i} = rolling friction of wheel i.

$\omega_i, \dot{\omega}_i$ = angular velocity and acceleration of wheel i.

4.3.2 The Simulation Algorithm in Eight Steps

In a manner that is similar to the methodology for dynamic modelling of automated vehicles presented in Section 4.2, the methodology developed in this section for numerical simulation of automated vehicle systems may also be presented as a series of steps. The following eight computational steps are required:

1. Calculation of the applied tractive forces and the steering angles,

2. Calculation of the constrained location and velocity vectors of joints A_i and B_i for corresponding wheel units,

3. Calculation of the direction and slip angles, as well as rotation angles of the casters,

4. Calculation of the forces acting on the wheel-ground contact points by the ground,

5. Calculation of the external forces contributed by each type of wheel along the x and y directions,

6. Calculation of total forces and moments acting on the vehicle system,

7. Combination of all forces acting on the vehicle system and the vehicle motion equations,

8. Integration to obtain the state of the system at the next time level.

132

The fundamental computations required in each of these steps are summarized in Table 4.3, and the flowchart of Fig. 4.5. Prior to the development of a dynamical simulation algorithm, it should be recognized that it is necessary to specify input currents (power variables) and steering angle (steering variables), but these inputs must satisfy the kinematic constraints of the system. The angular velocity and acceleration of the driving motor are also determined by applying the kinematic constraints of the vehicle system, namely the conditions of pure rolling and no side slip.

In Step 1, the tractive force F_{t_i} and steering angles are determined by using Eqns. (4.13) and (4.8). Vehicle configuration and parameters must also be known. The present state and the input current(s) must be known. These input currents can be calculated from the inverse dynamics of the vehicle, if the desired velocity and trajectory are given and the system has not redundancy [52]. In Step 2, the constrained location and velocity of joint B, for desired wheel units is determined by Eqns. (4.2 a or b) and (4.3), (4.4) and (4.6). These equations are repeated for convenience in Table 4.2. In Step 3, direction angles are obtained using Eqns. (4.5), (4.8), and (4.10), and the solution for the slip angles and rotation angles of the caster are obtained using Eqn. (4.11). Direction and slip angles are defined as intermediate variables, because these variables do not appear in the final dynamic equations. Step 3 is a preparatory step for calculating lateral forces in Step 4.

In Step 4, the external forces acting on each wheel unit are solved for by assuming that the load acting on each wheel unit has been specified. Using Eqns. (4.12), the lateral or side forces, as well as the resistances acting on the wheel-ground contact point by the ground can be computed. Those relationships are repeated in Table 4.3 for convenience.

In Step 5, the external forces acting at each wheel-ground contact point C_i by the ground along the x and y axes can be easily determined using Eqns. (4.19) through (4.22) for each wheel unit. In Step 6, the total external forces acting on the entire vehicle system along the x and y axes can be determined using Eqns. (4.23) and (4.24). The total external moments acting on the vehicle about the x and z axes can be computed by utilizing Eqns. (4.25) and (4.26).

In Step 7, the assembled dynamic equations for the vehicle have been used. The acceleration of the automated vehicle system with respect to frame $\{Q\}$ or frame $\{I\}$ will be obtained by applying dynamic motion equations (4.29) and (4.30). Finally, in Step 8 the next time level of position and velocity of the vehicle system can be obtained by integrating Eqns. (4.29) and (4.30) with time once and twice respectively. The flowchart of dynamical simulation of an automated vehicle system is shown in Fig. 4.5, and the numerical technique used in this simulation will be discussed in Section 4.4.

Table 4.3 *Dynamic Simulation Algorithm for an Automated Vehicle System*

Given: the system parameters m, m_s, h, h_s, I_{xz}, I_D, I_{s_z}, R_i, d_i, I_{s_i}, I_{B_i} ... (refer Table 4.1);

the location of each wheel $A_i \{x_{a_i}, y_{a_i}, z_{a_i}\}$, and initial angles δ_i, and ζ_i

where $i = 1, 2, ..., (n_d + n_s + n_{ds} + n_c)$;

the present state $\mathbf{P_0} = (X(0)_Q, Y(0)_Q, \varphi(0), \theta(0))^T$,

and $\mathbf{V_0} = (\dot{X}(0)_Q, \dot{Y}(0)_Q, p(0), \gamma(0))^T$;

the current I_i to each drive motor and steering angle $\delta_i(t)$ to each steerable wheel unit.

Step 1. Compute F_{t_i} from driving motor dynamical model:

$$F_{t_i} = \frac{N_i}{R_i} [K_{T_i} I_i - J_i N_i \frac{d\omega_i}{dt} - D_i N_i \omega_i - T_f] ,$$

$1 \leq i \leq n_d$ and $(n_d + n_s + 1) \leq i \leq (n_d + n_s + n_{ds})$.

Step 2. Compute $\mathbf{V}_{B_i} = \left(v_{B_{x_i}} \quad v_{B_{y_i}} \quad v_{B_{s_i}} \right)^T$, $v_{xy_{B_i}} = (v_{B_{x_i}}^2 + v_{B_{y_i}}^2)^{\frac{1}{2}}$,

$1 \leq i \leq (n_d + n_s + n_{ds})$;

and $\mathbf{V}_{A_i} = \left(v_{A_{x_i}} \quad v_{A_{y_i}} \quad v_{A_{s_i}} \right)^T$, $v_{xy_{A_i}} = (v_{A_{x_i}}^2 + v_{A_{y_i}}^2)^{\frac{1}{2}}$,

$(n_d + n_s + n_{ds} + 1) \leq i \leq (n_d + n_s + n_{ds} + n_c)$.

135

Step 3. Compute direction and slip angles:

$$\beta_i = \tan^{-1}\frac{v_{B_{y_i}}}{v_{B_{x_i}}}, \qquad \alpha_i = \beta_i - \delta_i, \qquad\qquad 1 \le i \le (n_d + n_s + n_{ds}),$$

$$\beta_i = \tan^{-1}\frac{v_{A_{y_i}}}{v_{A_{x_i}}}, \qquad \zeta_i = \frac{F_{c_i} \times d_i}{I_{s_i}}, \qquad\qquad (n_d + n_s + n_{ds} + 1) \le i \le n.$$

Step 4. Compute the external forces F_{f_i}, F_{l_i}, F_{c_i}:

$$F_{f_i} = k_1 (1 + k_2 v_{xy_i}) F_{s_{c_i}}, \qquad 1 \le i \le (n_d + n_s + n_{ds} + n_c);$$

$$F_{l_i} = -C_\alpha \alpha_i, \qquad\qquad 1 \le i \le (n_d + n_s + n_{ds});$$

$$F_{c_i} = k_{cn} F_{s_{c_i}} \operatorname{sign}(\beta_i - \zeta_i), \qquad (n_d + n_s + n_{ds} + 1) \le i \le (n_d + n_s + n_{ds} + n_c).$$

Step 5. Compute the external forces (X_i, Y_i) contributed by each wheel unit along the x

and y-axis.

Step 6. Compute $\sum X$, $\sum Y$, $\sum L$, $\sum N$

Step 7. Solve the dynamical equations of the vehicle for a_Q,

$$a_Q = \begin{pmatrix} \dot{u} \\ \dot{v} \\ \dot{\rho} \\ \ddot{\gamma} \end{pmatrix}, \qquad a = T \times \begin{pmatrix} \dot{u} \\ \dot{v} \\ \dot{\rho} \\ \ddot{\gamma} \end{pmatrix}$$

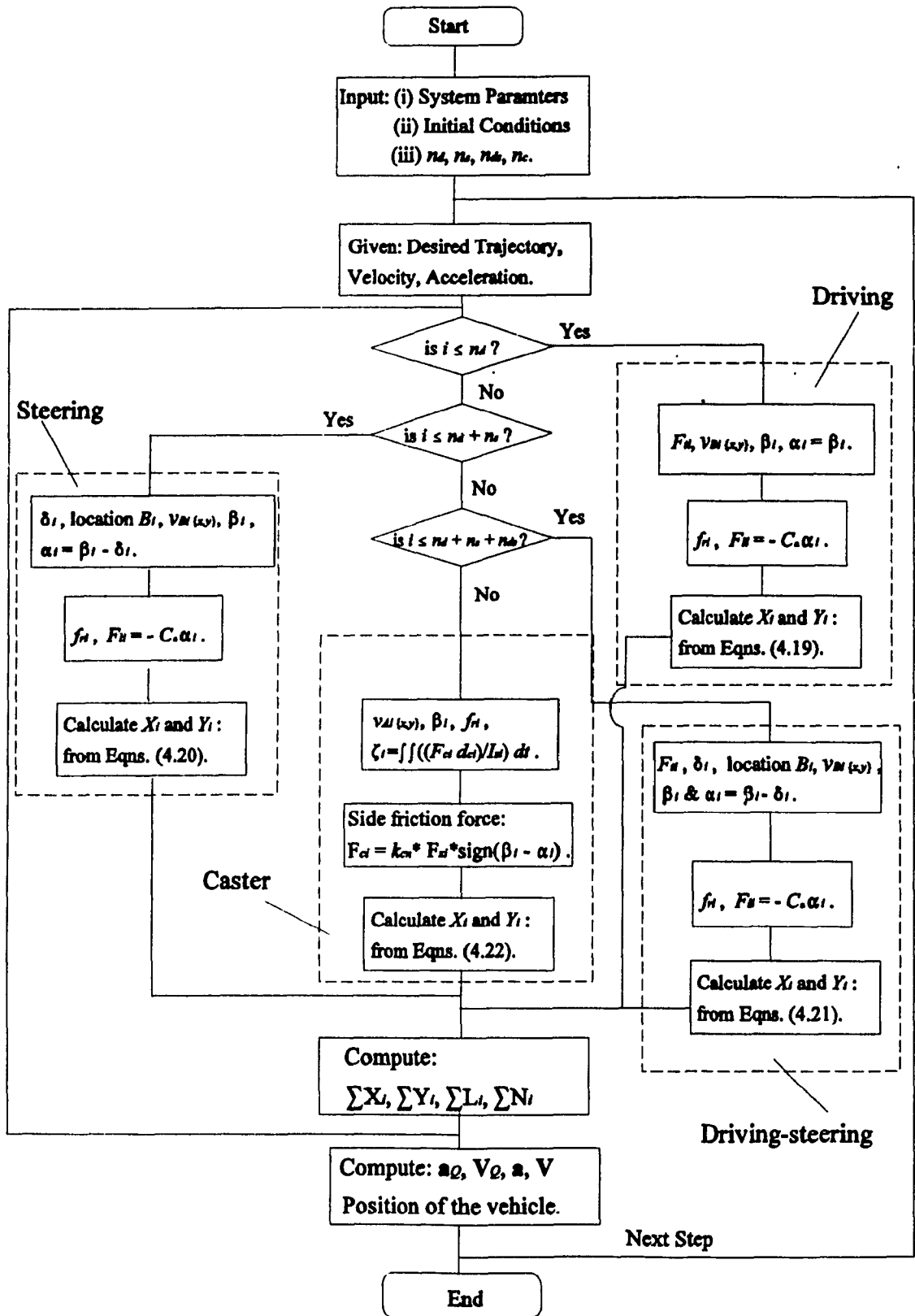**Step 8.** Integrate to obtain the next state positions and rates for the vehicle system.

Figure 4.5: Flowchart for Dynamical Simulation of Automated Vehicle System.

137

4.4 Summary

In this chapter, a systematic methodology for modelling and simulation of the dynamics of a class of automated vehicle has been developed. This methodology allows for arbitrary wheel configurations, combined sprung and unsprung masses, generation of the tractive forces, rolling friction and side friction at wheel-ground contact points, and nonholonomic constraints. Four types of wheel units, namely driving wheel units, steering wheel units, driving-steering wheel units and casters are considered to be employed on the automated vehicle systems.

The present approach to derivation of automated vehicle dynamical models renders the process considerably less difficult for users not familiar with the details of vehicle dynamics. It is possible to follow the simple steps provided in this chapter to obtain any desired dynamical model. This methodology may also be used to check models obtained by other techniques. In addition, although this model is designed to handle four DOFs automated vehicles, it can be extended to handle the six DOFs models since the z-direction variables (such as $\dot{Z}_Q$, z) have been retained throughout the modelling development.

For convenience to the users, a general procedure for deriving a dynamic model which incorporates n arbitrarily configured wheels is summarized the flowchart of Fig. 4.1. System parameters are summarized in Table 4.1, and assumptions and nomenclature for the model are summarised in Section 4.2.1. In order to facilitate tracking of all variables, Table 4.2 indicates all variables and equations generated or eliminated in each step. This permits the user to know the numerical degrees of freedom for the model so generated. Finally, the formal structure of the model is shown to lead to a parallel structure for numerical simulation on a digital computer. The flowchart for dynamical simulation of automated vehicle systems given by Fig. 4.5 illustrates this process.

138

Chapter 5

CASE STUDIES

5.1 Introduction

To demonstrate the methodology presented in Chapter 4, four different configurations of automated vehicle models are examined in this chapter. Dynamic models for these four case studies are derived by following the procedure given in Chapter 4. Results are given for numerical simulation on digital computer of two of these models. In these simulations, holonomic constraints and nonholonomic constraints of the automated vehicle are investigated.

For cases where the automated vehicle does not satisfy conditions of pure rolling and no side-slip at the wheel-ground contact point (holonomic constraints), there are redundancies in the dynamic models. The total number of redundant variables in the dynamic model is: $N_R = (n_d + n_s + 2n_{ds}) - $ (DOFs of the vehicle). The expression $(n_d + n_s + 2n_{ds})$ represents the total number of power and steering variables in the system.

For cases where automated vehicles satisfy conditions of pure rolling and no side-slip at the wheel-ground contact point (which are defined as nonholonomic constraints), the power variables (ω_i and $\dot{\omega}_i$) and steering variables (δ_i and $\dot{\delta}_i$) of the entire system can be determined from the nonholonomic constraints. In doing so, the total number of variables in the system is reduced, and the redundancy of the system becomes $N_R = (n_d + n_{ds}) - $ (DOFs of the vehicle). The remaining variables represent currents supplied to the DC motors. In addition, if there are no redundancies in the system, input currents can be determined from the inverse dynamics of the vehicle [52], in which currents can be expressed as functions of the desired linear velocities, yaw rate, and orientation of the vehicle with respect to the inertial frame $\{I\}$.

139

The first case study in this chapter is a model and simulation of the CONCIC-3 AGV [19] (with double steering wheelbase configuration). In this model, there are two sets of driving-steering wheel units (one each at the front and rear of the AGV), and two casters (located at either side of the geometric centre of the AGV). The second case study is a model and simulation of the CONCIC-2 AGV [21] (with differential driving wheel unit configuration). In this model, the two driving wheel units are employed at either side of the geometric centre of the AGV, and there are two casters (one each at the front and rear of the AGV). The third case study is a model of a vehicle with two pairs of driving-steering wheel units (one each at the front and rear of the vehicle). The fourth case study is an omnidirectional AGV with six-wheeled configuration. In this model, there are two driving-steering wheel units (one each at the front and rear of the vehicle), and there are two pairs of casters (one each at the front and rear of the vehicle).

5.2 Case Study 1: CONCIC-3 AGV

The CONCIC - 3 AGV has a double-steering wheelbase configuration with two motorized driving-steering wheel units (one each in the front and rear of the AGV), and two casters (one located on each side of the AGV), as shown in Fig. 5.1.

Assumptions:

- The AGV has three DOFs (u, v, γ).

- Sprung mass m_s is neglected, thus, the reference frame origin is located at the centre of the total mass of the AGV.

- Each wheel supports an equal fraction of the total AGV weight,

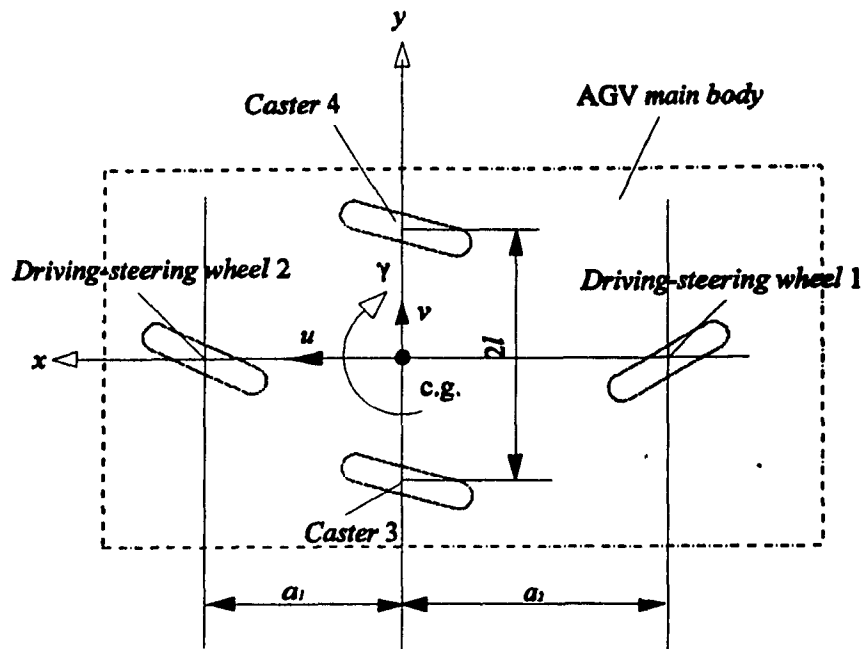- Offsets of the driving-steering wheel units and casters are equal to zero.

140

Figure 5.1: Schematic of CONCIC-3 AGV.

5.2.1 Dynamic Model of the CONCIC-3 AGV

The dynamic model of the CONCIC-3 AGV is developed by following the steps given in Chapter 4, as outlined below.

Step 1. Specification of the AGV system:

i) Driving wheel units: $n_d = 0$.

ii) Steering wheel units: $n_s = 0$.

iii) Driving-steering wheel units: $n_{ds} = 2$.

In this case, since the offset of each driving-steering wheel unit is equal to zero, the locations of joints A_i and B_i are coincident with each other. Locations of joints B_i for the two driving-steering wheel units are specified by the following equations ($i = 1, 2$):

141

$$\begin{cases} x_{b1} = -a_1 = -0.39 \ (m) \ , \\ y_{b1} = 0 \ (m) \ , \end{cases} \qquad \begin{cases} x_{b2} = a_1 = 0.32 \ (m) \ , \\ y_{b1} = 0 \ (m) \ , \end{cases} \qquad (5.1.1)$$

iv) Casters (in this case the offsets $d_3 = d_4 = 0$): $\quad n_c = 2$.

The locations of joints A_i for the two casters are ($i = 3, 4$):

$$\begin{cases} x_{a3} = 0 \ (m) \ , \\ y_{a3} = -l = 0.26 \ (m) \ , \end{cases} \qquad \begin{cases} x_{a4} = 0 \ (m) \ , \\ y_{a4} = l = 0.26 \ (m) \ , \end{cases} \qquad (5.1.2)$$

The total number of wheel units n employed on the CONCIC-3 AGV and the total number of steering and power variables N_{var} introduced to the system are given by the following equations:

$$\begin{aligned} n &= n_d + n_s + n_{ds} + n_c = 4 \ , \\ N_{var} &= n_d + n_s + 2 \ n_{ds} = 4 \ . \end{aligned} \qquad (5.1.3)$$

Step 2. Determination of intermediate variables (β_i, α_i, ζ_i and f_{r_i}) for each wheel unit:

Step 2.1 Calculate the constrained velocities at joint B_i, and determine the direction angle (β_i) of each driving-steering wheel unit:

iii) The constrained velocities of the two driving-steering wheels at joints B_1 and B_2 are:

$$\mathbf{V}_{B_1} = \begin{pmatrix} v_{x_{B_1}} \\ v_{y_{B_1}} \end{pmatrix} = \begin{pmatrix} u \\ v - 0.39\,\gamma \end{pmatrix} ,$$

$$\mathbf{V}_{B_2} = \begin{pmatrix} v_{x_{B_2}} \\ v_{y_{B_2}} \end{pmatrix} = \begin{pmatrix} u \\ v + 0.32\,\gamma \end{pmatrix} . \qquad (5.1.4)$$

142

iv) The constrained velocities for the two casters at joints A_3 and A_4 are:

$$\mathbf{V}_{A_3} = \begin{pmatrix} v_{x_{A_3}} \\ v_{y_{A_3}} \end{pmatrix} = \begin{pmatrix} u + 0.26\,\gamma \\ v \end{pmatrix},$$

$$\mathbf{V}_{A_4} = \begin{pmatrix} v_{x_{A_4}} \\ v_{y_{A_4}} \end{pmatrix} = \begin{pmatrix} u - 0.26\,\gamma \\ v \end{pmatrix}.$$

(5.1.5)

In this case, the rolling friction factor of each wheel unit is taken as constant ($f_{r_i} = 0.023$), the magnitudes of velocity vectors $\mathbf{V}_{B_1}, \mathbf{V}_{B_2}, \mathbf{V}_{A_3}$ and $\mathbf{V}_{A_4}$ in the xy plane do not need to be calculated. The direction angle (β_i) of each wheel unit ($i = 1, 2, 3, 4$):

$$\beta_1 = \tan^{-1}\frac{v_{y_{B_1}}}{v_{x_{B_1}}} = \tan^{-1}\frac{v + 0.32\,\gamma}{u},$$

$$\beta_2 = \tan^{-1}\frac{v_{y_{B_2}}}{v_{x_{B_2}}} = \tan^{-1}\frac{v - 0.39\,\gamma}{u},$$

$$\beta_3 = \tan^{-1}\frac{v_{y_{A_3}}}{v_{x_{A_3}}} = \tan^{-1}\frac{v - 0.6\gamma}{u - 0.26\gamma},$$

$$\beta_4 = \tan^{-1}\frac{v_{y_{A_4}}}{v_{x_{A_4}}} = \tan^{-1}\frac{v - 0.6\gamma}{u + 0.26\gamma}.$$

(5.1.6)

Step 2.2 Calculate the slip angles and rotation angles (α_i, ζ_i):

$$\alpha_1 = \beta_1 - \delta_1,$$

$$\alpha_2 = \beta_2 - \delta_2,$$

$$\zeta_3 = 0,$$

$$\zeta_4 = 0.$$

(5.1.7)

143

In the above equations, steering angles of the two driving-steering wheel units can be considered as independent input variables (commands) given to the AGV system. They are determined by applying kinematic constraint 2 as follows:

$$\delta_1 = \tan^{-1}\frac{-\dot{X}_Q \sin(\theta) + \dot{Y}_Q \cos(\theta) + x_{a_1}\gamma}{\dot{X}_Q \cos(\theta) + \dot{Y}_Q \sin(\theta) - y_{a_1}\gamma},$$

$$\delta_2 = \tan^{-1}\frac{-\dot{X}_Q \sin(\theta) + \dot{Y}_Q \cos(\theta) + x_{a_2}\gamma}{\dot{X}_Q \cos(\theta) + \dot{Y}_Q \sin(\theta) - y_{a_2}\gamma}.$$

$$(5.1.8)$$

These are functions of the desired linear velocity, yaw rate and location of each driving-steering wheel unit. In this step, the rolling friction factors are taken as constants, therefore only $2n$ intermediate variables need to be determined. The two steering variables are accounted for in the above equations, and now it only remains to incorporate the power variables.

Step 3. Calculation of the external forces (F_{l_i}, F_{f_i}, F_{c_i} and F_{t_i}) acting on each wheel at wheel-ground contact points:

Step 3.1 External forces depend on the slip angle, and friction between the wheel and floor as follows:

$$F_{l_1} = -C_\alpha \, \alpha_1 \, ,$$

$$F_{l_2} = -C_\alpha \, \alpha_2 \, ,$$

$$F_{c_3} = k_\alpha F_{s_3} \, \text{sign}\,(\beta_3 - \zeta_3) \, ,$$

$$F_{c_4} = k_\alpha F_{s_4} \, \text{sign}\,(\beta_4 - \zeta_4) \, ,$$

$$F_{f_i} = f_{r_i} F_{s_i} \, , \quad (i = 1, 2, 3, 4)$$

$$(5.1.9)$$

Step 3.2 External forces depend on the motor characteristics as follows:

$$F_{t_1} = \frac{N_1}{R_1} (K_{T_1} I_1 - J_1 N_1 \dot{\omega}_1 - D_1 N_1 \omega_1 - T_{t_1}) \, ,$$

$$F_{t_2} = \frac{N_2}{R_2} (K_{T_2} I_2 - J_2 N_2 \dot{\omega}_2 - D_2 N_2 \omega_2 - T_{t_2}) \, .$$

(5.1.10)

In Eqns. (5.1.10), the currents of the two driving-steering wheel units are I_1 and I_2. These currents can be determined from the inverse dynamic model of the AGV, since the system has no redundancy. They can be also considered as independent input variables (commands) applied to the system to study the dynamic behaviour of the AGV. The angular velocities and accelerations of the two driving-steering wheel units are ω_1, ω_2 and $\dot{\omega}_1$, $\dot{\omega}_2$, respectively, which can be determined by applying the kinematic constraints provided in Section 2.5. These angular velocities are expressed by following equations:

$$\begin{cases} \omega_1 = \dfrac{\dot{X}_Q \cos(\theta + \delta_1) + \dot{Y}_Q \sin(\theta + \delta_1) + (x_{a_1} \sin(\delta_1) - y_{b_1} \cos(\delta_1)) \cdot \dot{\gamma}}{R_1} \, , \\[4mm] \omega_2 = \dfrac{\dot{X}_Q \cos(\theta + \delta_2) + \dot{Y}_Q \sin(\theta + \delta_2) + (x_{a_1} \sin(\delta_1) - y_{b_2} \cos(\delta_2)) \cdot \dot{\gamma}}{R_2} \, , \end{cases}$$

(5.1.11)

and the angular acceleration of the two driving-steering wheel units $\dot{\omega}_1$, $\dot{\omega}_2$ can be determined by differentiating Eqns. (5.1.11) with respect to time (refer to Eqn. (4.18)). The accelerations and velocities of the vehicle with respect to the X, Y axes of inertial frame {I} are $\ddot{X}_Q$, $\ddot{Y}_Q$ and $\dot{X}_Q$, $\dot{Y}_Q$, respectively. The orientation and yaw rate of the vehicle are θ

and γ, respectively. In this step, all remaining power variables are determined if all input currents have been given .

Step 4. Formulating the total external forces acting on the wheel-ground contact points along the x and y axes:

i) Driving wheel units & ii) Steering wheel units do not need to be considered.

iii) Two driving-steering wheel units (refer to Eqns. (4.21)):

$$
\left\{
\begin{array}{l}
X_1 = (F_{t_1} - F_{f_1})\cos \delta_1 + |F_{l_1}| \cos (\delta_1 - \text{sign}(\alpha_1)\dfrac{\pi}{2}) , \\[4mm]
Y_1 = (F_{t_1} - F_{f_1})\sin \delta_1 + |F_{l_1}| \sin (\delta_1 - \text{sign}(\alpha_2)\dfrac{\pi}{2}) ,
\end{array}
\right.
\tag{5.1.12}
$$

and

$$
\left\{
\begin{array}{l}
X_2 = (F_{t_2} - F_{f_2})\cos \delta_2 + |F_{l_1}| \cos (\delta_2 - \text{sign}(\alpha_2)\dfrac{\pi}{2}) , \\[4mm]
Y_2 = (F_{t_2} - F_{f_2})\sin \delta_2 + |F_{l_1}| \sin (\delta_2 - \text{sign}(\alpha_2)\dfrac{\pi}{2}) ,
\end{array}
\right.
\tag{5.1.13}
$$

iv) Two casters (refer to 4.22) :

$$
\left\{
\begin{array}{l}
X_3 = -F_{f_3} \cos \zeta_3 + F_{c_3} \cos (\zeta_3 + \text{sign}(\zeta_3)\dfrac{\pi}{2}) , \\[4mm]
Y_3 = -F_{f_3} \sin \zeta_3 + F_{c_3} \sin (\zeta_3 + \text{sign}(\zeta_3)\dfrac{\pi}{2}) ,
\end{array}
\right.
\tag{5.1.14}
$$

and

146

$$\left\{ \begin{array}{l} X_4 = -F_{f_4} \cos \zeta_4 + F_{c_4} \cos \left(\zeta_4 + \text{sign} \left(\zeta_4 \right) \dfrac{\pi}{2} \right) , \\[4mm] Y_4 = -F_{f_4} \sin \zeta_4 + F_{c_4} \sin \left(\zeta_4 + \text{sign} \left(\zeta_4 \right) \dfrac{\pi}{2} \right) , \end{array} \right.$$

(5.1.15)

Step 5. Total external forces and moments acting on the AGV system:

a) Total external forces acting on the AGV along the x direction:

$$\sum X = (F_{t_1} - F_{f_1}) \cos \delta_1 + | F_{l_1} | \cos \left(\delta_1 - \text{sign} \left(\alpha_1 \right) \dfrac{\pi}{2} \right)$$

$$+ (F_{t_2} - F_{f_2}) \cos \delta_2 + | F_{l_2} | \cos \left(\delta_2 - \text{sign} \left(\alpha_2 \right) \dfrac{\pi}{2} \right)$$

$$- F_{f_3} \cos \zeta_3 + F_{c_3} \cos \left(\zeta_3 + \text{sign} \left(\zeta_3 \right) \dfrac{\pi}{2} \right)$$

(5.1.16)

$$- F_{f_4} \cos \zeta_4 + F_{c_4} \cos \left(\zeta_4 + \text{sign} \left(\zeta_4 \right) \dfrac{\pi}{2} \right) ,$$

b) Total external forces acting on the AGV along the y direction.

$$\sum Y = (F_{t_1} - F_{f_1}) \sin \delta_1 + | F_{l_1} | \sin \left(\delta_1 - \text{sign} \left(\alpha_1 \right) \dfrac{\pi}{2} \right)$$

$$+ (F_{t_2} - F_{f_2}) \sin \delta_2 + | F_{l_2} | \sin \left(\delta_2 - \text{sign} \left(\alpha_2 \right) \dfrac{\pi}{2} \right)$$

$$- F_{f_3} \sin \zeta_3 + F_{c_3} \sin \left(\zeta_3 + \text{sign} \left(\zeta_3 \right) \dfrac{\pi}{2} \right)$$

(5.1.17)

$$- F_{f_4} \sin \zeta_4 + F_{c_4} \sin \left(\zeta_4 + \text{sign} \left(\zeta_4 \right) \dfrac{\pi}{2} \right) ,$$

c) Total external moments acting on the AGV above the z (yaw) axis:

$$\sum N = \sum_{i=1}^{2} -((F_{t_i} - F_{f_i}) \cos \delta_i + |F_{l_i}| \cos (\delta_i - \text{sign}(\alpha_i) \frac{\pi}{2}) y_{e_i}$$

$$- \sum_{i=3}^{4} (-F_{f_i} \cos \zeta_i + F_{c_i} \cos (\zeta_i + \text{sign}(\zeta_i) \frac{\pi}{2}) y_{e_i}$$

$$+ \sum_{i=1}^{2} ((F_{t_i} - F_{f_i}) \sin \delta_i + |F_{l_i}| \sin (\delta_i - \text{sign}(\alpha_i) \frac{\pi}{2}) x_{e_i}$$

$$+ \sum_{i=3}^{4} (-F_{f_{latn}} \zeta_i + F_{c_i} \cos (\zeta_i + \text{sign}(\zeta_i) \frac{\pi}{2}) x_{e_i} .$$

(5.1.18)

Step 6. Assemble motion equations of the AGV with external forces and moments:

$$m(\dot{u} - \gamma v) = \sum X ,$$

$$m(\dot{v} + \gamma u) = \sum Y ,$$

$$I_z \dot{\gamma} = \sum N .$$

(5.1.19)

Finally, substituting external forces and moments obtained in Step 5 into Eqn. (4.1.19), the equations of motion for the CONCIC-3 AGV can be expressed as follows:

$$m(\dot{u} - \gamma v) = (F_{t_1} - F_{f_1}) \cos \delta_1 + |F_{l_1}| \cos (\delta_1 - \text{sign}(\alpha_1) \frac{\pi}{2})$$

$$+ (F_{t_2} - F_{f_2}) \cos \delta_2 + |F_{l_2}| \cos (\delta_2 - \text{sign}(\alpha_2) \frac{\pi}{2})$$

$$- F_{f_3} \cos \zeta_3 + F_{c_3} \cos (\zeta_3 + \text{sign}(\zeta_3) \frac{\pi}{2})$$

$$- F_{f_4} \cos \zeta_4 + F_{c_4} \cos (\zeta_4 + \text{sign}(\zeta_4) \frac{\pi}{2}) ,$$

(5.1.20)

$$m(\dot{v} + \gamma u) = (F_{t_1} - F_{f_1}) \sin \delta_1 + |F_{l_1}| \sin (\delta_1 - \text{sign}(\alpha_1) \frac{\pi}{2})$$

$$+ (F_{t_2} - F_{f_2}) \sin \delta_2 + |F_{l_2}| \sin (\delta_2 - \text{sign}(\alpha_2) \frac{\pi}{2})$$

$$- F_{f_3} \cos \zeta_3 + F_{c_3} \sin (\zeta_3 + \text{sign}(\zeta_3) \frac{\pi}{2})$$

$$- F_{f_4} \sin \zeta_4 + F_{c_4} \sin (\zeta_4 + \text{sign}(\zeta_4) \frac{\pi}{2}) ,$$

$$I_z \dot{Y} = (F_{f_3} \cos \zeta_3 - F_{c_3} \cos (\zeta_3 + \text{sign} (\zeta_3) \frac{\pi}{2})) (-l)$$

$$+ (F_{f_4} \cos \zeta_4 - F_{c_4} \cos (\zeta_4 + \text{sign} (\zeta_4) \frac{\pi}{2})) (l)$$

$$- ((F_{t_1} - F_{f_1}) \sin \delta_1 + |F_{l_1}| \sin (\delta_1 - \text{sign} (\alpha_1) \frac{\pi}{2})) (a_2)$$

$$+ ((F_{t_2} - F_{f_2}) \sin \delta_2 + |F_{l_2}| \sin (\delta_2 - \text{sign} (\alpha_2) \frac{\pi}{2})) (a_1) .$$

This is a sixth order system of nonlinear ordinary differential equations.

Step 7. Obtain the forward dynamical model of the CONCIC-3 AGV:

Rearranging Eqn. (5.22) in matrix form, the acceleration vector of the CONCIC-3 AGV with respect to frame $\{Q\}$ can be expressed by following equation:

$$\mathbf{a}_Q = \begin{pmatrix} \dot{u} \\ \dot{v} \\ \dot{Y} \end{pmatrix} = A^{-1} (B + D), \tag{5.1.21}$$

and the acceleration of the AGV with respect to inertial frame $\{I\}$ can be determined by the following equation:

$$\mathbf{a} = T \times \mathbf{a}_Q \tag{5.1.22}$$

where T is a transformation matrix and

$$A = \begin{bmatrix} m & 0 & 0 \\ 0 & m & 0 \\ 0 & 0 & I_z \end{bmatrix}, \qquad B = \begin{pmatrix} \sum X \\ \sum Y \\ \sum N \end{pmatrix}, \qquad D = \begin{pmatrix} v \, Y \\ -u \, Y \\ 0 \end{pmatrix} .$$

149

Step 8. Integrating the forward dynamical model :

Given the initial position $\mathbf{P}_0$ $\{X_Q(0), Y_Q(0), \theta(0)\}$ and velocity $\mathbf{V}_0$ $\{\dot{X}_Q(0), \dot{Y}_Q(0), \gamma(0)\}$ of the AGV with respect to frame $\{I\}$, the instantaneous velocities and position with respect to frame $\{I\}$ can be determined by integrating the above equation with respect to the time.

Comparison of results for the conventional and general approach: Comparing Eqns. (5.20) with the dynamical model of the CONCIC-3 AGV developed by Dr. Mostafa G. Mehrabi [19], we have the following notational correspondences:

$$u = V_u \, ,$$
$$\dot{u} = \dot{V}_u \, ,$$
$$v = V_w \, ,$$
$$\dot{v} = \dot{V}_w \, ,$$
$$\gamma = \Omega \, ,$$
$$\dot{\gamma} = \dot{\Omega} \, ;$$

$$\delta_1 = \delta_{fw} \, ,$$
$$\delta_2 = \delta_{rw} \, ,$$
$$\zeta_3 = \gamma_r \, ,$$
$$\zeta_4 = \gamma_l \, ,$$
$$a_1 = a \quad a_2 = b \, ,$$
$$l = c \, ;$$

$$F_{t_1} - F_{f_1} = F_{Rr_2} \, ,$$
$$F_{t_1} = F_{Rr_1} \, ,$$
$$F_{t_2} - F_{f_2} = F_{Rr_2} \, ,$$
$$F_{t_2} = F_{Rr_1} \, .$$

The above correspondences show that the dynamical equations obtained from the general approach are identical to the dynamical equations obtained using the conventional approach.

5.2.2 Dynamic Simulation of the CONCIC-3 AGV

5.2.2.1 Simulation Inputs

The complete dynamic model of the CONCIC-3 AGV has been derived in Section 5.2.1 following the formal structure provided in Chapter 4, Section 4.2. In this section, the dynamic

simulation of the CONCIC-3 AGV is studied based on the formal steps provided in Section 4.3.2. System parameters are given in Appendix D, Table D.1. Simulations have been carried out using the following initial conditions.

(i) Initial position of the AGV with respect to frame $\{I\}$:

$$\begin{cases} X_{\varrho} = 0 \ , \\ Y_{\varrho} = 0 \ , \\ \theta(0) = 0 \ . \end{cases} \tag{5.1.23}$$

(ii) Initial velocities and accelerations of the AGV with respect to frame $\{I\}$:

$$\begin{cases} \dot{X}_{\varrho} = 0 \ , \\ \dot{Y}_{\varrho} = 0 \ , \\ \dot{\gamma}(0) = 0 \ , \end{cases} \qquad \begin{cases} \ddot{X}_{\varrho} = 0 \ , \\ \ddot{Y}_{\varrho} = 0 \ , \\ \ddot{\gamma}(0) = 0 \ . \end{cases} \tag{5.1.24}$$

(iii) Initial caster angular displacements: $\zeta_3 = 0$, and $\zeta_4 = 0$.

Steering variables are computed using Eqns. (5.1.8), with the condition that the slip angle must less then 4 degrees. Tractive forces are determined by Eqns. (5.1.10), (5.1.11) and (4.18 b), and the currents are considered as inputs. Nonholonomic constraints of the automated vehicle system must be satisfied. In this case study, currents are given as step inputs to the two DC driving motors, and distinct steering angles are given to the two steering wheels. A different set of simulation inputs is shown in Fig. 5.2. For all cases, the steering angle input steps are $\delta_1 = -0.039$ rad $(= 2.23$ deg) and $\delta_2 = 0.032$ rad $(= 1.83$ deg).

5.2.2.2 Simulation Results for the CONCIC-3 AGV

Simulation results of the CONCIC-3 AGV are shown in Figs. 5.3 through 5.9. Given two constant currents ($I_1 = I_2 = 4$ amp) and two steering angle steps (when $t \geq 0.5$ sec, $\delta_1 = -0.039$ rad and $\delta_2 = 0.032$ rad), the slip angle of each wheel unit responds as shown in Fig.5.3. Results show that: (i) steering causes the wheel side-slip, (ii) slip angles increase with time, (iii) slip angles of the front and rear wheel units are larger than the slip angles of the two casters located at each side of the AGV. In conjunction with the slip angles, there are some lateral forces acting on each wheel unit due to steering. Results (see Fig.5.4) also show that (i) lateral forces increase with time, (ii) lateral forces acting on the two driving-steering wheel units located at the front and rear of the AGV are larger than the lateral forces acting on the two casters located at two sides of the AGV.

Figs. 5.5 and 5.6 show how the slip angles and lateral forces respond to different input currents with two constant steering angles. These results show that: (i) when step input currents $I_1 = I_2 \geq 2.0$ amp, the slip angles and lateral forces increase with input current as well as time, (ii) when $I_1 = I_2 < 2.0$ amp, the slip angles and lateral forces increase with decreasing input current. Therefore in order to satisfy the conditions of pure roll and non side-slip for automated vehicle systems, all power and steering variables have to be maintained within certain limits. These limits may be determined by applying kinematic constraints 1 and 2 provided in Chapter 2. Figs. 5.7 and 5.8 also show that: (i) when input currents are larger than a certain value, the longitudinal, lateral and angular velocities of the vehicle increase with current as well as time, (ii) when input currents are less than a certain value, the vehicle moves sideways rather than forward. In addition, Fig. 5.9 provides the trajectories of the CONCIC-3 AGV with different input current and steering variables.
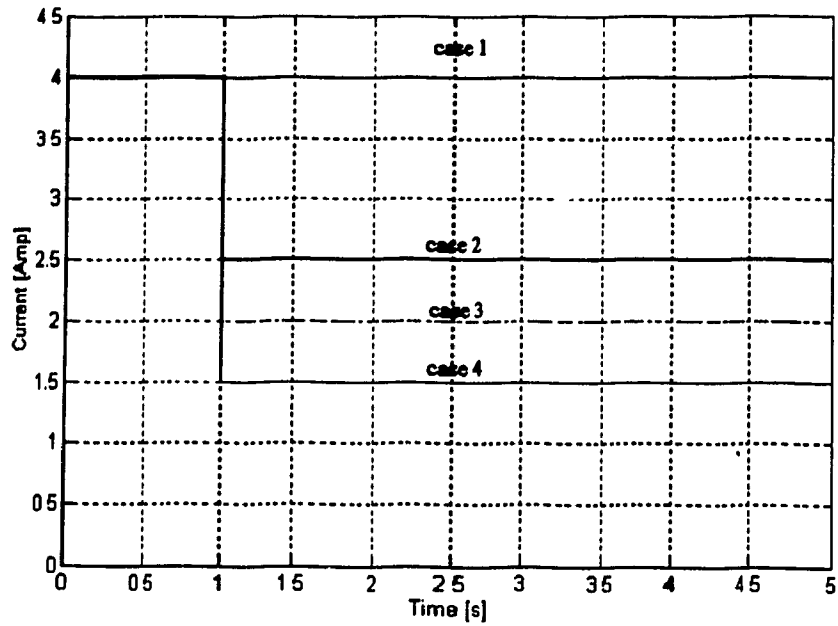
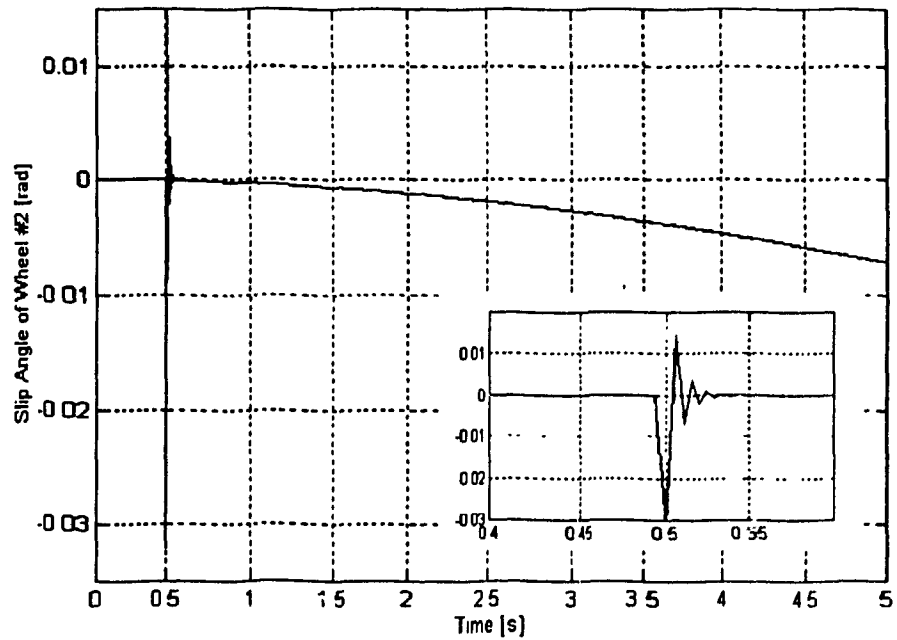**a)** Step input currents for the two DC driving motors.
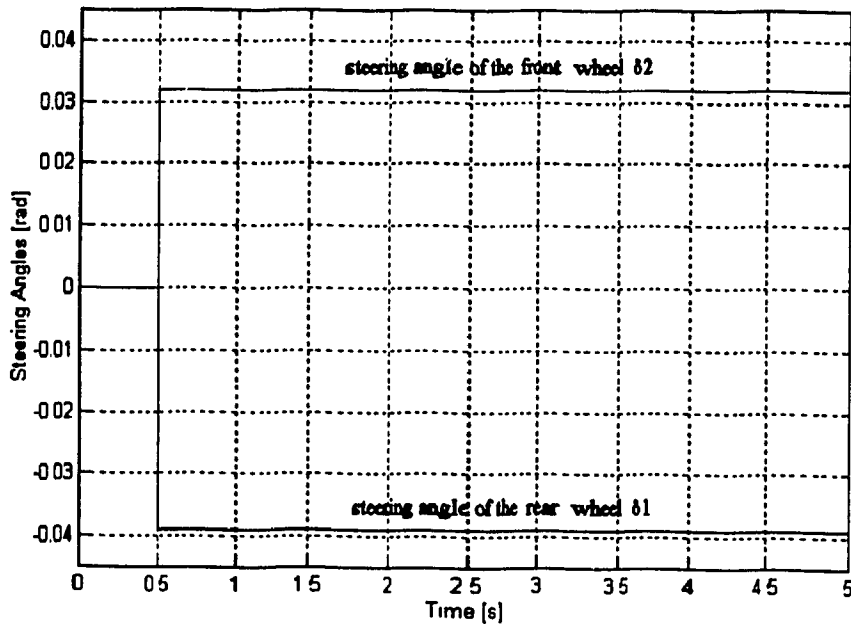
b) Steering angle st ?p inputs for the two driving-steering wheel units.
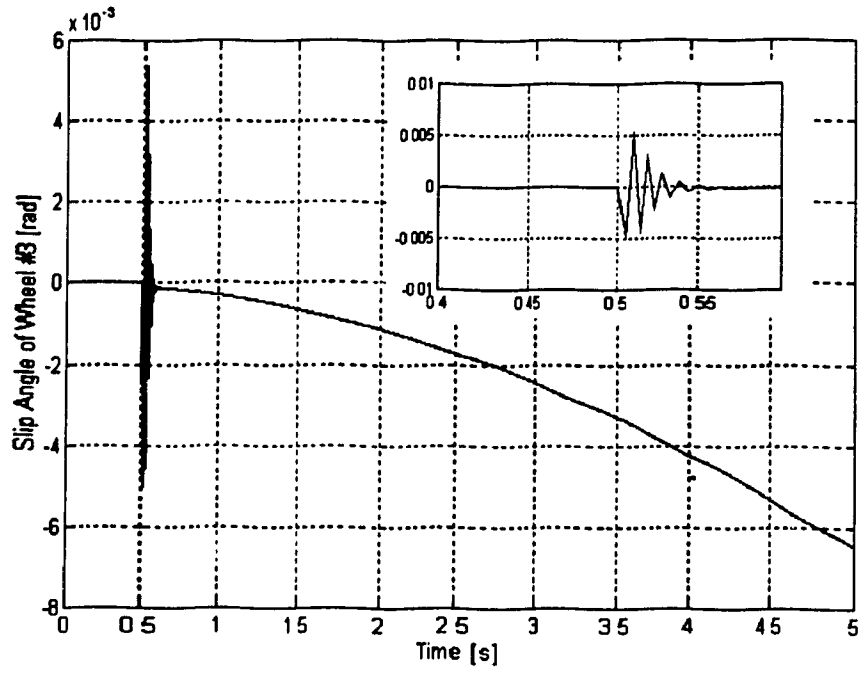
Figure 5.2: Simulation Inputs for CONCIC-3 AGV.

153
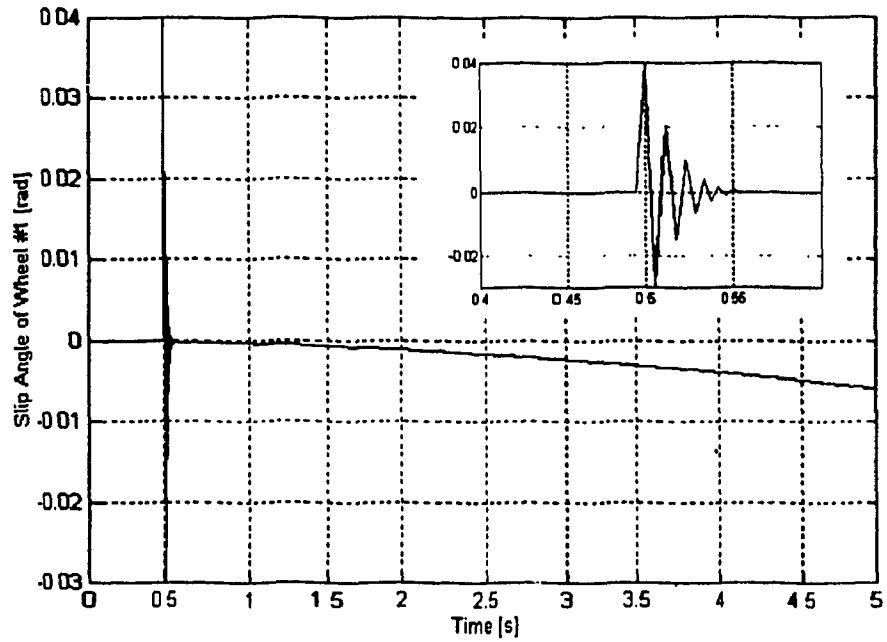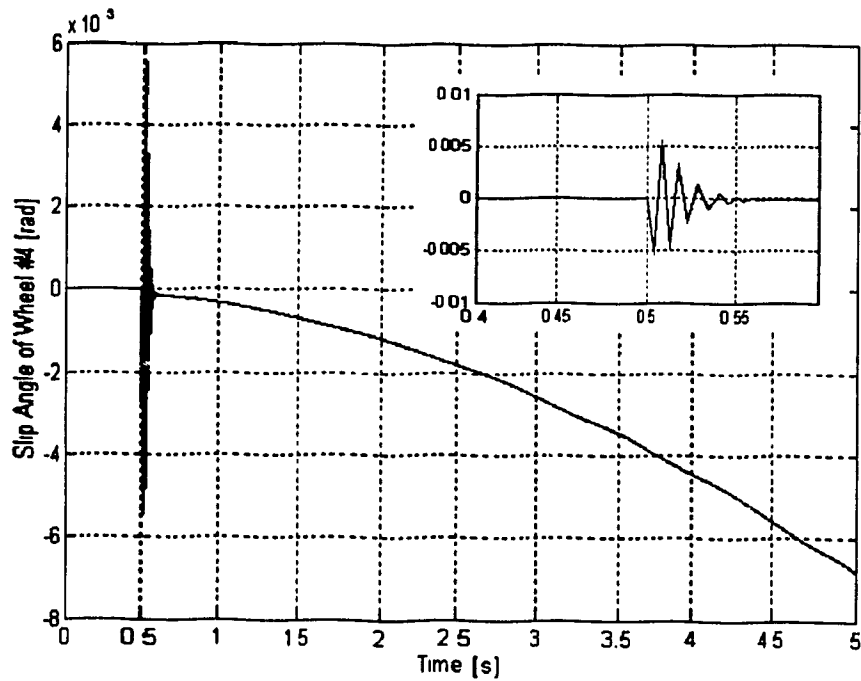
a) Slip angle of the rear driving-steering wheel unit of CONCIC-3 AGV.

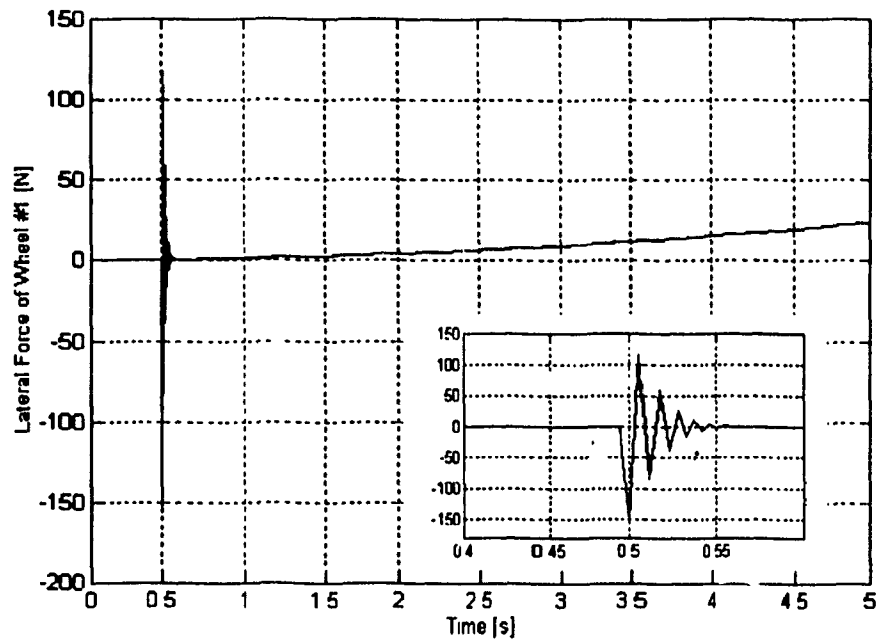b) Slip angle of the front driving-steering wheel unit of CONCIC-3 AGV.

154

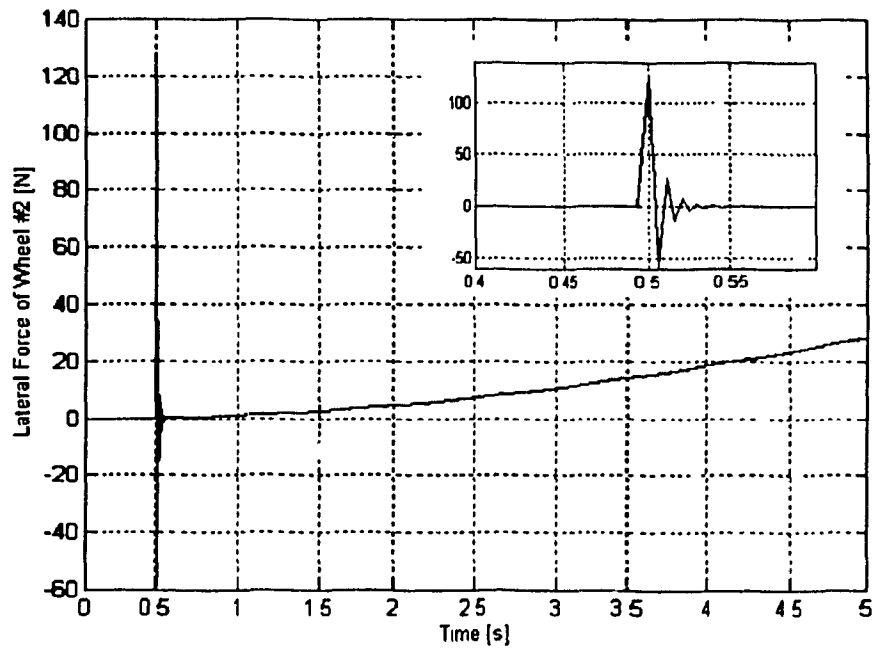c) Slip angle of the left caster of the CONCIC-3 AGV.
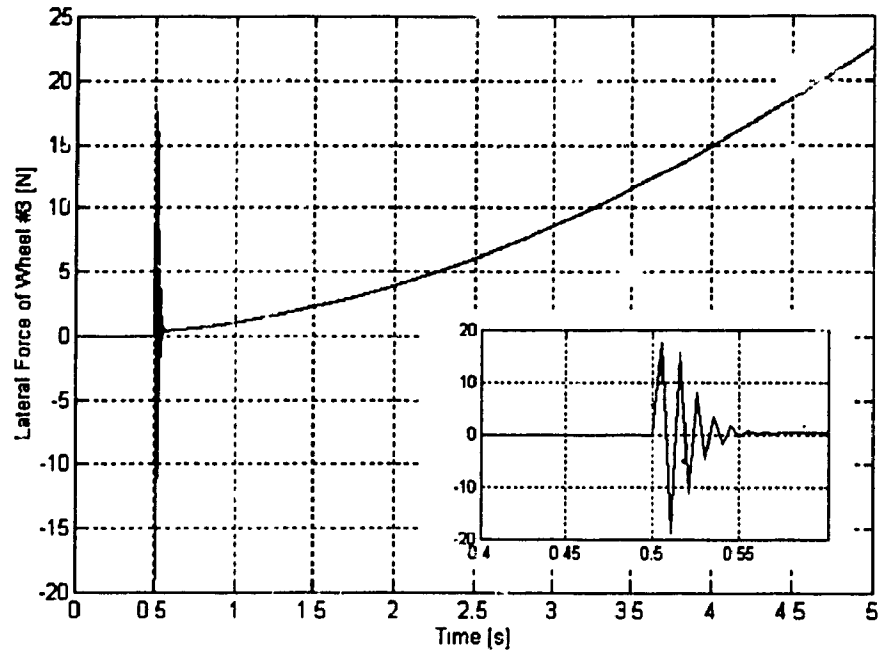

d) Slip angle of the right caster of the CONCIC-3 AGV.

Figure 5.3: Slip angle of each wheel for Case 1 current inputs (Fig. 5.2(a)) with steering angle inputs as shown in Fig. 5.2 (b).

155

a) Lateral force acting on the rear driving-steering wheel unit.

b) Lateral force acting on the front driving-steering wheel unit.

156

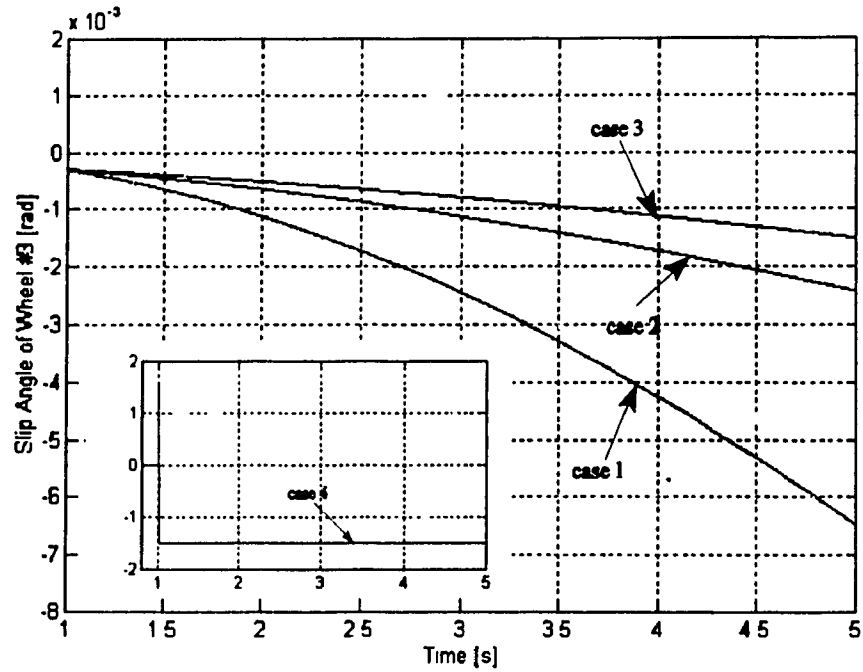c) Lateral force acting on the left caster.
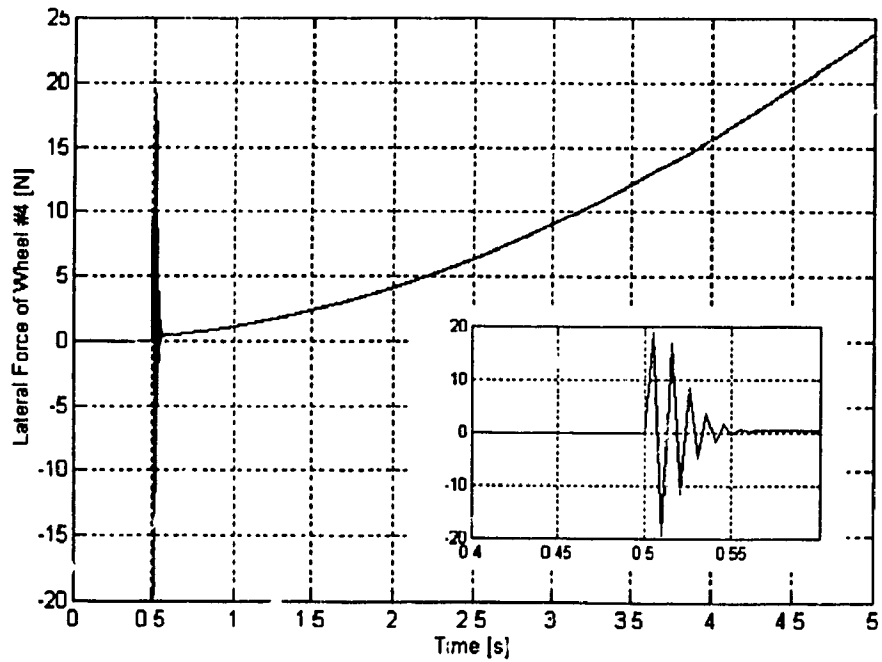
d) Lateral force acting on the right caster.

Figure 5.4: Lateral forces acting on each wheel unit of the AGV for Case 1 current inputs (Fig. 5.2 (a)), with steering angle inputs as shown in Fig. 5.2 (b).
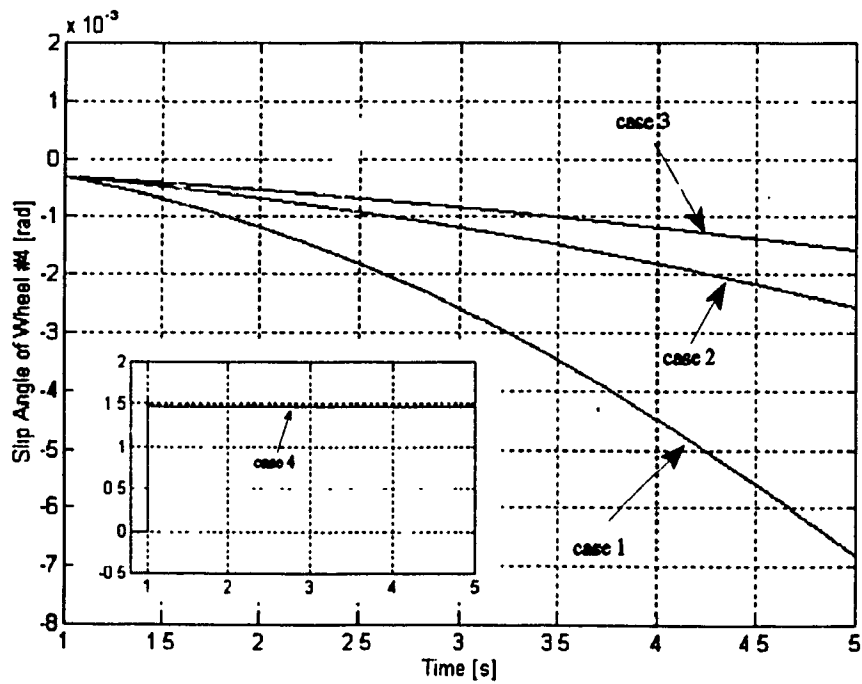
157
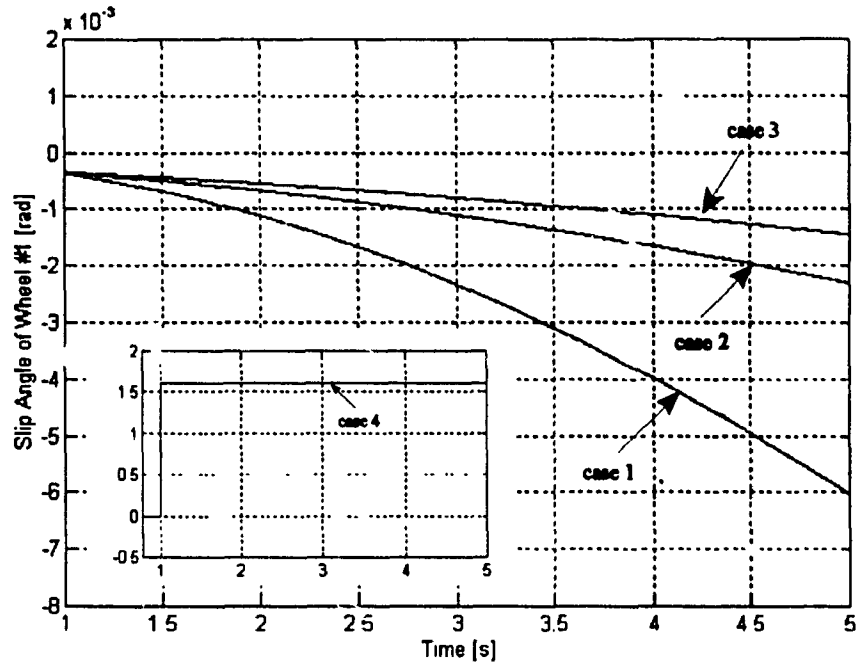
a) Rear wheel slip angles.
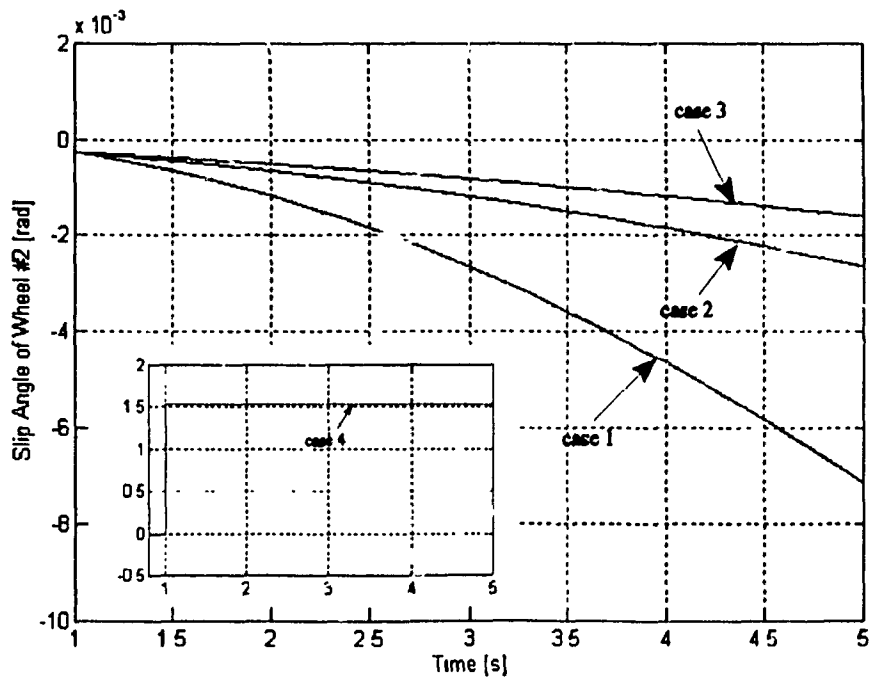
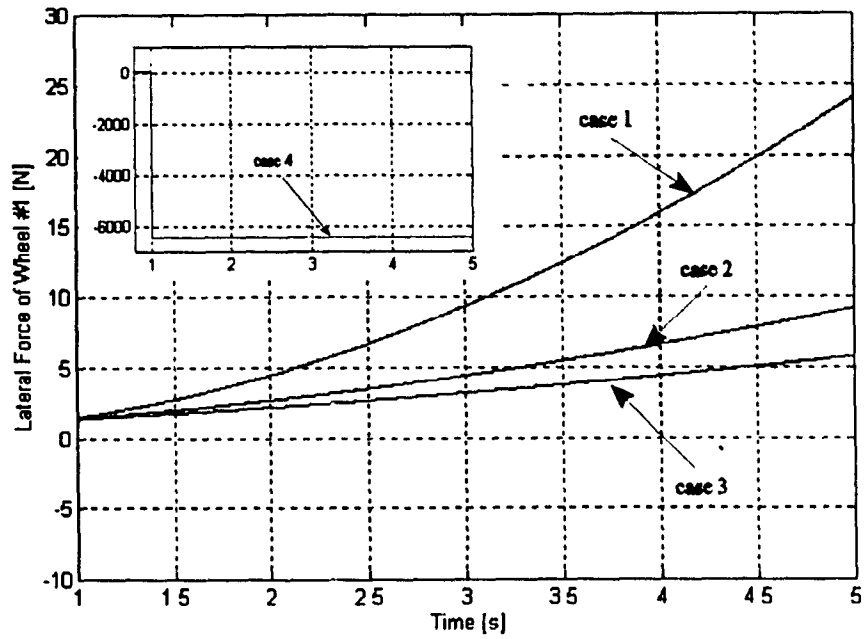
b) Front wheel slip angles.

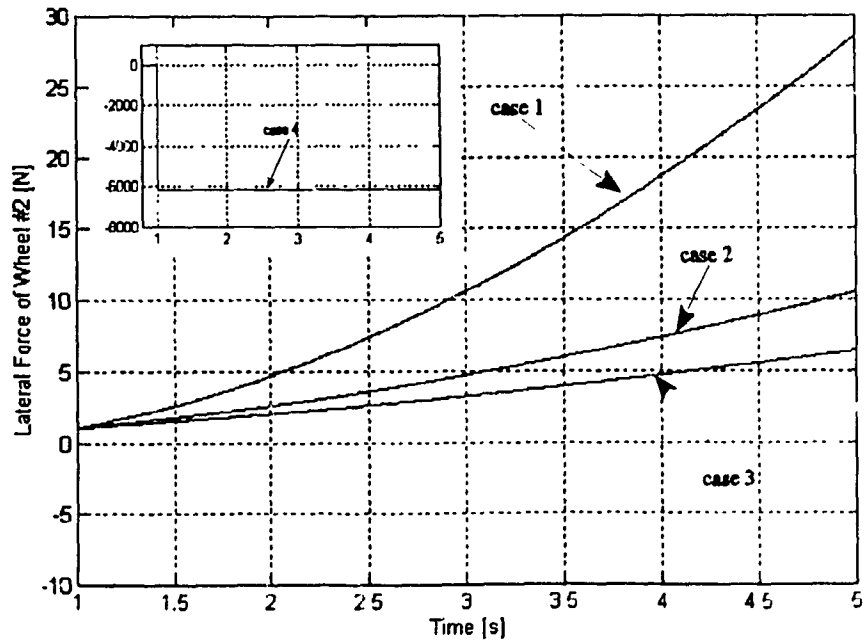158

c) Left caster slip angles.
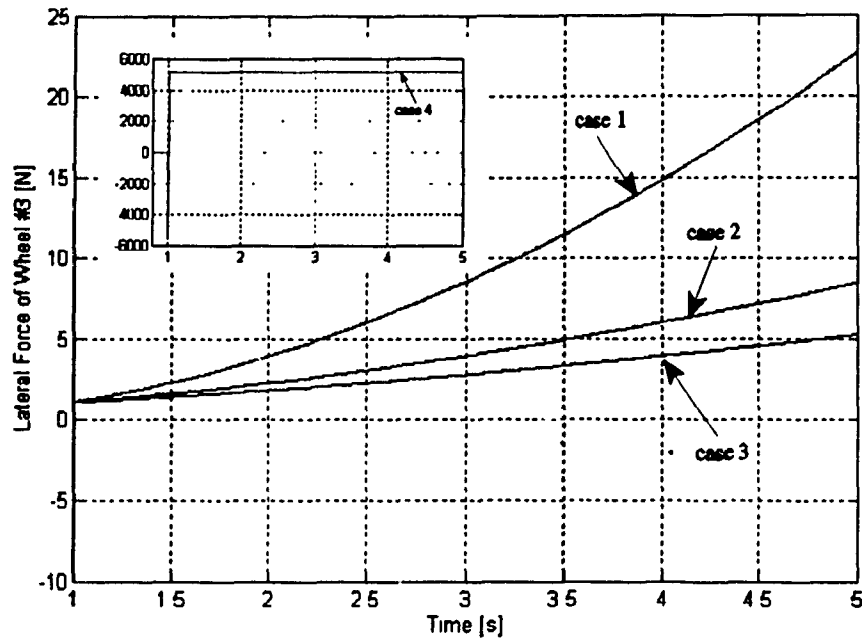

d) Right caster slip angles.

Figure 5.5: Slip angles of each wheel unit for various current step inputs, with constant steering angles ($\delta_1 = -0.039$ rad, $\delta_2 = 0.032$ rad) for CONCIC-3 AGV.
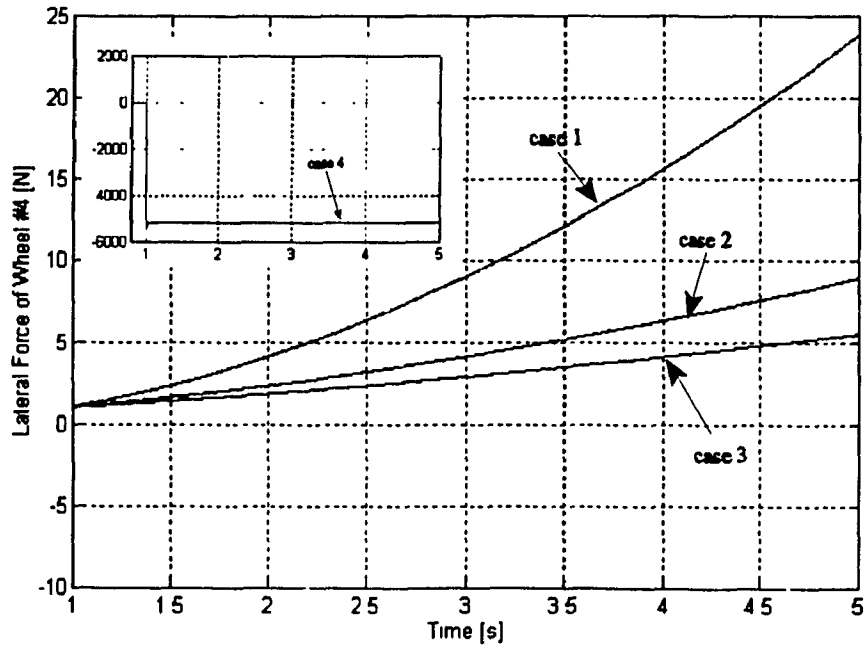
159

a) Lateral forces of the rear driving-steering wheel unit.

b) Lateral forces of the front driving-steering wheel unit
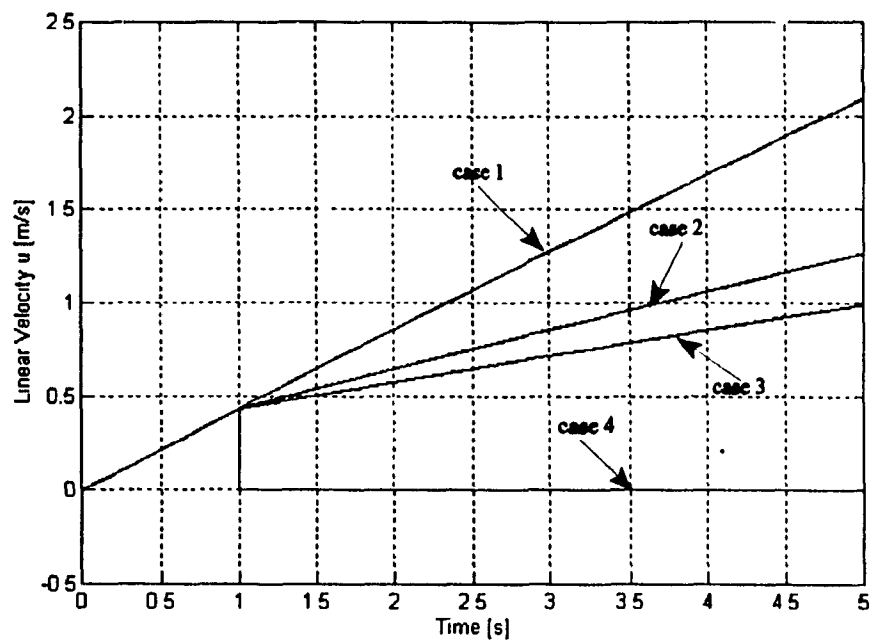
160

c) Lateral forces of the left caster.

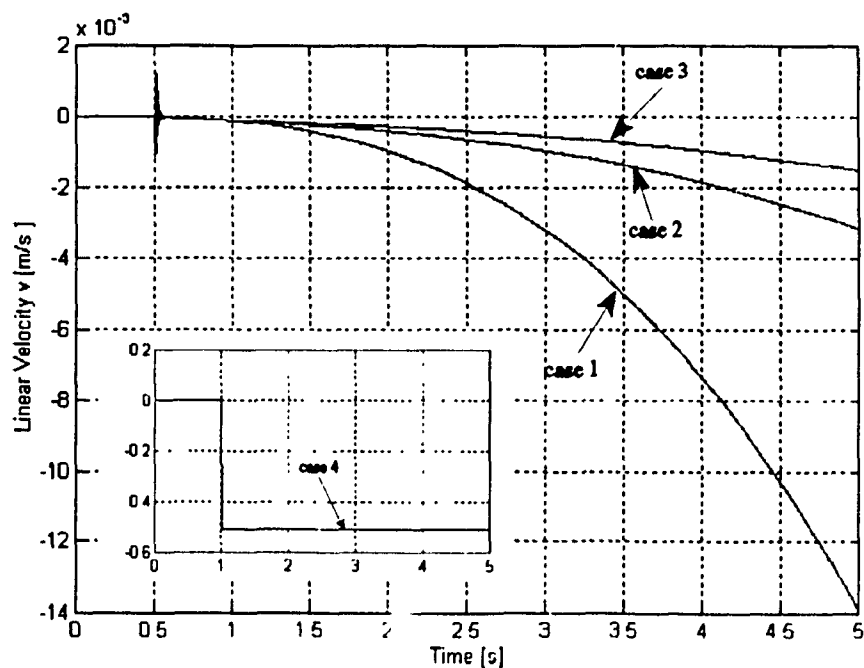
d) Lateral forces of the right caster.

Figure 5.6: Lateral force of each wheel corresponding to various current step inputs, with constant steering angles ($\delta_1 = -0.039$ rad, $\delta_2 = 0.032$ rad) for CONCIC-3 AGV.

161

a) Longitudinal velocities of the CONCIC-3 AGV with respect to frame $\{Q\}$.

b) Lateral velocities of the CONCIC-3 AGV with respect to frame $\{Q\}$.

162
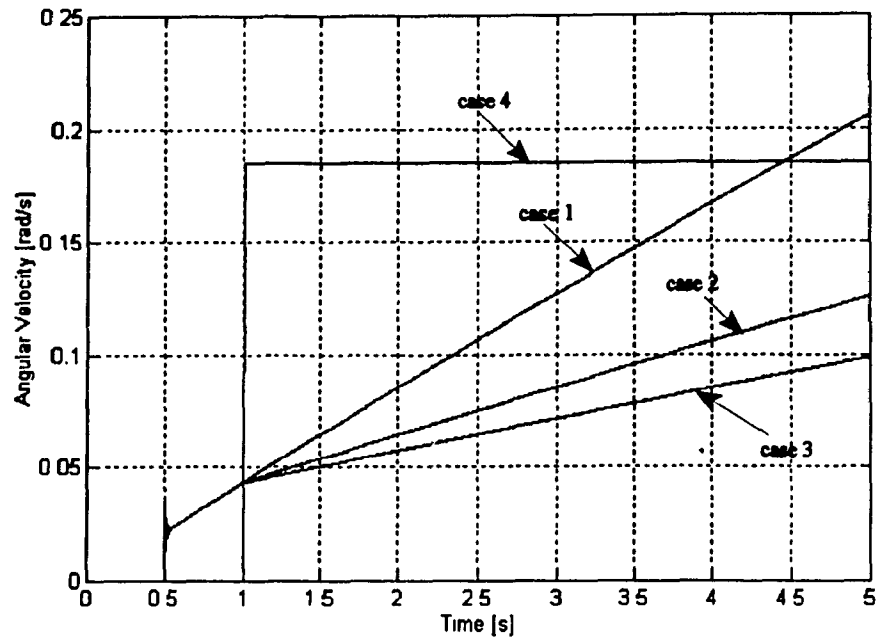
c) Angular velocities of the CONCIC-3 AGV.

Figure 5.7: Linear and angular velocity responses of the CONCIC-3 AGV with respect to frame $\{Q\}$ for various step current inputs.
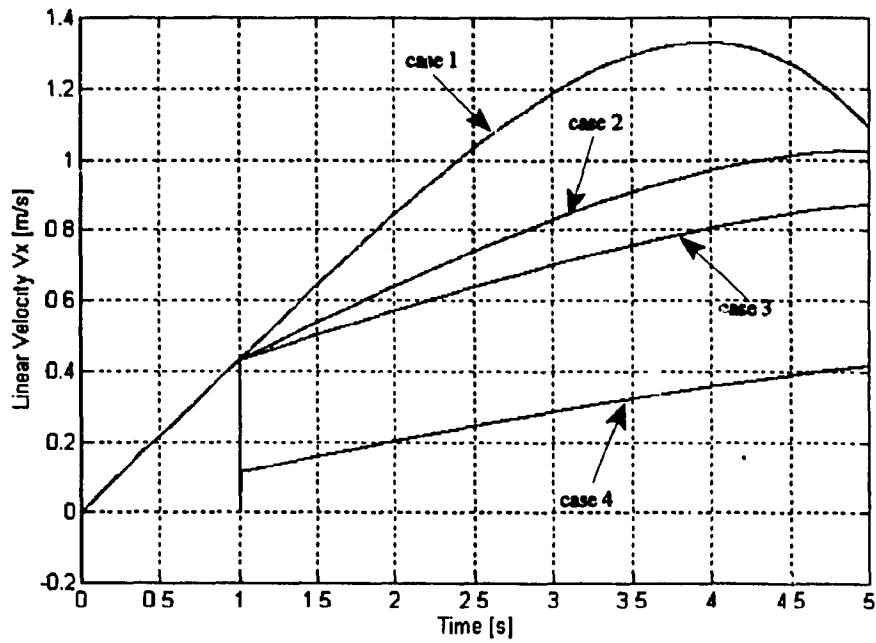
a) Linear velocities of the CONCIC-3 AGValong the X-direction.
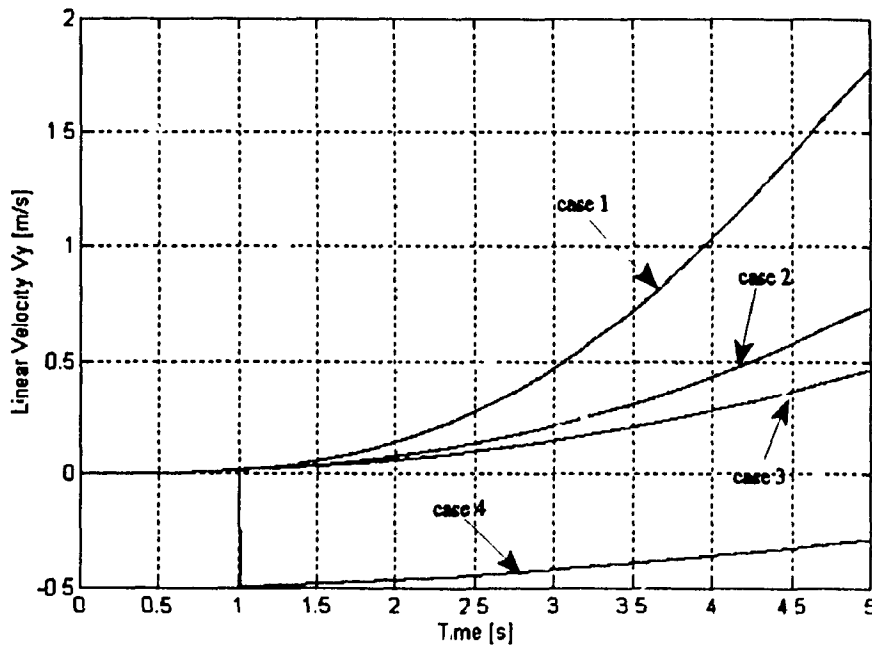
b) Linear velocities of the CONCIC-3 AGV along Y-direction.

Figure 5.8: Linear velocities of the CONCIC-3 AGV with respect to frame $\{I\}$ for various current steps, with constant steering angles $\delta_1 = -0.039$ rad, $\delta_2 = 0.032$ rad.

164
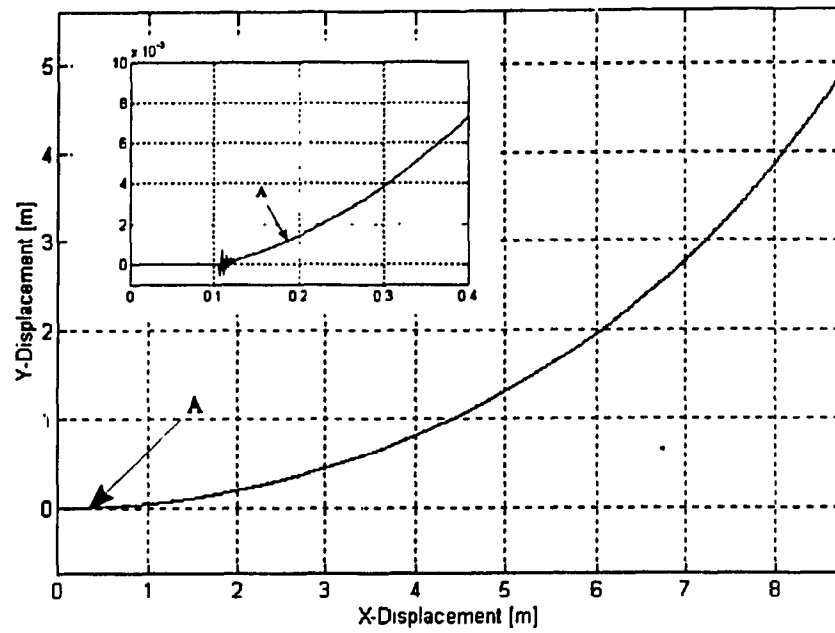
a) Current step input $I_1 = I_2 = 4$ (Amp)
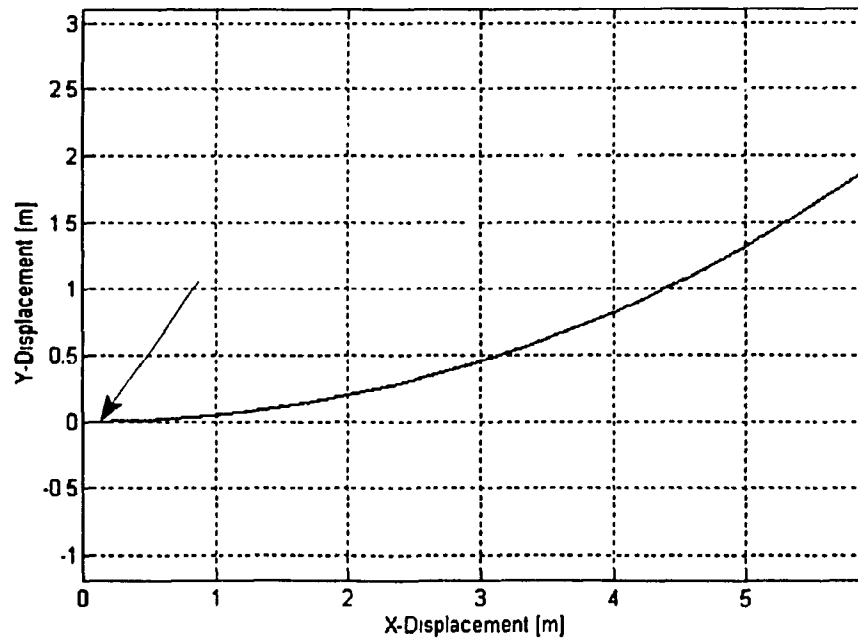
b) Current step input $I_1 = I_2 = 2.5$ Amp (t ≥ 1 s).

165
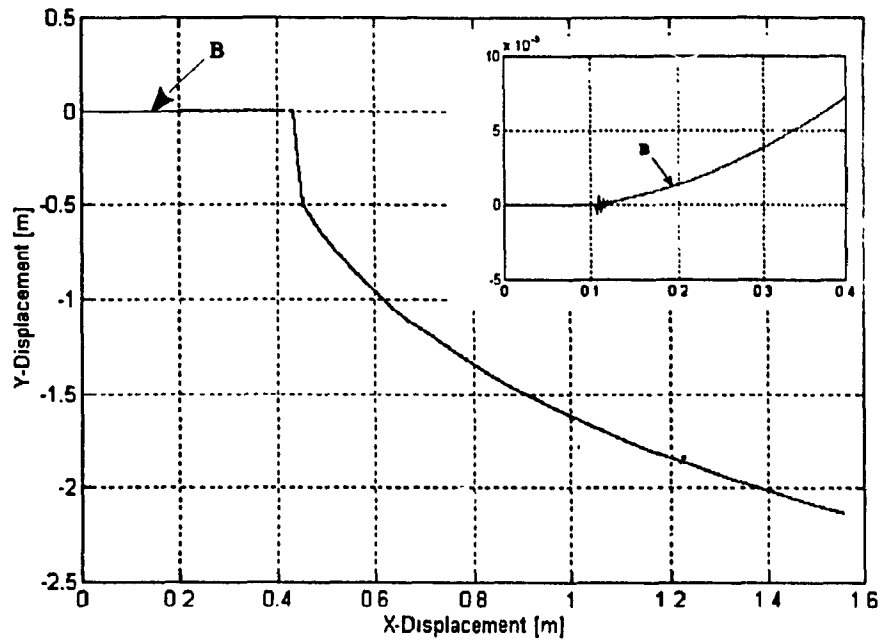
c) Current step input $I_1 = I_2 = 1.5$ Amp (t ≥ 1 s).

Figure 5.9: Trajectories of the CONCIC-3 AGV for various current step inputs, with constant steering angles $\delta_1 = -0.39$ rad, $\delta_2 = 0.32$ rad.

5.3 Case Study 2: CONCIC-2 AGV

The CONCIC-2 AGV [21] is shown in Fig. 5.10. The two driving wheels are mounted at either side of the geometric centre of the AGV, and the two casters are located at the front and rear. The AGV is considered as having two DOFs (u and γ), and sprung mass m_s is neglected. Each wheel supports an equal fraction of the total AGV weight.

Figure 5.10: Schematic of CONCIC-2 AGV.

5.3.1 Dynamic Model of the CONCIC-2 AGV

The dynamic model of the CONCIC-2 AGV is developed by following the steps given in Chapter 4, as outlined below:

Step 1. Specification of the CONCIC-2 AGV system:

i) Driving wheel units: $n_d = 2$.

Locations of joints B_i for the two driving wheel units are specified by the following equations:

$$\begin{cases} x_{b1} = 0 \ (m) \ , \\ y_{b1} = -l = -0.26 \ (m) \ , \end{cases} \qquad \begin{cases} x_{b2} = 0 \ (m) \ , \\ y_{b2} = l = 0.26 \ (m) \ . \end{cases} \qquad (5.2.1)$$
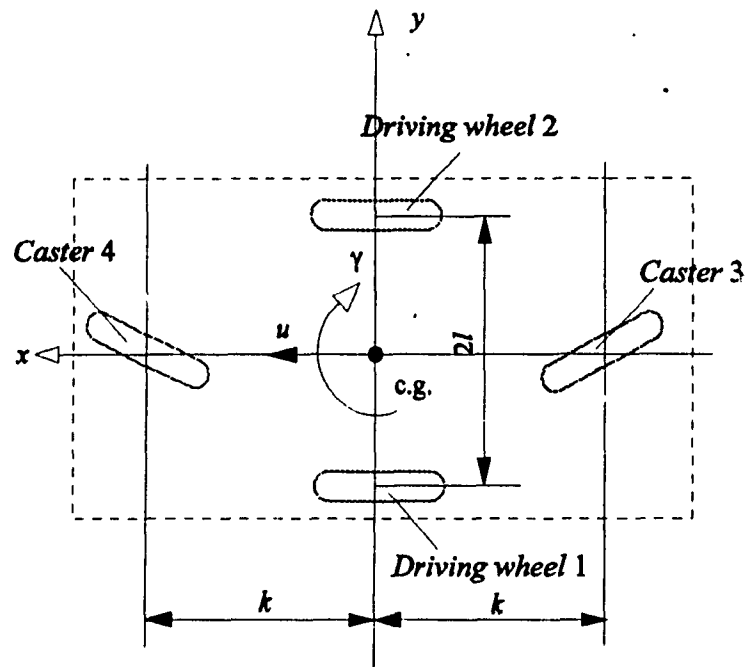
ii) Steering wheel units: $\qquad\qquad n_s = 0.$

iii) Driving-steering wheel units: $\qquad n_{ds} = 0.$

iv) Casters (in this case the offset $d_3 = d_4 \neq 0$): $\qquad n_c = 2.$

The locations joints A_i for two casters are:

$$\begin{cases} x_{a3} = -k = -0.39 \ (m) \ , \\ y_{a3} = 0 \ (m) \ , \end{cases} \qquad \begin{cases} x_{a4} = k = 0.39 \ (m) \ , \\ y_{a4} = 0 \ (m) \ . \end{cases} \qquad (5.2.2)$$

The total number of wheel units n employed on the CONCIC-2 AGV and the total number of variables N_{var} introduced in the system are given by the following equations:

$$n = n_d + n_s + n_{ds} + n_c = 4 \ , \qquad\qquad (5.2.3)$$

$$N_{var} = n_d = 2 \ .$$

Step 2. Setting up the intermediate variables (β_i, α_i, ζ_i and f_{r_i}) for each wheel unit:

Step 2.1 Calculate the constrained velocities, direction and steering angles of each wheel unit:

The constrained velocities of the two driving-steering wheel units at joint B_1 and B_2 are:

$$\mathbf{V}_{B_1} = \begin{pmatrix} v_{x_{B_1}} \\ v_{y_{B_1}} \end{pmatrix} = \begin{pmatrix} u + l\gamma \\ v \end{pmatrix} \ ,$$

$$\qquad\qquad\qquad\qquad\qquad\qquad\qquad (5.2.4)$$

$$\mathbf{V}_{B_2} = \begin{pmatrix} v_{x_{B_2}} \\ v_{y_{B_2}} \end{pmatrix} = \begin{pmatrix} u - l\gamma \\ v \end{pmatrix} \ .$$

The magnitudes of V_{B_1} and V_{B_2} in the xy plane are:

$$v_{xy_{B_1}} = \sqrt{(u + l\gamma)^2 + (v)^2} \ ,$$

$$v_{xy_{B_2}} = \sqrt{(u - l\gamma)^2 + (v)^2} \ .$$

(5.2.5)

The constrained velocities for the two casters at joint A_3 and A_4 are:

$$V_{A_3} = \begin{pmatrix} v_{x_{A_3}} \\ v_{y_{A_3}} \end{pmatrix} = \begin{pmatrix} u \\ v - k\gamma \end{pmatrix},$$

(5.2.6)

$$V_{A_4} = \begin{pmatrix} v_{x_{A_4}} \\ v_{y_{A_4}} \end{pmatrix} = \begin{pmatrix} u \\ v + k\gamma \end{pmatrix}.$$

The magnitudes of V_{A_3} and V_{A_4} in the xy plane are:

$$v_{xy_{A_3}} = \sqrt{(u)^2 + (v - k\gamma)^2} \ ,$$

$$v_{xy_{A_4}} = \sqrt{(u)^2 + (v + k\gamma)^2} \ .$$

(5.2.7)

The direction angle (β_i) of each wheel unit:

$$\beta_1 = \tan^{-1} \frac{v_{y_{B_1}}}{v_{x_{B_1}}} = \tan^{-1} \frac{v}{u + l\gamma} \ ,$$

$$\beta_2 = \tan^{-1} \frac{v_{y_{B_2}}}{v_{x_{B_2}}} = \tan^{-1} \frac{v}{u - l\gamma} \ ,$$

(5.2.8)

$$\beta_3 = \tan^{-1} \frac{v_{y_{A_3}}}{v_{x_{A_3}}} = \tan^{-1} \frac{v - k\gamma}{u} \ ,$$

$$\beta_4 = \tan^{-1} \frac{v_{y_{A_4}}}{v_{x_{A_4}}} = \tan^{-1} \frac{v + k\gamma}{u} \ .$$

169

Step 2.2 Calculate the slip angle and rotation angle (α_i, ζ_i) and rolling friction factor (f_{r_i}):

$$\alpha_1 = \beta_1 ,$$

$$\alpha_2 = \beta_2 ,$$

$$\zeta_3 = 0 ,$$

$$\zeta_4 = 0 ,$$

$$f_{r_1} = k_1(1 + k_2 \, v_{xy_{B_1}}) ,$$ (5.2.9)

$$f_{r_2} = k_1(1 + k_2 \, v_{xy_{B_2}}) ,$$

$$f_{r_3} = k_1(1 + k_2 \, v_{xy_{A_4}}) ,$$

$$f_{r_2} = k_1(1 + k_2 \, v_{xy_{A_4}}) .$$

Step 3. Determination of the external forces (F_{l_i}, F_{f_i}, F_{C_i} and F_{t_i}) acting on each wheel at wheel-ground contact points:

Step 3.1 External forces depend on the slip angle and friction between of the wheel and floor as follows:

$$F_{l_1} = -C_\alpha \, \alpha_1 ,$$

$$F_{l_2} = -C_\alpha \, \alpha_2 ,$$

$$F_{C_3} = k_{\alpha} \, F_{s_3} \, \text{sign} (\beta_3 - \zeta_3) ,$$ (5.2.10 a)

$$F_{C_4} = k_{\alpha} \, F_{s_4} \, \text{sign} (\beta_4 - \zeta_4) ,$$

and

$$F_{f_1} = k_1 (1 + k_2 v_{xy_{B_1}}) F_{z_1} ,$$

$$F_{f_2} = k_1 (1 + k_2 v_{xy_{B_2}}) F_{z_2} ,$$

$$F_{f_3} = k_1 (1 + k_2 v_{xy_{A_3}}) F_{z_3} ,$$ (5.2.10 b)

$$F_{f_4} = k_1 (1 + k_2 v_{xy_{A_4}}) F_{z_4}$$

Step 3.2 External forces depends on the motor characteristics as follows:

$$F_{t_1} = \frac{N_1}{R_1} (K_{T_1} I_1 - J_1 N_1 \dot{\omega}_1 - D_1 N_1 \omega_1 - T_{f_1}) ,$$

(5.2.11)

$$F_{t_2} = \frac{N_2}{R_2} (K_{T_2} I_2 - J_2 N_2 \dot{\omega}_2 - D_2 N_2 \omega_2 - T_{f_2}) .$$

In Eqns. (5.2.11), the currents of the two driving wheel units are I_1 and I_2. These currents can be considered as independent input variables (commands) applied to the system to study the dynamic behaviour of the CONCIC-2 AGV. They can also be determined from the inverse dynamics of the AGV, since the system has not redundant (i.e., $N_R = n_d$ - (DOFs of the vehicle) = 0). The angular velocities (ω_1, ω_2) and accelerations ($\dot{\omega}_1$, $\dot{\omega}_2$) of the two driving wheel units are determined by applying kinematic constraint 1 (referring to Eqns. (4.15) and (4.16)). These angular velocities are expressed by the following equations:

$$\begin{cases} \omega_1 = \dfrac{\dot{X}_Q \cos(\theta + \delta_1) + \dot{Y}_Q \sin(\theta + \delta_1) + l \cdot \dot{\gamma}}{R_1} , \\[4mm] \omega_2 = \dfrac{\dot{X}_Q \cos(\theta + \delta_2) + \dot{Y}_Q \sin(\theta + \delta_2) - l \cdot \dot{\gamma}}{R_2} . \end{cases}$$ (5.2.12)

Differentiating Eqns. (5.2.12) with respect to time yields:

$$\begin{cases} \omega_1 = \dfrac{\ddot{X}_\varrho \cos(\theta) + \ddot{Y}_\varrho \sin(\theta) - (\dot{X}_\varrho \sin(\theta) - \dot{Y}_\varrho \cos(\theta))\gamma + l\cdot\dot{\gamma}}{R_1}, \\[4mm] \omega_2 = \dfrac{\ddot{X}_\varrho \cos(\theta) + \ddot{Y}_\varrho \sin(\theta) - (\dot{X}_\varrho \sin(\theta) - \dot{Y}_\varrho \cos(\theta))\gamma - l\cdot\dot{\gamma}}{R_2}. \end{cases} \qquad (5.2.13)$$

The accelerations and velocities of the vehicle with respect to the X, Y-axes of the inertial frame $\{I\}$ are $\ddot{X}_\varrho$, $\ddot{Y}_\varrho$ and $\dot{X}_\varrho$, $\dot{Y}_\varrho$, respectively. The orientation and yaw rate of the vehicle are θ and γ, respectively. In this step, the two power variables should be determined.

Step 4. Formulating the total external forces acting on the wheel-ground contact points along x and y-axes.

i)Two Driving wheel units:

$$\begin{cases} X_1 = F_{t_1} - F_{f_1}, \\[2mm] Y_1 = F_{l_1}, \end{cases} \qquad (5.2.14)$$

and

$$\begin{cases} X_2 = F_{t_2} - F_{f_2}, \\[2mm] Y_2 = F_{l_2}. \end{cases} \qquad (5.2.15)$$

ii) Steering and iii) Driving-steering wheel units are not included in the model.

172

iv) Two casters:

$$\left\{ \begin{array}{l} X_3 = -F_{f_3} \cos \zeta_3 + F_{c_3} \cos (\zeta_3 + \text{sign}\,(\zeta_3)\dfrac{\pi}{2}) \ , \\[3mm] Y_3 = -F_{f_3} \sin \zeta_3 + F_{c_3} \sin (\zeta_3 + \text{sign}\,(\zeta_3)\dfrac{\pi}{2}) \ , \end{array} \right. \qquad (5.2.16)$$

and

$$\left\{ \begin{array}{l} X_4 = -F_{f_4} \cos \zeta_4 + F_{c_4} \cos (\zeta_4 + \text{sign}\,(\zeta_4)\dfrac{\pi}{2}) \ , \\[3mm] Y_4 = -F_{f_4} \sin \zeta_4 + F_{c_4} \sin (\zeta_4 + \text{sign}\,(\zeta_4)\dfrac{\pi}{2}) \ . \end{array} \right. \qquad (5.2.17)$$

Step 5. Total external forces and moments acting on the AGV system:

a) Total external forces acting on the AGV along the x direction:

$$\begin{aligned} \sum X =\ & (F_{t_1} - F_{f_1}) + (F_{t_2} - F_{f_2}) \\[2mm] & - F_{f_3} \cos \zeta_3 + F_{c_3} \cos (\zeta_3 + \text{sign}\,(\zeta_3)\ \dfrac{\pi}{2}) \\[2mm] & - F_{f_4} \cos \zeta_4 + F_{c_4} \cos (\zeta_4 + \text{sign}\,(\zeta_4)\dfrac{\pi}{2}) \ . \end{aligned} \qquad (5.2.18)$$

b) Total external moments acting on the AGV above the z (yaw) axis:

$$\begin{aligned} \sum N =\ & (F_{t_1} - F_{f_1})\ l - (F_{t_2} - F_{f_2})\ l \\[2mm] & + (F_{f_3}\sin \zeta_3 - F_{c_3}\sin (\zeta_i + \text{sign}\,(\zeta_i)\ \dfrac{\pi}{2})\ k \\[2mm] & - (F_{f_4}\sin \zeta_4 + F_{c_4} \sin (\zeta_4 + \text{sign}\,(\zeta_4)\ \dfrac{\pi}{2})\ k \ . \end{aligned} \qquad (5.2.19)$$

173

Step 6. Assemble motion equations of the AGV with external forces and moments:

$$m \, \dot{u} = \sum X \, ,$$

$$I_z \dot{\gamma} = \sum N \, .$$

(5.2.20)

Substituting external forces and moments obtained in Step 5 into Eqn. (5.2.20), the equation

of motion for the CONCIC-2 AGV can be expressed as follows:

$$m \cdot \dot{u} = F_{t_1} - F_{f_1} + F_{t_2} - F_{f_2} - F_{f_3} \cos \zeta_3 + F_{C_3} \cos (\zeta_3 + \text{sign} (\zeta_3) \frac{\pi}{2}))$$

$$- F_{f_4} \cos \zeta_4 + F_{C_4} \cos (\zeta_4 + \text{sign} (\zeta_4) \frac{\pi}{2})) \, ,$$

$$I_z \dot{\gamma} = (F_{t_1} - F_{f_1}) \, l - (F_{t_2} - F_{f_2}) \, l$$

(5.2.21)

$$+ (F_{f_3} \sin \zeta_3 - F_{C_3} \sin (\zeta_3 + \text{sign} (\zeta_3) \frac{\pi}{2})) \, k$$

$$+ (-F_{f_4} \sin \zeta_4 + F_{C_4} \sin (\zeta_4 + \text{sign} (\zeta_4) \frac{\pi}{2})) \, k \, .$$

Step 7. Obtain the forward dynamical model of CONCIC-2 AGV :

Rearrange Eqn. (5.2.21) in matrix form, the acceleration vector of the CONCIC-2 AGV with

respect to frame $\{Q\}$ can be determined by the following equation:

$$\mathbf{a}_Q = \begin{pmatrix} \dot{u} \\ \dot{\gamma} \end{pmatrix} = A^{-1} B \, ,$$

(5.2.22)

and the acceleration of the AGV with respect to the inertial frame $\{I\}$ can be determined by

the following equation:

$$\mathbf{a} = T \times \mathbf{a}_Q$$

(5.2.23)

where, T is the transformation matrix and

$$A = \begin{bmatrix} m & 0 \\ 0 & I_s \end{bmatrix}, \qquad B = \begin{pmatrix} \sum X \\ \sum N \end{pmatrix}.$$

Step 8. Integrating the forward dynamical model :

Given the initial position $P_0 \{X_Q(0),\ Y_Q(0),\ \theta(0)\}$ and velocities $V_0 \{\ \dot{X}_Q(0),\ \dot{Y}_Q(0),\ \gamma(0)\}$ of the CONCIC-2 AGV with respect to frame $\{I\}$, the instantaneous velocities and position with respect to the frame $\{I\}$ can be determined by integrating the above equation with respect to the time.

Comparison the results for the conventional and the general approach:

Comparing Eqn. (5.2.21) with dynamical model of the CONCIC-2 AGV developed by Min Huang [21], we have the following notational correspondences:

$$u = V_y,$$
$$F_{f_1} = F_{2f}, \qquad F_{d} = F_{2}t, \qquad \zeta_3 = \delta_f,$$

$$\dot{u} = \dot{V}_y,$$
$$F_{f_2} = F_{1f}, \qquad F_{d} = F_{1}t, \qquad \beta_f = \zeta_3 + sign\,(\zeta_3)\,\frac{\pi}{2},$$

$$v = V_x,$$
$$F_{f_3} = F_{ff}, \qquad \zeta_4 = \delta_4,$$

$$\dot{v} = 0,$$
$$F_{f_4} = F_{rf}, \qquad \beta_r = \zeta_4 + sign\,(\zeta_4)\,\frac{\pi}{2},$$

$$\gamma = -\Omega_z,$$
$$F_{c_3} = F_{fh}, \qquad \cos\,(\zeta_3 + sign\,(\zeta_3)\,\frac{\pi}{2}) = \cos\beta_f,$$

$$\dot{\gamma} = -\dot{\Omega}_z\,;$$
$$F_{c_4} = F_{rn}\,; \qquad \cos\,(\zeta_4 + sign\,(\zeta_4)\,\frac{\pi}{2}) = \cos\beta_r\,.$$

The above correspondences show that the dynamical equations obtained from the general approach are identical to the dynamical equations obtained using the conventional approach.

5.3.2 Dynamic Simulation of the CONCIC-2 AGV

5.3.2.1 Simulation Inputs

The complete dynamic model of the CONCIC-2 AGV has been derived in Section 5.3.1 following the formal structure provided in Chapter 4, Section 4.2. In this section, the dynamic simulation of the CONCIC-2 AGV is studied based on the formal steps provided in Section 4.3.2. System parameters are given in Appendix D, Table D.2. Simulations have been carried out using the following initial conditions.

(i) Initial position of the AGV with respect to the frame $\{I\}$ is,

$$\left\{ \begin{array}{l} X_\varrho = 0 \ , \\ Y_\varrho = 0 \ , \\ \theta(0) = 0 \ . \end{array} \right. \tag{5.2.24}$$

(ii) Initial velocities and accelerations of the AGV with respect to frame $\{I\}$,

$$\left\{ \begin{array}{l} \dot{X}_\varrho = 0 \ , \\ \dot{Y}_\varrho = 0 \ , \\ \dot{\gamma}(0) = 0 \ , \end{array} \right. \qquad \left\{ \begin{array}{l} \ddot{X}_\varrho = 0 \ , \\ \ddot{Y}_\varrho = 0 \ , \\ \ddot{\gamma}(0) = 0 \ . \end{array} \right. \tag{5.2.25}$$

(iii) Initial angles of the casters are: $\zeta_3 = \dfrac{\pi}{12}$, and $\zeta_4 = -\dfrac{\pi}{12}$.

Power variables (I_1 and I_2) are considered as input variables to the system. These variables are precalculated based the condition that the slip angle of each wheel must be less than 4 degrees. Nonholonomic constraints of the automated vehicle system are satisfied. Two different value of current are given to the two DC driving motors, and the ratio of the two input currents are I1: I2 = 1:0.85.

176

5.3.2.2 Simulation Results for the CONCIC-2 AGV

Simulation results of the CONCIC-2 AGV are shown in Figs. 5.11 through 5.14. Linear and angular accelerations of the AGV with respect to frame $\{Q\}$ in response to the step input currents are shown in Fig. 5.11. The results show that (i) when both driving motors are powered, forward and angular accelerations exhibit high-amplitude, high-frequency transient oscillatory behaviour, and (ii) these transients die out, leaving a non-oscillatory steady-state motion. Corresponding velocities and trajectories are shown in Figs. 5.12 and 5.13.

Response curves showing slip angles of the two driving wheel units, as well as the rotation angles of the two casters to the input step currents $I_1 = 1.6$ and $I_2 = 1.36$ amp are shown in Fig. 5.14. Corresponding side forces acting on each caster are shown in Fig. 5.15. Results show that: (i) slip angles of the two driving wheel units are equal to zero, and the corresponding lateral force acting on each driving wheel unit is then equal to zero, (ii) rotation angles of the two casters exhibit high-amplitude, high-frequency transient behaviour, but quickly stabilize to a constant value, (iii) there are also side forces acting initially on each caster, which rapidly decrease to zero.

These results prove that given the proper input power variables to the system, nonholonomic constraints of the automated vehicle system can be satisfied (see Fig. 5.14). Since the direction of caster orientation is not coincident with its direction angle, there are side forces acting on the caster (see Figs. 1.4 and 5.15). In other words, side forces push the caster to move along the direction of the velocity vector at joint A_i (i 3, 4) In addition, good performance of the AGV may be obtained from a range of possible combinations of differential power values to the two driving wheel units, as shown in Fig. 5.13
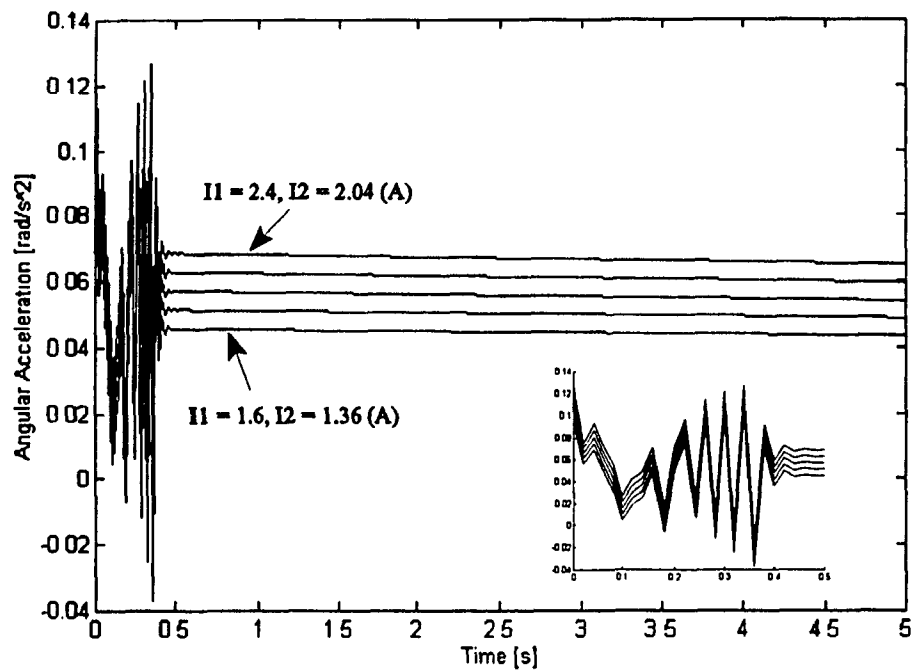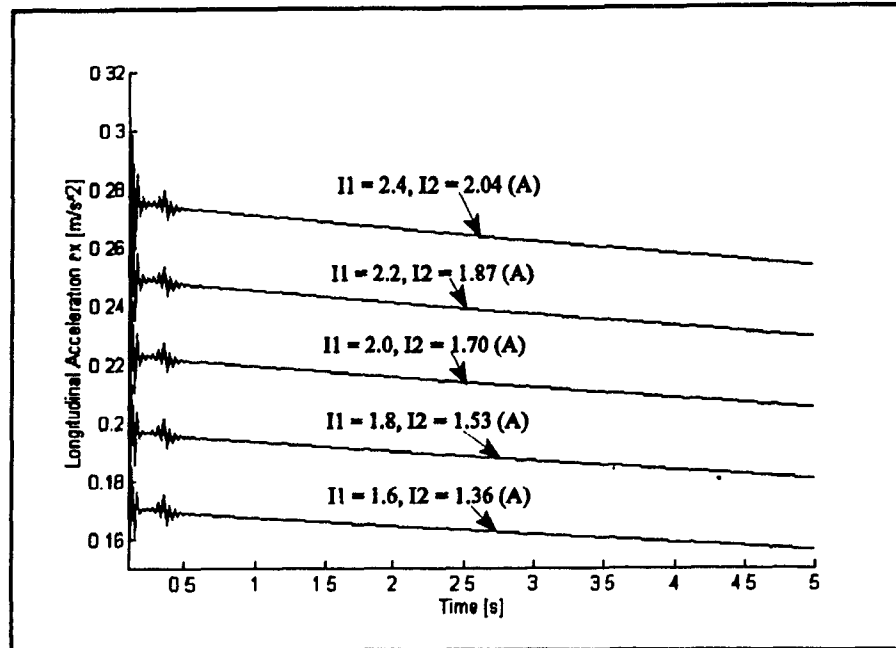
Figure 5.11: Forward and angular acceleration of the CONCIC-2 AGV with respect to

frame $\{Q\}$ for various current step inputs.

178
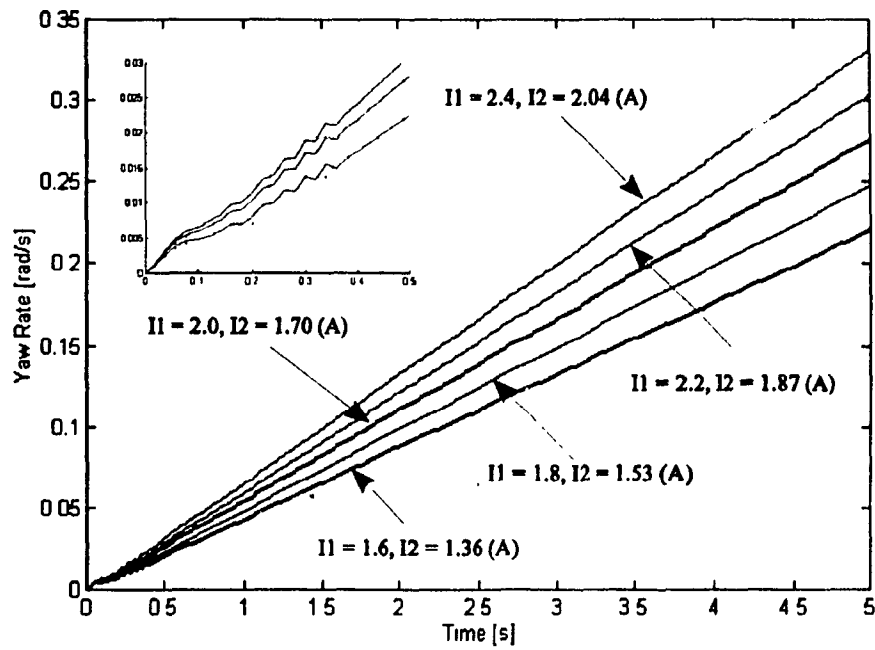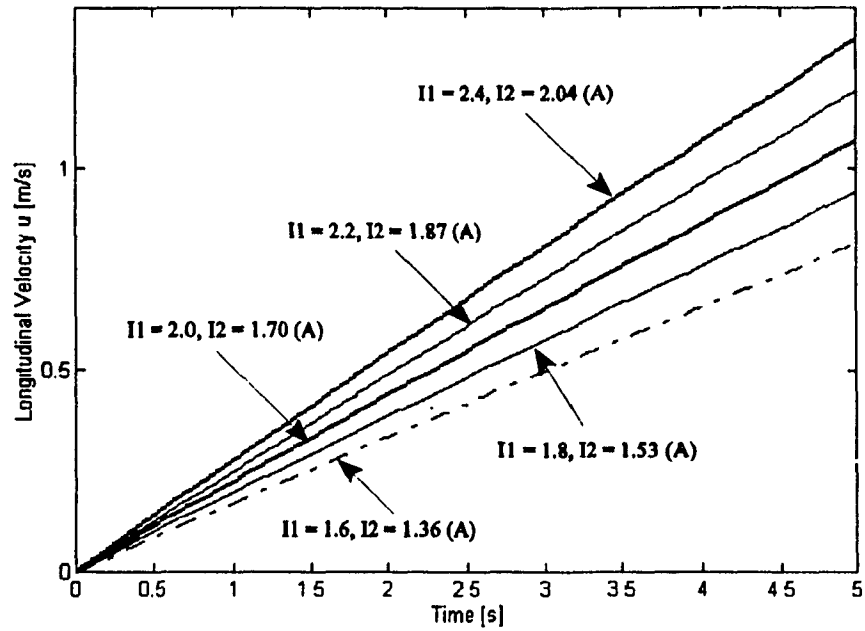
Figure 5.12: Forward velocity and yaw rate of the CONCIC-2 AGV with respect to frame {*Q*} for various current step inputs.

179
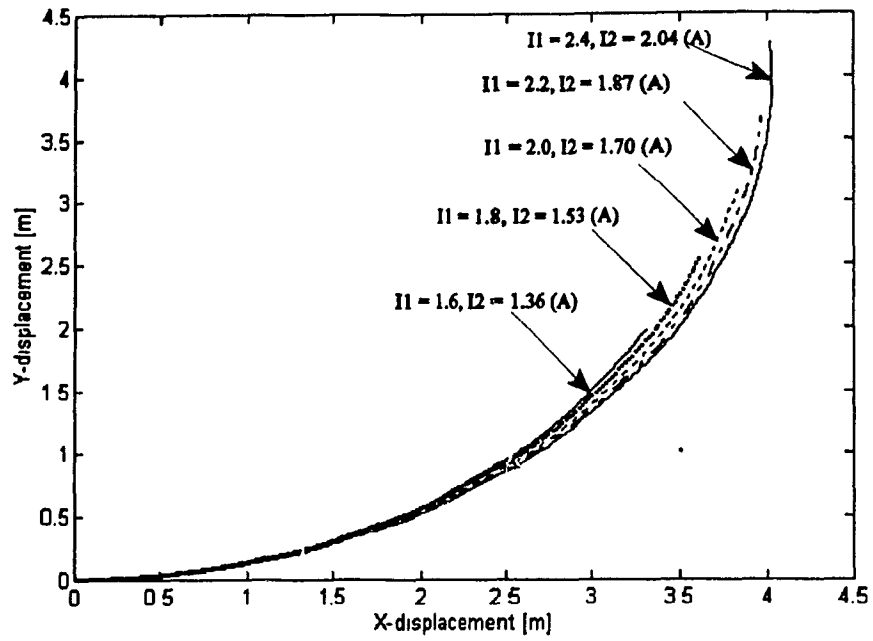
Figure 5.13: Trajectory of the CONCIC-2 AGV for various current step inputs.
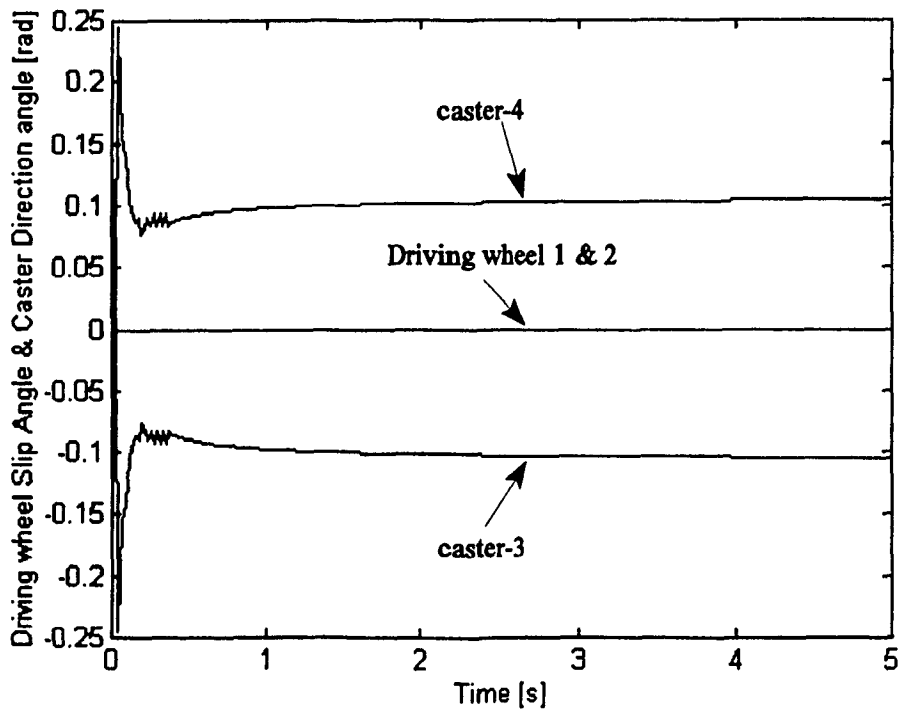
Figure 5.14: Angular responses for $I_1 = 1.6$ Amp, $I_2 = 1.36$ Amp.

180

a) Side Forces Actes on the Front Caster Along the x-Direction

b) Side Forces Actes on the Front Caster Along the y-Direction

c) Side Forces Actes on the Rear Caster Along the x-Direction
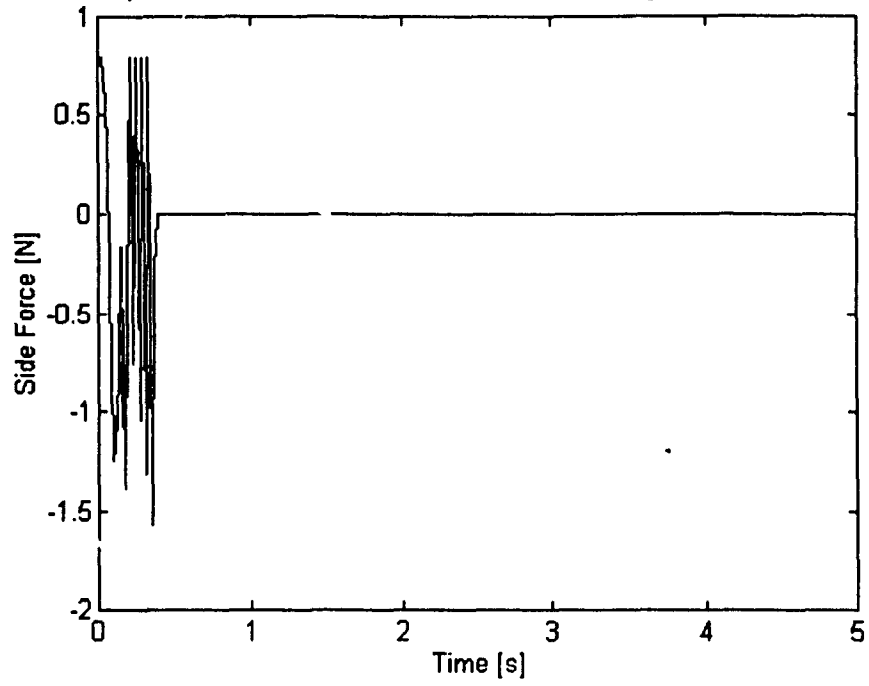
d) Side Forces Actes on the Rear Caster Along the y-Direction
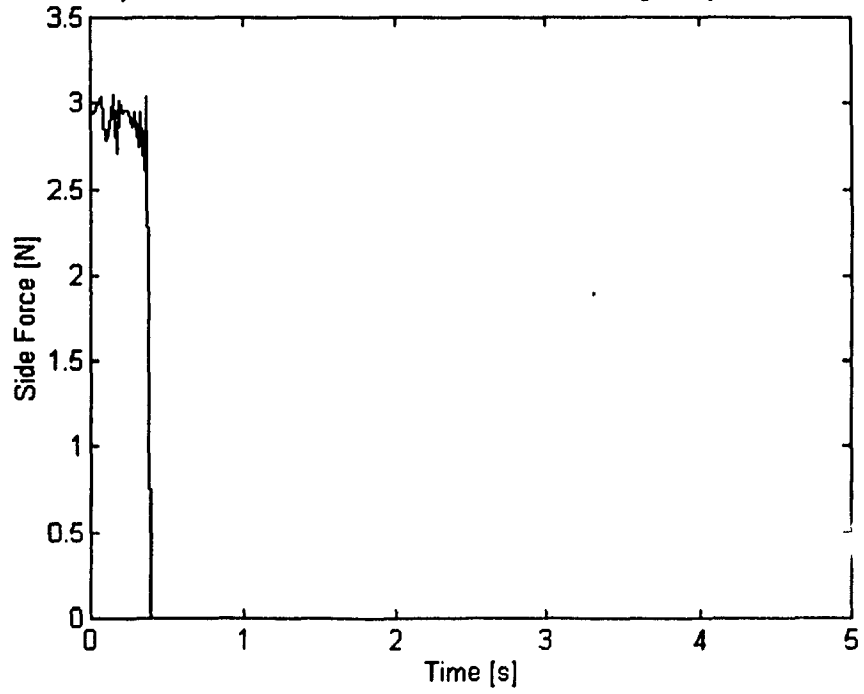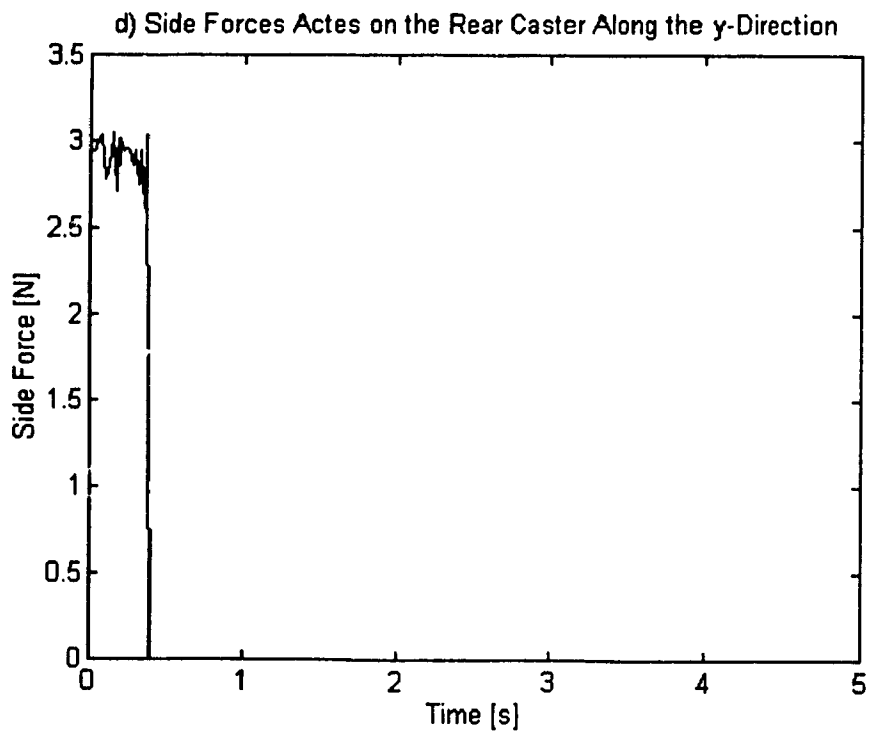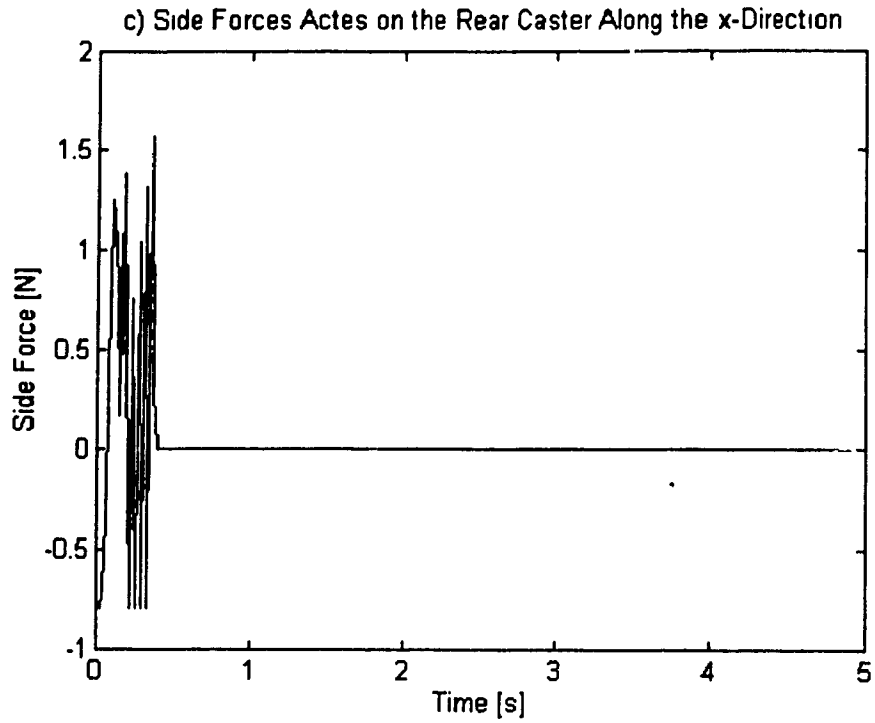
Figure 5.15: Side forces acting on each caster for step inputs I_1 = 1.6 Amp, I_2 = 1.36 Amp.

5.4 Case Study 3: An automated vehicle with four driving-steering wheel units

An automated vehicle, with four drivin$_{\xi}$-steering wheel units configuration, is shown in Fig.5.16. Each pair of driving-steering units is located at the front and the rear of the automated vehicle respectively.

Assumptions:

- The automated vehicle has three DOFs (u, v, γ),

- Four driving-steering units are Type A,

- All wheel units are considered to have same characteristics and load acting on each of them has been precalculated (referring to Appendix C).
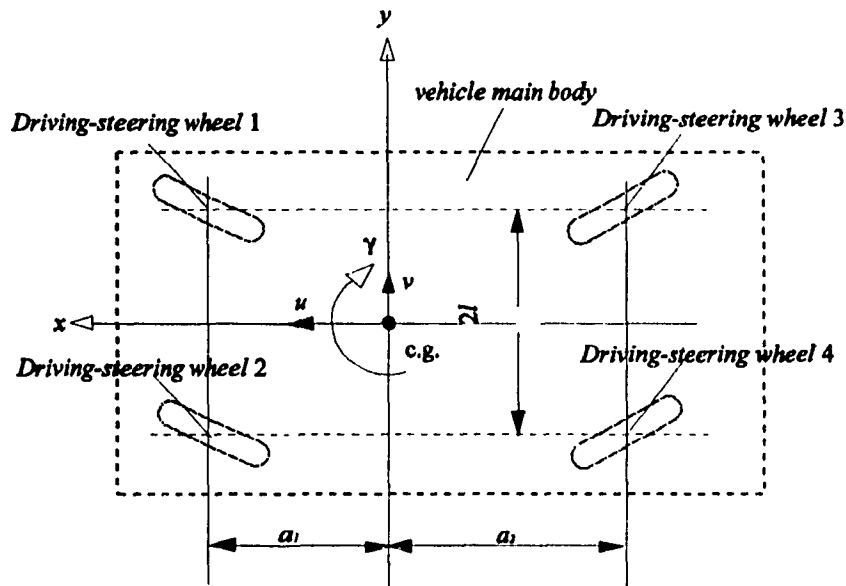
Figure 5.16: Schematic of four driving-steering wheel units automated vehicle.

5.4.1 Dynamic Model of the Four Driving-Steering Wheel Units Automated Vehicle

In this case study, the vehicle only consists of one type of wheel unit, the dynamical model of the vehicle is developed by following steps provided in Chapter 4, as outline below.

183

Step 1. Specification of the automated vehicle system:

i) Driving wheel units: $\qquad\qquad\qquad$ $n_d = 0$.

ii) Steering wheel units: $\qquad\qquad\qquad$ $n_s = 0$.

iii) Driving-steering wheel units: $\qquad\qquad$ $n_{ds} = 4$.

Locations of each joints A_i for the four driving-steering wheel units are specified by the following equations ($i = 1, 2, 3, 4$):

$$\begin{cases} x_{a_1} = a_1 = 0.32 \ (m) \ , \\ y_{a_1} = l = 0.26 \ (m) \ , \end{cases} \qquad \begin{cases} x_{a2} = a_1 = 0.32 \ (m) \ , \\ y_{a_2} = -l = -0.26 \ (m) \ , \end{cases}$$

$$(5.3.1)$$

$$\begin{cases} x_{a_3} = -a_2 = -0.39 \ (m) \ , \\ y_{a_3} = l = 0.26 \ (m) \ , \end{cases} \qquad \begin{cases} x_{a_4} = -a_2 = -0.39 \ (m) \ , \\ y_{a_4} = -l = -0.26 \ (m) \ . \end{cases}$$

According Eqns. (4.2 a), the locations of each joint B_i for four driving-steering wheel units are determined by the following equations:

$$\begin{cases} x_{b_1} = a_1 + d \cos \xi_1 \ (m) \ , \\ y_{b_1} = l + + d \sin \xi_1 \ (m) \end{cases} \qquad \begin{cases} x_{b_2} = a_1 - d \cos \xi_2 \ (m) \ , \\ y_{b_2} = -l + d \sin \xi_2 \ (m) \ , \end{cases}$$

$$(5.3.2)$$

$$\begin{cases} x_{b_3} = -a_2 + d \cos \xi_3 \ (m) \ , \\ y_{b_3} = l + d \sin \xi_3 \ (m) \ , \end{cases} \qquad \begin{cases} x_{b_4} = -a_2 + d \cos \xi_4 \ (m) \ , \\ y_{b_4} = -l + d \sin \xi_4 \ (m) \ . \end{cases}$$

In Eqns. (5.3.2), the offset of the steering column for each wheel unit is d, and the angle between the x_{A_i} and the steering column $A_i B_i$ is $\xi_i = \text{sign} \ (y_{a_i}) \dfrac{\pi}{2} + \delta_i$ (where, $i = 1, 2, 3, 4$).

184

iv) Casters: $n_c = 0$.

The total number of wheel units n employed on the vehicle and total number of power and steering variables are introduced to the system are:

$$n = n_d + n_s + n_{ds} + n_c = 4 ,$$
(5.3.3)

$$N_{v,s,r} = 2 \, n_{ds} = 8 .$$

Step 2. Determination of intermediate variables (β_i, α_i, ζ_i and f_{r_i}) for each wheel unit:

Step 2.1 Calculate the constrained velocities and direction angle for each wheel unit.

The constrained velocities of the four driving-steering wheel units at joint B_1, B_2, B_3, B_4 are:

$$\mathbf{V}_{B_1} = \begin{pmatrix} v_{x_{B_1}} \\ v_{y_{B_1}} \end{pmatrix} = \begin{pmatrix} u - \gamma y_{b_1} \\ v + \gamma x_{b_1} \end{pmatrix},$$

$$\mathbf{V}_{B_2} = \begin{pmatrix} v_{x_{B_2}} \\ v_{y_{B_2}} \end{pmatrix} = \begin{pmatrix} u - \gamma y_{b_2} \\ v + \gamma x_{b_2} \end{pmatrix},$$

(5.3.4)

$$\mathbf{V}_{B_3} = \begin{pmatrix} v_{x_{B_3}} \\ v_{y_{B_3}} \end{pmatrix} = \begin{pmatrix} u - \gamma y_{b_3} \\ v + \gamma x_{b_3} \end{pmatrix},$$

$$\mathbf{V}_{B_4} = \begin{pmatrix} v_{x_{B_4}} \\ v_{y_{B_4}} \end{pmatrix} = \begin{pmatrix} u - \gamma y_{b_4} \\ v + \gamma x_{b_4} \end{pmatrix}.$$

The magnitudes of $\mathbf{V}_{B_1}$, $\mathbf{V}_{B_2}$, $\mathbf{V}_{B_3}$ and $\mathbf{V}_{B_4}$ in the xy plane are expressed by the following equations (where $i = 1, 2, 3, 4$):

$$v_{xy_{B_i}} = \sqrt{(u - \gamma y_{b_i})^2 + (v + \gamma x_{b_i})^2} .$$
(5.3.5)

185

The direction angle (β_i) of each driving-steering wheel units are determined by the following equations:

$$\beta_1 = \tan^{-1}\frac{V_{y_{B_1}}}{V_{x_{B_1}}} = \tan^{-1}\frac{v + \gamma(d\cos\xi_1 + x_{a_1})}{u - \gamma(d\sin\xi_1 + y_{a_1})} \; ,$$

$$\beta_2 = \tan^{-1}\frac{V_{y_{B_2}}}{V_{x_{B_2}}} = \tan^{-1}\frac{v + \gamma(d\cos\xi_2 + x_{a_2})}{u - \gamma(d\sin\xi_2 + y_{a_2})} \; ,$$

$$\beta_3 = \tan^{-1}\frac{V_{y_{B_3}}}{V_{x_{B_3}}} = \tan^{-1}\frac{v + \gamma(d\cos\xi_3 + x_{a_3})}{u - \gamma(d\sin\xi_3 + y_{a_3})} \; ,$$

$$\beta_4 = \tan^{-1}\frac{V_{y_{B_4}}}{V_{x_{B_4}}} = \tan^{-1}\frac{v + \gamma(d\cos\xi_4 + x_{a_4})}{u - \gamma(d\sin\xi_4 + y_{a_4})} \; .$$

(5.3.6)

In Eqns. (5.3.6), the steering variables (δ_1, δ_2, δ_3, and δ_4) of the driving-steering wheel units are determined by applying kinematic constraint 2, that the wheel-ground contact point satisfies the condition of non slipping. Referring Eqns.(4.8 a), the steering angles for Type A driving-steering wheel units are expressed by the following equations:

$$\delta_1 = \tan^{-1}\frac{\dot{X}_Q\sin(\theta) + \dot{Y}_Q\cos(\theta) + x_{a_1}\gamma}{\dot{X}_Q\cos(\theta) + \dot{Y}_Q\sin(\theta) - y_{a_1}\gamma} \; ,$$

$$\delta_2 = \tan^{-1}\frac{\dot{X}_Q\sin(\theta) + \dot{Y}_Q\cos(\theta) + x_{a_2}\gamma}{\dot{X}_Q\cos(\theta) + \dot{Y}_Q\sin(\theta) - y_{a_2}\gamma} \; ,$$

(5.3.7)

$$\delta_3 = \tan^{-1}\frac{\dot{X}_Q\sin(\theta) + \dot{Y}_Q\cos(\theta) + x_{a_3}\gamma}{\dot{X}_Q\cos(\theta) + \dot{Y}_Q\sin(\theta) - y_{a_3}\gamma} \; ,$$

$$\delta_4 = \tan^{-1}\frac{\dot{X}_Q\sin(\theta) + \dot{Y}_Q\cos(\theta) + x_{a_4}\gamma}{\dot{X}_Q\cos(\theta) + \dot{Y}_Q\sin(\theta) - y_{a_4}\gamma} \; .$$

In Eqns. (5.3.7), the desired linear velocities of the vehicle with respect to the inertial frame $\{I\}$ are $\dot{X}_Q$ and $\dot{Y}_Q$, respectively. The angular velocity and orientation of the vehicle are γ and θ respectively. In this step, the four steering variables are accounted for in Eqns. (5.3.7), and now it only remains to incorporate four power variables.

Step 2.2. Calculate the slip angle (α_i), and rolling friction factor (f_{r_i}):

The slip angle (α_i) of each wheel is obtained from follow equations:

$$\alpha_i = \beta_i - \delta_i,$$ (5.3.8)

and the rolling friction factor (f_{r_i}) may be decided by the following equations:

$$f_{r_i} = k_1(1 + k_2 v_{xy_{B_i}}),$$ (5.3.9)

where, $i = 1, 2, 3, 4$, and k_1 and k_2 are rolling friction coefficients of each wheel. In this case, there are no caster involved in the system, therefore, rotation angles (ζ_i) don't need to be considered.

Step 3. Determination of the external forces (F_{l_i}, F_{f_i}, F_{c_i} and F_{t_i}) acting on each wheel at wheel-ground contact points:

Step 3.1 External forces depend on the slip angle and friction between the wheel and floor:

The lateral forces F_{l_i} and rolling friction forces F_{f_i} of each wheel unit are computed from following equations:

$$F_{l_i} = -C_\alpha \alpha_i,$$

$$F_{f_i} = k_1 (1 + k_2 v_{xy_{B_i}}) F_{z_i},$$ (5.3.10)

187

where, i = 1, 2, 3, 4, and $C_{\alpha i}$ is cornering stiffness [N/rad] of each wheel. In this step the side forces F_{C_i} doesn't need to be considered, since there is no caster involved in the system.

Step 3.2 External forces depend on the motor characteristics as follows.

The applied tractive force of each driving wheel are determined by the following equations:

$$ F_{t_i} = \frac{N_i}{R_i} (K_{T_i} I_i - J_i N_i \dot{\omega}_i - D_i N_i \omega_i - T_{fi}) , \qquad (5.3.11) $$

where, $N_1 \sim N_4$ = gear ratio $\qquad\qquad$ K_{ti} = motor torque constant [N.m/A]

$\quad\ I_i \quad$ = current [Amp] $\qquad\qquad\qquad$ T_{fi} = static friction of motor [Nm]

$\quad\ J_i \quad$ = driving wheel moment of inertia [kg.m^2]

$\quad\ D_i \quad$ = viscous damping factor [N.m.s/rad]

In Eqns. (5.3.11), the angular velocities ω_i and accelerations $\dot{\omega}_i$ are determined by applying kinematic constraint 1. Referring to Eqns. (4.17 a) and (4.18 a), the angular velocities and accelerations of these four Type A driving-steering wheel units are expressed by the following equations (where i = 1, 2, 3, 4):

$$ \omega_i = \frac{\dot{X}_Q \cos(\theta + \delta_i) + \dot{Y}_Q \sin(\theta + \delta_i) + (x_{a_i}\sin(\delta_i) - y_{a_i}\cos(\delta_i))\dot{\gamma}}{R_i} , \qquad (5.3.12) $$

$$ \dot{\omega}_i = \frac{Num1 + Num2 + Num3}{R_i} , $$

with, $\quad Num1 = \ddot{X}_Q \cos(\theta + \delta_i) - \dot{X}_Q \sin(\theta + \delta_i)(\dot{\gamma} + \dot{\delta}_i),$

$\qquad\qquad Num2 = \ddot{Y}_Q \sin(\theta + \delta_i) + \dot{Y}_Q \cos(\theta + \delta_i)(\dot{\gamma} + \dot{\delta}_i),$

$\qquad\qquad Num3 = (x_{a_i}\cos(\delta_i) + y_{a_i}\sin(\delta_i))\dot{\delta}_i\dot{\gamma} + (x_{a_i}\sin(\delta_i) - y_{a_i}\cos(\delta_i))\ddot{\gamma}.$

They are a function of the linear velocities, yaw rate, angular acceleration and orientation of the vehicle with respect to the inertial frame $\{I\}$.

Step 4. Formulating the total external forces acting on the wheel-ground contact points along the x and y axes:

i) Driving wheel units, ii) Steering wheel units, and iv) Caster do not need to be considered.

iii) Four driving-steering wheel units (i =1, 2, 3, 4):

$$\begin{cases} X_i = (F_{t_i} - F_{f_i})\cos\delta_i + |F_{l_i}| \cos(\delta_i - \text{sign}(\alpha_i)\frac{\pi}{2}) \ , \\ Y_i = (F_{t_i} - F_{f_i})\sin\delta_i + |F_{l_i}| \sin(\delta_i - \text{sign}(\alpha_i)\frac{\pi}{2}) \ . \end{cases} \qquad (5.3.13)$$

Step 5. Total forces and moments acting on the vehicle system:

a) Total external forces acting on the automated vehicle along the x-direction:

$$\begin{aligned} \sum X = &(F_{t_1} - F_{f_1}) \cos\delta_1 + |F_{l_1}| \cos(\delta_1 - \text{sign}(\alpha_1)\frac{\pi}{2}) \\ &+ (F_{t_2} - F_{f_2}) \cos\delta_2 + |F_{l_2}| \cos(\delta_2 - \text{sign}(\alpha_2)\frac{\pi}{2}) \\ &+ (F_{t_3} - F_{f_3}) \cos\delta_3 + |F_{l_3}| \cos(\delta_3 - \text{sign}(\alpha_3)\frac{\pi}{2}) \qquad (5.3.14) \\ &+ (F_{t_4} - F_{f_4}) \cos\delta_4 + |F_{l_4}| \cos(\delta_4 - \text{sign}(\alpha_4)\frac{\pi}{2}) \ . \end{aligned}$$

b) Total external forces acting on the automated vehicle along the y-direction:

$$\begin{aligned} \sum Y = &(F_{t_1} - F_{f_1}) \sin\delta_1 + |F_{l_1}| \sin(\delta_1 - \text{sign}(\alpha_1) \frac{\pi}{2}) \\ &+ (F_{t_2} - F_{f_2}) \sin\delta_2 + |F_{l_2}| \sin(\delta_2 - \text{sign}(\alpha_2) \frac{\pi}{2}) \\ &+ (F_{t_3} - F_{f_3}) \sin\delta_3 + |F_{l_3}| \sin(\delta_3 - \text{sign}(\alpha_3) \frac{\pi}{2}) \qquad (5.3.15) \\ &+ (F_{t_4} - F_{f_4}) \sin\delta_4 + |F_{l_4}| \sin(\delta_4 - \text{sign}(\alpha_4) \frac{\pi}{2}) \ . \end{aligned}$$

189

c) Total moments acting on the automated vehicle above the z (yaw)- axis:

$$\sum N = \sum_{i=1}^{4} -((F_{t_i} - F_{f_i})\cos\delta_i + |F_{l_i}|\cos(\delta_i - \text{sign}(\alpha_i)\frac{\pi}{2}))\, y_{a_i}$$
$$+ \sum_{i=1}^{4} ((F_{t_i} - F_{f_i})\sin\delta_i + |F_{l_i}|\sin(\delta_i - \text{sign}(\alpha_i)\frac{\pi}{2}))\, x_{a_i}. \qquad (5.3.16)$$

Step 6. Assemble the motion equations of the automated vehicle with external forces and moments:

$$m(\dot{u} - \gamma v) - \gamma\, p\, h_s\, m_s = \sum X ,$$
$$m(\dot{v} + \gamma u) + m_s\, \dot{p}\, h_s = \sum Y , \qquad (5.3.17)$$
$$I_z\dot{\gamma} - I_{xz}\dot{p} = \sum N .$$

Finally, substituting external forces and moments obtained from Step 5 into Eqns. (5.3.17), the equations of motion for the vehicle system are expressed as follows:

$$m(\dot{u} - \gamma v) - \gamma\, p\, h_s\, m_s = (F_{t_1} - F_{f_1})\cos\delta_1 + |F_{l_1}|\cos(\delta_1 - \text{sign}(\alpha_1)\frac{\pi}{2})$$
$$+ (F_{t_2} - F_{f_2})\cos\delta_2 + |F_{l_2}|\cos(\delta_2 - \text{sign}(\alpha_2)\frac{\pi}{2})$$
$$+ (F_{t_3} - F_{f_3})\cos\delta_3 + |F_{l_3}|\cos(\delta_3 - \text{sign}(\alpha_3)\frac{\pi}{2})$$
$$+ (F_{t_4} - F_{f_4})\cos\delta_4 + |F_{l_4}|\cos(\delta_4 - \text{sign}(\alpha_4)\frac{\pi}{2})$$

$$m(\dot{v} + \gamma u) + m_s\, \dot{p}\, h_s = (F_{t_1} - F_{f_1})\sin\delta_1 + |F_{l_1}|\sin(\delta_1 - \text{sign}(\alpha_1)\frac{\pi}{2}) \qquad (5.3.18)$$
$$+ (F_{t_2} - F_{f_2})\sin\delta_2 + |F_{l_2}|\sin(\delta_2 - \text{sign}(\alpha_2)\frac{\pi}{2})$$
$$+ (F_{t_3} - F_{f_3})\sin\delta_3 + |F_{l_3}|\sin(\delta_3 - \text{sign}(\alpha_3)\frac{\pi}{2})$$
$$+ (F_{t_4} - F_{f_4})\sin\delta_4 + |F_{l_4}|\sin(\delta_4 - \text{sign}(\alpha_4)\frac{\pi}{2})$$

$$I_z \dot{\gamma} - I_{xz} \ddot{\beta} = \sum_{i=1}^{4} -((F_{t_i} - F_{f_i}) \cos \delta_i + |F_{l_i}| \cos(\delta_i - \text{sign}(\alpha_i) \frac{\pi}{2})) y_{e_i}$$

$$+ \sum_{i=1}^{4} ((F_{t_i} - F_{f_i}) \sin \delta_i + |F_{l_i}| \sin(\delta_i - \text{sign}(\alpha_i) \frac{\pi}{2})) x_{e_i} .$$

This is a six order system of nonlinear ordinary differential equations.

Step 7. Obtain the forward dynamical model of the automated vehicle:

Rearrange Eqns. (5.3.18) in matrix form. The accelerations of the four steering-driving wheel units vehicle with respect to the reference frame $\{Q\}$ can be expressed by the following equation:

$$\mathbf{a}_Q = A^{-1} (B + D), \tag{5.3.19}$$

and the acceleration of the vehicle with respect to the initial frame $\{I\}$ can be expressed by the following equation:

$$\mathbf{a} = T \times \mathbf{a}_Q , \tag{5.3.20}$$

where:

$$\mathbf{a}_Q = \begin{pmatrix} \dot{u} \\ \dot{v} \\ \ddot{\gamma} \end{pmatrix}, \qquad T = \begin{bmatrix} \cos(\theta) & -\sin(\theta) & 0 \\ \sin(\theta) & \cos(\theta) & 0 \\ 0 & 0 & 1 \end{bmatrix},$$

and

$$A = \begin{bmatrix} m & 0 & 0 \\ 0 & m & 0 \\ 0 & 0 & I_s \end{bmatrix}, \qquad B = \begin{pmatrix} \sum X \\ \sum Y \\ \sum N \end{pmatrix}, \qquad D = \begin{pmatrix} (vm + h_s m_s \rho)\gamma \\ -mu\gamma \\ 0 \end{pmatrix}.$$

Step 8. Integrating the forward dynamical model:

Given initial position and velocities of the automated vehicle as: $\mathbf{P}_\bullet = \{X_Q(0),\ Y_Q(0),\ \theta(0)\}^T$

and $\mathbf{V}_\bullet = \{\dot{X}_Q(0),\ \dot{Y}_Q(0),\ \gamma(0)\}^T$, then, the instantaneous velocities of the vehicle with

respect to the reference frame $\{Q\}$ and inertial frame $\{I\}$ can be determined by integrating

Eqns. (5.3.19) and (5.3.20) with respect to time. The instantaneous position of the vehicle

with respect to frame $\{I\}$ can also be obtained by integrating Eqn. (5.3.20) with respect to

time twice.

In this case study, although kinematic constraints 1 and 2 have been applied to

determine the system steering and power variables introduced by the steering and driving

motors, there is one redundancy ($N_R = n_{ds}$ - DOFs $= 4 - 3 = 1$) remaining in the system. The

currents (I_1, I_2, I_3, I_4) applied on each driving motor therefore cannot be determined from the

inverse dynamic model of vehicle. In order to study the dynamic behaviour and control this

system, this extra redundancy must be eliminated, but this is beyond the scope of the present

thesis.

5.5 Case Study 4: Six Wheeled AGV

An AGV with six wheel configuration is shown in Figs. 5.17 and 5.18. There are two motorized driving-steering wheel units located at front and rear of the AGV, as well as two pairs of casters located at two sides of the front and rear of the AGV respectively. This AGV has two important manoeuvrability characteristics: the ability to turn sharply and the ability to keep within a narrow path when turning. It can move sideways by turning the driving-steering wheels to left or right 90^0, and it is referred to as an omnidirectional AGV [30] and [31]. The dynamic model of a realistic hypothetical six wheeled AGV can be developed based on use of parameters for the *hardware trim assembly* and *engine assembly* AGVs in use at General Motors Oshawa (Ontario, Canada) plant, and the following assumptions:

- The AGV main body is considered to have three degrees of freedom (u, v, γ),

- Sprung mass m_s is neglected,

- All driving-steering wheels utilized on the AGV are considered to have identical characteristics,

- All casters are considered to have identical characteristics,

- All six wheels located on the AGV are regarded to support an equivalent proportion of the AGV main body weight,

- Reference frame $Q(x, y, z)$ is located at the AGV mass centre.

The AGV specifications are as follows [66]:

- Vehicle length, width and height: 160 in (4.06 m), 90 in (2.28 m) and 111.5 in

193

(2.83 m), respectively. (i.e., a_1 = 0.93 m, a_2 = 0.93 m, l = 0.74 m, and h = 2.28 m,

h_1 = 0.75 m, h_2 = 1.05 m (refer to Fig. 5.17),

- Maximum payload of the AGV: 2,400 lb (1088.12 kg),

- AGV total weight with payload and batteries: 5,000 lb (2267.95 kg),

- Stopping accuracy is ± 0.39 in (± 0.99 mm),

- Forward and reverse speeds are up to 200 ft/min (1.02 m/s) and 130 ft/min (0.66 m/s),

- Acceleration of the AGV is approximately 1.5~3 ft/s^2 (0.457~0.9 m/s^2).
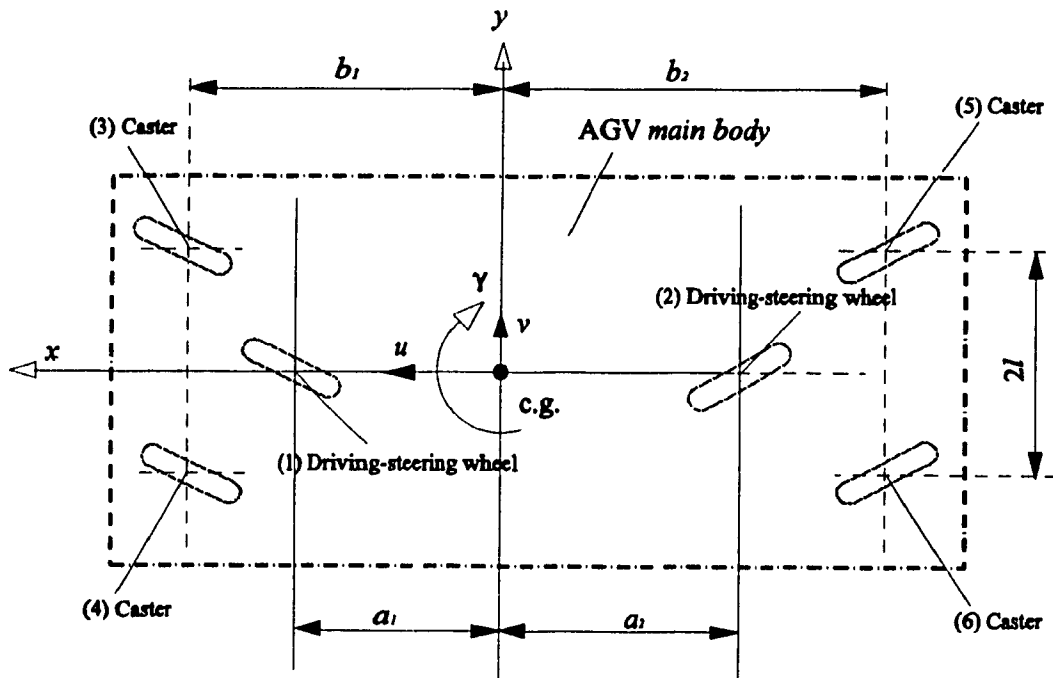
Figure 5.17: Schematic of a Six Wheels Configuration AGV.
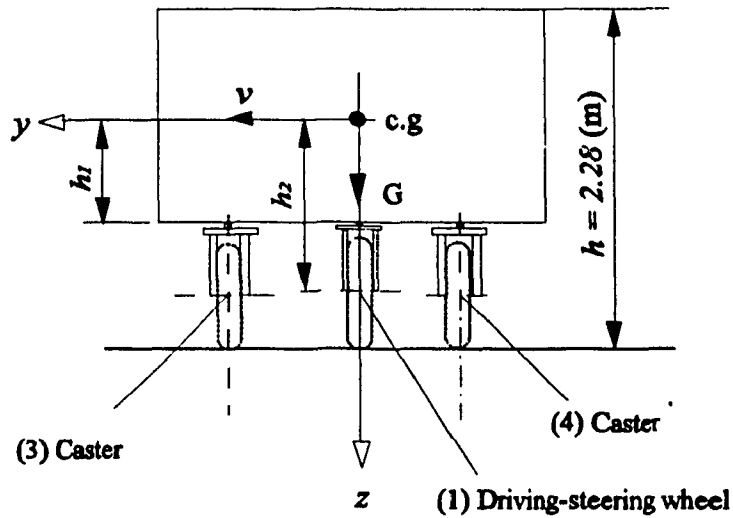
Figure 5.18: Front View of the Six Wheels AGV.

5.5.1. Dynamic Model of a six wheel configuration AGV:

Step 1. Specification of an AGV system:

i) Driving wheel units: $\qquad$ $n_d = 0$.

ii) Steering wheel units: $\qquad$ $n_s = 0$.

iii) Driving-steering wheel units: $\qquad$ $n_{ds} = 2$.

In this cases, since the offset of each driving-steering wheel units is equal to zero, the locations of joints A_i and B_i are coincident with each other. Locations of the two driving-steering wheel units are specified by the following equations ($i = 1, 2$):

$$
\begin{cases}
x_{b_1} = a_1 = 0.93 \ (m) \ , \\
y_{b_1} = 0 \ (m) \ ,
\end{cases}
\qquad
\begin{cases}
x_{b_2} = - a_2 = -0.93 \ (m) \ , \\
y_{b_2} = 0 \ (m) \ .
\end{cases}
\tag{5.4.1}
$$

195

iv) Casters (the offset of each caster is $d_3 = d_4 = d_5 = d_6 = 0.0\,4$ m): $n_c = 4$.

The locations of the four casters are specified by the following equations:

$$\begin{cases} x_{e_3} = b_1 = 1.53 \ (m) \ , \\ y_{e_3} = l = 0.74 \ (m) \ , \end{cases} \qquad \begin{cases} x_{e_4} = b_1 = 1.53 \ (m) \ , \\ y_{e_4} = -l = -0.74 \ (m) \ , \end{cases}$$

(5.4.2)

$$\begin{cases} x_{e_5} = -b_2 = -1.53 \ (m) \ , \\ y_{e_5} = l = 0.74 \ (m) \ , \end{cases} \qquad \begin{cases} x_{e_6} = -b_2 = -1.53 \ (m) \ , \\ y_{e_6} = -l = -0.74 \ (m) \ . \end{cases}$$

The total number of the wheel units n employed on the AGV and the total number of the steering and power variables N_{var} introduced to the system are given by the following equations:

$$n = n_d + n_s + n_{ds} + n_c = 6 \ ,$$

$$N_{var} = 2 \ n_{ds} = 4 \ .$$

(5.4.3)

Step 2. Determination of intermediate variables (β_p, α_p, ζ_l and f_{r_l}) for each wheel unit.

Step 2.1 Calculate the constrained velocities and direction angle of each wheel unit:

The constrained velocities of the two driving-steering wheel units at joint B_1 and B_2 are:

$$V_{B_1} = \begin{pmatrix} v_{x_{B_1}} \\ v_{y_{B_1}} \end{pmatrix} = \begin{pmatrix} u \\ v + 0.93 \, \gamma \end{pmatrix},$$

(5.4.4)

$$V_{B_2} = \begin{pmatrix} v_{x_{B_2}} \\ v_{y_{B_2}} \end{pmatrix} = \begin{pmatrix} u \\ v - 0.93 \, \gamma \end{pmatrix}.$$

196

The magnitudes of V_{B_1} and V_{B_2} in the xy plane are expressed by the following equations:

$$v_{xy_{B_1}} = \sqrt{u^2 + (v + 0.93\gamma)^2} \; ,$$

$$(5.4.5)$$

$$v_{xy_{B_2}} = \sqrt{u^2 + (v - 0.93\gamma)^2} \; .$$

The constrained velocity vectors for the four casters at joint A_3, A_4 and A_5, A_6 are expressed by the following equations:

$$V_{A_3} = \begin{pmatrix} v_{x_{A_3}} \\ v_{y_{A_3}} \end{pmatrix} = \begin{pmatrix} u - 0.74\gamma \\ v + 1.53\gamma \end{pmatrix} ,$$

$$V_{A_4} = \begin{pmatrix} v_{x_{A_4}} \\ v_{y_{A_4}} \end{pmatrix} = \begin{pmatrix} u + 0.74\gamma \\ v + 1.53\gamma \end{pmatrix} ,$$

$$(5.4.6)$$

$$V_{A_5} = \begin{pmatrix} v_{x_{A_5}} \\ v_{y_{A_5}} \end{pmatrix} = \begin{pmatrix} u - 0.74\gamma \\ v - 1.53\gamma \end{pmatrix} ,$$

$$V_{A_6} = \begin{pmatrix} v_{x_{A_6}} \\ v_{y_{A_6}} \end{pmatrix} = \begin{pmatrix} u + 0.74\gamma \\ v - 1.53\gamma \end{pmatrix} .$$

The magnitudes of V_{A_3}, V_{A_4} and V_{A_5}, V_{A_6} in the $x \, y$ plane are determined by the following equations:

$$v_{xy_{A_3}} = \sqrt{(u - 0.74\gamma)^2 + (v + 1.53\gamma)^2} \; ,$$

$$v_{xy_{A_4}} = \sqrt{(u + 0.74\gamma)^2 + (v + 1.53\gamma)^2} \; ,$$

$$(5.4.7)$$

$$v_{xy_{A_5}} = \sqrt{(u - 0.74\gamma)^2 + (v - 1.53\gamma)^2} \; ,$$

$$v_{xy_{A_6}} = \sqrt{(u + 0.74\gamma)^2 + (v - 1.53\gamma)^2} \; .$$

197

The direction angle (β_i) of each wheel unit:

$$\beta_1 = \tan^{-1} \frac{V_{y_{B_1}}}{V_{x_{B_1}}} = \tan^{-1} \frac{v + 0.93\,\gamma}{u} \,,$$

$$\beta_2 = \tan^{-1} \frac{V_{y_{B_2}}}{V_{x_{B_2}}} = \tan^{-1} \frac{v - 0.93\,\gamma}{u} \,,$$

$$\beta_3 = \tan^{-1} \frac{V_{y_{A_3}}}{V_{x_{A_3}}} = \tan^{-1} \frac{v + 1.53\,\gamma}{u - 0.74\,\gamma} \,,$$

$$\beta_4 = \tan^{-1} \frac{V_{y_{B_4}}}{V_{x_{B_4}}} = \tan^{-1} \frac{v + 1.53\,\gamma}{u + 0.74\,\gamma} \,,$$

$$\beta_5 = \tan^{-1} \frac{V_{y_{A_5}}}{V_{x_{A_5}}} = \tan^{-1} \frac{v - 1.53\,\gamma}{u - 0.74\,\gamma} \,,$$

$$\beta_6 = \tan^{-1} \frac{V_{y_{A_6}}}{V_{x_{A_6}}} = \tan^{-1} \frac{v - 1.53\,\gamma}{u + 0.74\,\gamma} \,.$$

(5.4.8)

Step 2.2 Calculate the slip angles and rotation angles (α_p, ζ_i) and rolling friction factor (f_{r_i}):

The slip angles of two driving-steering wheel unites:

$$\alpha_1 = \beta_1 - \delta_1 \,,$$

$$\alpha_2 = \beta_2 - \delta_2 \,,$$

(5.4.9)

where, the steering angles (δ_1 and δ_2)of the two driving-steering wheel units are determined by applying kinematic constraints of the AGV. Each steering angle can be expressed as function of the linear velocities $\dot{X}_\varrho(t)$ and $\dot{Y}_\varrho(t)$, the yaw rate $\gamma(t)$ and the orientation $\theta(t)$ of the vehicle as following equations (referring to Eqn. (4.8 a)):

$$\delta_1 = \tan^{-1} \frac{-\dot{X}_\varrho \sin(\theta) + \dot{Y}_\varrho \cos(\theta) + 0.93\,\gamma}{\dot{X}_\varrho \cos(\theta) + \dot{Y}_\varrho \sin(\theta)} \,,$$

(5.4.10)

198

$$\delta_2 = \tan^{-1} \frac{-\dot{X}_Q \sin(\theta) + \dot{Y}_Q \cos(\theta) - 0.93\,\gamma}{\dot{X}_Q \cos(\theta) + \dot{Y}_Q \sin(\theta)} .$$

The steering rates of the two driving-steering wheel units are obtained by differentiating Eqns. (5.4.10) with respect to the time. The rotation angles for four casters are determined by the following equations ($i = 3, 4, 5, 6$):

$$\zeta_i = \zeta_i(0) + \int\int_0^t \frac{F_{C_i} d_i}{I_{C_i}} \, dt . \qquad (5.4.11)$$

In Eqn. (5.4.11), the polar moment of inertia and the offset of each caster are I_{C_i} and d_i, respectively. In addition, the friction factor for the six wheel units may be chosen as follows:

$$f_{r_1} = k_1(1 + k_2 v_{xy_{B_1}}) ,$$

$$f_{r_2} = k_1(1 + k_2 v_{xy_{B_2}}) ,$$

$$f_{r_3} = k_1(1 + k_2 v_{xy_{A_3}}) ,$$

$$f_{r_4} = k_1(1 + k_2 v_{xy_{A_4}}) , \qquad (5.4.12)$$

$$f_{r_5} = k_1(1 + k_2 v_{xy_{A_5}}) ,$$

$$f_{r_6} = k_1(1 + k_2 v_{xy_{A_6}}) .$$

The rolling friction coefficients of each wheel in Eqns. (5.4.12) are k_1 and k_2. The friction factors represented in Eqns. (5.4.12) can also determined by taking other consideration (refer to Appendix B).

199

Step 3. Determination of the external forces (F_{l_i}, F_{f_i}, F_{c_i} and F_{t_i}) acting on each wheel unit

at the wheel-ground contact points:

Step 3.1 External forces depend on the slip angle as well as the friction between the wheel

and floor as follow :

Lateral forces acting on the two driving-steering wheels at the wheel-ground contact points

are be determined by the following equations:

$$F_{l_1} = -C_\alpha \, \alpha_1 \, ,$$

$$F_{l_2} = -C_\alpha \, \alpha_2 \, .$$

$$(5.4.13)$$

The side forces acting on the four casters at the wheel-ground contact points are determined

from the following equations ($i = 3, 4, 5, 6$):

$$F_{c_i} = k_{cn} \, F_{z_i} \, \text{sign}\,(\beta_i - \zeta_i) \, .$$

$$(5.4.14)$$

The rolling frictions acting on the six wheel units at the wheel-ground contact points may

decided by the following equations ($i = 1, 2, 3, 4, 5, 6$):

$$F_{f_i} = f_{r_i} \, F_{z_i} \, .$$

$$(5.4.15)$$

Step 3.2 External forces depend on the motor characteristics:

The applied tractive forces acting on the two driving-steering wheel units are determined by

the following equations:

$$F_{t_1} = \frac{N_1}{R_1} \, (K_{T_1} \, I_1 - J_1 \, N_1 \, \dot{\omega}_1 - D_1 \, N_1 \, \omega_1 - T_{f_1}) \, ,$$

$$(5.4.16)$$

$$F_{t_2} = \frac{N_2}{R_2} \, (K_{T_2} \, I_2 - J_2 \, N_2 \, \dot{\omega}_2 - D_2 \, N_2 \, \omega_2 - T_{f_2}) \, ,$$

200

where, N_1, N_2 = gear ratio $\quad\quad K_{T1}, K_{T2}$ $\quad\quad$ = motor torque constant [N.m/A]

$\quad\quad\quad I_1, I_2$ = current [Amp] $\quad\quad$ J_1, J_2 = driving wheel moment of inertia [kg.m^2]

$\quad\quad\quad T_{f1}, T_{f2}$ = static friction of motor [Nm],

$\quad\quad\quad D_1, D_2$ = viscous damping factor [N.m.s/rad].

In Eqns. (5.4.16), the currents of two driving-steering wheel units can be determined from the inverse dynamic model of the AGV, since the system has no redundancy. They can be also considered as independently input variables (commands) applied to the system to study the dynamic behaviour of the AGV. The angular velocities (ω_1, ω_2) and acceleration and ($\dot{\omega}_1$, $\dot{\omega}_2$) of the two driving motor can expressed as a function of the linear velocities, yaw rate, angular acceleration and orientation of the vehicle with respect to the inertial frame $\{I\}$. The angular velocities of the two driving-steering wheel units can be expressed by the following equations:

$$\omega_1 = \frac{\dot{X}_Q\cos(\theta + \delta_1) + \dot{Y}_Q\sin(\theta + \delta_1) + (0.93\sin(\delta_1))\gamma}{R_1},$$

$$\omega_2 = \frac{\dot{X}_Q\cos(\theta + \delta_2) + \dot{Y}_Q\sin(\theta + \delta_2) - (0.93\sin(\delta_2))\gamma}{R_2}.$$

(5.4.17)

and angular accelerations of the two driving-steering wheel units can be obtained by differentiating the above equations with respect to the time.

Step 4. Formulating the total external forces acting on the wheel-ground contact points along

the x and y directions:

i) Driving wheel units: Do not need to be considered.

ii) Steering wheel units: Do not need to be considered.

iii) Two driving-steering wheel units ($i = 1, 2$):

$$\begin{cases} X_i = (F_{t_i} - F_{f_i})\cos \delta_i + |F_{l_i}| \cos (\delta_i - \text{sign} (\alpha_i)\frac{\pi}{2}) \,, \\[4mm] Y_i = (F_{t_i} - F_{f_i})\sin \delta_i + |F_{l_i}| \sin (\delta_i - \text{sign} (\alpha_i)\frac{\pi}{2}) \,, \end{cases}$$

(5.4.18)

iv) Four casters (i =3, 4,, 5, 6):

$$\begin{cases} X_i = -F_{f_i} \cos \zeta_i + F_{c_i} \cos (\zeta_i + \text{sign} (\zeta_i)\frac{\pi}{2}) \,, \\[4mm] Y_i = -F_{f_i} \sin \zeta_i + F_{c_i} \sin (\zeta_i + \text{sign} (\zeta_i)\frac{\pi}{2}) \,. \end{cases}$$

(5.4.19)

Step 5. Total external forces and moments acting on the AGV system:

a) Total forces acting on the AGV along the x direction:

$$\sum X = \sum_{i=1}^{2} ((F_{t_i} - F_{f_i}) \cos \delta_i + |F_{l_i}| \cos (\delta_i - \text{sign} (\alpha_i) \frac{\pi}{2}))$$

$$- \sum_{i=3}^{6} (F_{f_i} \cos \zeta_i + F_{c_i} \cos (\zeta_i + \text{sign} (\zeta_i) \frac{\pi}{2})) \,.$$

(5.4.20)

b) Total forces acting on the AGV system along the y direction:

$$\sum Y = \sum_{i=1}^{2} ((F_{t_i} - F_{f_i}) \sin \delta_i + |F_{l_i}| \sin(\delta_i - \text{sign}(\alpha_i) \frac{\pi}{2}))$$

$$- \sum_{i=3}^{6} (F_{f_i} \sin \zeta_i + F_{c_i} \sin(\zeta_i + \text{sign}(\zeta_i) \frac{\pi}{2})) \ . \tag{5.4.21}$$

c) The total moments acting on the AGV system above the z (yaw) axis:

$$\sum N = -\sum_{i=1}^{2} ((F_{t_i} - F_{f_i}) \cos \delta_i + |F_{l_i}| \cos(\delta_i - \text{sign}(\alpha_i) \frac{\pi}{2})) \ y_{b_i}$$

$$- \sum_{i=3}^{6} (F_{f_i} \cos \zeta_i - F_{c_i} \cos(\zeta_i + \text{sign}(\zeta_i) \frac{\pi}{2})) \ y_{a_i}$$

$$- \sum_{i=1}^{2} ((F_{t_i} - F_{f_i}) \sin \delta_i + |F_{l_i}| \sin(\delta_i - \text{sign}(\alpha_i) \frac{\pi}{2})) \ x_{b_i} \tag{5.4.22}$$

$$+ \sum_{i=3}^{6} (F_{f_i} \sin \zeta_i + F_{c_i} \sin(\zeta_i + \text{sign}(\zeta_i) \frac{\pi}{2})) \ x_{a_i} \ .$$

Step 6. Assemble the motion equations of the AGV with external forces and moments:

$$m(\dot{u} - \gamma v) = \sum X \ ,$$

$$m(\dot{v} + \gamma u) = \sum Y \ , \tag{5.5.23}$$

$$I_z \dot{\gamma} = \sum N \ .$$

Finally, substituting external forces and moments obtained from Step 5 into Eqns. (5.4.23),

the equations of motion for the vehicle system are expressed by the following equations:

$$m(\dot{u} - \gamma v) = \sum_{i=1}^{2} ((F_{t_i} - F_{f_i}) \cos \delta_i + |F_{l_i}| \cos(\delta_i - \text{sign}(\alpha_i) \frac{\pi}{2}))$$

$$- \sum_{i=3}^{6} (F_{f_i} \cos \zeta_i + F_{c_i} \cos(\zeta_i + \text{sign}(\zeta_i) \frac{\pi}{2})) \ ,$$

$$m(\dot{v} + \gamma u) = \sum_{l=1}^{2} ((F_{t_l} - F_{f_l})\sin\delta_l + |F_{t_l}|\sin(\delta_l - \text{sign}(\alpha_l)\frac{\pi}{2}))$$ (5.4.24)
$$- \sum_{l=3}^{6} (F_{f_l}\sin\zeta_l + F_{c_l}\sin(\zeta_l + \text{sign}(\zeta_l)\frac{\pi}{2})) ,$$

$$I_z\dot{\gamma} = -\sum_{l=1}^{2} ((F_{t_l} - F_{f_l})\cos\delta_l + |F_{t_l}|\cos(\delta_l - \text{sign}(\alpha_l)\frac{\pi}{2})) y_{b_l}$$

$$- \sum_{l=3}^{6} (F_{f_l}\cos\zeta_l - F_{c_l}\cos(\zeta_l + \text{sign}(\zeta_l)\frac{\pi}{2})) y_{a_l}$$

$$-\sum_{l=1}^{2} ((F_{t_l} - F_{f_l})\sin\delta_l + |F_{t_l}|\sin(\delta_l - \text{sign}(\dot{\alpha}_l)\frac{\pi}{2})) x_{b_l}$$

$$+ \sum_{l=3}^{6} (F_{f_l}\sin\zeta_l + F_{c_l}\sin(\zeta_l + \text{sign}(\zeta_l)\frac{\pi}{2})) x_{a_l} .$$

This is a sixth order system of nonlinear ordinary differential equations.

Step 7. Obtained the forward dynamical model of the AGV:

Rearranging Eqns. (5.4.24) in matrix form, the accelerations of the AGV with respect to the reference frame $\{Q\}$ can be expressed by the following equations:

$$\mathbf{a}_Q = A^{-1} (B + D),$$ (5.4.25)

and the acceleration of the AGV with respect to the inertial frame $\{I\}$ can be determined by the following equations:

$$\mathbf{a} = T \times \mathbf{a}_Q ,$$ (5.4.26)

where:

204

$$\mathbf{a}_Q = \begin{pmatrix} \dot{u} \\ \dot{v} \\ \dot{\gamma} \end{pmatrix}, \qquad T = \begin{bmatrix} \cos(\theta) & -\sin(\theta) & 0 \\ \sin(\theta) & \cos(\theta) & 0 \\ 0 & 0 & 1 \end{bmatrix},$$

and

$$A = \begin{bmatrix} m & 0 & 0 \\ 0 & m & 0 \\ 0 & 0 & I_z \end{bmatrix}, \qquad B = \begin{pmatrix} \sum X \\ \sum Y \\ \sum N \end{pmatrix}, \qquad D = \begin{pmatrix} vm\gamma \\ -um\gamma \\ 0 \end{pmatrix}.$$

Step 8. Integrating the forward dynamical model:

Given initial position and velocities of the automated vehicle as: $\mathbf{P}_\bullet = \{X_Q(0),\ Y_Q(0),\ \theta(0)\}^\mathsf{T}$

and $\mathbf{V}_\bullet = \{\dot{X}_Q(0),\ \dot{Y}_Q(0),\ \gamma(0)\}^\mathsf{T}$, then, the instantaneous velocities and position of the vehicle with respect to the reference frame $\{I\}$ can be determined by integrating Eqn. (5.4.26).

The dynamic model of the six wheeled AGV has been derived by following the steps provided in Chapter 4, Section 4.2. The dynamic simulation of this system can be carried out by following the steps provided in Section 4.3. In addition, the system has no redundancy, therefore, currents applied to the system can be determined from the inverse dynamic model of the AGV, if the desired acceleration and velocity are given. These currents can also be input variables to the system. This simulation procedure is very similar to that of the CONCIC-3 AGV, and the interested reader can refer to Section 5.2 for more details.

205

5.6 Summary

In this Chapter, the methodology for derivation and simulation of automated vehicle dynamic models is demonstrated. Dynamic models of four vehicles with different wheel configurations are derived following the steps provided in Chapter 4, Section 4.2. Results show that the present methodology is appropriate to a class of automated vehicles (defined in Section 2.2) with arbitrary wheel configurations. The derivation procedure is seen to be easily followed. External forces and moments acting on the vehicle, as well as inertial forces and moments of inertia of the vehicle are all obtained. Referring to Table 4.2, all variables and equations originated or eliminated in each step are itemized. The final required control variables and the redundancy of the system are emphasized for each case.

The dynamic simulations for case 1 and case 2 are also carried out by following the steps provided in Chapter 4, Section 4.3. For these two cases, there are no redundancy in the systems. Therefore, the currents (power variables) can be considered as independent input variables applied to the systems (in order to study the behaviours of the system). They can also be determined from the inverse dynamic model of the vehicle (in order to control of the system), if the desired accelerations and velocities of the vehicle are given. The manner of using inverse dynamic model to determine input currents is often applied to the computer torque control of the AGV [48].

Chapter 6

CONCLUSIONS AND RECOMMENDATIONS

6.1 Conclusions

This thesis derives and demonstrates a systematic methodology for the automated derivation

of dynamic models of a class of automated vehicles with n wheels of arbitrary configuration.

In addition, a systematic methodology is derived and demonstrated for numerical simulation

of this class of vehicles on digital computer. In order to achieve these objectives, this research

has covered the following areas:

(i) Description of general assumptions, definitions and conventional notations, as well

as kinematic constraints for automated vehicle systems.

(ii) An automated vehicle dynamic model is assembled by considering the vehicle main

body and each wheel unit as a separate rigid body, going through the necessary force

balances and characteristics of the salient components.

(iii) Development of a systematic methodology to derive and simulate dynamic

models for a class of vehicle with n arbitrary wheel configurations, a combination

of sprung and unsprung masses, generation of tractive forces, rolling friction and

lateral forces (side friction forces) at wheel-ground contact points, and nonholonomic

constraints.

(vi) Determination of redundancies in the automated vehicle system dynamic model.

(v) Four automated vehicles with different wheel configurations have been examined

to show how the methodology may be put to use. Results show that this methodology yields models in a very short time, providing the much needed help for investigating performance of different designs of automated vehicles. In addition, this methodology is considered preferable to those currently available due to its improved flexibility.

In Chapter 2, general assumptions, definitions and conventional notations are introduced and discussed in detail. Expressions for the positions and velocities of three and four DOFs automated vehicles have been derived based on these usages. Two kinematic (Nonholonomic) constraints are detailed, both of which must be satisfied by all wheel units utilized on the types of vehicles considered in this thesis. These constraints are the pure rolling and non-slipping conditions at wheel-ground contact points.

Based on derivations in Sections 2.4.1 and 2.4.2, we can conclude that if the geometric relationship of all joints with respect to the reference frame is known, then the characteristics of these joints can be completely described. These characteristics are described by a set of equations written in terms of the position, velocity, orientation, and their time derivatives. The complete mathematical description of all wheel unit joints with respect to their corresponding reference frames can be combined with knowledge of kinematic constraints to either design the control law or compute the simulation input motion parameters. The theory of combining the mathematical description of wheel unit joints and their kinematic constraints together can be used to reduce the redundancy of the dynamic model, and can also be used to develop a general kinematic model for arbitrary wheel configurations, but this is beyond the scope of the present thesis.

In Chapter 3, an automated vehicle is considered which is composed of distinct individual rigid bodies. This vehicle consists of a main body, and arbitrary combinations of driving wheel units, steering wheel units, driving-steering units and casters. The vehicle main body and each wheel unit are considered to be connected by two possible types of joints. Equations of motion for each rigid body have been derived in detail. The forward dynamical model of a vehicle with arbitrary wheel configurations has been developed by integrating together subsystems comprising the vehicle main body and each wheel unit.

Furthermore, in this model the sprung mass m_s and unsprung mass m are considered explicitly. Two principal types of steering wheel units and/or driving-steering wheel units are generally employed on automated vehicle systems, and are investigated in detail in Chapter 3, Sections 3.3.3 and 3.3.4. Equations of motion for these types of wheel units have been derived, and kinematic constraints have also been detailed.

In Chapter 4, a systematic methodology for modelling and simulation of the dynamics of a class of automated vehicle has been developed. This methodology allows for arbitrary wheel configurations, combined sprung and unsprung masses, generation of the tractive forces, rolling friction and side friction at wheel-ground contact points, and nonholonomic constraints. Four types of wheel units, namely driving wheel units, steering wheel units, driving-steering wheel units and casters are considered to be employed on the automated vehicle systems.

The present approach to derivation of automated vehicle dynamical models renders the process considerably less difficult for users not familiar with the details of vehicle dynamics. It is possible to follow the simple steps provided in this chapter to obtain any

desired dynamical model. This methodology may also be used to check models obtained by other techniques. In addition, although this model is designed to handle four DOFs automated vehicles, it can be extended to handle the six DOFs models since the z-direction variables (such as $\dot{Z}_Q$, z) have been retained throughout the modelling development.

The general procedure for deriving a dynamic model which incorporates n arbitrarily configured wheels is summarized the flowchart of Fig. 4.1. System parameters are summarized in Table 4.1, and assumptions and nomenclature for the model are summarised in Section 4.2.1. In order to facilitate tracking of all variables, Table 4.2 indicates all variables and equations generated or eliminated in each step. This permits the user to know the numerical degrees of freedom for the model so generated. Finally, the formal structure of the model is shown to lead to a parallel structure for numerical simulation on a digital computer. The flowchart for dynamical simulation of automated vehicle systems given by Fig. 4.5 illustrates this process.

In Chapter 5, the methodology for derivation and simulation of automated vehicle dynamic models is demonstrated. Dynamic models of four vehicles with different wheel configurations are derived following the steps provided in Chapter 4, Section 4.2. Results show that the present methodology is appropriate to a class of automated vehicles (defined in Section 2.2) with arbitrary wheel configurations. The derivation procedure is seen to be easily followed. External forces and moments acting on the vehicle, as well as inertial forces and moments of inertia of the vehicle are all obtained. Referring to Table 4.2, all variables and equations originated or eliminated in each step are itemized. The final required control variables and the redundancy of the system are emphasized for each case.

210

Appendix A of this thesis presents a detailed review of the dynamic characteristics of a rigid body. This leads to the use of D'Alembert's principle for the analysis of automated vehicle systems. Appendix B of this thesis presents a detailed discussion of the mechanics of wheels. Based on this discussion, an expression for the friction factor at the wheel-ground contact point is adopted. An expression is also adopted for the lateral forces acting on each wheel. From these considerations, a simplified wheel model is derived. Tractive forces provided to the system by DC motors in driving wheels are studied to derive an expression representing their effect on the vehicle system. Appendix C studies the vertical forces acting on individual wheel units to determine overall vehicle load distributions. The effect of forward speed and rolling motion on this distribution is also studied. Examples of statically indeterminate vehicle structures are given. Appendix D provides actual system parameters for two automated vehicles, namely CONCIC-2 and CONCIC-3. These data are used in the dynamic simulations of Chapter 5.

6.2 Recommendations for Future Work

This methodology could be further generalized to include consideration of pitch and bounce modes, boosting the number of DOFs from four to six. More detailed vehicle suspension models could be incorporated into the methodology. More detailed analysis of vehicle load distributions (including statically indeterminate problems) should be considered. An investigation into the development of strategies for the elimination of redundancies in vehicle dynamic models should be conducted. This would result in the system being more easily and directly controllable. Additional types of motors and wheel units should be considered.

211

Consideration of area wheel-ground contact regions instead of point wheel-ground contact regions should be considered for more realistic tire models. Experimental verification of a variety of case studies should be carried out to assess the accuracy of the models and simulations. A sensitivity analysis should be carried out to determine the effect of parametric variations on system response. Furthermore, incorporating this automated modelling as an extension or as a toolbox to other packages (such as Working Model of Knowledge Revolution [60]) should be explored.

REFERENCES

[1] Imai, H., Fujiwara, K., and Kawashima, Y. (Mitsubishi Electric Corp., Japan). "Advanced Automated Transportation Systems", *International Trends in Manufacturing Technology, Automated Guided Vehicle Systems*, 1987 IFS (Publications) Ltd, UK. pp. 311-324.

[2] Lane, D. *Project Engineer, Whirlpool Corporation.* "Flexible and Smart Assembly with AGVs", *Material Handling Engineering*, March 1994.

[3] Castleberry, G., "AGVs Critical to Development of Factories of the Future", *Journal: Robotic World* [RBW], ISSN: 0737-7908, vol. 10, iss: 3, Sept. 1992, pp. 10-12.

[4] Nelms, D.W, "Delta's Automated Cargo", *Journal: Air Transport World* [ATW], ISSN:0002-2543, vol. 29, iss. 8, Aug. 1992, pp. 57-58.

[5] Delta Air Lines Inc.. "Systems: Demand Rockets, Delta Automates Air Cargo Operations", *Journal: Modern Materials Handling* [MMH], ISSN: 0026-8038, vol. 47, iss. 5, Apr. 1992, pp. 12-13.

[6] Dunkin, A. "Automated Guided Vehicle Systems", *Industrial Engineering* Aug. 1994, pp. 47.

[7] "Automated System: Key Component in Strategy for Growth", *Journal: Logistics Today* [LOG], ISSN: 0262-4354, vol. 12, iss. 1, Jan.-Feb. 1993, pp. 16-18.

[8] Lai, S. and Hsieh, S., "Algorithms, AGVs, Operations Research, Functions, Models", *Journal of Computers & Industrial Engineering* [CIE], ISSN: 0360-8352, vol. 23, iss. 1-4, Nov. 1992, pp. 181-185.

[9]   Tanya, S. and Sanljiv, S., "A Program for Dispatching and Routing AGVs", *Journal: Computers & Industrial Engineering* [CIE], ISSN: 0360-8352, vol. 23, iss. 1-4, Nov. 1992, pp. 187-190.

[10]   Hong Kong Ingenuity Ltd., "Inside Knowledge", *Asian Business Journal* [ABS] ISSN: 0254-3729, vol. 31, iss. 6, June 1995, p. 57.

[11]   Saha, S., and Angeles, J. "Kinematics and Dynamics of a Three-Wheeled 2-DOF AGV", *Proceeding of the IEEE International Conference on Robotics and Automation*, vol. 3, pp. 1572-1577, Scottsdale, Arizona, 1989.

[12]   Tanaka, N., "The concept of the advanced robot for support of offshore oil exploration", *Proceedings of the IEEE International Conference on Advancea Robotics*, Tokyo, Japan, Sept. 1985, pp. 507-511.

[13]   Meieran, H. B., and Gelhaus, F. E., "Mobile robots designed for hazardous environments", *Robotics Engineering*, March, 1986, pp. 10-16.

[14]   Auton, B. "Three Views on the Changing Role of Lift Trucks in Semi-Automated and Automated Warehouses." *Beverage World*, August 1995, pp. 74-82.

[15]   Anderson, T., and Longmore-Ethridge, A., " Security Works", *Security Management*, November 1993, pp. 17-19.

[16]   Routh, G. "Industrial Engineers Play Critical Role in Boeing Celebration", *IEE Solutions*, July 1995.

[17]   Rajagopalan, R., "Guidance and Control of Automated Guided Vehicle Employing Binary Camera Vision", *Ph.D Thesis*, Concordia University, Montréal, Canada, Sept. 1991.

[18] Matsumoto, N. and Tomizuka, M., "Vehicle Lateral Velocity and Yaw Rate Control With Two Independent Control Inputs", *Journal of Dynamic System, Measurement and Control*, Dec. 1992, vol. 114, pp. 606-612.

[19] Mehrabi, M. G. "Path Tracking Control of Automated Vehicles: Theory and Experiment", *Ph.D Thesis*, Concordia University, Montréal, Canada, September 1993.

[20] Cheng, R. M. H., Coubert, Y., Favreau, P., and A. Fahim", Investigation of an Automated Guided Vehicle (AGV) Driven by Camera Vision", *Proceedings of the International Conference on Intelligent Autonomous Systems*, pp. 162-167, Amsterdam, Netherlands, 1986.

[21] Huang, M., "Dynamic Modelling and Simulation of an AGV(CONCIC-2AGV)", *Master's Thesis*, Concordia University, Montréal, Canada, April 1991.

[22] Cheng, R. M. H., and Rajagopalan, R., "Kinematics of Automated Guided Vehicles with an Inclined Steering Column", *ASME International Computers in Engineering Conference*, San Francisco, California, Aug. 1988.

[23] Cheng, R.M.H., and Huang, M., "Dynamic Modelling and Simulation of an AGV (The CONCIC-2 Vehicle)", *IFToMM Congress*, Prague, Czechoslovakia, August 1991.

[24] Cheng, R. M. H., and Mehrabi, M. G., "Dynamic Modelling of Wheeled Mobile Robots and Automated Transit Vehicles Using Dimensionless 'Roll Number'", *The 1st IEEE Conference on Control Applications*, 1992, Dayton, Ohio, pp. 160-167.

[25] Jarvis, R., "Robot Navigation," *Journal of Industrial Robotics* [IRO] ISSN: 0143-991X, vol. 21, iss. 2, 1994, p. 3.

[26] Boegli, P., "A Comparative Evaluation of AGV Navigation Techniques", *International Trends in Manufacturing Technology, Automated Guided Vehicle Systems*, 1987 IFS (Publications) Ltd, UK, pp. 65-77.

[27] Rajagopalan, R. and Cheng, R. M. H., "Guidance and Control of Automated Guided Vehicles Using Binary Camera Vision", *SME Transactions on Robotics Research*, vol. II, Sept. 1992.

[28] Hessburg, T., Peng, H., Tomizuka, M., Zhang, W., and Kamei, E., "A Study of Lateral Control for Vehicles", American Control Conference, San Diego, CA., 1991 pp. 3084-3089.

[29] Cheng, R. M. H., and Rajagopalan, R., "Kinematics of Automatic Guided Vehicles with an Inclined Steering Column and Offset Distance: Criterion for Existence of Inverse Kinematic Solution", *Journal of Robotic Systems*, 1992, pp. 1058-1081.

[30] Muir, P.F, and Neuman, C.P., "Dynamic Modelling of Multibody Robotic Mechanisms: Incorporating Closed-Chains, Friction, Higher-Pair Joints, and Unactuated and Unsensed Joints", *Proceedings of the IEEE International Conference on Robotics and Automation*, 1988, pp. 1546-1551.

[31] Muir, P.F. and Neuman, C.P., "Kinematic Modelling of Automated Guided Vehicles", Technical Report No. CMU-RI-TR-86-12, The Robotic Institute, CMU, PA, 1986.

[32] Muir, P.F. and Neuman, C.P., "Resolved Motion Rate and Resolved Acceleration Servocontrol of Wheeled Mobile Robots", *Proceeding of the IEEE 1990 International Conference on Robotics and Automation*, pp. 1133-40 vol.2.

[33] Wang, Y., Linnett, J. and Roberts, J. "A unified approach to inverse and direct

kinematics for four kinds of wheeled mobile robots and its applications", to appear in *Proceeding of the IEEE 1996 International Conference on Robotics and Automation*.

[34]   d'Andréa-Novel, B., Bastin, G., and Campion, G., "Modelling and control of Non Holonomic Wheeled Mobile Robots", *Proceedings of the 1991 IEEE International Conference on Robotics and Automation*, Sacramento, California, April 1991, pp. 1130-1135.

[35]   Cyril, X., Cheng, R. M. H., and Sankar, T. S., "Dynamics of Wheeled Mobile Robots (AGVs)", *Proceeding of the 4th International Conference on CAD/CAM, Robotics and Factories of the Future*, vol. 2, pp. 264-273, India, 1989

[36]   Lilly, K. W., "Efficient Dynamic Simulation of Robotic Mechanisms", Kluwer Academic Publishers, 1993.

[37]   Craig, J. J., "Introduction to Robotics: Mechanics and Control - Second Edition", Addison-Wesley Publishing Company, Inc., 1989.

[38]   Li, Z. X., Canny, J., and Heinzinger, G., "Robot Motion Planning with Nonholonomic Constraints", *Robotics Research. Fifth International Symposium*, pp. 309-16.

[39]   Johnson, B. W., "Microcomputei Based Adaptive Control for an Electric Wheelchair Guidance System", *University of Virginia*, 1983.

[40]   Verma, M. K., and Gillespie, T. D., "Roll Dynamics of Commerial Vehicles", *Vehicle System Dynamics*, vol. 9, 1980, pp. 1-17.

[41]   Tousi. S., Bajaj, A. K. and Soedel, W., "On the Stability of a Flexible Vehicle Controlled by a Human Pilot", *Vehicle System Dynamics*, vol. 17, 1988, pp. 37-56.

[42]   Constantine, C. J., and Law, E. H., "The Effects of Roll Control for Passenger Cars

during Emergency Maneuvers", *Concepts in Vehicle dynamics and simulation*, SAE SP-1016, pp. 31-51.

[43]   Xia, X., "A Nonlinear Analysis of Close Loop Driver / Vehicle Performance with Four Wheel Steering Control", *Ph.D. Dissertation, Department of Mechanical Engineering, Clemson University, Clemson, SC. Dec. 1990.*

[44]   Constantine, C. J., Bowman, J. E. and Law, E. H. "Development of Models and Computer Programs for Lateral Dynamics of Automobiles During Combined Braking and Steering Maneuvers", Department of Mechanical Engineering Technical Report TR-90-132-ME-MMS, Clemson University, Clemson, SC, June 1991.

[45]   Lee, C S. G., and Chang, P. R., "Efficient Parallel Algorithms for Robot Forward Dynamic Computation", *Proceedings of the International Conference on Robotics and Automation*, 1987, pp. 654-659.

[46]   Leahy, M. B., "Industrial Manipulator Control With Feedforward Dynamic Compensation", *Proceedings of the 27th Conference of Decision and Control*, Austin, Texas, Dec. 1989, pp. 598-601.

[47]   Craig, J. J., Hsu, P., and Sastry, S. S., "Adaptive Control of Mechanical Manipulators", *The International Journal of Robotics* Research, vol. 6, no. 2, pp. 16-28, summer 1987.

[48]   Khosal, P. K. and Kanaoa, T., "Experimental Evaluation of the Feedforward Compensation and Computed-Torque Control Schemes", *Proceedings of the American Control Conference*, pp. 790-798, Seattle, WA, June 1986.

[49]   An, C. H., Atkeson, C. G., Griffiths J. D., and Hollerbach, J. M., "Experimental

Evaluation of Feedforward and Computed Torque Control", *Proceedings of the International Conference on Robotics and Automation*, pp. 165-168, Raleigh, NC, March 31 - April 3, 1987.

[50]   Leahy, M. B. Jr. "Dynamics Based Control of Vertical Articulated Manipulators", *1988 IEEE International Conference on Robotics and Automation*, pp. 1048-56, April 1988.

[51]   Canudas C., Roskam, R., "Path Following of a 2-DOF Wheeled Mobile Robot under Path and Input Torque Constraints", *Proceedings of the 1991 IEEE International Conference on Robotics and Automation*, Sacramento, California, April 1991, pp. 1142-1147.

[52]   Barakat, N, " Comput Torque Control of a Differentially Driven Automate Guided Vehicle", *Master's Thesis*, Concordia University, Montréal, Canada, 1996.

[53]   Feng, L., Koren, Y., and Borenstein, J., "A Model-Reference Adaptive Motion Control for a Differential-Drive Mobile Robot", *Proceeding of the IEEE International Conference on Robotics and Automation*, San Diego, May 1994.

[54]   Koshiyama, A., and Yamafuji, K., "Design and Control of All-Direction Steering Type Mobile Robot", *The International Journal of Robotics Research*, vol. 12, no. 5, Oct. 1993, pp. 411-419.

[55]   Li, Z., "Motion Planning with Nonholonomic Constraints", *Master's Thesis*, Mathematics Department, University of California at Berkeley, Berkeley, Ca. 94720, 1989.

[56]   Toumassoud, P., and Jehl, O., "Motion Planning for a Mobile Robot with a Kinematic

Contraint", *Proceedings of the IEEE International Conference on Robotics and Automation*, 1988.

[57] Sarkar, N., Yun, X., and Kumar, V., "Control of Mechanical Systems With Rolling Constraints: Application to Dynamic Control of Mobile Robots", *The International Journal of Robotics Research*, vol. 13, no.1, Feb. 1994, pp. 55-69.

[58] Helferty, J. J. and Biswas, H., "Neuromorphic Control of Robotics Manipulators", *Proceedings of the IEEE International Conference on Robotics and Automation*, Sacramento, California, vol. 3, pp. 2436-2441, 1991.

[59] d'Andréa-Novel, B., Bastin, G., and Campion, G., "Modelling and control of Non Holonomic Wheeled Mobile Robots", *Proceedings of the 1991 IEEE International Conference on Robotics and Automation*, Sacramento, California, April 1991, pp. 1130-1135.

[60] Gramoll Kurt, "Using 'Working Model' to Introduce Design into a Freshman Engineering Course" 1994 *ASEE Conf. Proc., Edmonton, Canada*, Session 2525, June, 1994.

[61] Xi, S. Z. "Vehicle Theory", *Publication of Mechanical Inc.of China*, Aug. 1998.

[62] Burdick, J. W., "An Algorithm for Generation of Efficient Manipulator Dynamic Equations", *Proceedings of the IEEE International Conference on Robotics and Automation*, pp. 212-218, 1986.

[63] Gillespie T. D., " Fundamental of Vehicle Dynamics" , *Society of Automotive Engineers, Inc.* 1992.

[64] Beer, F. P., and Russell-Johnston, E., "Vector Mechanics for Engineers: STATICS

and DYNAMICS", *Third Edition*, McGraw-Hill Inc., 1977.

[65]   Conte, S., and De Boor, C., "Elementary Numerical Analysis: An Algorithmic

Approach - 2nd Edition", Mcgraw-Hill Inc., 1972.

[66]   Shoup, T. E., "Numerical Methods for the Personal Computer", Prentice-Hall Inc.,

1983.

[67]   "Specifications of hardware trim assembly and engine assembly AGVs", General

Motors Corporation, Oshawa, Ontario, Canada.   .

[68]   Ellis, J. R., "Vehicle Dynamics", *London Business Books Limited*, 1969.

[69]   Ellis, J. R., "Road Vehicle Dynamics", *London Business Books Limited*, 1989.

[70]   Wong, J. Y., "Theory of Ground Vehicles", John Wiley & Sons, Inc., 1978.

[71]   Dixon J. C., "Tyres, Suspension and Handling", Cambridge University Press

1991.

[72]   Timoshenko, S., "Strength of Materials", D. Van Nostrand Company, 1958.

[73]   Williams, C. D., "Analysis of Statically Indeterminate Structures", *International

Textbook Company*, 1959.

[74]   Bruch, C. D., "Strength of Materials for Technology", John Wiley & Sons Inc.,

1978.

[75]   "DC Motors Speed Controls Servo Systems", Robbins & Myers/Electro-Craft, *an

engineering handbook*, 1989.

Appendix A

A REVIEW OF THE CHARACTERISTICS OF A RIGID BODY

Xi [61], Gillespie [63], Ellis [68] [69] and Wong [70] point out that D'Alembert's principle is frequently applied to problems in vehicle dynamics and automated vehicle dynamics [21] [39]. This principle is also used in the present research for analysis of the dynamics of automated vehicle systems. Here, a review of the relevant characteristics of a rigid body is given in order to understand how this principle is applied in the analysis of automated vehicle systems.

A.1. Velocities and Accelerations of a Point on a Rigid Body

A Cartesian (x, y, z) axis system is shown in Fig. A.1. Instantaneous linear velocities and accelerations of the origin along the x, y, z directions are represented by u, v, w and a_x, a_y, a_z respectively. Angular velocities and angular accelerations about the x, y, z axes are represented by p, q, γ and $\dot{p}, \dot{q}, \dot{\gamma}$ respectively. Angular velocity directions are defined by the right hand rule as shown in Fig. A.1.

It is desired to study the motion of an arbitrary point on the rigid body in order to facilitate examination of the kinematic relationships between the vehicle main body and each wheel unit. Consider an arbitrary point $P_i(x, y, z)$ and let $v_{P_x}, v_{P_y}, v_{P_z}$ be linear velocities of the point parallel to the x, y and z axes, respectively. From inspection of Fig. A.1, the velocity vector at this point can be expressed as $v_P = v_{P_x} \mathbf{i} + v_{P_y} \mathbf{j} + v_{P_z} \mathbf{k}$. In addition, the component of the velocity vector v_P in the xy plane can be expressed as $v_{P(x,y)} = v_{P_x} \mathbf{i} + v_{P_y} \mathbf{j}$, where the

velocity vector $v_{P(x,y)}$ is the heading of the rigid body at point P, in the xy plane. The angle between the x axis and the velocity vector $v_{P(x,y)}$ is defined as the direction angle (β_P) of the velocity $v_{p(x,y)}$. The positive sense of angle β_P is as shown in Fig. A.1. Thus, the general expressions can be formulated as follows to describe the motion of point P_i.
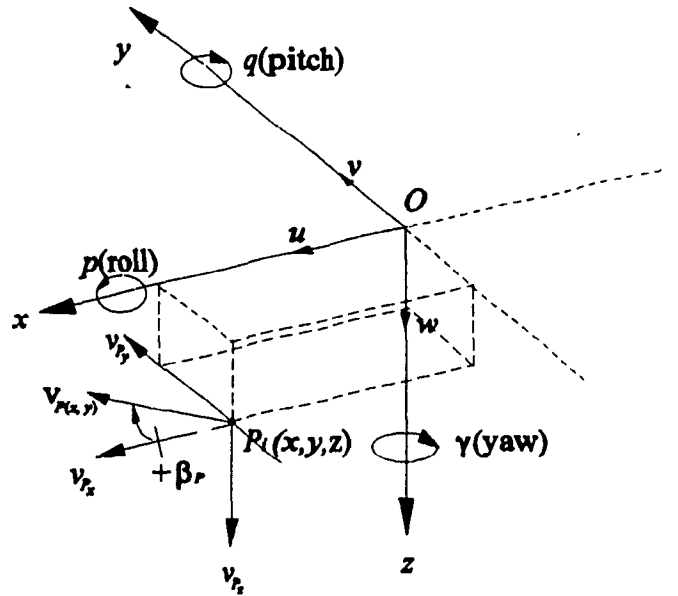

Figure A.1: Body Centred Axis System.

(1) The linear velocities v_{P_x}, v_{P_y}, v_{P_z} can be represented by a vector v_P:

$$v_P = (u - \gamma y + qz)i + (v + \gamma x - pz)j + (w - qx + py)k$$

which can expressed in matrix form as:

$$v_P = \begin{pmatrix} v_{P_x} \\ v_{P_y} \\ v_{P_z} \end{pmatrix} = \begin{pmatrix} u \\ v \\ w \end{pmatrix} + \begin{bmatrix} 0 & -\gamma & q \\ \gamma & 0 & -p \\ -q & p & 0 \end{bmatrix} \begin{pmatrix} x \\ y \\ z \end{pmatrix} \qquad (A.1)$$

(2) The linear accelerations of point P_i can be represented as a vector $\mathbf{a}_P$:

$$\mathbf{a}_P = \{\, a_x - \gamma v + qw - (q^2 + \gamma^2)x + (qp - \dot{\gamma})y + (\gamma p + \dot{q})z \,\}\mathbf{i}$$

$$+ \{\, a_y + \gamma u - pw - (p^2 + \gamma^2)y + (\gamma q - \dot{p})z + (pq + \dot{\gamma})x \,\}\mathbf{j}$$

$$+ \{\, a_z - qu + pv - (p^2 + q^2)z + (p\gamma - \dot{q})x + (q\gamma + \dot{p})y \,\}\mathbf{k}$$

which can be expressed in matrix form as:

$$
\mathbf{a}_P = \begin{pmatrix} a_{P_x} \\ a_{P_y} \\ a_{P_z} \end{pmatrix} = \begin{pmatrix} \dot{u} \\ \dot{v} \\ \dot{w} \end{pmatrix} + \begin{bmatrix} 0 & -\dot{\gamma} & \dot{q} \\ \dot{\gamma} & 0 & -\dot{p} \\ -\dot{q} & \dot{p} & 0 \end{bmatrix} \begin{pmatrix} x \\ y \\ z \end{pmatrix} + \begin{bmatrix} 0 & -\gamma & q \\ \gamma & 0 & -p \\ -q & p & 0 \end{bmatrix} \begin{pmatrix} \dot{x} \\ \dot{y} \\ \dot{z} \end{pmatrix}
$$

$$
= \begin{pmatrix} \dot{u} \\ \dot{v} \\ \dot{w} \end{pmatrix} + \begin{bmatrix} 0 & -\dot{\gamma} & \dot{q} \\ \dot{\gamma} & 0 & -\dot{p} \\ -\dot{q} & \dot{p} & 0 \end{bmatrix} \begin{pmatrix} x \\ y \\ z \end{pmatrix} + \begin{bmatrix} 0 & -\gamma & q \\ \gamma & 0 & -p \\ -q & p & 0 \end{bmatrix} \begin{pmatrix} v_{P_x} \\ v_{P_y} \\ v_{P_z} \end{pmatrix}
$$

Substituting Eqn. (A.1) into the above equation, the acceleration at any point P_i can be rewritten as:

$$
\mathbf{a}_P = \begin{pmatrix} v_{P_x} \\ v_{P_y} \\ v_{P_z} \end{pmatrix} = \begin{pmatrix} a_x \\ a_y \\ a_z \end{pmatrix} + \begin{bmatrix} 0 & -\dot{\gamma} & \dot{q} \\ \dot{\gamma} & 0 & -\dot{p} \\ -\dot{q} & \dot{p} & 0 \end{bmatrix} \begin{pmatrix} x \\ y \\ z \end{pmatrix}
$$

$$
+ \begin{bmatrix} 0 & -\gamma & q \\ \gamma & 0 & -p \\ -q & p & 0 \end{bmatrix} \left(\begin{pmatrix} u \\ v \\ w \end{pmatrix} + \begin{bmatrix} 0 & -\gamma & q \\ \gamma & 0 & -p \\ -q & p & 0 \end{bmatrix} \begin{pmatrix} x \\ y \\ z \end{pmatrix} \right)
$$

(A.2)

Eqns. (A.1) and (A.2) define the velocity and acceleration of point $P(x, y, z)$ in a rigid body

when the reference axes are fixed relative to the body. Instantaneous linear velocities and accelerations of the origin of the x, y, z system are u, v, w and a_x, a_y, a_z respectively. In addition, rotational velocities and accelerations of the axes are p, q, γ and $\dot{p}$, $\dot{q}$, $\dot{\gamma}$.

(3) The magnitude of velocity v_P is:

$$v_P = \sqrt{ v_{P_x}^2 + v_{P_y}^2 + v_{P_z}^2 }$$

$$= \sqrt{ (u - \gamma y + qz)^2 + (v + \gamma x - pz)^2 + (w - qx + py)^2 }$$

and the magnitude of velocity $v_{P(x,y)}$ (component of v_P in the xy plane) is

$$v_{P_{(x,y)}} = \sqrt{ v_{P_x}^2 + v_{P_y}^2 }$$

$$= \sqrt{ (u - \gamma y + qz)^2 + (v + \gamma x - pz)^2 } \qquad (A.3)$$

(4) Direction angle β_P (which is the angle between the x axis and the velocity vector $v_{P(x,y)}$) is given by:

$$\beta_P = \tan^{-1} \frac{v_{P_y}}{v_{P_x}} = \tan^{-1} \frac{v + \gamma x - pz}{u - \gamma y + qz} . \qquad (A.4)$$

The sign of angle β_P depends on the sign of (v_{P_y} / v_{P_x}): if $(v_{P_y} / v_{P_x}) > 0$, then β_P is positive, if $(v_{P_y} / v_{P_x}) < 0$, then β_P is negative. In other words, if β_P is clockwise the sign of β_P is positive, otherwise it is negative.

A.2. Differential Equations of a Six DOF Rigid Body

Based on D'Alembert's principle, the inertial forces and moments acting on a body form a

system in equilibrium. Thus, referring to Fig. A.1, the motion of a six DOF rigid body of the

"body-centred system" type can be represented by the following differential equations:

$$\sum X = \sum \delta m \; \dot{u} = m \; (\dot{u} - \gamma v + qw)$$

$$\sum Y = \sum \delta m \; \dot{v} = m \; (\dot{v} - pw + \gamma u) \qquad\qquad (A.5)$$

$$\sum Z = \sum \delta m \; \dot{w} = m \; (\dot{w} - qu + pv)$$

$$\sum L = \sum \delta m (y\dot{w} - z\dot{v}) = I_x \dot{p} - (I_y - I_z)\gamma q + I_{yz}(\gamma^2 - q^2) - I_{xz}(pq + \dot{\gamma}) + I_{xy}(p\gamma - \dot{q})$$

$$\sum M = \sum \delta m (z\dot{u} - x\dot{w}) = I_y \dot{q} - (I_z - I_x)\gamma p + I_{zx}(p^2 - \gamma^2) - I_{xy}(\dot{q}\gamma + \dot{p}) + I_{yz}(qp - \dot{\gamma})$$

$$\sum N = \sum \delta m (x\dot{v} - y\dot{u}) = I_z \dot{\gamma} - (I_x - I_y)pq + I_{xy}(q^2 - p^2) - I_{yz}(\gamma p + \dot{q}) + I_{xz}(\gamma q - \dot{p})$$

where $\quad \sum X = \sum \delta m a_x =$ Total external force in the x direction

$\sum Y = \sum \delta m a_y =$ Total external force in the y direction

$\sum Z = \sum \delta m a_z =$ Total external force in the x direction

$\sum L = \sum \delta m (ya_z - za_y) =$ Total moments about the x axis

$\sum M = \sum \delta m (za_x - xa_z) =$ Total moments about the y axis

$\sum M = \sum \delta m (xa_y - ya_x) =$ Total moments about the z axis

The moments and products of inertia of the rigid body are defined as:

$$I_x = \sum \delta m \; (y^2 + z^2) = \text{moment of inertia about } ox$$

$$I_y = \sum \delta m \; (x^2 + z^2) = \text{moment of inertia about } oy$$

$$I_z = \sum \delta m \; (x^2 + y^2) = \text{moment of inertia about } oz$$

$$I_{xy} = \sum \delta m \; xy \qquad = \text{product of inertia about } ox \text{ and } oy$$

$$I_{xz} = \sum \delta m \; xz \qquad = \text{product of inertia about } ox \text{ and } oz$$

$$I_{yz} = \sum \delta m \; yz \qquad = \text{product of inertia about } oy \text{ and } oz.$$

If the origin of the reference system is located at the centre of mass of the rigid body, then

$$\sum \delta mx = \sum \delta my = \sum \delta mz = 0,$$

and $\qquad \sum \delta m = m = \text{Total mass of the rigid body.}$

A.3. Differential Equations of a Four DOF Rigid Body

When the linear translational motion of a rigid body along the z axis (bounce) and the rotational motion about the y axis (pitch) are neglected, i.e., $w = \dot{w} = 0$, $q = \dot{q} = 0$, the system is reduced to four DOFs. The equations of motion (A.5) can then be reduced to:

$$
\begin{aligned}
\sum X &= m \, (\dot{u} - \gamma v) \;, \\
\sum Y &= m \, (\dot{v} + \gamma u) \;, \\
\sum L &= I_x \, \dot{p} + I_{yz} \, \gamma^2 - I_{xz} \dot{\gamma} + I_{xy} p \gamma \;, \\
\sum N &= I_z \dot{\gamma} - I_{xy} p^2 - I_{yz} \gamma p - I_{xz} \dot{p} \;.
\end{aligned}
\tag{A.6}
$$

If the sides of the rigid body are symmetric with respect to the xoz plane, then $I_{xy} = I_{yz} = 0$. The equations of motion of the four DOF rigid body can thus be further simplified to:

$$
\begin{aligned}
\sum X &= m \, (\dot{u} - \gamma v) \;, \\
\sum Y &= m \, (\dot{v} + \gamma u) \;, \\
\sum L &= I_x \, \dot{p} - I_{xy} \, \dot{\gamma} \;, \\
\sum N &= I_z \dot{\gamma} - I_{xz} \, \dot{p} \;.
\end{aligned}
\tag{A.7}
$$

227

Appendix B

MECHANICS OF A WHEEL/TIRE

In addition to aerodynamic and gravitational forces, there are forces and moments affecting the motion of a vehicle through the wheel-ground contact. An understanding of the basic characteristics of the wheel-ground contact is therefore essential for any study of performance characteristics, ride quality, and handling behaviour of a vehicle. Wong [70] specifies that the wheel of a vehicle is generally required to fulfil the following five functions: (1) to support the weight of the vehicle, (2) to cushion the vehicle over surface irregularities, (3) to provide sufficient traction for driving and braking, (4) to provide adequate steering control and directional stability. Thus, the study of the mechanics of wheels is of fundamental importance for an understanding of the performance and characteristics of vehicles. For this purpose, Appendix B deals with the forces and moments acting by the ground, rolling resistance and cornering properties.

B.1 Forces and Moments Acting on a Wheel/Tire

As shown in Fig. B.1, there are three forces and three moments acting on the wheel from the ground. The *tractive* (longitudinal) *force* F_x is the component in the x-direction of the resultant force acting on the wheel by the ground. The *lateral* (side) *force* F_y is the component in the y-direction which is a function of both the slip angle α and camber angle γ. The *normal* (vertical) *force* F_z is the component in the z-direction of the resultant force acting on the wheel by the ground. The *overtiring moment* M_x is the moment about the x-axis acting on the wheel by the ground. The *rolling resistance moment* M_y is the moment about the y-axis acting

228

on the wheel by the ground. The *aligning torque* M_z is the moment about the z-axis acting on the wheel by the ground.
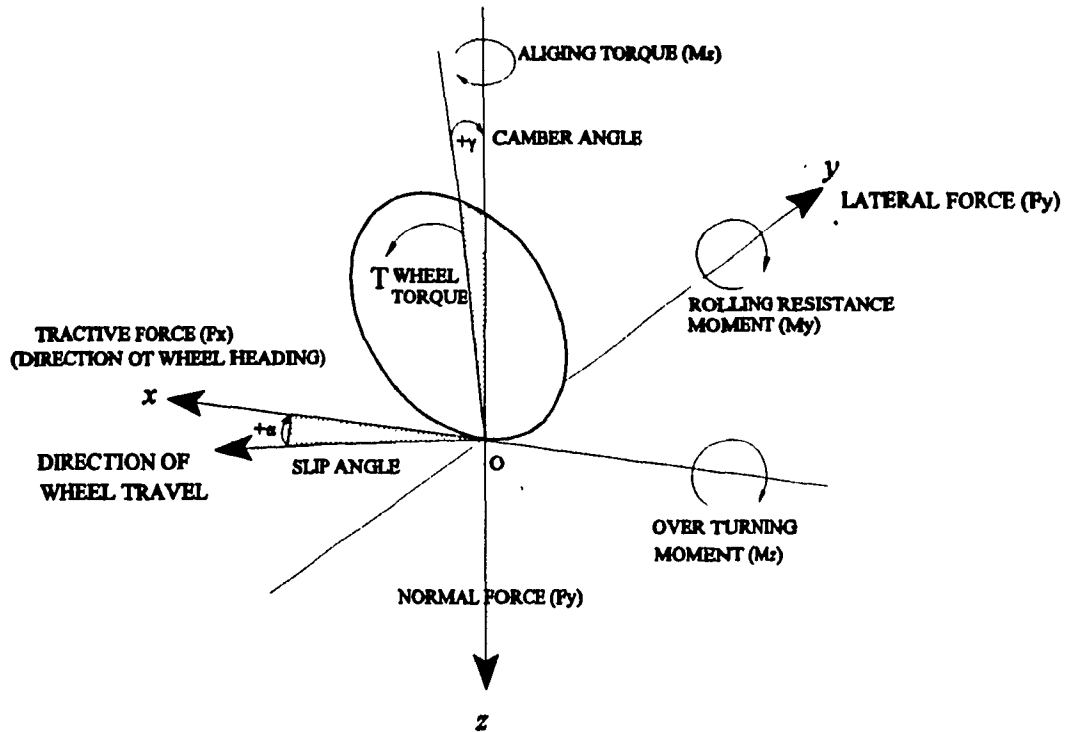

Figure B.1: Wheel Axis System.

In addition, there are two important angles associated with a rolling wheel: the camber angle γ and the slip angle α. The camber angle γ is the angle formed between the wheel plane and the xz plane. The slip angle α is the angle formed between the direction of wheel travel and the line of intersection of the wheel plane with the road surface (the x-axis). The lateral force at wheel-ground contact is a function of both camber angle and slip angle. The positive sense of both camber angle and slip angle are shown in Fig. B.1.

229

B.2. Rolling Resistance

There are a number of factors [70] affecting the rolling resistance of pneumatic wheels/tires. Wheel construction has significant influence on rolling resistance. Inflation pressure affects the flexibility of the wheel/tire. In additional, rolling resistance is also affected by driving speed, because of the increase of work in deforming the tread and of vibration in the wheel/tire carcass with increase of speed. Operating temperature, wheel/tire diameter, and the tractive force also have effects on the rolling resistance of a wheel/tire.

The complex relationships between design and operational parameters of the wheel/tire and its rolling resistance make it extremely difficult to develop an analytic method for predicting the rolling resistance of wheels/tires. Determination of the rolling resistance therefore relies almost entirely on experimental data. Wong [70] reports that, based on experimental results, many empirical formulas have been proposed to calculate rolling resistance of a wheel/tire on hard surfaces. Wong also shows that in many performance calculations, it is often sufficient to consider the resistance coefficient as a linear function of speed. For the most common range of inflation pressure and for speeds up to 128 km/h (80 mph), the following equation gives values of rolling resistance f_r for a car wheel/tire on hard (concrete) surfaces:

$$f_r = k_1 (1 + k_2 V)$$

(B.1)

where, $k_1 = 0.007$, $k_2 = 0.01$ [s/m], and V = velocity of wheel centre [m/s]. Eqn. (B.1) predicts the values of f_r with acceptable accuracy. Furthermore, in many cases, the effect of speed may be ignored, and the value of f_r is treated as constant for different surfaces.

B.3 Cornering Properties

There are many parameters affecting cornering properties of a wheel/tire such as type of wheel/tire, normal load, slip and camber angles, inflation pressure, etc. Ellis [68] reports that the steering angle, slip angle and normal force are considered to be the most important effects of wheel cornering properties, and the effects of camber angle can be neglected. The effects of steering angle, slip angle and normal force on the cornering properties of a wheel/tire may be described as follows:

Wong [70] reports that for small steering angles, the lateral force versus steer angle relation is linear, but as the angle is increased the response falls off due to sliding at the rear of the contact patch where tread deflection is greatest. The relation between steering angle δ and lateral force F_y can thus be represented as follows:

$$F_y = C_1 \delta + C_2 \delta \mid \delta \mid + C_3 \delta^3 \tag{B.2}$$

Each of the coefficients (C_1, C_2, C_3) is a function of the normal force F_z. In addition, lateral force is also a function of slip angle. when the camber angle γ is zero, the lateral force F_y is called the cornering force, which is linearly dependent on slip angle of the wheel/tire up to approximately 4 degrees. Dixon [71] reports that, for small α (non-sliding regime), the lateral force is given by the following equation:

$$F_y = F_l = -C_s \alpha \tag{B.3}$$

where C_s is the cornering stiffness of a given wheel/tire which varies with a number of operational parameters including inflation pressure, normal load, tractive (or braking)

231

effort, and lateral force. Wong [70] shows that cornering stiffness C_{α} can be regarded as constant within a limited range of operating conditions, and has a typical value 50 kN/rad (870 N/deg) for a car tire. The negative sign in Eqn. (B.3) indicates that the lateral force always opposes the slip angle.

Dixon [71] also reports that to improve comparability between wheels/tires of different load ratings, it is often convenient to divide the cornering stiffness by the normal force F_z to give the cornering (stiffness) coefficient C_{α} (subscript α for slip angle). Coefficient C_{α} has a typical value of 0.16/deg or 10/rad for radial-ply. Thus, the lateral force can also be represented by normal force, slip angle and the cornering coefficient as follows:

$$F_y = C_{\alpha} F_z \alpha \qquad (B.4)$$

Here, the slip angle α is the angle between the direction of the velocity vector of the wheel/tire (direction of wheel/tire travel) and the direction of wheel/tire heading. Both steer angle and normal force are strongly dependent on vehicle configuration.

B.4. A Simplified Wheel/Tire Model

B.4.1 Behaviour of a Wheel/Tire

Generally, when a driving torque T is applied to a pneumatic wheel/tire, a tractive force F_t is developed at the wheel-ground contact patch as shown in Fig. B.2 [70]. At the same time, the wheel/tire tread in front of and within the contact patch is subjected to compression. A corresponding shear deformation of the side wall of the wheel/tire also

232

develops.

As tread elements are compressed before entering the contact region, the distance that the wheel/tire travels when subject to a driving torque will be less than that in free rolling. This phenomenon is usually referred to as defamation slip. In addition, when the wheels/tires travel on the ground, the ground may have some deformation. Therefore, considering the deformations of both the wheel/tire and ground, we can simplify the contact region normal forces acting on the wheel/tire by the ground to a point acting force F_z. The acting point C is shown in Fig. B.2, where ε is the positive offset from wheel/tire axis centre (obtainable from experiment).
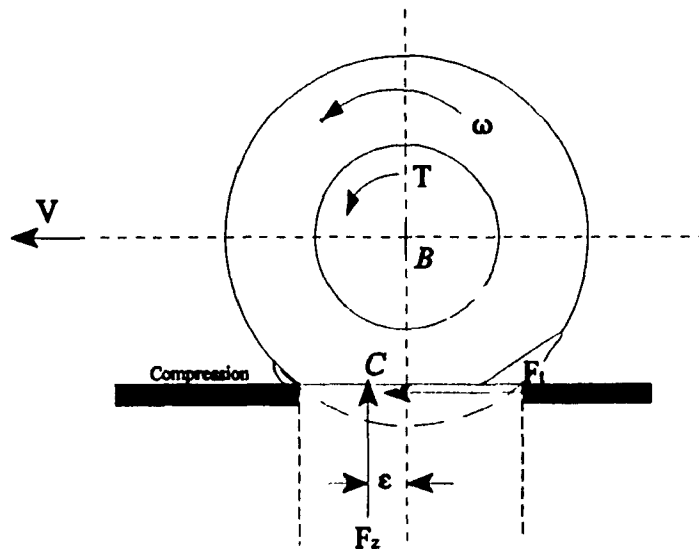

Figure B.2: Behaviour of a wheel/tire under the action of a driving torque [70].

Under the action of a breaking torque on the wheel/tire, a negative offset ε will be created and the breaking force F_b will oppose the breaking torque. In addition, when there is an

233

angular acceleration (deceleration) acting on the wheel/tire, the friction F_f will also be produced at point C to oppose it.

B.4.2 A Special Case

Base on the mechanics of the wheel/tire discussed in Sections B.1 through B.4.1, if the deformation of the wheel/tire has been considered, generally, the tractive force F_x (F_x = F_t - F_f), lateral force F_l(F_l = F_y = $-C_S \alpha$) and normal force F_z acting on the wheel/tire by the ground can be simplified as in Fig. B.3. All three forces are acting through the action point C. Thus, overtiring moment M_x can be determined as the product of normal force F_z and offset ϵ. Aligning torque M_z can be determined as the product of lateral force F_l and offset ϵ. Rolling resistance moment M_y is determined as the product of normal force F_z and the shift of the centre of the normal force. The signs of the overtiring moment M_x, rolling resistance moment M_y, and aligning torque M_z are decided by the right hand rule, and the positive sense of these are shown in Fig. B.3.

However, if a wheel employed on the vehicle is made of hard rubber, the deformation of the wheel is very small, and this wheel can be considered as non-deformable. In addition, if the vehicle moves on a hard, smooth and dry surface, then the wheel-ground contact region may be regarded as point contact, and the offset ϵ will be equal to zero. Forces at the action point C will then coincide with the origin of the wheel axis system. The overtiring moment M_x, aligning torque M_z, and rolling resistance moment M_y then no longer exist in the wheel axis system. Only the three external forces, tractive force F_x, lateral force F_l, and normal force F_z, act on the wheel-ground contact point C by the ground.

It is necessary to point out that, in the present research, we mostly deal with the simplified wheel model. Each wheel is considered as a non-deformable wheel, and the wheel-ground contact region is assumed to be a point contact. Overtiring moment M_x, aligning torque M_z, and rolling resistance moment M_y are not taken in account.
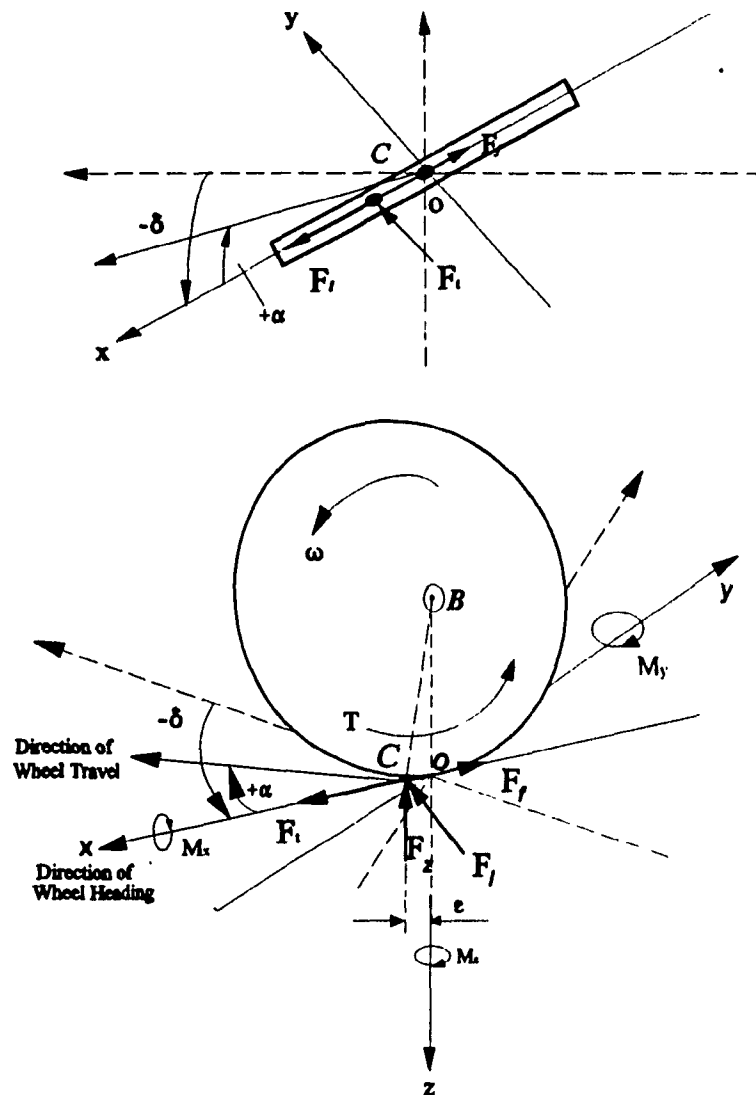

Figure B.3: Free Body Diagram of a Wheel/Tire.

B.5. Tractive Force

Tractive forces are applied to the vehicle via DC motors, and these forces are therefore dependent on motor characteristics and not on wheel and floor characteristics. The DC motor in the motor-wheel unit is a permanent magnet DC motor with torque-current curve as shown in Fig. B.4. The torque T_g generated by the motor can be calculated by the following formula [75] [21]:

$$T_g = K_T I , \qquad \qquad (B.5)$$

where the motor current is I, and the torque constant is defined as K_T.

Fig.B.5 shows a motor and load system. The moment of inertia of the motor referred to the motor shaft (with the wheel as load in the case of automated vehicle system) is defined as J. The viscous damping factor, static friction torque and load torque of the motor shaft are defined as D, T_f and T_m respectively. The angular displacement of the motor rotation is Θ. The dynamic equation of this system can be expressed as :

$$T_g = J\frac{d^2\Theta}{d^2t} + D\frac{d\Theta}{dt} + T_f + T_m . \qquad (B.6)$$

Substituting T_g from Eqn. (B.5) into Eqn. (B.6),

$$T_m = K_T I - J\frac{d^2\Theta}{d^2t} - D\frac{d\Theta}{dt} - T_f . \qquad (B.7)$$

The torque transferred to the wheel from the motor shaft is

$$T_\omega = N \, T_m , \qquad \qquad (B.8)$$

236

where the gear ratio is N. The tractive force acting on the wheel unit by the DC motor is expressed as follows:

$$F_t = \frac{T_\omega}{R} = \frac{NT_m}{R} = \frac{N}{R}(K_T I - J\frac{d^2\Theta}{d^2 t} - D\frac{d\Theta}{dt} - T_f) , \qquad (B.7)$$

where the radius of the motorized wheel is R. The angular velocity and angular acceleration of the motorized wheel are ω and $\dot{\omega}$ respectively, and the angular velocity and angular acceleration of the motor are $\dfrac{d\Theta}{dt} = N\omega$ and $\dfrac{d^2\Theta}{d^2 t} = N\dot{\omega}$ respectively. Thus, Eqn. (B.7) can be rewritten as:

$$F_t = \frac{N}{R}(K_T I - J N \dot{\omega} - D N \omega - T_f) . \qquad (B.8)$$

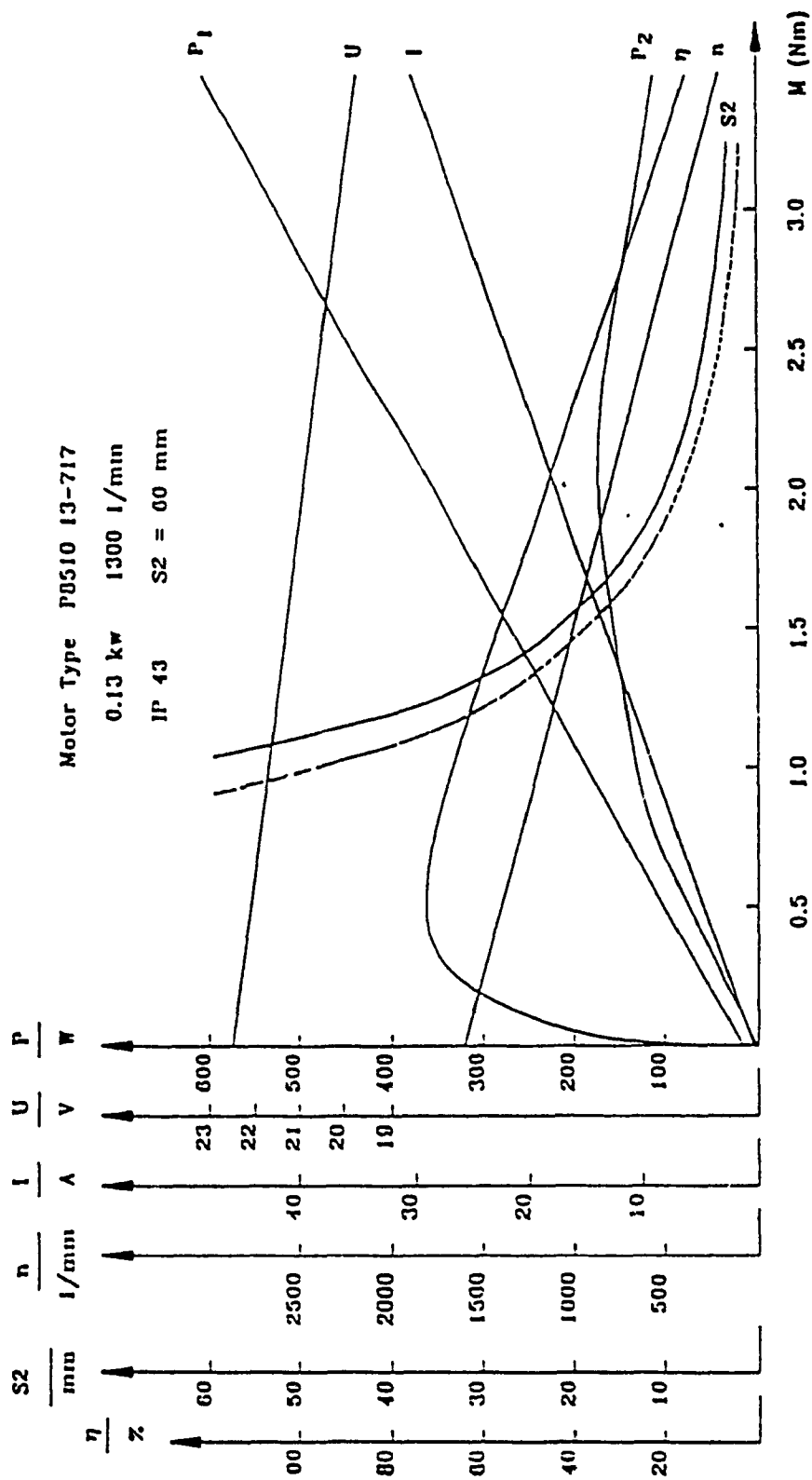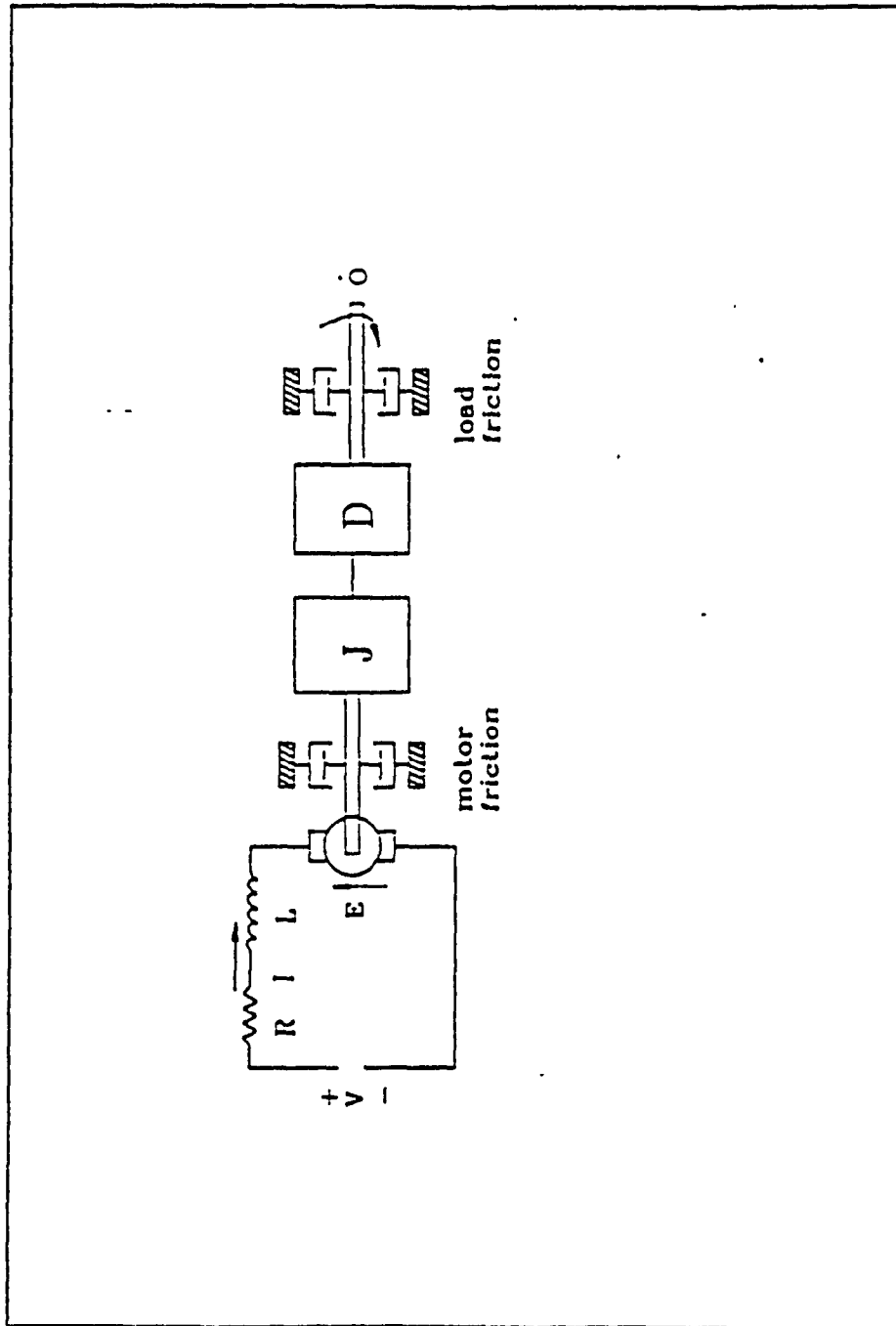**Figure B.4:** Driving Motor Characteristics [21].

Figure B.5: Model of DC Motor and Load System [75].

239

Appendix C

VERTICAL FORCES ACTING ON THE INDIVIDUAL WHEELS

C.1. Introduction

The load acting on each wheel unit is, generally speaking, dependent on the vehicle configuration when the vehicle is stationary. When the vehicle is climbing or descending a hill or turning a curve, the load acting on each wheel unit will vary. The load acting on each wheel unit will also be redistributed when the vehicle has pitch, bounce and rolling motions. In this research, an automated vehicle is considered to move on a smooth horizontal plane, and bounce and pitch motions are therefore neglected. It is assumed that the number of aligning wheels in the y-direction is less than three. The vertical forces acting on each wheel unit will be determined by detailed consideration of each specific case.

C.2 Forward Motion of the Automated Vehicle with No Lateral Acceleration and Roll about the x-axis

An automated vehicle is assumed to be driven in the forward direction on a flat floor, with no rolling and lateral acceleration involved.

Case 1. Four Wheel Units Configuration Automated Vehicle.

Fig. C.1 shows an automated vehicle with four wheel units configuration, with each pair of wheel units aligned along the y-direction. Vertical reaction forces at each wheel unit can be obtained from the fundamental equations of statics [72] [73] [74], which take the moments at contact points $C_{1,2}$ and $C_{3,4}$ respectively, i.e.:

240

$$F_{s_{1,2}} = \frac{W L_2 + a_x m h_g}{L_1 + L_2} ,$$

$$F_{s_{3,4}} = \frac{W L_1 - a_x m h_g}{L_1 + L_2} ,$$

(C.1)

$$F_{s_1} = \frac{W L_2 + a_x m h_g}{2 (L_1 + L_2)} , \qquad F_{s_2} = \frac{W L_2 + a_x m h_g}{2 (L_1 + L_2)} ,$$

$$F_{s_3} = \frac{W L_1 - a_x m h_g}{2 (L_1 + L_2)} , \qquad F_{s_4} = \frac{W L_1 - a_x m h_g}{2 (L_1 + L_2)} .$$

Case 2. Three Wheel Units Configuration Automated Vehicle.

If there are only three wheel units located on the vehicle main body, and one pair of wheel units (assuming, for example, wheel units 3 and 4) is located aligned along the y-direction, the vertical reaction forces acting on the wheel can be easily determined from the equations of static equilibrium, expressed as follows:

$$F_{s_1} = \frac{W L_2 + a_x m h_g}{L_1 + L_2} ,$$

$$F_{s_{2,3}} = \frac{W L_1 - a_x m h_g}{L_1 + L_2} ,$$

(C.2)

$$F_{s_2} = \frac{W L_2 - a_x m h_g}{2 (L_1 + L_2)} , \qquad F_{s_3} = \frac{W L_1 - a_x m h_g}{2 (L_1 + L_2)} .$$

In Eqns. (C.1) and (C.2), the distance between the centre of the front wheel(s) and the centre of the total mass is L_1. The distance between the centre of the rear wheel(s) and the

241

centre of the total mass is L_2. The distance from the ground to the centre of the total mass is

h_g. The weight of the AGV is W and the mass of the AGV is m. The forward acceleration of

the centre of mass along the x-direction is a_x.
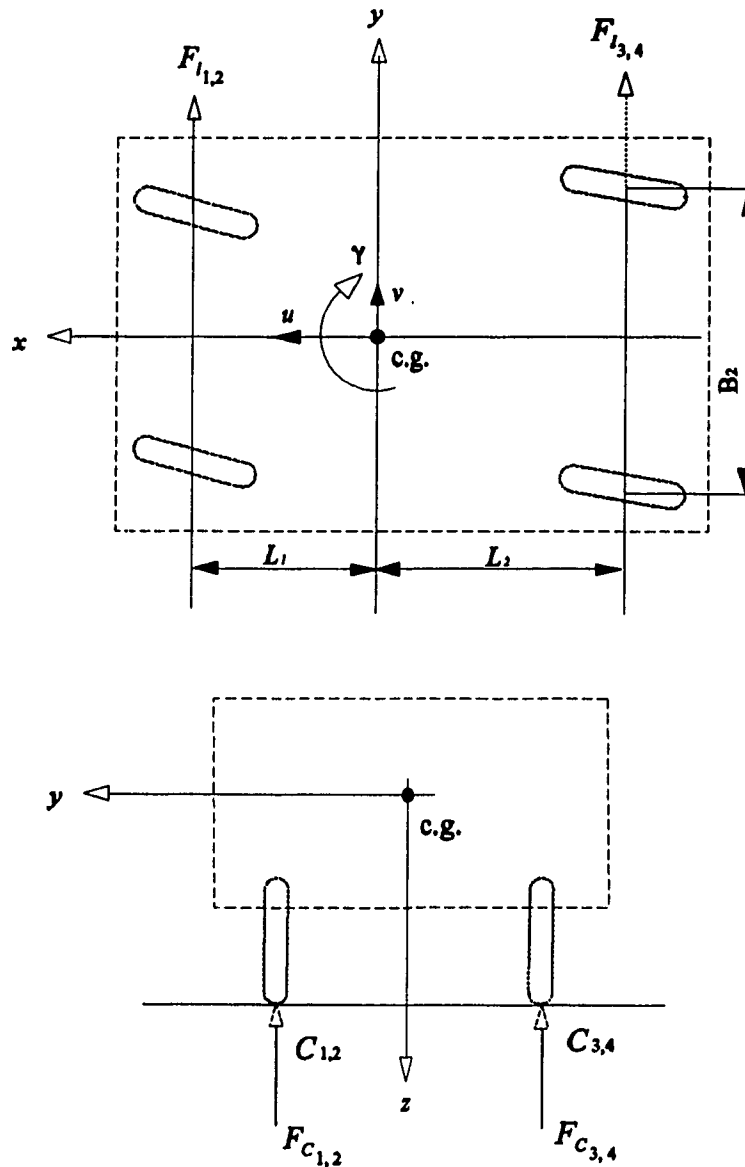

Fig.C.1: Schematic of Four Wheel Units Automated Vehicle
with Lateral and Vertical Forces.

242

Case 3. Statically indeterminate problems occur when the number of wheel units employed on the AGV main body exceeds three, and one of the following conditions has been met.

Condition 1: total number of wheel axes is larger than two (coincident axes are counted as one axis as shown in Fig. C.1 (a) and (b)).

Condition 2: total number of wheel units in parallel is more than three, i.e., the number of wheel-ground contact points from a side view of the vehicle is larger than three as shown in Fig. C.2 (b).

The redundant constraints will then be increased in the AGV system, and the structure of the vehicle is considered statically indeterminate, i.e., the problem of calculating vertical reaction forces based on considerations of static equilibrium alone involves more unknowns than equations. Fundamental equations of statics are not sufficient to calculate all of the vertical reaction forces acting on the wheels, so that additional equations, based on consideration of the deflection of the AGV frame or the tires, must be derived. There are numerous methods for solving this type of problem, such as the method of superposition and the moment-area method [72] [73].

This is, however, a very complex problem and in some instances it is possible to avoid derivation of an explicit solution. The vertical load acting on each wheel can be determined by the designer based on certain standards and assumptions. For example, the load acting on each wheel unit must supply enough friction forces to satisfy the conditions of pure rolling and no side slipping. There are some examples given as follows.

243
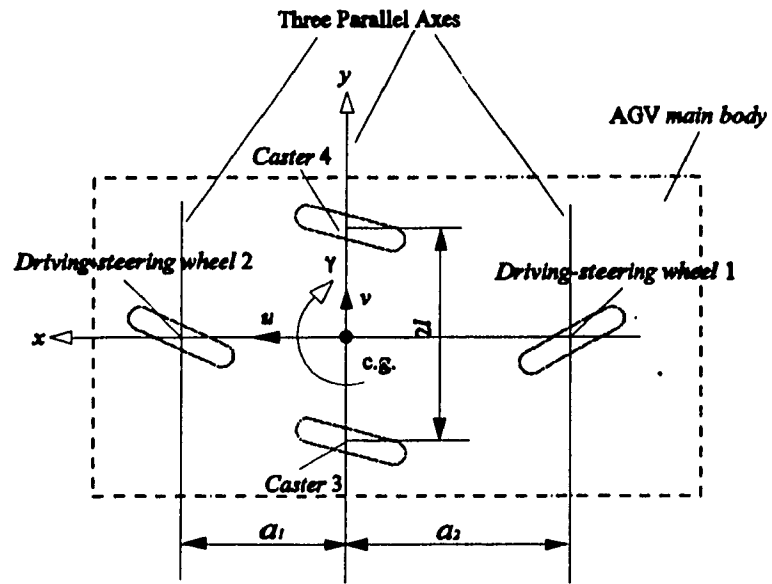
(a) Three axes in parallel
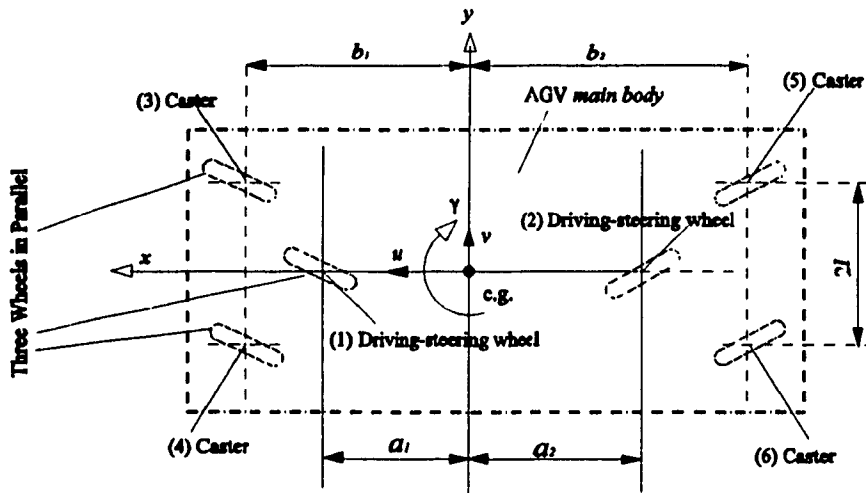
(b) Four axes in parallel

Figure C.2: Statically Indeterminate Structures.

244

Example 1: CONCIC-3 AGV.

The CONCIC-3 AGV has a double steering wheelbase configuration with two sets of driving-steering wheels units in the front and rear of the AGV. In addition, there are two casters fixed at two sides of the AGV to provide stability as shown in Fig.5.1. In this case [19], the designer can consider the total mass to be supported by the front and rear driving-steering wheel units for the purpose of simplifying analysis and controller design. The casters are assumed to be lightly contacted with the ground just enough to provide static equilibrium. Thus, the static vertical reaction forces are:

$$F_{z_1} = \frac{W \, a_1}{a_1 + a_2},$$

$$F_{z_2} = \frac{W \, a_2}{a_1 + a_2}, \qquad\qquad (C.3)$$

$$F_{z_3} = F_{z_4} \approx 0 \, .$$

In Eqns. (C.3), the total weight of the CONCIC-3 AGV is W, and the distance from the front driving-steering wheel unit, as well as the rear driving-steering wheel unit to the centre of the total mass are a_1 and a_2, respectively.

Example 2: CONCIC - 2 AGV.

The CONCIC-2 has two driving wheel units employed at two sides of the AGV, and two casters in the front and rear of the AGV as shown in Fig. 5.10. The axes of the two side driving wheel units are aligned. The two casters have separate axes at the front and rear of the AGV. The number of wheel units is greater than three, and the total number of axes is

greater than two. Therefore, vertical forces acting on the wheels cannot be determined by the fundamental equations of statics. In this case, the designer [21] can consider that each of the wheels supports the same load, which is one of the fourth of total weight, based on the assumptions: (a) the AGV main body, driving wheel units and casters are rigid bodies, and (b) each wheel unit truly supports the AGV main body, i.e., each wheel absolutely attached on the ground. Thus, the static vertical reaction forces are:

$$F_{s_{1,2,3,4}} = \frac{\text{Weight of total vehicle main body}}{4} + .$$

(C.4)

Weight of each wheel unit .

Example 3 Six wheels employed on an AGV

There are a number of six wheel configuration AGVs in use in the General Motors plant at Oshawa, Ontario, Canada as shown in Fig. 5.17. One feature in common with the CONCIC-3 AGV is the doubled steering wheelbase configuration with two sets of driving-steering wheel units in the front and rear of the AGV. Unlike the CONCIC-3, however, are the two pairs of the casters employed on the front and rear of the AGV. In this case, the four casters support the most of the AGV weight and the two driving-steering wheels only lightly support the AGV main body. The loads acting on the two steering-driving wheel units are determined by applying the kinematic constraint that the load must offer suitable tractive forces to permit motion of the AGV.

$$F_{s_{1,4}} = \frac{W\,b_1 + a_x\,m\,h_s}{b_1 + b_2} - F_{s_1} , \qquad F_{s_1} = \frac{F_{t_1}}{f_{r_1}}$$

(C.4)

$$F_{s_{3,6}} = \frac{W\,b_2 - a_x\,m\,h_s}{b_1 + b_2} - F_{s_2} , \qquad F_{s_2} = \frac{F_{t_2}}{f_{r_2}} .$$

The above three examples have illustrated that the static vertical load acting on each wheel unit is also often determined by specific requirements or assumptions. It is necessary to simplify the AGV model to reduce redundant constraints by using some suitable assumptions. In addition, it is essential to reduce redundant constraints in the AGV system from the viewpoint of system controllability [17].

C.3 An AGV Moves on an Arbitrary Path, with Rolling Motion About the x-axis and Lateral Acceleration Considered.

When an AGV is driving on an arbitrary path, and lateral acceleration or rolling motion are involved in the AGV system, the vertical load acting on each wheel unit will be shifted from the left side to the right side or *vice versa*. For above-discussed Cases 1 and 2, the shift value can be determined by following procedure.

C.3.1 Determination of the side forces acting on each wheel unit caused by the lateral inertial force $a_{s_y} \cdot m_s$,

$$a_{s_y} m_s = F_{l_{1,2}} + F_{l_{3,4}},$$

$$F_{l_{1,2}} = a_{s_y} m_s \frac{L_2}{L_1 + L_2},$$

$$F_{l_{3,4}} = a_{s_y} m_s \frac{L_1}{(L_1 + L_2)},$$

(C.5)

where the lateral acceleration of the sprung mass is a_{s_y} and the sprung mass is m_s. As long as an AGV moves at constant forward speed (u) in a circular path with radius R, the lateral acceleration $a_{s_y} = \frac{u^2}{R}$. Otherwise, the lateral acceleration should be determined by Eqn.

(3.6). Furthermore, in Eqn. (C.5), when there is no sprung mass involved in the system, the lateral acceleration a_{s_y} and sprung mass m_s should be replaced by the lateral acceleration a_y and the total mass m .

C.3.2 Determination of the side forces acting on each wheel unit caused by the lateral inertial force $a_{u_{y_i}} \cdot m_{u_i}$,

$$ F_{l_{u_i}} = a_{u_{y_i}} \cdot m_{u_i} , \qquad \text{where} \qquad \{ i = 1, 2, 3, 4 \} . \qquad \text{(C.6)} $$

The unsprung mass of each wheel unit is m_{u_i}. The lateral acceleration of the centre of each wheel is $a_{u_{y_i}}$. Based on the location of joints A_i or B_i, the acceleration of each wheel unit can be determined by applying Eqn.(A.4). In addition, when the AGV moves at constant forward speed (u) in a circular path with radius R , $a_{u_{y_i}} = \dfrac{u^2}{R \pm B_i / 2}$. The distance between the two aligned wheel units is B_i, and the sign of B_i is dependent on the AGV turning direction. The sign of B_i is negative for the wheel nearer to the centre of the turning path. Otherwise, it will be positive.

C.3.3 Rotating Moments Caused by the Rolling Angle ϕ :

$$ M_{\phi_1} = C_{\phi_1} \phi , $$
$$ M_{\phi_2} = C_{\phi_2} \phi , \qquad \text{(C.7)} $$

where the rolling stiffness of the two front wheel units and rear wheel units are C_{ϕ_1} and C_{ϕ_2} [N.m/rad] respectively, and the rolling angle of the AGV is ϕ (as shown in Fig. C.3) .
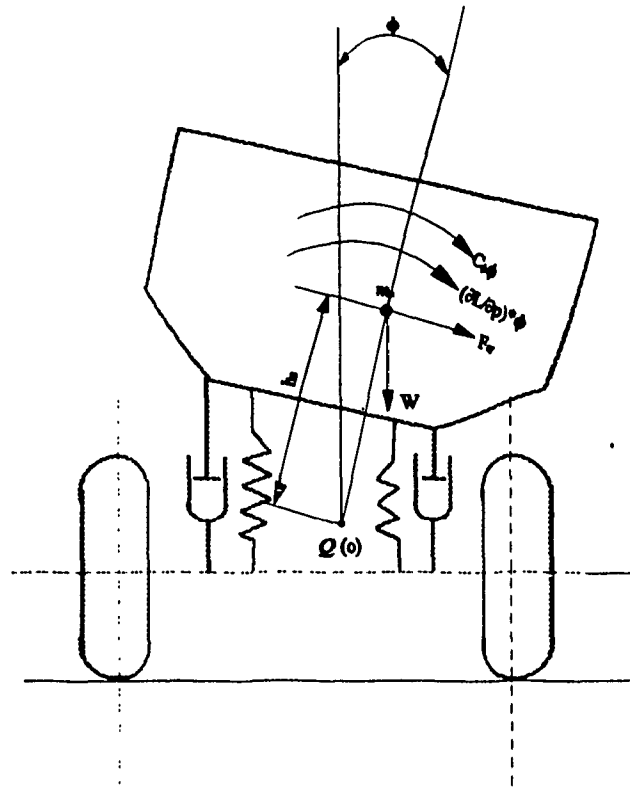
248

Figure C.3: Schematic of Rotating Moments Caused
by Rolling Motion.

C.3.4 The load shift ΔZ_i ($i = 1, 2, \ldots, n$)

Assuming the AGV is turning to the left side, the forces acting on the front two wheels are

shown in Fig. C.4. Taking the moment at wheel-ground contact point 1, the following

equations are obtained :

$$\sum M_1 = F_{l_{1,2}} h + M_{\phi_1} + (F_{l_{u_1}} + F_{l_{u_2}}) R_{1,2} + \Delta Z_2 B_1 = 0,$$

$$\Delta Z_2 B_1 = -\{ F_{l_{1,2}} h + M_{\phi_1} + (F_{l_{u_1}} + F_{l_{u_2}}) R_{1,2} \},$$

$$\Delta Z_2 = - \frac{F_{l_{1,2}} h + M_{\phi_1} + (F_{l_{u_1}} + F_{l_{u_2}}) R_{1,2}}{B_1},$$

(C.8)

249

where the negative sign of ΔZ_2 illustrates that the load acting on the right wheel has been reduced.
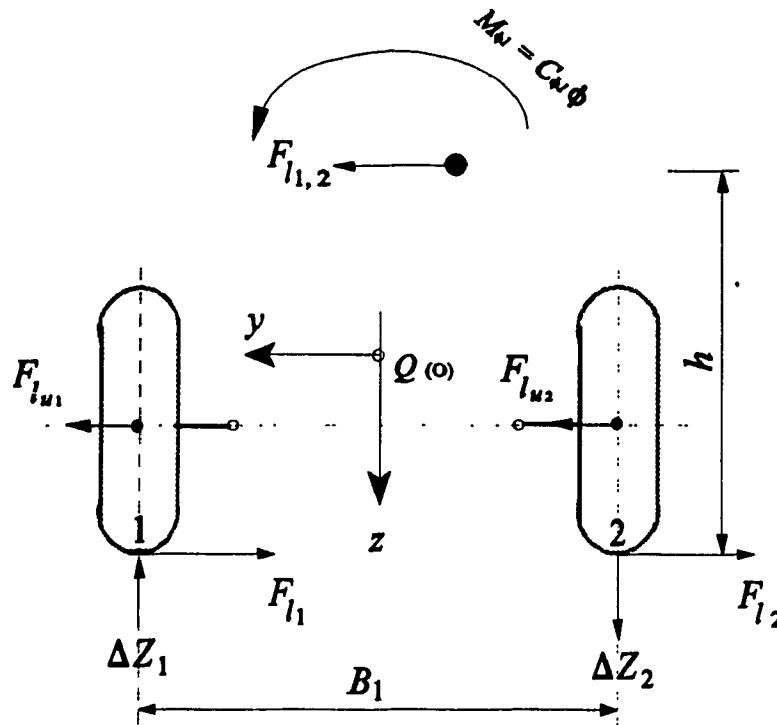

Figure C.4: Schematic of the AGV model for analysis of the load distribution from the left side wheel to the right side wheel.

Similarly, taking the moment at wheel-ground contact point 2, the following equations are obtained:

$$\sum M_2 = F_{l_{1,2}} h + M_{\phi_1} + (F_{l_{u_1}} + F_{l_{u_2}}) R_{1,2} - \Delta Z_1 B_1 ,$$

$$\Delta Z_1 B_1 = F_{l_{1,2}} h + M_{\phi_1} + (F_{l_{u_1}} + F_{l_{u_2}}) R_{1,2} ,$$

$$\Delta Z_1 = \frac{F_{l_{1,2}} h + M_{\phi_1} + (F_{l_{u_1}} + F_{l_{u_2}}) R_{1,2}}{B_1} ,$$

(C.9)

where the positive sign of ΔZ_1 indicates that the load acting on the left wheel has been increased. Comparing Eqns. (C.8) and (C.9), the following result is proved:

$$\Delta Z_1 = - \Delta Z_2 ,\tag{C.10}$$

This means that the same value of load has been shifted from right side wheel -2 to left side wheel-1 (See Fig. C.4, which is the front view of the AGV).

Similarly, the load shift value between the two rear wheels (3 and 4) can be determined by the following equations:

$$\sum M_3 = F_{l_{3,4}} h + M_{\phi_2} + (F_{l_{u_3}} + F_{l_{u_4}}) R_{3,4} + \Delta Z_4 B_2 = 0,$$

$$\Delta Z_4 B_2 = -\{ F_{l_{3,4}} h + M_{\phi_2} + (F_{l_{u_3}} + F_{l_{u_4}}) R_{3,4} \},$$

$$\Delta Z_4 = \frac{F_{l_{3,4}} h + M_{\phi_2} + (F_{l_{u_3}} + F_{l_{u_4}}) R_{3,4}}{B_2} ,\tag{C.11}$$

and

$$\sum M_4 = F_{l_{3,4}} h + M_{\phi_2} + (F_{l_{u_3}} + F_{l_{u_4}}) R_{3,4} - \Delta Z_3 B_2 = 0,$$

$$\Delta Z_3 B_2 = F_{l_{3,4}} h + M_{\phi_2} + (F_{l_{u_3}} + F_{l_{u_4}}) R_{3,4} ,$$

$$\Delta Z_3 = \frac{F_{l_{3,4}} h + M_{\phi_2} + (F_{l_{u_3}} + F_{l_{u_4}}) R_{3,4}}{B_2} ,\tag{C.12}$$

also,

$$\Delta Z_3 = - \Delta Z_4 .\tag{C.13}$$

251

In the above equations, the distance between the sprung mass m_s centroid and the ground is h. The distance between the unsprung mass m_{ui} centroid and the ground is conventionally taken as the wheel radius R_i. The distance between left and right wheels in the front or rear are B_1 and B_2, respectively.

C.4 Total Vertical Force Acting on Each Wheel Unit

By taking consideration of the load shifts caused by lateral acceleration and rolling motion while the automated vehicle moves on a curved path, the total vertical force acting on each wheel will be determined as follows.

Case 1: Four Wheel Units Configuration Automated Vehicle

$$F_{Z_1} = \frac{W L_2 - a_x m h_g}{2(L_1 + L_2)} + \Delta Z_1$$

$$= \frac{W L_2 - a_x m h_g}{2(L_1 + L_2)} + \frac{F_{l_{1,2}} h + M_{\phi_1} + (F_{l_{u_1}} + F_{l_{u_2}}) R_{1,2}}{B_1},$$

$$F_{Z_2} = \frac{W L_2 - a_x m h_g}{2(L_1 + L_2)} - \Delta Z_2$$

$$= \frac{W L_2 - a_x m h_g}{2(L_1 + L_2)} - \frac{F_{l_{1,2}} h + M_{\phi_1} + (F_{l_{u_1}} + F_{l_{u_2}}) R_{1,2}}{B_1},$$

$$F_{Z_3} = \frac{W L_1 + a_x m h_g}{2(L_1 + L_2)} + \Delta Z_3$$ (C.14)

$$= \frac{W L_1 + a_x m h_g}{2(L_1 + L_2)} + \frac{F_{l_{3,4}} h + M_{\phi_2} + (F_{l_{u_3}} + F_{l_{u_4}}) R_{3,4}}{B_2},$$

$$F_{Z_4} = \frac{W L_1 + a_x m h_g}{2(L_1 + L_2)} - \Delta Z_4$$

$$= \frac{W L_1 + a_x m h_g}{2(L_1 + L_2)} - \frac{F_{l_{3,4}} h + M_{\phi_2} + (F_{l_{u_3}} + F_{l_{u_4}}) R_{3,4}}{B_2}.$$

252

Case 2: Three Wheel Units Configuration Automated Vehicle.

$$F_{z_1} = \frac{W L_2 - a_x m h_s}{2(L_1 + L_2)},$$

$$F_{z_2} = \frac{W L_2 + a_x m h_s}{2(L_1 + L_2)} + \Delta Z_2$$

$$= \frac{W L_2 + a_x m h_s}{2(L_1 + L_2)} + \frac{F_{l_{2,3}} h + M_\phi + (F_{l_{w_2}} + F_{l_{w_3}}) R_{2,3}}{B_2}, \qquad (C.15)$$

$$F_{z_3} = \frac{W L_1 + a_x m h_s}{2(L_1 + L_2)} - \Delta Z_3$$

$$= \frac{W L_1 + a_x m h_s}{2(L_1 + L_2)} - \frac{F_{l_{2,3}} h + M_\phi + (F'_{l_{w_2}} + F_{l_{w_3}}) R_{2,3}}{B_2},$$

Case 3: Statically Indeterminate Configuration.

For this case, vertical forces acting on the wheel should be determined using some assumptions. Generally, the vertical forces should take care of the static load, and dynamic loads caused by forward accelerations, lateral accelerations, and roll and yaw motions.

Table D.1 System Parameters of CONCIC-3 AGV

Parameter	Description
Vehicle Main Body	
m = 124.5 kg	Total mass of the vehicle
ms = 0.00 kg	Sprung mass
Iz = 14.6 kg m²	Yaw moment of inertia
Ixz = 0 kg m²	Moment of inertia about the xz-plane
Ix = 6.0 kg m²	Roll moment of inertia
h = 0.31 m	Distance from the total mass centre to the ground
Configuration Location of each joint A_i with respect to frame $\{Q\}$	
x_{a1} = -0.39 m	Distance between the y-axis and joint A_1 (the rear wheel)
y_{a1} = 0.00 m	Distance between the x-axis and joint A_1
$_{2}$ = 0.32 m	Distance between the y-axis and joint A_2 (the front wheel)
y_{a2} = 0.00 m	Distance between the x-axis and joint A_2
x_{a3} = 0.00 m	Distance between the y-axis and joint A_3 (the left wheel)
y_{a3} = -0.26 m	Distance between the x-axis and joint A_3
x_{a4} = 0.00 m	Distance between the y-axis and joint A_4 (the right wheel)
y_{a4} = 0.26 m	Distance between the x-axis and joint A_4
Wheel Units	
m_{d1} = m_{d2} = 9.5 kg	Mass of each driving-steering wheel unit
R_1 = R_2 = 0.0075 m	Radius of the two driving-steering wheel units
I_{g_i} = 0.002 kg m²	Rotational inertia of the driving wheel

J_i = 0.0025 kg m^2	Moment of inertia of the driving wheel (referred to motor shaft)
$C_{\alpha 1}$ = $C_{\alpha 2}$ = 4000 N/rad	Cornering stiffness of rear and front wheel units
f_{ri} = 0.023 N/N	Rolling resistance for each wheel unit, i = 1, 2, 3, 4
Casters	
m_{d3} = m_{d4} = 2.4 kg	Mass
R_3 = R_4 = 0.06 m	Radius
I_{z3} = I_{z3} = 0.001 kg m^2	Polar moment of inertia .
d_3 = d_4 = 0 m	Offset
$C_{\alpha 3}$ = $C_{\alpha 4}$ = 3000 N/rad	Cornering stiffness of left and right casters (N/rad).
Driving Motor	
T_m = 0.088 s	Mechanical time constant
T_e = 0.078 s	Electrical time constant
K_T = 0.114 N m/A	Motor torque constant
D_i = 0.0228 kg m^2/s	Mechanical damping coefficient
J_i = 0.0025 kg m^2	Moment of inertia (referred to motor shaft)
N_{d_1} = N_{d_2} = 9.9	Gear ratio
T_{f_1} = T_{f_2} = 0 N m	Static friction
Steering Motor	
T_s = 18.0 N m	Stall Torque
τ_{st} = 0.00378 s	Electrical time constant
k_{ts} = 3.0 N m/A	Motor torque constant
ω_f = 45 rpm	No load speed

255

Table D.2 SYSTEM PARAMETERS OF CONCIC-2 AGV

Parameter	Description
Vehicle Main Body	
m = 124.4 kg	Total mass of the vehicle
m_s = 0.00 kg	The sprung mass
I_z = 14.6 kg m^2	Yaw moment of inertia
I_{xz} = 0 kg m^2	Moment of inertia about the xz-plane
I_x = 0 kg m^2	Roll moment of inertia
h = 0.31 m	Distance from the total mass centre to the ground
Configuration Location of each joint A_i with respect to frame $\{Q\}$	
x_{b1} = 0.00 m	Distance between the y-axis and joint B_1 (the right wheel)
y_{b1} = -0.26 m	Distance between the x-axis and joint B_1
x_{b2} = 0.00 m	Distance between the y-axis and joint B_2 (the left wheel)
y_{b2} = 0.26 m	Distance between the x-axis and joint B_2
x_{a3} = -0.39 m	Distance between the y-axis and joint A_3 (the rear wheel)
y_{a3} = 0.00 m	Distance between the x-axis and joint A_3
x_{a4} = 0.39 m	Distance between the y-axis and joint A_4 (the front wheel)
y_{a4} = 0.00 m	Distance between the x-axis and joint A_4
Wheel Units	
$m_{d1} = m_{d2}$ = 9.5 kg	Mass of each driving-steering wheel unit
$R_1 = R_2$ = 0.0075 m	Radius of the two driv· ·· ·steering wheel units
I_{B_i} = 0.0025 kg m^2	Driving wheel rotational inertia
k_{ci} = 0.007	Coefficient of rolling friction for each wheel unit, i = 1, 2, 3, 4
k_{c2} = 0.01s/m	Coefficient of rolling friction for each wheel unit

Casters	
$m_{d3} = m_{d4} = 2.4$ kg	Mass of each caster
$R_3 = R_4 = 0.06$ m	Radius
$I_{z3} = I_{z4} = 0.001$ kg m^2	Polar moment of inertia for each caster
$d_3 = d_4 = 0.04$ m	Offset for each caster
$k_{cn} = 0.01$	Coefficient of side friction for each caster, $i = 3, 4$
Driving Motor	
$k_e = 0.163$ V s/m	Voltage constant
$K_T = 0.114$ N m/A	Torque constant
$D_i = 0.0001$ kg m^2/s	Mechanical damping coefficient
$J_i = 0.0025$ kg m^2	Moment of inertia (referred to motor shaft)
$N_{d_1} = N_{d_2} = 9.9$	Gear ratio
$T_{f_4} = T_{f_3} = 0$ Nm	Static friction